

Graphs on Euclidean, Spherical and Hyperbolic Surfaces

by

Alexandra Wesolek

M.Sc., Freie Universitaet Berlin, 2019

B.Sc., Freie Universitaet Berlin, 2016

Thesis Submitted in Partial Fulfillment of the
Requirements for the Degree of
Doctor of Philosophy

in the
Department of Mathematics
Faculty of Science

© Alexandra Wesolek 2023
SIMON FRASER UNIVERSITY
Spring 2023

Copyright in this work is held by the author. Please ensure that any reproduction or re-use is done in accordance with the relevant national copyright legislation.

Declaration of Committee

Name: Alexandra Wesolek

Degree: **Doctor of Philosophy**

Thesis title: **Graphs on Euclidean, Spherical and Hyperbolic Surfaces**

Committee: **Chair:** Veselin Jungic
Teaching Professor, Mathematics

Bojan Mohar
Supervisor
Professor, Mathematics

Matt DeVos
Committee Member
Associate Professor, Mathematics

Pavol Hell
Examiner
Professor Emeritus, Computing Science

Pavel Valtr
External Examiner
Professor, Applied Mathematics
Charles University

Abstract

This thesis is on the interplay of surfaces and graphs embedded on them. In order to showcase the interactions between the two, it discusses a game commonly played on graphs and surfaces: The Cops and Robber game. The goal in studying this game is to find strategies for the robber to escape from one or more cops and for the cop(s) to catch the robber. This thesis discusses strategies of the players when the game is played on surfaces and higher dimensional manifolds of constant curvature. What properties of a manifold make it easy for the robber to escape the cops? The results in this thesis suggest that the number of cops needed to catch the robber is related to the dimension of the manifold, whereas the number of cops needed to come arbitrarily close to the robber is related to how uniform its curvature is.

The relationship between topology and graph theory often stems from representations of graphs as points and curves in topological spaces. This thesis discusses parameters that influence the quality of representations, such as the number of edge crossings of graphs drawn in the plane. For example, we ask how we can decompose the edges of a drawing into two or more subdrawings such that the sum of the edge crossings in each subdrawing is as small as possible. To study this question, we consider random drawings of the complete graph, where vertices are points which are chosen uniformly at random from a Euclidean square, and the edges are straight lines. We show a strategy to decompose such a random graph drawing into two subdrawings, such that the sum of the crossings is small. More generally, this thesis studies intersection graphs of random geometric objects and properties of those intersection graphs such as the density of small substructures or the existence of spanning substructures.

Finally, we consider representations of graphs in higher dimensional spaces and their energy as a measure of quality. The energy is a well-studied parameter since it is related to planar drawings of graphs as well as spectral drawings. We provide a new semidefinite graph drawing algorithm that minimises the energy of a representation with respect to a new set of constraints.

Keywords: Cops and Robber; random intersection graphs; graph drawing; plane decomposition

Dedication

To my family.

Thank you for being unique and sharing your philosophies every step of the way.

Thank you for reminding me what is most important in life.

To my mother.

Whom I admire for her intelligence and kindness.

Acknowledgements

Most importantly, I would like to thank my family. Without you I would have never made it this far. Thank you to my mother, Anna Wesolek, for being such an inspiration in my life. Thank you to my father, Christoph Wesolek, for going out of his way to make sure I am healthy. Thank you to my siblings Joanna Brauner, Michael Wesolek and Piotr Wesolek for always believing in me and for sharing laughter's and love. Thank you to my niece and nephews Hanna Wesolek, Franek Wesolek, Luke Wesolek, Paul Brauner and Moritz Brauner for filling me with happiness.

I am thankful to my supervisors Bojan Mohar and Matt DeVos for going on many mathematical journeys with me, it has been very inspiring learning from you. Further, I sincerely appreciate the calming conversations you had with me when I was feeling overwhelmed. Thank you especially for all our meetings during the pandemic, those that were online and outside in the park. It helped me pass this difficult time. Thank you also for the freedom you gave me, such as letting me have collaborations with researchers outside of SFU. It made my PhD experience diverse and adventurous.

I would like to thank the reviewers of this thesis, Pavol Hell and Pavel Valtr, for helpful remarks on the thesis and interesting questions during the thesis defence.

I am indebted to Marthe Bonamy. I am very lucky to have met such a brilliant person which has been my collaborator, mentor, good friend and inspiration. Thank you for the endless advice you shared with me, especially in difficult times. Thank you for opening doors for me in academia and making Bordeaux my second home. Thank you for being you.

I am thankful to Danielle Rogers for all the fun research discussions we had in CECM, which made me love maths and forget all the stress in the world. Thank you for always making sure everyone is included and respected, it is worth gold. Thank you for making academia a better place and inspiring me to be a better person.

Thank you for all the laughs in the office. Thank you especially to Abhinav Shantanam, Aniket Mane, Jesse Champion Loth, Kevin Halasz and Sebastian Gonzalez Herмосillo de la Maza for all the conversations we had. I hope these are not the last acknowledgements I add you to. ;) Thank you for reassuring me that everything will be fine in the end.

Thank you to my friends in graduate school, Javier, Juan, Mackenzie, Parisa, Sam, Sebastian, Stefan, and Yassi. Thank you for all the lovely memories, which I will carry along

the way. Thank you also to my friends at Labri in Bordeaux, Claire, Clément, Jonathan, Paul and Timothé(e) for making my days warmer and brighter.

I am thankful to all my collaborators. I am in particular thankful for the research visits in Victoria with Natasha Morrison and in Lyon with Édouard Bonnet, Stéphan Thomassé, Nicolas Bousquet and Théo Pierron. It was such an important experience to see other places and ways in which mathematics was done. Thank you also to my collaborators Alberto Espuny Díaz, Carla Groenland, Carole Muller, Claire Hilaire, Colin Geniet, Dan Cranston, Dieter Mitsche, Éva Czabarka, Hugues Déprés, Jaques Verstraëte, Jakob Pekarek, JD Nir, Jiaxi Nie, Jonathan Narboni, Josef Tkadlec, Julien Duron, László Székely, Linda Cook, Louis Esperet, Lyuben Lichev, Paweł Rzażewski, Raimund Seidel, Ruy Fabila-Monroy, Sergey Norin, Sergio Cabello, Vesna Iršič and Yuga Higashikawa for all the inspiring mathematical discussions, I learned so much from you.

I am thankful to Marni Mishna, Mary Catherine Kropinski, Nathan Ilten and Veselin Jungic for discussions on inclusive learning environments and personal support. Your work is inspiring, thank you for supporting students in exceptional ways.

I am grateful for my funding from the Vanier Canada Scholarship Program and everyone who supported my application. Doing the PhD without the funding would have been a great challenge. The scholarship gave me the freedom to do community work and start research collaborations around the world.

I would like to thank the many people behind the scenes, especially Casey Bell, Christie Carlson, Dale Yamaura, Rachel Tong and Stacey Openshaw. The university would not work without you. I would also like to thank the contracted food and cleaning services at SFU, thank you for providing a nice working environment.

I would like to thank my friends from the Solidarity and Social Justice Committee at TSSU. It has been so inspiring to learn from you, your teachings will guide me throughout my life. Thank you especially to Catherine, Chantelle, Hanieh, Hannah, Kayla, Maria Cristina, Marissa, Mona, Muriel, Rahil, Seamus, Sherry, Terra-Lea, Tiara and Wei Chun for holding so much space for the important conversations in life. Meeting you made it worth living across the world from home. Thank you to the Indigenous scholars from which we could learn along the way such as Audrey and Harsha.

Finally I would like to thank my partner, Tabriz Popatia, who has been a constant source of energy. Thank you for always believing in me, and reminding me of my accomplishments, no matter how small they were. Thank you for all your kindness and patience.

Table of Contents

Declaration of Committee	ii
Abstract	iii
Dedication	iv
Acknowledgements	v
Table of Contents	vii
List of Figures	ix
1 Introduction	1
1.1 Basic Definitions for Surfaces	5
1.2 Thesis Structure and Acknowledgement of Collaborations	8
2 Cops and Robber Game on Geodesic Spaces	10
2.1 Cops and Robber Game on Graphs	10
2.2 Cops and Robber Game on Geodesic Spaces	12
2.2.1 Guarding	13
2.2.2 Lion and Man	14
2.3 Cops and Robber Game on Surfaces	16
2.3.1 Cops and Robber with Strategies from the Lion and Man Game	17
2.3.2 Generalised Radial Strategy	20
2.3.3 Higher-dimensional Spheres	25
2.3.4 Covering Space Method and its Application to the Flat Torus	26
2.3.5 Hyperbolic Surfaces	30
2.3.6 n-Dimensional Hyperbolic Space	44
2.3.7 Manifolds of Constant Curvature	44
3 Random Graphs from Surfaces	46
3.1 Models for Random Graphs	47
3.1.1 Binomial Random Graph $G(n, p)$	47

3.1.2	Random Graphs from Graphons	48
3.2	Representations of Graphons	51
3.3	Random Intersection Graphs of Geodesic Segments	53
3.3.1	The Euclidean Square $[0, 1]^2$ and Sylvester's Four Point Problem . .	58
3.3.2	Coloured Crossing Number in $[0, 1]^2$	60
3.3.3	Torus with Euclidean Metric	67
3.3.4	Sphere	68
3.3.5	Hyperbolic Surfaces	79
3.4	Random Intersection Graphs of Disks	82
3.4.1	Random Geometric Graph $G^d(n, r)$	82
3.4.2	Thresholds for Spanning Substructures	84
4	Decomposing Drawings into Plane Subdrawings	90
4.1	Large Substructures	90
4.2	Small Substructures	92
4.2.1	Packability	92
4.2.2	Convex-Nonpackable CGGs	94
4.2.3	Strong Packability	99
4.2.4	Paths and Caterpillars	102
5	Spectral Graph Theory for Graph Drawings	106
5.1	Tutte's Spring Embedding	106
5.2	Eigenvector Embeddings of Graphs	108
5.3	Drawings of Distance Regular Graphs	109
5.4	Semidefinite Graph Drawing Algorithm	111
5.4.1	Strong Duality	114
5.5	The Energy of Regular Graphs	114
5.6	Spectral Graph Drawings for Graphs of Higher Genus	118
6	Conclusion	120
6.1	Open Questions	120
6.2	Work not in this Thesis	121
	Author's Publications	123
	Bibliography	125
A	Code for finding crossing probability of $S(2)$	134

List of Figures

Figure 1.1	Triangulation as viewed from one side of the double torus.	1
Figure 1.2	A sphere, a torus and a projective plane. The projective plane can be obtained from a half-sphere by identifying antipodal points on the boundary.	2
Figure 1.3	The torus, which can be obtained from an Euclidean square $[0, 1]^2$ by identifying opposite sides of the square. A Klein-bottle which can be obtained from an Euclidean Square $[0, 1]^2$ by identifying two pairs of consecutive edges along the boundary of the square.	3
Figure 1.4	Tessellation of the plane by a square and by a parallelogram spanned by $(0, 1)$ and $(1/2, \sqrt{3}/2)$. The thick polygon is the corresponding fundamental polygon of the torus.	5
Figure 1.5	The surface $S(g)$ with its fundamental domain $P\left(4g, \frac{2\pi}{4g}\right)$ as a standard geometric model for the double torus.	7
Figure 2.1	Two cops c_1, c_2 capture the robber r	11
Figure 2.2	The cop's position c is at the same distance to A as the robber's position r . By staying on the same distance to A as the robber, the cop can guard the depicted half of the great circle through A and B	13
Figure 2.3	The lion's position on the cylinder at time step $\sqrt{a^2 + b^2}$ (for some small a, b) when the starting position of the lion is $(0, 1, 0)$ and the starting position of the man is $(0, 0, 0)$	15
Figure 2.4	Depicted is the point p which is the closest point on Or^k from the robber's position r^{k+1}	16
Figure 2.5	The case where the angle at r^k in the triangle $Or^k r^{k+1}$ is smaller than π	17
Figure 2.6	One move in the cop's strategy.	18
Figure 2.7	The robber and the cop approaching the circles with radius ℓ_R and ℓ_C , respectively.	18
Figure 2.8	A schematic setup when X is starshaped. A is the boundary of X , C_d and $C_{d'}$ are the cycles of distance d and d' from x_0 . The distance between $\phi_d(y_1)$ and $\phi_d(y_2)$ is smaller than the distance between y_1 and y_2	21

Figure 2.9	The first move of the robber and the cop in the ε -approaching game. The point $(\frac{3}{4}, \frac{1}{2})$ is at most τ_0 away from r^1	27
Figure 2.10	A hyperbolic right angled triangle with vertices A, B, C , the right angle is at C . The points X_1, X_2, X_3 are on the geodesic \overline{AC}	31
Figure 2.11	Copies of the fundamental polygon $P(4g, \frac{2\pi}{4g})$ in \mathcal{D} . Depicted is a point and one copy of this point in each of the depicted copies of the fundamental polygon.	34
Figure 2.12	A schematic picture of cop's position c_1 and robber's position r at time step k	35
Figure 2.13	The point $\phi(r^{k+1})$ is the reflection point of r^{k+1} over g_k	36
Figure 2.14	The case when the second last move of the robber is of type (b)	38
Figure 2.15	A step K_1^+ in comparison to a step K_1^- . In both cases the distance of r^k to p^k is the same and hence the move of cop c_1 is the same.	42
Figure 3.1	A graphon $W : [0, 1]^2 \rightarrow [0, 1]$, the values at which W is 1 are depicted in black, the value of W is 0 else. The graphon arises from the intersection graphs of random intervals of length $2r$ in $[0, 1]$ for $r = 0.2$	48
Figure 3.2	A set of edges whose intersection graph is bipartite.	49
Figure 3.3	On the left the adjacency matrix of the intersection graph of the edges e_1, \dots, e_{10} . Row and column i corresponds to the edge e_i . On the right the corresponding graphon.	49
Figure 3.4	The thickness of edges determines with what density edge e_i is picked.	49
Figure 3.5	Possible values for triangle densities $t(K_3)$ given edge densities $t(K_2)$	51
Figure 3.6	A uniformly random drawing of a complete graph on the sphere.	54
Figure 3.7	The case $A_{w,h}^{(1)}$ with a point at the bottom-left corner.	63
Figure 3.8	The case $A_{w,h}^{(2)}$ with points at the bottom-left and top-right corner. The left depicts the case $C_{w,h}^{(2)}$ and the right figure the case $D_{w,h}^{(2)}$	65
Figure 3.9	The left part shows a drawing D_4 of a $K_{4,4}$ on parts $\{v_1, \bar{v}_1, v_2, \bar{v}_2\}$ and $\{w_1, \bar{w}_1, w_2, \bar{w}_2\}$. The angles α and β are in the triangle formed by w_2, v_2 and a crossing, whereas γ and δ are in a triangle formed by v_1, w_1 and the same crossing. The right-hand side shows part of a $D_4^{(3)}$ drawing with the circles of w_2 and v_2 each containing 3 vertices and with nine edges for each incident bundle emanating from these two nodes.	70
Figure 3.10	Possible crossings in the blow up: Bundle-bundle crossings (C), bundle crossings (B) and node crossings (N).	71

Figure 3.11	L_x are the vertices on the arc between the extremal two edges leading from x to B . The dashed arc in this figure contains vertices in W_y	72
Figure 3.12	(A), (B), (C) and (D) are special areas of vertices of a node. An illustration where $0 < \alpha \leq \frac{\pi}{2}$	73
Figure 3.13	An illustration of the antipodal argument for the total number of node crossings at one of the nodes. The edges incident with any x and y ($x \neq y$) yield precisely n^2 node crossings.	74
Figure 3.14	Triangles of type (CCC) and (CCN).	74
Figure 3.15	Two edges from node A leading to antipodal nodes B and \bar{B} can cross. If $d = \min\{d_1, d_2\}$ and $r \leq d$, then $ L_x = O(rn)$	75
Figure 3.16	If w_2, v_2 approach w_1, v_1 , respectively, then all angles $\alpha, \beta, \gamma, \delta$ converge to zero.	79
Figure 3.17	Sylvester's four point probability for an equilateral triangle with growing hyperbolic radius r_H , which was translated into Euclidean radius $r_E = \tanh(\frac{r_H}{2})$	81
Figure 3.18	A random point set in $S(2)$	82
Figure 3.19	On the left, copies of a point w_2 . On the right, a polygon which contains a point w_1 and the closest copy of w_2 to w_1 . The geodesic segment between them on the Poincaré disk is as long as their distance on the surface.	83
Figure 3.20	A picture of a bounding box $R_{z_1 z_2}$ of a point set $W_{z_1 z_2}$. The number of points in $W_{z_1 z_2} \cap \sigma_3(i)$ and $W_{z_1 z_2} \cap \sigma_3(j)$ differs by the number of points in $\sigma_3(i)$ which are on the boundary of R_{z_1, z_2}	88
Figure 4.1	A partition of K_7 into plane C_3 's and a K_6 with a C_4 packing. The grey edges are edges which are not covered by a C_4	90
Figure 4.2	A drawing of the complete graph K_{26} which can not be decomposed into $\lfloor \frac{26}{2} \rfloor$ spanning trees. The vertices are in general position and all vertices except the central vertex are on the convex hull.	91
Figure 4.3	Four plane triangulated cycles. The first, Θ_1 , is geometric-packable. For each of the remaining three, the question of geometric-packability remains open.	93
Figure 4.4	Packing C_4 's into a sequence of convex drawings.	93
Figure 4.5	The inductive step in packing Θ_1	94
Figure 4.6	When G is a 4-cycle with a crossing, $p(6, G) = 3$	95
Figure 4.7	The set of thick blue edges is convex, but the set of thin red edges is not.	96
Figure 4.8	Θ_5 is not convex-packable.	97

Figure 4.9	$G_1 \notin \mathcal{P}(C_4)$ and $G_2 \in \mathcal{P}^*(C_4)$ and $G_3 \in \mathcal{P}(C_4) \setminus \mathcal{P}^*(C_4)$	98
Figure 4.10	Two convex C_4 's in D_{12}	98
Figure 4.11	A typical \mathcal{C}_4 in an asymptotic C_4 -packing of the convex complete graphs.	99
Figure 4.12	An edge labelling of Θ_2 used to show it is strongly packable.	101
Figure 4.13	Edge labellings showing that Θ_3 , Θ_4 , and Θ_1 are all strongly packable.	102
Figure 4.14	A plane path is transformed into a convex plane caterpillar.	102
Figure 4.15	An edge-labelling of a caterpillar where all leaves are adjacent to either v_1 or v_{s+1}	103
Figure 4.16	An edge-labelling of a caterpillar where v_i is adjacent to i leaves for all $1 \leq i \leq s + 1$	104
Figure 5.1	An example of Tutte's spring embedding on the right. The vertices of the outer face of the general drawing (left) are mapped to vertices of a triangle (right), which are on the outer face of the spring embedding.	107
Figure 5.2	Platonic solids.	110
Figure 5.3	Semidefinite drawings of Platonic solids.	114
Figure 5.4	A semidefinite drawing of the Petersen graph.	119

Chapter 1

Introduction

Surfaces and graphs are often studied alongside each other. Graphs can be used to discretise a surface or represent a region separation of it. Graphs obtained this way have nice structures and in fact appear in many real-world applications. Therefore, graphs that can be drawn on a surface without edge crossings have been studied extensively. A *drawing*

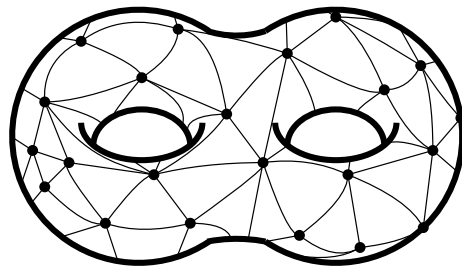


Figure 1.1: Triangulation as viewed from one side of the double torus.

of a graph G on a surface S consists of a mapping f of the vertex set $f : V(G) \rightarrow S$ and a set of simple curves $f_{uv} : [0, 1] \rightarrow S$ for $uv \in E(G)$ with endpoints $f(u)$ and $f(v)$, representing the edges of G . Additional assumptions are that f is injective, $f_{uv}((0, 1))$ is disjoint from $f(V)$, and no two curves can have infinitely many intersection points. These assumptions make the drawing non-degenerate. A common point $x \in f_e([0, 1]) \cap f_{e'}([0, 1])$ for $e, e' \in E(G)$ which is not an endpoint is called a *crossing*.

Two famous topological applications of graphs are the four colour theorem, where graphs are used to encode adjacencies of regions in plane maps, and the classification theorem for compact surfaces where triangular graphs are used to approximate a surface and determine its topological properties. A *topological surface* is a connected topological space which is locally homeomorphic to an (Euclidean) disk. The classification theorem says that every compact topological surface is homeomorphic to some member of one of these three families:

- the sphere,

- the connected sum of g tori for $g \geq 1$,
- the connected sum of g real projective planes for $g \geq 1$.

Figure 1.2 depicts the sphere, the torus and the projective plane. We denote by g the

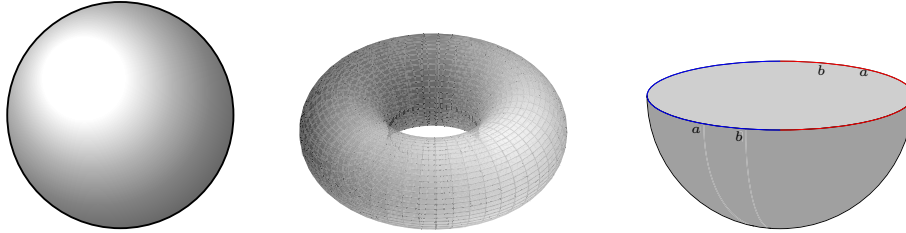


Figure 1.2: A sphere, a torus and a projective plane. The projective plane can be obtained from a half-sphere by identifying antipodal points on the boundary.

genus of the surface, the genus of the sphere is 0. A connected sum of surfaces can be obtained by cutting a small disk from each of the surfaces and gluing the surfaces along the boundary of the disks. Early versions of the classification theorem were stated in 1861 by Möbius [76] and in 1866 by Jordan [58] and the theorem was finally (rigorously) proved in 1921 by Brauer [23]. We refer the reader to the nice exposition on the classification theorem by Gallier and Xu [37]. An important tool in the proof is to show that surfaces can be triangulated, which means a surface has a 2-cell embedding of a graph where each face is a triangle, see Figure 1.1. An *embedding* of a graph is a drawing of a graph on a surface such that none of its edges cross; if each face is homeomorphic to an Euclidean disk then the embedding is a *2-cell embedding*.

An elegant proof of the fact that surfaces can be triangulated was given by Thomassen in [109]. Given a triangulation of a surface, the faces are homeomorphic to convex triangles, and hence it can be shown that the surface is homeomorphic to a 2-cell complex. Then it is shown that a compact surface is homeomorphic to one of the following standard surfaces:

- $S(4g, aba^{-1}b^{-1})$ has a face which is a polygon with $4g$ vertices and the boundary edges a_1, \dots, a_{4g} are identified such that $a_{4i-3} = a_{4i-1}^{-1}$ and $a_{4i-2} = a_{4i}^{-1}$ for $i = 1, \dots, g$.
- $S(2g, aa)$ has a face which is a polygon with $2g$ vertices and the boundary edges a_1, \dots, a_{2g} are identified such that $a_{2i+1} = a_{2(i+1)}$ for $i = 0, \dots, g - 1$.

Figure 1.3 depicts the torus $S(4, aba^{-1}b^{-1})$ and the Klein bottle $S(4, aa)$. The classification theorem can be alternatively stated using the Euler characteristic and orientability. Given a graph G defined by a 2-cell embedding on a surface S , the *Euler characteristic* of S is

$$\chi(S) = v(G) - e(G) + f(G), \quad (1.1)$$

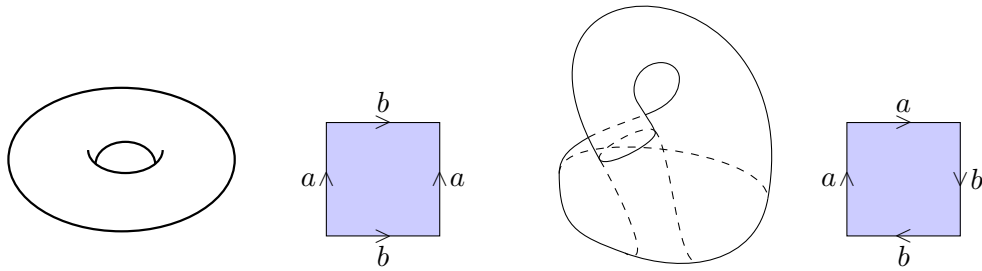


Figure 1.3: The torus, which can be obtained from an Euclidean square $[0, 1]^2$ by identifying opposite sides of the square. A Klein-bottle which can be obtained from an Euclidean Square $[0, 1]^2$ by identifying two pairs of consecutive edges along the boundary of the square.

where $v(G)$ is the number of vertices of G , $e(G)$ is the number of edges of G and $f(G)$ is the number of faces of the embedding. The number $\chi(S)$ is a topological invariant of the surface S .

Theorem 1.1 ([23]). Every compact topological surface can be topologically characterised by its Euler characteristic and orientability.

In graph theory the Euler characteristic is used to study classes of graphs which are embeddable in an oriented surface of genus g . An important graph class is the class of *planar graphs*, these are graphs which have an embedding on the sphere (or alternatively, Euclidean plane). The Euler characteristic of a planar graph is 2, and this fact is often referred to as Euler's formula. It finds many applications in graph theory, for example in the use of the discharging method.

In the following we call a *surface* a real, smooth topological surface equipped with a Riemannian metric. We will sometimes also consider higher dimensional manifolds. An *n-dimensional topological manifold* is a topological space in which each point has a neighbourhood that is homeomorphic to an open unit ball in \mathbb{R}^n . We call a *manifold* a real, smooth topological manifold equipped with a Riemannian metric.

For a topological space X , the *covering space* of X is a topological space C together with a continuous surjective map $p: C \rightarrow X$ such that for every $x \in X$, there exists an open neighbourhood U of x , such that $p^{-1}(U)$ is a union of disjoint open sets in C , each of which is mapped homeomorphically onto U by p (i.e. it is a local homeomorphism). If X and C are both metric spaces and p is not only a local homeomorphism but also a local isometry, then we say that the covering space C of X *locally preserves distances*. For example, consider the torus obtained from an Euclidean square $[0, 1]^2$ as in Figure 1.3. Its covering space is the Euclidean plane \mathbb{R}^2 , where $p(x, y)$ is the point in $[0, 1]^2$ obtained by an appropriate integer shift of x, y . More precisely, $p(x, y) = (x - \lfloor x \rfloor, y - \lfloor y \rfloor)$, where $\lfloor \cdot \rfloor$ is the rounding down function.

Every complete, connected manifold of constant negative curvature -1 (resp. $1, 0$) has the hyperbolic n -space \mathbb{H}^n (resp. the sphere \mathbb{S}^n , Euclidean space \mathbb{R}^n) as a distance preserving covering space, hence we will call it a hyperbolic manifold, (resp. spherical, Euclidean). When we say curvature, we mean sectional curvature, which we define in Section 1.1. Further, a hyperbolic (spherical or Euclidean) compact manifold is the quotient of \mathbb{H}^n (resp. $\mathbb{S}^n, \mathbb{R}^n$) under the action of a (discrete) group of isometries (see [9]).

Theorem 1.2 (Killing-Hopf [52, 63]). Any compact Riemannian manifold of constant curvature -1 (resp. $1, 0$) is isometric to \mathbb{H}^n/Γ (resp. $\mathbb{S}^n/\Gamma, \mathbb{R}^n/\Gamma$) where Γ is a group of isometries on \mathbb{H}^n (resp. $\mathbb{S}^n, \mathbb{R}^n$) acting freely and properly discontinuously.

A group Γ acts freely on a topological space X if every $g \in \Gamma$ which is not the identity element has no fixed points, that means $g(x) \neq x$ for all $x \in X$. A group Γ acts properly discontinuously on a topological space X if for every compact set $K \subset X$ there are only finitely many group elements $g \in \Gamma$ such that $g(K) \cap K \neq \emptyset$.

As an example of how to apply the Killing-Hopf Theorem, we consider locally Euclidean surfaces. By Theorem 1.2, any such surface is isometric to \mathbb{R}^2/Γ , where Γ is a group of isometries acting freely. Since rotations and reflections have fixed points, they do not act freely, hence Γ consists of translations and proper glide reflections. Since the group Γ acts properly discontinuously, the group can be generated by two isometries (see [105]). If Γ is generated by two translations, they can be characterised by two translation vectors t_1, t_2 centred at $(0, 0)$ and \mathbb{R}^2/Γ is isometric to a torus by identifying opposite sides of the parallelogram defined by t_1, t_2 . Otherwise the two isometries are a translation and a glide reflection, which have perpendicular directions, and \mathbb{R}^2/Γ is isometric to a Klein bottle by joining opposite sides of the defined parallelogram, with one pair of sides being joined with a twist. The covering space of \mathbb{R}^2/Γ can be characterised by a lattice. Figure 1.4 shows two lattices of the torus whose parallelograms are spanned by $(0, 1), (1, 0)$ and $(0, 1), (1/2, \sqrt{3}/2)$, respectively.

For a point $P \in \mathbb{R}^2$, its orbit in \mathbb{R}^2/Γ is $\{g(P) \mid g \in \Gamma\}$. The orbit space can be visualised by considering a *fundamental region*, a connected subset of the plane which contains a representative of each Γ -orbit with at most one representative of each Γ -orbit in its interior. When the boundary of the region is a polygon, we call the fundamental region a *fundamental polygon*. The parallelograms of the lattice defined by translation vectors t_1, t_2 are fundamental polygons, but fundamental polygons can be obtained in different ways. For example, when considering the lattice spanned by the translation vectors t_1, t_2 of a fundamental polygon of a torus, the Voronoi cell of a lattice point in the Voronoi diagram on all lattice points (intersection points of lines) is a fundamental polygon, see Figure 1.4. The *Voronoi cell* of a point P in a point set $Q \subset \mathbb{R}^2$ consists of every point \mathbb{R}^2 in the Euclidean plane whose distance to P is less than or equal to the distance to any other point in Q .

A torus can be obtained from the fundamental polygon obtained by such a Voronoi cell in Figure 1.4 (b) by gluing opposite sides of the polygon.

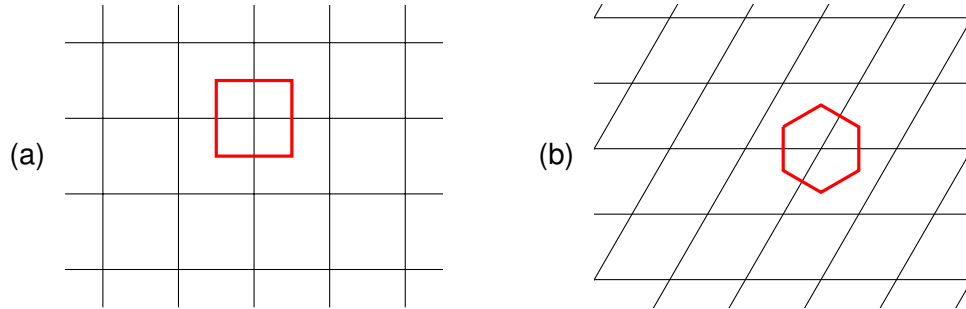


Figure 1.4: Tesselation of the plane by a square and by a parallelogram spanned by $(0, 1)$ and $(1/2, \sqrt{3}/2)$. The thick polygon is the corresponding fundamental polygon of the torus.

1.1 Basic Definitions for Surfaces

For standard terminology for graphs we refer the reader to Diestel's book [27], in the following we introduce the needed terminologies for surfaces. We start by defining a geodesic space. Let (X, d) be a metric space. For $x, y \in X$, an (x, y) -path is a continuous map $\gamma : I \rightarrow X$ where $I = [0, 1]$ is the unit interval on \mathbb{R} , $\gamma(0) = x$ and $\gamma(1) = y$. One can define the *length* $\ell(\gamma)$ of the path γ by taking the supremum over all finite sequences $0 = t_0 < t_1 < t_2 < \dots < t_n = 1$ of the values $\sum_{i=1}^n d(\gamma(t_{i-1}), \gamma(t_i))$. Clearly, the length of every (x, y) -path is at least $d(x, y)$. The metric space X is a *geodesic space* if for every $x, y \in X$ there is an (x, y) -path whose length is equal to $d(x, y)$. An (x, y) -path γ is *isometric* if $\ell(\gamma) = d(x, y)$. Observe that for $0 \leq t < t' \leq 1$ the subpath $\gamma|_{[t, t']}$ is also isometric. Therefore the set $\gamma(I) = \{\gamma(t) \mid t \in I\}$ is an isometric subset of X . With a slight abuse of terminology, we say that the image $\gamma(I) \subset X$ is an *isometric path* or *geodesic segment* in X . If there exists a unique isometric path between x, y then we will denote it by $\overline{xy} \subset X$. A continuous map $\gamma : \mathbb{R} \rightarrow X$ is a *geodesic* if it is locally isometric, i.e., for every $t \in \mathbb{R}$ there is an $\varepsilon > 0$ such that the subpath $\gamma|_J$ on the interval $J = [t - \varepsilon, t + \varepsilon]$ is isometric.

The geodesic spaces that we are most interested in are compact surfaces. The *diameter* of a compact surface S is the maximum distance between points in S

$$\text{diam}(S) = \max\{d(x, y) \mid x, y \in S\}.$$

The *systolic girth*, denoted as $\text{sys}(S)$, is the length of a shortest noncontractible curve on the surface. We focus on surfaces with nice geometries, those that are Euclidean, spherical or hyperbolic. That means, they have constant (sectional) curvature. We give a formal definition of sectional curvature which is used in Theorem 1.2, but we will mainly apply Theorem 1.2 directly. The sectional curvature $K(\sigma_p)$ depends on a two-dimensional linear

subspace σ_p of the tangent space at a point p of the manifold M . Suppose σ_p is spanned by u, v , then

$$K(\sigma_p) = \frac{\langle R(u, v)v, u \rangle}{\langle u, u \rangle \langle v, v \rangle - \langle u, v \rangle^2},$$

where R is the Riemann curvature tensor defined by $R(u, v)w = \Delta_u \Delta_v w - \Delta_v \Delta_u w - \Delta_{[u, v]}w$. If the dimension of the manifold M is 2 then the sectional curvature is the Gaussian curvature. We refer to [1] for more information on the Gaussian curvature.

We will denote the n -dimensional ball, sphere and flat torus for $n \geq 1$ by

- $B^n = \{(x_1, \dots, x_{n-1}, z) = (\underline{x}, z) \in \mathbb{R}^n \mid x_1^2 + \dots + x_{n-1}^2 + z^2 \leq 1\}$,
- $\mathbb{S}^n = \{(x_1, \dots, x_n, z) = (\underline{x}, z) \in \mathbb{R}^{n+1} \mid x_1^2 + \dots + x_n^2 + z^2 = 1\}$,
- $T^n = \mathbb{S}^1 \times \dots \times \mathbb{S}^1$.

Geodesic segments (or *geodesic arcs*) in \mathbb{S}^2 are arcs of great circles whose length is at most π . The *great circle* on \mathbb{S}^n is the intersection of \mathbb{S}^n with a 2-plane that passes through the origin in the Euclidean space \mathbb{R}^{n+1} . For a point $P \in \mathbb{S}^2$, its *antipodal point* \bar{P} is the point diametrically opposite to P . For a subset $A \subset \mathbb{S}^2$, its *antipodal set* \bar{A} contains the antipodal point of each point in A .

We denote by \mathcal{D}^n the n -dimensional *Poincaré disk*, which means the disk $\{(x_1, \dots, x_n) \mid x_1^2 + \dots + x_n^2 < 1\}$ equipped with the hyperbolic metric $4 \frac{dx_1^2 + \dots + dx_n^2}{(1 - x_1^2 - \dots - x_n^2)^2}$. For brevity, we write $\mathcal{D} = \mathcal{D}^2$. We define by $P(k, \theta)$ the regular k -gon in the Poincaré disk \mathcal{D} centred at $O = (0, 0)$ with angle θ at the vertices. We denote its vertices by v_1, \dots, v_k in counter-clockwise direction and let a_i be the (oriented) edge from v_i to v_{i+1} and a_i^{-1} be the reversed edge from v_{i+1} to v_i (we consider the indices modulo k). We are going to consider three standard hyperbolic surfaces for $g \geq 2$, where one of them is non-orientable.

- Let $S(g)$ be the orientable surface obtained from $P\left(4g, \frac{2\pi}{4g}\right)$ by identifying the (oriented) edges a_{4i-3} with a_{4i-1}^{-1} and a_{4i-2} with a_{4i}^{-1} for $i = 1, \dots, g$. The surface $S(2)$ is depicted in Figure 1.5.
- Let $S'(g)$ be the orientable surface obtained from $P\left(4g + 2, \frac{2\pi}{2g+1}\right)$ by identifying opposite (oriented) edges a_i, a_{i+2g+1}^{-1} for $i = 1, \dots, 2g$.
- Let $N(g)$ be the non-orientable surface obtained from $P\left(2g, \frac{2\pi}{2g}\right)$ by identifying the (oriented) edge a_{2i+1} with $a_{2(i+1)}$ for $i = 0, \dots, g - 1$ for $g \geq 1$.

We recall some geometric properties of the hyperbolic plane. Given a point P and a geodesic h there is a unique geodesic that is orthogonal to h and goes through P , we will denote this geodesic as $o_h(P)$. The closest point on h from P is the intersection point of h and the orthogonal $o_h(P)$.

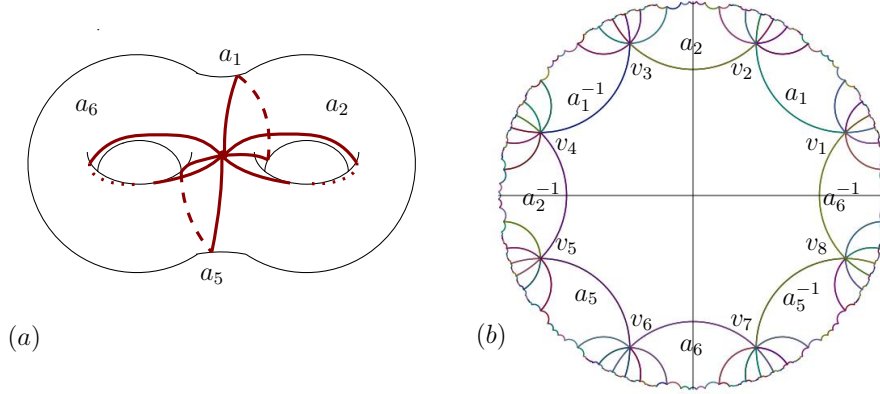


Figure 1.5: The surface $S(g)$ with its fundamental domain $P\left(4g, \frac{2\pi}{4g}\right)$ as a standard geometric model for the double torus.

We will use that the hyperbolic plane is a metric space and the *triangle inequality* holds, that is for three points $A, B, C \in \mathcal{D}$, $d(A, B) + d(B, C) \geq d(A, C)$. Equality holds if and only if B is on the geodesic segment \overline{AC} . In order to work with the geometry on the Poincaré disk, we will use laws of hyperbolic geometry (for a reference, see [6, 106]). Among the many identities of hyperbolic functions, we will use that in a triangle A, B, C with right angle at C and angle α, β at A, B , respectively, it holds that

$$\cosh(d(A, B)) = \cot(\alpha) \cot(\beta), \tag{1.2}$$

$$\tanh(d(A, C)) = \cos(\alpha) \tanh(d(A, B)), \tag{1.3}$$

$$\cosh(d(A, C)) = \frac{\cos(\beta)}{\sin(\alpha)}. \tag{1.4}$$

Theorem 1.3 (Pythagoras' Theorem for Hyperbolic Triangles). Any triangle ABC in the hyperbolic plane with a right angle at vertex C satisfies

$$\cosh(d(A, B)) = \cosh(d(A, C)) \cosh(d(B, C)).$$

We are also going to use the following hyperbolic laws.

Theorem 1.4 (Hyperbolic Law of Cosine). Any triangle ABC in the hyperbolic plane with angle γ at C satisfies

$$\cosh(d(A, B)) = \cosh(d(A, C)) \cosh(d(B, C)) - \sinh(d(A, C)) \sinh(d(B, C)) \cos(\gamma).$$

Theorem 1.5 (Hyperbolic Law of Sine). Any triangle ABC in the hyperbolic plane with angle α at A and β at B satisfies

$$\frac{\sin(\alpha)}{\sinh(d(B, C))} = \frac{\sin(\beta)}{\sinh(d(A, C))}$$

Theorem 1.6 (Hyperbolic 4-Parts Law). Any triangle ABC in the hyperbolic plane with angle β at B and angle γ at C satisfies

$$\cos \gamma \cosh d(B, C) = \sinh d(B, C) \coth d(A, C) - \sin \gamma \cot \beta.$$

A *Lambert Quadrilateral* is a quadrilateral in the hyperbolic disk with three right angles, and note that then the fourth angle is smaller than π . Any two sides of a Lambert quadrilateral determines the length of the other sides, see [106].

We now state some basic properties of the fundamental polygon $P\left(4g, \frac{2\pi}{4g}\right)$ of $S(g)$. Let v_1, \dots, v_{4g} be its vertices and let w_i for $i = 1, \dots, 4g$ be the midpoint on the geodesic between v_i and v_{i+1} (vertices modulo $4g$). The polygon consists of $8g$ triangles of the form Ov_iw_i or Ow_iv_{i+1} , where $O = (0, 0)$. Each of them is an isosceles triangle with one right angle and two angles of size $\alpha = \beta = \frac{2\pi}{8g}$. By Equation (1.4), the hyperbolic length of a *leg* of the isosceles triangle, which is one of the two sides of equal length, is

$$d(O, w_i) = d(w_i, v_i) = \operatorname{acosh}\left(\frac{\cos(\beta)}{\sin(\alpha)}\right) = \operatorname{acosh}\left(\cot\left(\frac{\pi}{4g}\right)\right).$$

We will now consider the Poincaré disk \mathcal{D} and compare hyperbolic distances to Euclidean distance (by considering \mathcal{D} as a subspace of the Euclidean plane). If r is the hyperbolic distance of a point $P \in \mathcal{D}$ from the origin $O = (0, 0)$, then the Euclidean distance from O to P is

$$r_E = \tanh\left(\frac{r}{2}\right).$$

Considering the polygon $P\left(4g, \frac{2\pi}{4g}\right)$ in \mathcal{D} , this means that the Euclidean distance from O to w_i is $\tanh\left(\frac{1}{2} \operatorname{acosh}\left(\cot\left(\frac{\pi}{4g}\right)\right)\right)$. The triangle Ov_iw_i has a right angle at w_i and the hyperbolic length of the hypotenuse $\overline{Ov_i}$ is $\operatorname{acosh}(\cot(\alpha) \cot(\beta)) = \operatorname{acosh}\left(\cot\left(\frac{\pi}{4g}\right)^2\right)$ hence the Euclidean distance from O to v_i is $\tanh\left(\frac{1}{2} \operatorname{acosh}\left(\cot\left(\frac{\pi}{4g}\right)^2\right)\right)$.

1.2 Thesis Structure and Acknowledgement of Collaborations

We briefly discuss the structure of this thesis and the collaborations on the chapters, which we discuss in more detail at the beginning of each chapter.

We start the thesis with discussing the Cops and Robber game on surfaces. The results are joint work with Vesna Iršič and Bojan Mohar. The results for spherical and Euclidean manifolds are published [W13], while the results for hyperbolic manifolds are in preparation for publication [W12].

Chapter 3 is on intersection graphs of random geodesic segments on surfaces and intersection graphs of random disks in the Euclidean plane. The former is related to geodesic

drawings of graphs on surfaces and crossing numbers. Section 3.3 includes joint work with Marthe Bonamy and Bojan Mohar [W4] on triangle densities in intersections graphs of random graph drawings which are almost crossing optimal. Section 3.3.2 is on a coloured Sylvester four point problem and was developed at the Crossing Number Workshop 2022. It is joint work with Sergio Cabello, Éva Czabarka, Ruy Fabila-Monroy, Yuga Higashikawa, Raimund Seidel, László Székely, and Josef Tkadlec [W7]. It is in preparation to be published. Section 3.4.2 is on random intersection graphs of disks, so called random geometric graphs, and is joint work with Alberto Espuny Díaz, Lyuben Lichev and Dieter Mitsche, currently in preparation for publication [W10].

In Chapter 4 and Chapter 5 we consider straight line drawings of graphs. Chapter 4 is on almost-decompositions of straight line drawings into plane subdrawings and is joint work with Daniel W. Cranston, Jiaxi Nie and Jacques Verstraëte [W8]. Chapter 5 is on a semidefinite program for graph drawings and is joint work with Matthew DeVos and Danielle Rogers. It is currently in preparation for publication [W9]. A similar chapter has also been submitted for the master's thesis of Danielle Rogers.

Chapter 2

Cops and Robber Game on Geodesic Spaces

The Cops and Robber game is a pursuit-evasion game. The game is played on graphs [5, 15, 22, 35, 59, 73], and as a new variant on geodesic spaces [79, 80]. The cops are trying to come as close to the robber as possible (for graphs, to occupy the same vertex) while the robber is trying to escape from the cops. We start this chapter by discussing the Cops and Robber game on graphs in Section 2.1 and geodesic spaces in Section 2.2. In the latter section we also discuss the related Lion and Man game, since some of the common strategies we use originate from this game. Mohar [80] showed an interesting interplay between graphs and surfaces, see Theorem 2.5. Section 2.3 presents our results on the Cops and Robber game on surfaces of constant curvature and related topological spaces [W12, W13]. One of our main result is that on compact n -dimensional manifolds of constant curvature 0, 1 or -1 , two cops are enough such that one cop can come arbitrarily close to the robber. The results in this chapter are joint work with Vesna Iršič and Bojan Mohar and we worked on them while Vesna Iršič held a postdoctoral position at Simon Fraser University from 2021-2022. We thank Tibor Marcinek for his hyperbolic canvas on Geogebra which we used to make some of the figures in Section 2.3.5.

2.1 Cops and Robber Game on Graphs

The standard Cops and Robber game on a graph G is played as follows. First, the cops c_1, \dots, c_k choose their starting positions $c_1^0, \dots, c_k^0 \in V(G)$. Then, the robber chooses a starting vertex $r^0 \in V(G)$. Each round of the game has two turns, the first one for the cops and the second for the robber.

At their turn, a player makes a step to an adjacent vertex or stays at their current position. After round k we denote the position of cop c_i as c_i^k , and of the robber r as r^k . The cops capture the robber if one of the cops eventually occupies the same position as

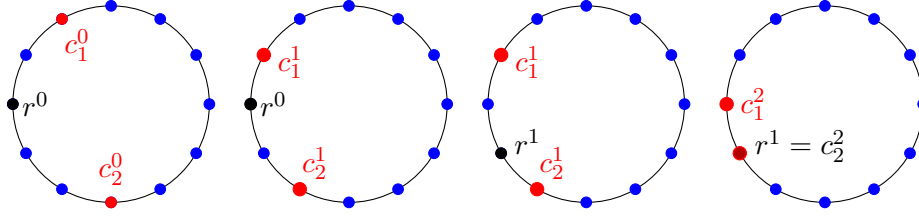


Figure 2.1: Two cops c_1, c_2 capture the robber r .

the robber, this means $c_i^k = r^k$ or $c_i^k = r^{k-1}$ for some $i, k \in \mathbb{Z}_+$ (the positive integers). See Figure 2.1 for an example where two cops capture the robber on a cycle.

The cops win the game if they capture the robber, the robber wins if the cops do not capture him, which means that the robber can escape the cops. The cop number of a graph $c(G)$ is the minimum number of cops that can capture the robber regardless of the robber's strategy and starting positions. The Cops and Robber game was first introduced for only one cop and one robber [87, 99]. Shortly after, Aigner and Fromme [5] generalised the game to playing with multiple cops, and they also showed the classical result on planar graphs.

Theorem 2.1 ([5]). The cop number of every planar graph is at most three.

The smallest known planar graph with cop number three is the dodecahedral graph [98], but it is still an open question whether there are smaller planar graphs with cop number three. In order to prove Theorem 2.1, Aigner and Fromme established an essential tool in the Cops and Robber game, which is guarding an isometric path.

Theorem 2.2 ([5]). If P is a shortest (i.e. isometric) path between two vertices, then one cop can guard P .

If a cop is guarding a path, that means as soon as the robber makes a step onto the path, he is caught. The *genus of a graph* is the smallest genus of a surface in which the graph can be drawn without edge crossings. Planar graphs have genus zero. The asymptotic behaviour of the cop number of graphs of higher genus is not known. Schröder [104] bounded the cop number of a graph G of genus g by $c(G) \leq \lfloor \frac{3}{2}g \rfloor + 3$. Bowler, Erde, Lehner and Pitz [21] improved this bound to $c(G) \leq \frac{4}{3}g + 3$ and Erde and Lehner [30] recently announced a bound of $c(G) \leq (1 + o(1))(3 - \sqrt{3})g$, where for $f_1, f_2 : \mathbb{N} \rightarrow \mathbb{R}$ we say $f_1(g) = o(f_2(g))$ if $f_1(g)/f_2(g) \rightarrow 0$ when $g \rightarrow \infty$. Further we say $f_1(g) = O(f_2(g))$ if $|f_1(g)|/f_2(g) \leq C$ for some $C > 0$ when $g \rightarrow \infty$. There are graphs with cop number $g^{\frac{1}{2}-o(1)}$ [77], which follows from a lower bound of the cop number on random graphs [15]. Mohar conjectured that the upper bound is close to the lower bound.

Conjecture 2.3 ([77, 80]). If G is a graph embeddable in a surface of genus g . Then

$$c(G) = O(\sqrt{g}).$$

Conjecture 2.3 is a tough conjecture, hence the current upper bounds are far from optimal.

2.2 Cops and Robber Game on Geodesic Spaces

The Cops and Robber game was recently extended to geodesic spaces X by Mohar [79]. The robber selects an initial position for all of the players $c_1^0, \dots, c_k^0, r^0 \in X$ and an agility function $\tau : \mathbb{N} \rightarrow \mathbb{R}_+$ such that $\sum_{n \geq 1} \tau(n) = \infty$. Each round of the game has two turns, the first one for the robber and the second one for the cops. In the n -th round, a player makes a step of length at most $\tau(n)$ (at their turn). As on graphs, we will denote the position of cop c_i after round n as c_i^n , and of the robber r as r^n . We say the cops win the game if

$$\inf_{n,i} d(c_i^n, r^n) = 0. \quad (2.1)$$

Otherwise we say that the robber wins the game, which means that he can stay at distance at least ε away from the cops, for some $\varepsilon > 0$. We say the cops catch the robber if the infimum in Equation 2.1 is a minimum, which means after some round k , a cop c_i occupies the same position as the robber. For a geodesic space we denote by $c(X)$ the minimum number of cops that can win the game regardless of the strategy of the robber, and by $c_0(X)$ the minimum number of cops that can catch the robber.

Given an $\varepsilon > 0$, $c_\varepsilon(X) = k$ is defined as the minimum number of cops c_1, c_2, \dots, c_k that guarantee that

$$\inf_{n,i} d(c_i^n, r^n) \leq \varepsilon.$$

With this notation, the following result holds.

Theorem 2.4 ([80]). If X is a compact geodesic space, then

$$c(X) = \sup\{c_\varepsilon(X) \mid \varepsilon > 0\}.$$

This theorem says that to show that n cops can win a game on some geodesic space X , it is enough to show that they can win the ε -approaching game, for every $\varepsilon > 0$. Mohar showed a nice connection between the cop number of graphs and surfaces.

Theorem 2.5 ([80]). Suppose that G is a graph of genus g with $c(G) \geq 3$. Then there is a surface S of genus g , such that

$$c(G) \leq c(S) \leq c_0(S) \leq c(G) + 1.$$

2.2.1 Guarding

Let X be the game space and let $A \subseteq X$. The *shadow* of the robber on A is a mapping $\sigma: X \rightarrow X$ such that $\sigma|_A = id|_A$, the identity function on A , and $d(x, y) \geq d(\sigma(x), \sigma(y))$, which means that σ is a 1-Lipschitz function. If a cop comes to the point $\sigma(r)$, where r is the robber's position, then we say that the cop *caught the shadow* $\sigma(r)$ of the robber. Once the cop is in the robber's shadow, she can stay in the shadow forever. While the cop is in the robber's shadow, we say she *guards* A . If the robber enters A , then the cop will catch the robber.

Mohar proved the isometric path property used on graphs for geodesic spaces. Given an isometric path I between two points A and B , he defined $\sigma(x)$ to be the point on I at distance $\min(d(x, A), d(B, A))$ to A . Clearly, $\sigma|_I = id|_I$ and by the triangle inequality $d(x, y) \geq |d(x, A) - d(y, A)| = d(\sigma(x), \sigma(y))$.

Lemma 2.6 ([80]). Let I be an isometric path in X starting at A and ending at B . Then one cop c can guard I after spending time equal to the length of I on the path to adjust himself. Moreover, if c guards the path at time step k then $c^k = \sigma(r^k)$.

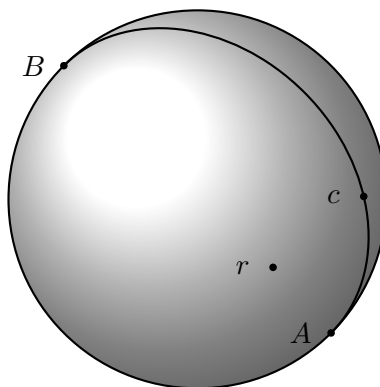


Figure 2.2: The cop's position c is at the same distance to A as the robber's position r . By staying on the same distance to A as the robber, the cop can guard the depicted half of the great circle through A and B .

Figure 2.2 depicts the isometric path strategy. The main difficulty for the cop is usually to get into the shadow of the robber. The following lemma gives a lower bound for the cop number of a geodesic space by the cop number of its shadow.

Lemma 2.7 ([W13]). Let A and X be geodesic spaces, and let $A \subseteq X$ be such that there exists a 1-Lipschitz mapping $\sigma: X \rightarrow A$ with the property $\sigma|_A = id|_A$. Then $c(X) \geq c(A)$ and $c_0(X) \geq c_0(A)$.

Proof. Let $c(X) = k$. We describe a strategy which ensures that k cops can win a game on A . Cops imagine that the game is played on X , they make their optimal moves in X ,

and then use σ to determine their moves in A . Since σ is well-defined and 1-Lipschitz, the mapped movements of the cops are legal, and if k cops can win the game on X , their images also win on A . The same argument works for catching the robber. \square

2.2.2 Lion and Man

The Cops and Robber game played on geodesic spaces is related to other pursuit-evasion games played on surfaces such as differential games or the Lion and Man game [24, 64, 68, 103]. The Lion and Man game was introduced by Rado (see Littlewood's Miscellany [68]). In order to explain the Lion and Man game, let an *infinite path* be a 1-Lipschitz map $f : [0, \infty] \rightarrow S$ (which means the speed of Lion and Man is at most 1) and let B_{x_0} be the set of infinite paths starting at x_0 . A player's strategy in the Lion and Man game is a map $\Phi : B_{x_0} \rightarrow B_{y_0}$ such that if two paths f_1, f_2 agree on $[0, t_0]$, then their images $\phi(f_1), \phi(f_2)$ agree on $[0, t_0]$ (which means man and lion can not look ahead).

Our results on Euclidean balls are inspired by the proofs for the Lion and Man game. Therefore we give a summary of studied strategies and the results on the strategies in the Lion and Man game.

A sketch of the strategy for the lion on a disk

The lion starts in the centre of the disk O . She stays for the remainder of the game on the line between the centre O and the man, moving as close to the man as possible.

The lion's strategy ensures that she is coming closer and closer to the man (in fact, arbitrarily close). It was first believed that the lion's strategy would ensure a capture of the man, but Besicovitch showed that this is not true.

A sketch of Besicovitch's strategy for the man on a disk

The man starts in a point different from the lion and not on the boundary of the disk. He makes a small step perpendicular to the line L defined by the man's position and the origin of the disk. The step is in the direction of the halfplane bounded by L that does not contain the lion, or if the lion is on L , then the direction is arbitrary.

The man's strategy ensures that the lion can not catch him. The step that the man makes has to be small enough, such that the man does not reach the boundary, but large enough so that the man can walk for infinitely long. Besicovitch showed that such a step size exist.

Theorem 2.8 (See [68]). A man can escape a lion in a circular arena, but the lion can come arbitrarily close to the man.

Croft [24] extended the Lion and Man game to considering multiple lions. He changed the name of the players, birds are trying to catch a fly. It turns out that n birds are needed to catch the fly on B^n .

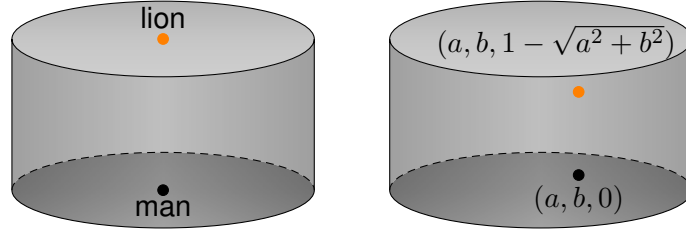


Figure 2.3: The lion's position on the cylinder at time step $\sqrt{a^2 + b^2}$ (for some small a, b) when the starting position of the lion is $(0, 1, 0)$ and the starting position of the man is $(0, 0, 0)$.

Generalised strategy for a fly in a ball B^n with $n - 1$ birds

The fly starts in a position different to the birds and not on the boundary of the ball. It makes a small step perpendicular to the hyperplane H defined by the birds' positions in the direction that contains the origin (or an arbitrary direction if the hyperplane H contains the origin).

While the Lion and Man game has a nice and easy definition, Bollobás, Leader and Walters [16] showed that both the lion and man can have a winning strategy, which means the lion can make sure that the man does not occupy the same point as the lion, whereas the lion can make sure she occupies the same point as the man. For the example given in [16], let $D = \{(x, y) \mid x^2 + y^2 \leq 1\}$ be an Euclidean disk and $I = [0, 1]$. Let $S = D \times I$ where the product space is equipped with the ℓ_∞ -metric, which means that for $x_1, x_2 \in D, y_1, y_2 \in I$, the distance $d((x_1, y_1), (x_2, y_2)) = \max\{d_D(x_1, x_2), d_I(y_1, y_2)\}$, where the distance d_D and d_I are the Euclidean distance in D and I , respectively. Suppose the lion starts at $(0, 1, 0)$ and the man starts at $(0, 0, 0)$. The lions strategy is to keep the disk coordinate the same as the man while moving closer in the interval $[0, 1]$. This is possible because of the ℓ_∞ -metric in the product space. After moving distance 1 on S , the lion occupies the same position as the man. The man's strategy is to make his disk-coordinate differ from the coordinate of the lion. If there exists a time step t such that the lion's disk coordinate is $(0, s)$ for all $0 \leq s \leq t$, then the man moves such that his disk coordinate is $[0, -s]$ for all $0 \leq s \leq t$.

The main issue here is that the lion and the man make decisions at the same time. This is not the case in the Cops and Robber game. Mohar [79] showed that an advantage of the Cops and Robber game on geodesic spaces is that either the cops or the robber have a winning strategy (for the ε -game), so the game is well defined.

2.3 Cops and Robber Game on Surfaces

In this section we consider the Cops and Robber game played on Euclidean, spherical and hyperbolic surfaces. We will first discuss the game on balls, using the strategies of the Lion and Man game, in order to establish some tools that we will need on surfaces.

Lemma 2.9. Let the Cops and Robber game be played on an Euclidean disk, a disk on the unit sphere of radius at most $\frac{\pi}{2}$ or a hyperbolic disk B^2 . If the cops position c^{k_0} is on the line between the centre O of B^2 and the position of the robber r^{k_0} , then the cop can guard the disk of radius $\frac{1}{2}(d(O, c^{k_0}) + d(O, r^{k_0}))$ and centre O .

Proof. Let $d_k = \frac{1}{2}(d(O, c^k) + d(O, r^k))$ and D_k be the disk of radius d_k and centre O . We explain the cop's strategy for the time steps $k \geq k_0$. First suppose that the geodesic segment from r^k to r^{k+1} passes through D_k , we show that the cop can catch the robber. We are allowed to subdivide the robber's step since this is only to the advantage of the robber, so we assume without loss of generality $d(O, r^{k+1}) = d_k$. We can assume $r^{k+1} \neq c^k$ and we consider the closest point p from r^{k+1} on the geodesic through O and r^k .

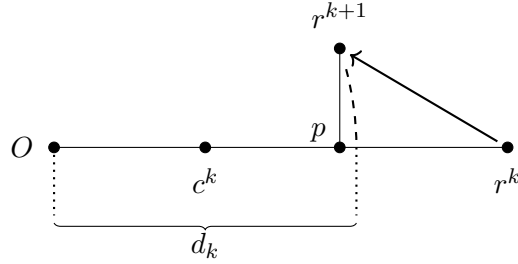


Figure 2.4: Depicted is the point p which is the closest point on Or^k from the robber's position r^{k+1} .

By Pythagoras' theorem (in the Euclidean or hyperbolic plane or for a right angled triangle on a spherical hemisphere),

$$d(O, p) < d_k,$$

hence $d(r^k, p) > d(c^k, p)$. But then using Pythagoras' theorem again on the triangles $c^k p r^{k+1}$ and $r^{k+1} p r^k$ which both have a right angle at p , it follows that $d(r^{k+1}, c^k) < d(r^{k+1}, r^k)$, so the cop can catch the robber.

We show now that if $d(O, r^{k+1}) > d_k$ and the cop does not pass through D , there exists a position of the robber on $\overline{Or^{k+1}}$ such that

$$d(0, c^{k+1}) - d(0, c^k) \geq d(0, r^k) - d(0, r^{k+1}). \quad (2.2)$$

By subdividing the robber's step, we can assume that the triangle $Or^k r^{k+1}$ has angle at most $\frac{\pi}{2}$ at O . Suppose first the angle at r^k in the triangle $Or^k r^{k+1}$ is smaller than π . The

cop moves to the point c^{k+1} on $\overline{Or^{k+1}}$ such that

$$d(0, c^{k+1}) - d(0, c^k) = d(0, r^k) - d(0, r^{k+1}).$$

We show now that this is a valid move, which means $d(c^k, c^{k+1}) \leq d(r^k, r^{k+1})$.

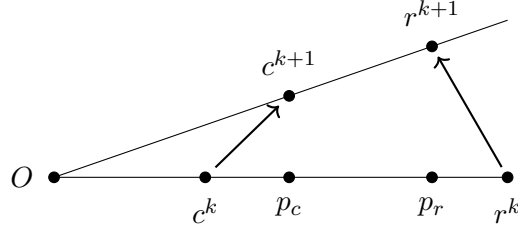


Figure 2.5: The case where the angle at r^k in the triangle $Or^k r^{k+1}$ is smaller than π .

If r^{k+1} is on the geodesic Or^k , then the cop moves as far as the robber, hence this is a valid move for the cop. Otherwise consider the closest points p_c, p_r on the geodesic Or^k of c^{k+1}, r^{k+1} , respectively. Using Pythagoras' theorem again, $d(O, c^{k+1}) > d(O, p_c)$ and $d(O, r^{k+1}) > d(O, p_r)$. But then $d(p_c, c^k) < d(O, c^{k+1}) - d(O, c^k)$ and $d(p_r, r^k) > d(O, r^k) - d(O, r^{k+1})$. But then using Pythagoras' theorem again, $d(c^k, c^{k+1}) < d(r^k, r^{k+1})$, hence 2.2 is a valid move.

Suppose now the angle at r^k in the triangle $Or^k r^{k+1}$ is larger than π . Then this is of advantage to the cop since the robber moves further away from O , i.e.

$$d(O, r^k) - d(O, r^{k+1}) < 0.$$

The cop can simply move at a right angle to Oc^k and

$$d(O, c^{k+1}) - d(O, c^k) \geq 0,$$

which establishes (2.2). As long as the cop has not caught the robber, the value d_k is increasing, and as soon as the robber passes through the disk D_k , he is caught. This proves the lemma. \square

2.3.1 Cops and Robber with Strategies from the Lion and Man Game

We show that a similar argument to Besicovitch's strategy can be used to prove that one cop suffices to win our version of the game on an Euclidean disk (the cop does not catch the robber, but gets arbitrarily close). Note that this result is later generalised (see the proof of Proposition 2.13).

Proposition 2.10 ([W13]). Let B^2 be a 2-dimensional Euclidean disk. Then $c(B^2) = 1$.

Proof. We can assume that B^2 is a unit disk. At the beginning of the game, the robber chooses agility τ with $\sum_k \tau(k) = \infty$, and an initial position of both players. Let O denote the centre of the disk B^2 , and let r^k and c^k denote positions of the robber and the cop after the k -th move, respectively.

The cop's strategy is to first move to the centre O of the disk, and in the next steps to move for the same distance as the robber while ending his move on the line connecting the centre of the disk and current robber's position while getting as close to robber as possible (see Figure 2.6). By Lemma 2.9, we may assume that $d(O, r^k)$ is increasing (otherwise the cop gets closer to the robber even sooner), and since $d(O, r^k) \leq 1$, the sequence converges, say $\ell_R = \lim_{k \rightarrow \infty} d(O, r^k)$.

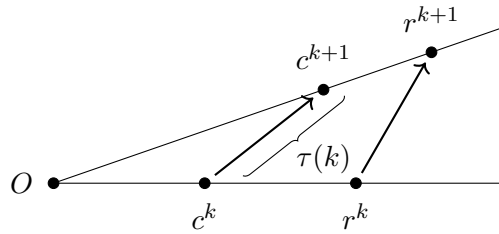


Figure 2.6: One move in the cop's strategy.

Thus $d(O, c^k)$ is also increasing for all $k \geq K_0$, where K_0 is the step of the game in which the cop reaches O . Thus $d(O, c^k)$ converges, say $\ell_C = \lim_{k \rightarrow \infty} d(O, c^k)$. If $\ell_R = \ell_C$, then the cop can get arbitrarily close to the robber, hence she wins the game.

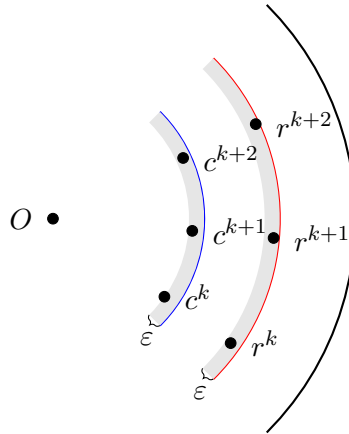


Figure 2.7: The robber and the cop approaching the circles with radius ℓ_R and ℓ_C , respectively.

Suppose that $\ell_R > \ell_C$. Take $\varepsilon = \pi(\ell_R - \ell_C)$. (Notice that $\varepsilon > 0$ since $0 < \ell_C < \ell_R \leq 1$.) Then there exists $K_1 \in \mathbb{N}$ such that for all $k \geq K_1$ we have $d(O, c^k) \geq \ell_C - \varepsilon$ and $d(O, r^k) \geq \ell_R - \varepsilon$. There also exists $M_1 \in \mathbb{N}$ such that $\sum_{i=K_1}^{M_1} \tau(i) \geq \varepsilon + 2\pi\ell_R$. In steps $i = K_1, \dots, M_1$, $\|d(O, r^k)\| \in [\ell_R - \varepsilon, \ell_R]$, so the robber travels the distance of at least one full circle of

circumference $2\pi\ell_R$ in these steps. But since $\|d(O, c^k)\| \in [\ell_C - \varepsilon, \ell_C]$ and the cop ends each of his moves on the line between O and the robber, she only needs to move for at most $2\pi\ell_C$ to ensure this. Thus she can move a bit closer to the robber in each step, and in steps K_1, \dots, M_1 she gains at least $2\pi\ell_R - 2\pi\ell_C$. Hence

$$d(O, c_{M_1}) \geq d(O, c_{K_1}) + 2\pi(\ell_R - \ell_C) \geq \ell_C - \varepsilon + 2\varepsilon = \ell_C + \varepsilon > \ell_C,$$

which is a contradiction. \square

Theorem 2.11 ([W13]). If $n \geq 1$, then $c(B^n) = 1$.

Proof. The cop's strategy is to first move to the centre O of B^n . Suppose that after k steps the cop is positioned in c^k which lies on the line between O and the robber's position is r^k . Then the line Or^k and the robber's position r^{k+1} in the next move span a 2-dimensional subspace in B^n which is isometric to B^2 . So the cop can use the strategy explained in Proposition 2.10 on every step to get arbitrarily close to the robber. \square

Let pr_2 be the projection on the z -coordinate, i.e., $\text{pr}_2(\underline{x}, z) = z$, and let pr_1 be the projection on the first $n - 1$ coordinates, i.e., $\text{pr}_1(\underline{x}, z) = \underline{x}$.

Theorem 2.12 ([W13]). If $n \geq 1$, then $c_0(B^n) = n$.

Proof. We first prove that the robber has a strategy to escape $n - 1$ cops from catching him (i.e. occupying the same point as the robber). The robber selects his initial position $(\frac{1}{2}, 0, \dots, 0)$ and positions all cops in $(\frac{1}{100}, 0, \dots, 0)$. He chooses agility $\tau: \mathbb{N} \rightarrow \mathbb{R}^+$ with $\tau(n) = \frac{1}{n+2}$.

Suppose that the robber is not caught after k steps of the game. Denote players position after k th step as $(r^k, c_0^k, \dots, c_{n-1}^k)$. Let Λ be the hyperplane containing points $r^k, c_1^k, \dots, c_{n-1}^k$. Construct a line λ , which contains r^k and is perpendicular to Λ . Let L be the point on λ such that $LO \perp \lambda$. The robber moves for time $\tau(k+1)$ along λ towards L (and possibly beyond L) at maximum speed. If $L \in \Lambda$, the robber may choose his direction arbitrarily. Denote the new position of the robber by r^{k+1} . Clearly, no cop can reach the point r^{k+1} in time $\tau(k+1)$. We still need to check that $r^{k+1} \in B^n$.

Denote $|Or^k| = r_k$, $|Or^{k+1}| = r_{k+1}$, and let α be the angle at r^k in the triangle $\triangle Or^k r^{k+1}$. Due to the choice of the direction of robber's move, $\alpha \in [0, \pi/2]$. The law of cosines gives

$$r_{k+1}^2 = r_k^2 + \tau(k+1)^2 - 2r_k\tau(k+1)\cos\alpha \leq r_k^2 + \tau(k+1)^2.$$

Using induction this yields

$$r_{k+1}^2 \leq \sum_{i=1}^{k+1} \tau(i)^2 < \sum_{i=1}^{\infty} \tau(i)^2 = \frac{\pi^2}{6} - \frac{5}{4} < 1,$$

so $r^{k+1} \in B^n$ and thus the robber is also not caught after $k + 1$ moves.

Next, we prove that n cops have a strategy to catch the robber using induction on n . For $n = 1$, one cop can clearly catch the robber on $B^1 = [-1, 1]$. Suppose n cops can catch the robber on B^n and observe the game on B^{n+1} . The robber chooses initial positions and agility function τ . First, the cops c_2, \dots, c_{n+1} all move into the hyperplane with $z = 0$. By induction, these n cops can catch the robber's projection $\text{pr}_1(r)$ in $B^{n+1} \cap \{z = 0\}$. Now one cop, say c_{n+1} , keeps pr_1 the same as robber's. If she has some agility left, then she also moves closer to the robber in z -coordinate. The cops c_1, \dots, c_n move to the hyperplane $z = \text{pr}_2(r)$. They maintain their position in the hyperplane with the same z coordinate as the robber has. If they have some agility left, they move according to their strategy to catch the robber in the n -dimensional ball $B^{n+1} \cap \{z = \text{pr}_2(r)\}$.

Let N_0 be the step in which both above conditions are fulfilled. The robber either stays close to the $z = \text{pr}_2(r)$ hyperplane or moves away from it. We can partition the set of indices $\{N_0, N_0 + 1, \dots\}$ into disjoint sets M_x and M_z in the following way:

$$M_z = \left\{ m \geq N_0 \mid d(\text{pr}_2(r^{m+1}), \text{pr}_2(r^m)) \geq \frac{\tau(m)}{2} \right\},$$

$$M_x = \{N_0, N_0 + 1, \dots\} \setminus M_z.$$

Note that if $m \in M_x$, then

$$d(\text{pr}_1(r^{m+1}), \text{pr}_1(r^m)) = \sqrt{\tau(m)^2 - d(\text{pr}_2(r^{m+1}), \text{pr}_2(r^m))^2} > \frac{\sqrt{3}}{2}\tau(m) > \frac{\tau(m)}{2}.$$

If $\sum_{m \in M_x} d(\text{pr}_1(r^{m+1}), \text{pr}_1(r^m))$ and $\sum_{m \in M_z} d(\text{pr}_2(r^{m+1}), \text{pr}_2(r^m))$ are finite, then the sum $\sum_{m \geq N_0} \frac{\tau(m)}{2}$ is finite, too. This implies that $\sum_{m \in \mathbb{N}} \tau(m) < \infty$, which is by definition not possible for an agility function τ . Hence at least one of the sums $\sum_{m \in M_x} d(\text{pr}_1(r^{m+1}), \text{pr}_1(r^m))$ and $\sum_{m \in M_z} d(\text{pr}_2(r^{m+1}), \text{pr}_2(r^m))$ must be infinite. If it is the first one (resp. the second one), then the cops c_1, \dots, c_n (resp. the cop c_{n+1}) can by induction catch the robber. \square

2.3.2 Generalised Radial Strategy

The radial strategy used to determine the cop number of the n -dimensional ball can be generalised in the following way.

Let X be a geodesic space and $x_0 \in X$ a fixed point. For $y \in X$, a *ray* is a simple (x_0, y) -path $R = R(x_0, y)$, $R: [0, 1] \rightarrow X$, with $R(0) = x_0$, $R(1) = y$, and the property $d(x_0, R(t)) < d(x_0, R(t'))$ if $0 \leq t < t' \leq 1$. We say that X is *starshaped* at x_0 if $X = \bigcup_{y \in A} R(x_0, y)$ for some $A \subseteq X$, $R(x_0, y) \cap R(x_0, z) = \{x_0\}$ for every distinct $y, z \in A$, and $d(x_0, y) = d(x_0, z)$ for every $y, z \in A$.

For example, in B^n , setting x_0 to be the centre of the ball, A to be ∂B^n , and taking rays as straight lines from x_0 to every point in A , satisfies the starshaped condition.

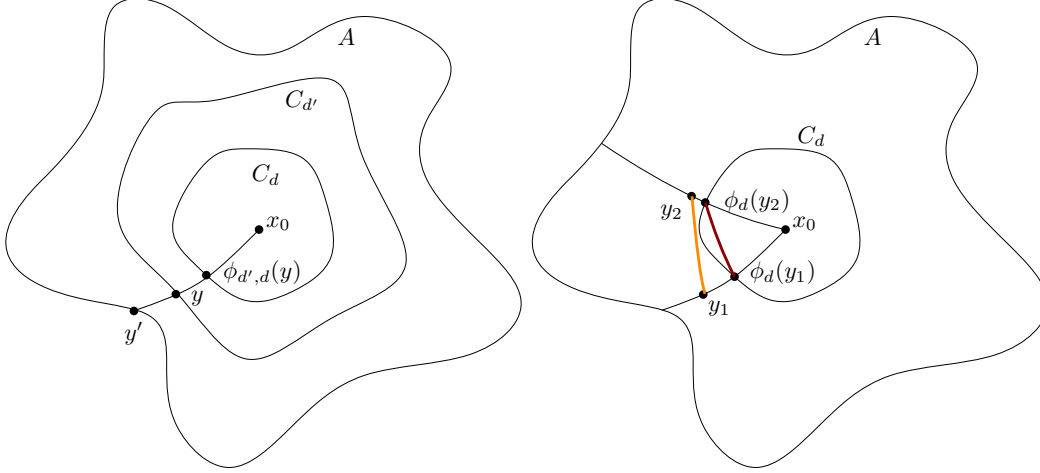


Figure 2.8: A schematic setup when X is starshaped. A is the boundary of X , C_d and $C_{d'}$ are the cycles of distance d and d' from x_0 . The distance between $\phi_d(y_1)$ and $\phi_d(y_2)$ is smaller than the distance between y_1 and y_2 .

Let X be starshaped at x_0 . Denote $C_d = \{t \in X \mid d(x_0, t) = d\}$. For every $d, d' \in (0, d(x_0, A)]$, we can define a mapping $\varphi_{d',d}: C_{d'} \rightarrow C_d$, see Figure 2.8.

For every $y \in C_{d'}$ there exists exactly one ray containing y , say $R(x_0, y')$, $y' \in A$. There exists exactly one point on $R(x_0, y')$ at distance d from x_0 . Take this point to be $\varphi_{d',d}(y)$. Notice that $\varphi_{d',d}^{-1} = \varphi_{d,d'}$. Sometimes we will use a simplified notation $\varphi_d(y) = \varphi_{d',d}(y)$ since $d' = d(x_0, y)$ is implicitly expressed with the choice of y .

For $d_1, d_2 \geq d$, define

$$\begin{aligned} \delta(d_1, d_2, d) &= \inf_{y_1 \in C_{d_1}, y_2 \in C_{d_2}, y_1 \neq y_2} \frac{d(y_1, y_2) - d(\varphi_{d_1,d}(y_1), \varphi_{d_2,d}(y_2))}{d(y_1, y_2)} = \\ &= \inf_{y_1 \in C_{d_1}, y_2 \in C_{d_2}, y_1 \neq y_2} \left(1 - \frac{d(\varphi_{d_1,d}(y_1), \varphi_{d_2,d}(y_2))}{d(y_1, y_2)} \right). \end{aligned}$$

Proposition 2.13 ([W13]). If X is starshaped at x_0 and $\delta(d_1, d_2, d) > 0$ for every $d_1 \geq d_2 \geq d$, $d_1 > d$, then $c(X) = 1$.

Proof. Let $\tau, \sum_n \tau(n) = \infty$, be the agility chosen by the robber. The cop's strategy is first to move to x_0 and then try to move closer to the robber, while ending each of his moves on the same ray g as the robber is on.

First, we prove that if the cop is positioned at distance d from x_0 while the robber is at distance more than d from x_0 and they are both on the same ray R , then the cop can guard C_d . Notice that since $\delta(d_1, d_2, d) > 0$, we have $d(y_1, y_2) > d(\varphi_{d_1,d}(y_1), \varphi_{d_2,d}(y_2))$ for every $y_1 \in C_{d_1}, y_2 \in C_{d_2}$. Thus if the robber moves such that his distance from x_0 remains greater than d , then the condition from the statement ensures that the cop can end his move on C_d , again on the same ray R as the robber is on.

If the robber moves closer to x_0 than d , then the cop first moves to the intersection point between the robber's trajectory and C_d (for which she spends at most the same distance as the robber did), and then follows along the robber's trajectory to catch him. Thus we may assume that $d(x_0, r_n)$ has a limit. (Otherwise the cop catches the robber or gets closer to him even sooner. Indeed, consider the projection of both players' steps on the interval $[0, d(x_0, A)]$, where the robber's position is $d(x_0, r_n)$ and the cop's position is $d(x_0, c_n)$. If the robber moves at least for distance $d = d(x_0, A)$ steps towards 0, then the cop caught the robber in $[0, d(x_0, A)]$, and hence in X .) Let $\ell_R = \lim_{n \rightarrow \infty} d(x_0, r_n)$. The cop's strategy is to first move to x_0 (for example along one of the rays R), and then use the "radial" strategy: ending each of his moves on the same ray R as the robber is on, while trying to get as close to the robber as possible. Since $\delta(d_1, d_2, d) > 0$ for all appropriate d_1, d_2, d , we easily conclude that for every distinct $y_1 \in C_{d_1}, y_2 \in C_{d_2}$, we have $d(y_1, y_2) > d(\varphi_{d_1, d}(y_1), \varphi_{d_2, d}(y_2))$. Thus $d(x_0, c_n)$ is also increasing (after the cop reaches x_0) and hence convergent. Let $\ell_C = \lim_{n \rightarrow \infty} d(x_0, c_n)$. If $\ell_R = \ell_C$, then the cop can get arbitrarily close to the robber, hence she wins the game.

Suppose that $\ell_R > \ell_C$. Let $\delta_0 = \delta(\frac{\ell_R + \ell_C}{2}, \frac{\ell_R + \ell_C}{2}, \ell_C) > 0$. Note that $\delta_0 \leq 1$ by definition. Take $\varepsilon = \frac{\ell_R - \ell_C}{2}$. There exists $N_0 \in \mathbb{N}$ such that for all $n \geq N_0$ we have $d(x_0, c_n) \geq \ell_C - \varepsilon$ and $d(x_0, r_n) \geq \ell_R - \varepsilon$. For $n \geq N_0$, denote $r = r_n, c = c_n, r' = r_{n+1}, R'$ is the ray on which r' lies, and \bar{c} is the point in $R' \cap C_{d(x_0, c)}$. The cop's strategy is to first move to \bar{c} , and then move along R' for the remainder of his agility.

Observe that, $d(r, r') \geq d(\varphi_{\ell_R - \varepsilon}(r), \varphi_{\ell_R - \varepsilon}(r'))$, and $d(c, \bar{c}) \leq d(\varphi_{\ell_C}(c), \varphi_{\ell_C}(\bar{c}))$ (here we are using the simplified notation for the function φ). Therefore

$$1 - \frac{d(c, \bar{c})}{d(r, r')} \geq 1 - \frac{\overbrace{d(\varphi_{\ell_C}(c), \varphi_{\ell_C}(\bar{c}))}^{\varphi_{\ell_C}(y_1), \varphi_{\ell_C}(y_2)}}{\underbrace{d(\varphi_{\ell_R - \varepsilon}(r), \varphi_{\ell_R - \varepsilon}(r'))}_{y_1, y_2}} \geq \delta_0.$$

Thus $d(c, \bar{c}) \leq (1 - \delta_0)d(r, r')$. This means that the cop can move closer to the robber along $g(r')$ for at least $d(r, r') - (1 - \delta_0)d(r, r') = \delta_0 d(r, r')$. Note that this holds for every step $n \geq N_0$. Since $\sum_n \tau(n) = \infty$, there exists $M_0 \in \mathbb{N}$ such that $\sum_{n=N_0}^{M_0} \tau(n) \geq \frac{\ell_R - \ell_C}{\delta_0}$.

Thus in steps $i = N_0, \dots, M_0$, the cop is able to move closer to the robber for at least $\sum_{n=N_0}^{M_0} \delta_0 \tau(n) \geq \delta_0 \cdot \frac{\ell_R - \ell_C}{\delta_0} = \ell_R - \ell_C$. But this means that $d(x_0, c_{M_0}) \geq d(x_0, c_{N_0}) + \ell_R - \ell_C \geq \ell_C - \varepsilon + \ell_R - \ell_C = \ell_R - \varepsilon > \ell_C$, which is a contradiction. \square

To illustrate the use of Proposition 2.13, we give another proof that $c(B^n) = 1$.

Lemma 2.14 ([W13]). The n -dimensional ball B^n satisfies the condition that $\delta(d_1, d_2, d) > 0$ for every $d_1 \geq d_2 \geq d, d_1 > d$.

Proof. Let x_0 be the centre of the ball B^n . Taking rays as straight lines between x_0 and the points on the boundary of B^n satisfies the starshaped condition. First, suppose that

$d_1 = d_2$. In this case, $d_2 > d$. Take distinct $y_1, y_2 \in C_{d_1}$. Triangles $\triangle x_0 \varphi_{d_1, d}(y_1) \varphi_{d_1, d}(y_2)$ and $\triangle x_0 y_1 y_2$ are similar. Thus

$$\frac{d}{d_1} = \frac{d(\varphi_{d_1, d}(y_1), \varphi_{d_1, d}(y_2))}{d(y_1, y_2)}.$$

So

$$\delta(d_1, d_1, d) = \inf_{y_1, y_2 \in C_{d_1}, y_1 \neq y_2} \left(1 - \frac{d(\varphi_{d_1, d}(y_1), \varphi_{d_1, d}(y_2))}{d(y_1, y_2)} \right) = 1 - \frac{d}{d_1} > 0.$$

Second, suppose that $d_1 > d_2$ and take $y_1 \in C_{d_1}$, $y_2 \in C_{d_2}$. Since $\triangle x_0 y_2 \varphi_{d_1, d_2}(y_1)$ is an isosceles triangle, the angle $\angle y_1 \varphi_{d_1, d_2}(y_1) y_2 > \frac{\pi}{2}$. Thus $d(y_1, y_2)^2 > (d_1 - d_2)^2 + d(\varphi_{d_1, d_2}(y_1), y_2)^2$. We have

$$\begin{aligned} \frac{d(\varphi_{d_1, d}(y_1), \varphi_{d_2, d}(y_2))^2}{d(y_1, y_2)^2} &< \frac{d(\varphi_{d_1, d_2}(y_1), y_2)^2}{(d_1 - d_2)^2 + d(\varphi_{d_1, d_2}(y_1), y_2)^2} = \\ &= 1 - \frac{(d_1 - d_2)^2}{(d_1 - d_2)^2 + d(\varphi_{d_1, d_2}(y_1), y_2)^2} \leq \\ &\leq 1 - \frac{(d_1 - d_2)^2}{(d_1 - d_2)^2 + 4}, \end{aligned}$$

where we used the bound $d(\varphi_{d_1, d_2}(y_1), y_2) \leq \text{diam}(B^n) = 2$. Thus

$$\delta(d_1, d_2, d) \geq \inf_{y_1 \in C_{d_1}, y_2 \in C_{d_2}} 1 - \sqrt{1 - \frac{(d_1 - d_2)^2}{(d_1 - d_2)^2 + 4}} > 0.$$

□

We remark that for B^n the described condition can be simplified to only requiring that for every $d' > d$,

$$\delta(d', d) = \inf_{y_1, y_2 \in C_{d'}, y_1 \neq y_2} \left(1 - \frac{d(\varphi_{d', d}(y_1), \varphi_{d', d}(y_2))}{d(y_1, y_2)} \right) > 0.$$

This can be rephrased as follows. For $y_1, y_2 \in C_d$, let $\alpha_d(y_1, y_2) := d(y_1, y_2)$. Our condition then requires that $\alpha_d(y_1, y_2)$ is strictly increasing in terms of d for every selection of y_1, y_2 .

We also prove that the radial strategy can be used on a hemisphere of an n -dimensional sphere. We start by stating the following technical lemma.

Lemma 2.15 ([W13]). Let $0 < d \leq d_2 \leq d_1 \leq \frac{\pi}{2}$, $d < d_1$. If $0 < \alpha \leq \frac{\pi}{2}$, then

$$\cos d_1 \cos d_2 + \sin d_1 \sin d_2 \cos \alpha < \cos^2 d + \sin^2 d \cos \alpha.$$

Proof. Let $\varphi, \psi: [0, \frac{\pi}{2}] \rightarrow \mathbb{R}$, $\psi(\alpha) = \cos d_1 \cos d_2 + \sin d_1 \sin d_2 \cos \alpha$ and $\varphi(\alpha) = \cos^2 d + \sin^2 d \cos \alpha$. Notice that $\varphi(0) = 1$ and

$$\psi(0) = \begin{cases} 1, & d_1 = d_2; \\ \cos d_1 \cos d_2 + \sin d_1 \sin d_2, & d_1 \neq d_2. \end{cases}$$

It is easy to see that $\cos d_1 \cos d_2 + \sin d_1 \sin d_2 < 1$ for every $0 < d_2 < d_1 \leq \frac{\pi}{2}$. On the other hand, $\varphi'(\alpha) = -\sin^2 d \sin \alpha$ and $\psi'(\alpha) = -\sin d_1 \sin d_2 \sin \alpha$. Since $d_1 > d$, $0 > \varphi'(\alpha) > \psi'(\alpha)$. Thus for every $\alpha \in (0, \frac{\pi}{2}]$, $1 > \varphi(\alpha) > \psi(\alpha)$. \square

Lemma 2.16 ([W13]). The n -dimensional hemisphere \mathbb{S}_+^n satisfies the condition $\delta(d_1, d_2, d) > 0$ for every $d_1 \geq d_2 \geq d, d_1 > d$.

Proof. The shortest paths between the north pole $N = (0, \dots, 0, 1)$ and the points on the boundary of S_+^n have all the conditions needed for rays, thus S_+^n is starshaped at N . Let τ' be the agility function chosen by the robber. Let τ be a subdivision of τ' such that the angle at N corresponding to each move is smaller than $\frac{\pi}{2}$. By [79, Lemma 5] this only goes in the favour of the robber.

Let $y_1 \in C_{d_1}, y_2 \in C_{d_2}, y_1 \neq y_2$. If y_2 lies on the geodesic between N and y_1 , then $d(\varphi_{d_1, d}(y_1), \varphi_{d_2, d}(y_2)) = 0$ and $1 - \frac{d(\varphi_{d_1, d}(y_1), \varphi_{d_2, d}(y_2))}{d(y_1, y_2)} = 1$, so this case can be excluded in the below calculations. Using the spherical law of cosines, we get

$$\begin{aligned} \cos(d(\varphi_{d_1, d}(y_1), \varphi_{d_2, d}(y_2))) &= \cos^2 d + \sin^2 d \cos \alpha, \\ \cos(d(y_1, y_2)) &= \cos d_1 \cos d_2 + \sin d_1 \sin d_2 \cos \alpha, \end{aligned}$$

where α is the angle between the geodesics from N to y_1 and from N to y_2 . Our choice of the agility function yields that $0 < \alpha \leq \frac{\pi}{2}$. Notice that this allows us to write

$$\delta(d_1, d_2, d) = \inf_{0 < \alpha \leq \pi/2} \left(1 - \frac{\arccos(\cos^2 d + \sin^2 d \cos \alpha)}{\arccos(\cos d_1 \cos d_2 + \sin d_1 \sin d_2 \cos \alpha)} \right).$$

To determine $\delta(d_1, d_2, d)$, let us consider the continuous function $f: (0, \frac{\pi}{2}] \rightarrow \mathbb{R}$,

$$f(\alpha) = 1 - \frac{\arccos(\cos^2 d + \sin^2 d \cos \alpha)}{\arccos(\cos d_1 \cos d_2 + \sin d_1 \sin d_2 \cos \alpha)}.$$

By Lemma 2.15, $f(\alpha) > 0$ for every $\alpha \in (0, \frac{\pi}{2}]$.

Since $d_1 > d$, $f(\frac{\pi}{2}) = 1 - \frac{\arccos(\cos^2 d)}{\arccos(\cos d_1 \cos d_2)} > 0$. If $d_1 \neq d_2$, then

$$\lim_{\alpha \searrow 0} f(\alpha) = 1 - \frac{\arccos(1)}{\arccos(\cos d_1 \cos d_2 + \sin d_1 \sin d_2)} = 1.$$

If $d_1 = d_2$, then we can write

$$f(\alpha) = 1 - \frac{\arccos(1 + \sin^2 d(\cos \alpha - 1))}{\arccos(1 + \sin^2 d_1(\cos \alpha - 1))},$$

from which we can see that $\lim_{\alpha \searrow 0} f(\alpha) > 0$.

As f is continuous and its limits at the boundary are bounded away from zero, it follows that $\inf_{\alpha \in (0, \pi/2]} f(\alpha) > 0$ and thus $\delta(d_1, d_2, d) > 0$. \square

2.3.3 Higher-dimensional Spheres

It turns out that a constant number of cops are also enough to win the game on n -dimensional spheres, while a linear number of cops is needed to catch the robber.

When studying the game on \mathbb{S}^n it is useful to consider a mirroring strategy of the cop. Let

$$\rho: \mathbb{S}^n \rightarrow \mathbb{S}^n, \rho((x_1, \dots, x_n, z)) = \begin{cases} (x_1, \dots, x_n, z), & z \leq 0, \\ (x_1, \dots, x_n, -z), & z \geq 0. \end{cases}$$

Lemma 2.17 ([W13]). One cop can guard a great circle in \mathbb{S}^n .

Remark: the cop essentially guards a whole hemisphere.

Proof. Given starting positions (r_1, c_1) of the robber and the cop, respectively, we change coordinates so that $c_1 = \rho(r_1)$ (this can be done with an orthogonal transformation, so distances are preserved). Now the cop's strategy is to move so that $c_n = \rho(r_n)$, thus guarding the great circle $\{(x_1, \dots, x_n, 0) \in \mathbb{S}^n\}$. \square

Theorem 2.18 ([W13]). If $n \geq 1$, then $c(\mathbb{S}^n) = 2$.

Proof. Let (r_1, c_1, c_2) be the starting positions of the robber and both cops. First, the coordinate system is fixed in such a way that $c_1 = \rho(r_1)$. Afterwards, the first cop uses the strategy from Lemma 2.17 to guard the lower hemisphere. So the robber is essentially limited to moving around in the upper hemisphere (otherwise he is caught). The second cop first moves to the north pole N and then uses the radial strategy. Proposition 2.13 and Lemma 2.16 ensure that she can get arbitrarily close to the robber. \square

It follows from [103] that exactly $n + 1$ cops are needed to catch the robber on \mathbb{S}^n , i.e.

$$c_0(\mathbb{S}^n) = n + 1.$$

Observe that two cops can win on \mathbb{S}^n even if each of them is using the radial strategy on a complementary hemisphere. This can easily be generalised to spaces that are union of a number of subsets, each satisfying the condition of Proposition 2.13.

2.3.4 Covering Space Method and its Application to the Flat Torus

Sometimes it is beneficial for the cops to imagine that the game is played on the covering space instead of on the space itself. The following result shows that if k cops can win the game on the covering space, then k cops can also win on the space itself.

Lemma 2.19 ([W13]). If C is the covering space of X that locally preserves distances, then $c(X) \leq c(C)$.

Proof. Let $p: C \rightarrow X$ be the covering map and let $c(C) = k$. While the game in X is played with k cops, the cops imagine the game is simultaneously played on C . If a cop moves to c in C , the same cop moves to $p(c)$ in X (which is possible due to the properties of the covering map). Thus since at least one cop can get arbitrarily close to the robber in C , the image of this cop in X also gets arbitrarily close to the robber. \square

In the following we consider the Cops and Robber game played on a flat torus, to demonstrate the usefulness of the covering space method. Recall that the covering space of T^n is \mathbb{R}^n .

Lemma 2.20 ([W13]). Let $\varepsilon > 0$. If the robber's position is on the line between two cops in \mathbb{R}^n , then the two cops can come to distance ε from the robber in \mathbb{R}^n .

Proof. Without loss of generality we may assume that $r^0 = (0, \dots, 0)$, $c_1^0 = (0, \dots, 0, a)$, $c_2^0 = (0, \dots, 0, -b)$, $a \geq b > 0$. Take $\varepsilon > 0$. We want to prove that the cops have a strategy to reduce $d(r^n, \{c_1^n, c_2^n\})$ to at most ε . Let $t = \frac{1}{2\varepsilon}(a^2 - \varepsilon^2)$, $\alpha = \arctan(\frac{a}{t})$ and $\beta = \arctan(\frac{b}{t})$. Note that the right-angled triangle with one of the angles α and legs of lengths a and t has the hypotenuse of length $t + \varepsilon$.

The cops partition each move of the robber into his first $n - 1$ coordinates x_1, \dots, x_{n-1} , and the last coordinate x_n , denoted by τ_n^x and τ_n^z , respectively. Note that in each step, at least one of these is greater than $\frac{\tau_n}{2}$. The cops move for τ_n^x in the same direction as the robber, but slightly towards him, the first cop following a line with slope $\pm\alpha$, and the second cop following a line with slope $\pm\beta$ (as long as this step ensures that the x_n coordinates of the first cop, resp. second cop, is larger, resp. smaller, than the x_n coordinate of the robber, otherwise they move on a smaller angle, directly towards the robber). They also move for τ_n^z in x_n -coordinate towards the robber. The first part of the move at angle α (β , resp.) ensures that the distance between the cops' and the robber's projections on the x_1, \dots, x_{n-1} -hyperplane are always at most ε apart, while the second part of the move ensures that the distance between the cops' projections on x_n -axis is getting smaller. Notice also that such moves ensure that after every move of the cops, the robber is at most at distance ε from the projections of cops' positions onto the x_1, \dots, x_{n-1} -hyperplane. If $\sum_{n=1}^k \tau_n^x > t$ for some k , then the latest after k steps the distance between the cops and the robber will be at most ε . Otherwise, since $\sum_n \tau_n = \infty$, it holds $\sum_n (\tau_n - \tau_n^x) = \sum_n \tau_n^z = \infty$, thus the cops

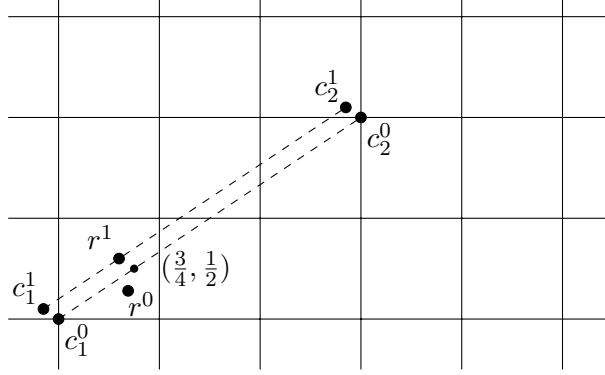


Figure 2.9: The first move of the robber and the cop in the ε -approaching game. The point $(\frac{3}{4}, \frac{1}{2})$ is at most τ_0 away from r^1 .

will eventually be on the same x_n -coordinate as the robber, and the robber will be at least ε -close. \square

Remark 2.21. The conclusion of Lemma 2.20 also holds if the robber is at distance less than ε from the line between the two cops. The details are left to the reader.

Using the covering space method we demonstrate that two cops win the game on T^n .

Theorem 2.22 ([W13]). For every $n \geq 1$, $c(T^n) = 2$.

Proof. As $\mathbb{S}^1 \subseteq T^n$ and the projection $T^n \rightarrow \mathbb{S}^1$ is a 1-Lipschitz mapping, Lemma 2.7 yields $c(T^n) \geq 2$.

The universal covering space of T^n is the Euclidean space \mathbb{R}^n . We will prove that with good initial positions two cops can win the game on \mathbb{R}^n , thus by Lemma 2.19, $c(T^n) \leq 2$ as well. Without loss of generality we may assume that $c_1^0 = c_2^0 = (0, \dots, 0) \in T^n$. The robber moves from r^0 to r^1 in his first move, see Figure 2.9. There exists a point with rational coordinates that is at most τ_0 away from r^1 , say $(\frac{p_1}{q_1}, \dots, \frac{p_n}{q_n})$, where $p_i, q_i \in \mathbb{N}_0$ for $i \in [n]$. Let $Q = q_1 q_2 \cdots q_n$. Imagine the cops' initial positions in the Euclidean space are $c_1^0 = (0, \dots, 0) \in \mathbb{R}^n$ and $c_2^0 = (Q \cdot \frac{p_1}{q_1}, \dots, Q \cdot \frac{p_n}{q_n})$. They first make the step $r^1 - (\frac{p_1}{q_1}, \dots, \frac{p_n}{q_n})$. As a result, r^1 now lies on the line between c_1^1 and c_2^1 . Using Lemma 2.20, these two cops can now come ε -close to the robber in the game on \mathbb{R}^n . Thus the two cops win the ε -approaching game on T^n . This implies that $c(T^n) \leq 2$. \square

On the other hand, $n + 1$ cops are needed to catch the robber on T^n .

Theorem 2.23 ([W13]). If $n \geq 1$, then $c_0(T^n) = n + 1$.

Proof. On T^n , n cops cannot catch a robber. The robber chooses the agility function $\tau = \frac{1}{8}$. Since the $\frac{1}{8}$ -ball around r^k can be entirely contained in the union of $\frac{1}{8}$ -balls around c_1^k, \dots, c_n^k if and only if $r^k = c_i^k$ for some $i \in [k]$, the robber has a direction in which he can move to escape being captured in this move.

Next, we prove in full detail that three cops suffice to catch the robber on T^2 . We imagine the game is played on the universal cover space of T^2 , so on \mathbb{R}^2 . Without loss of generality, $c_1^0 = c_2^0 = c_3^0 = (0, 0)$. Let the robber's initial position be $r^0 \in [0, 1]^2$ in the covering space \mathbb{R}^2 . We imagine the cops' initial positions are $c_1^0 = (0, -100)$, $c_2^0 = (200, 100)$ and $c_3^0 = (-200, 100)$. For $i \in [3]$, let ℓ_i be the ray starting at r^0 that goes through c_i^0 , and let ℓ_i^\perp be the bisector of the line segment between c_i^0 and r^0 . The selected initial conditions in the covering space ensure that the angle α_1 of the slope of ℓ_1 is in $[\arctan(100), \pi/2]$, the angle α_2 of the slope of ℓ_2 is in $[\arctan(\frac{99}{201}), \arctan(\frac{1}{2})]$ and the angle α_3 of the slope of ℓ_3 is in $[\pi - \arctan(\frac{1}{2}), \pi - \arctan(\frac{99}{201})]$. The angles of the lines ℓ_i^T are at $\alpha_i + \pi/2$ or $\alpha_i - \pi/2$.

A short calculation shows that the angles between the bisectors ℓ_i^\perp ($i \in [3]$) are between $\frac{\pi}{3} - \frac{\pi}{18} = \frac{5\pi}{18}$ and $\frac{\pi}{3} + \frac{\pi}{18} = \frac{7\pi}{18}$ and the angles between the rays ℓ_i ($i \in [3]$) are between $\frac{10\pi}{18}$ and $\frac{14\pi}{18}$.

The cops' strategy is to move in the same direction as the robber if the robber is moving away from the bisector between them, or to move to the reflection along the bisector of the robber's new position. This clearly maintains angles between lines ℓ_i^\perp , $i \in [3]$, and angles between lines ℓ_i , $i \in [3]$. Let $D_n = \sum_{i=1}^3 d(r^n, c_i^n)$. The above strategy ensures that D_n is decreasing. Indeed, when the robber moves from r^n to r^{n+1} , $d(r^n, r^{n+1}) = \tau_n$, he moves closer to either one or two bisectors between him and a cop. If he moves closer to only one of the bisectors (say closer to the cop c_j), then the angle between the move $r^n \rightarrow r^{n+1}$ and ℓ_j is at most $\frac{7\pi}{18}$, thus $D_n - D_{n+1} \geq 2\tau_n \cos(\frac{7\pi}{18})$. If the robber moves closer to two of the bisectors (say closer to the cops c_j and c_k), then at least one of the angles between the move $r^n \rightarrow r^{n+1}$ and ℓ_j or ℓ_k is smaller than one half of the angle between ℓ_j and ℓ_k , which is smaller than $\frac{7\pi}{18}$. Thus again, $D_n - D_{n+1} \geq 2\tau_n \cos(\frac{7\pi}{18})$.

Since $\sum_n \tau_n = \infty$, there exists $N_0 \in \mathbb{N}$ such that $\sum_{n=1}^{N_0} \tau_n \geq \frac{D_0+1}{2 \cos(\frac{7\pi}{18})}$. Thus $D_{N_0} = \sum_{i=1}^3 d(r^{N_0}, c_i^{N_0}) \leq D_0 - \sum_{n=1}^{N_0} 2\tau_n \cos(\frac{7\pi}{18}) \leq D_0 - 2 \cos(\frac{7\pi}{18}) \frac{D_0+1}{2 \cos(\frac{7\pi}{18})} = -1$, which is a contradiction. Hence the cops are able to catch the robber. This concludes the proof for $n = 2$.

In higher dimension ($n \geq 3$) the strategy is to choose the initial positions of the cops (in the covering space) such that the robber is caught in a simplex. Then, as in the previous argument, with every step of the robber, there is a cop which gets at least a positive fraction of the step closer to the robber. We skip the details, but show that there exists such a fixed positive fraction if the robber was caught in a regular n -simplex in \mathbb{R}^{n+1} .

Let $n + 1$ points $S = \{e_1 = (1, 0, \dots, 0), e_2 = (0, 1, 0, \dots, 0), \dots, e_{n+1} = (0, \dots, 0, 1)\}$ span the regular simplex Σ in \mathbb{R}^{n+1} . A point $x = (x_1, \dots, x_{n+1})$ lies in Σ if and only if $x_1 + \dots + x_{n+1} = 1$ and $x_i \geq 0$ for $i \in [n + 1]$. Let the robber's position after step r be $x = (a_1, \dots, a_{n+1})$ in the interior of Σ , let c_i be the reflection of x over the hyperplane Π_i spanned by $S \setminus \{e_i\}$. The normal of Π_i is $n_i = (1, \dots, 1, 0, 1, \dots, 1)$, where 0 is on the i -th coordinate, and e_{i-1} (index modulo $n + 1$) lies on Π_i . Then $c_i = x + 2 \frac{(e_{i-1} - x) \cdot n_i}{n} n_i$. Recall

that projection of a onto b is $\text{proj}_b a = \frac{a \cdot b}{b \cdot b} b$. Thus $c_i = x + \frac{2a_i}{n} n_i$ and $c_i - x = \frac{2a_i}{n} n_i$. Notice that $\|c_i - x\|^2 = \frac{4a_i^2}{n}$.

Let the robber's position after step $r + 1$ be $x' = (b_1, \dots, b_{n+1}) \in \Sigma$ and let $\|x' - x\| = \tau$. Since $\|x' - x\|^2 = \sum_{j=1}^{n+1} (b_j - a_j)^2 = \tau^2$, at least one of the terms is greater than $\frac{\tau^2}{n+1}$. Without loss of generality, $(b_1 - a_1)^2 \geq \frac{\tau^2}{n+1}$.

If $b_1 - a_1 < 0$, then $a_1 - b_1 \geq \frac{\tau}{\sqrt{n+1}}$. Thus $(x' - x) \cdot (c_1 - x) = \frac{2a_1}{n} (a_1 - b_1) \geq \frac{2a_1}{n} \frac{\tau}{\sqrt{n+1}}$. Therefore $\text{proj}_{c_1 - x}(x' - x) \geq \frac{\frac{2a_1}{n} \frac{\tau}{\sqrt{n+1}}}{\sqrt{n(n+1)} \|c_1 - x\|}$.

If $b_1 - a_1 \geq 0$, then $b_1 - a_1 \geq \frac{\tau}{\sqrt{n+1}}$. Since $0 = \sum_{j=1}^{n+1} (b_j - a_j) \geq \frac{\tau}{\sqrt{n+1}} + \sum_{j=2}^{n+1} (b_j - a_j)$, at least one of the terms is smaller than $\frac{-\tau}{n\sqrt{n+1}}$. Without loss of generality, $b_2 - a_2 \leq \frac{-\tau}{n\sqrt{n+1}}$, i.e., $a_2 - b_2 \geq \frac{\tau}{n\sqrt{n+1}}$. Thus $(x' - x) \cdot (c_2 - x) \geq \frac{2a_2}{n} \frac{\tau}{n\sqrt{n+1}}$ and $\text{proj}_{c_2 - x}(x' - x) \geq \frac{\frac{2a_2}{n} \frac{\tau}{n\sqrt{n+1}}}{\sqrt{n(n+1)} \|c_2 - x\|}$.

Thus it is always true that at least one of $\text{proj}_{c_i - x}(x' - x)$ is directed towards c_i and has norm greater or equal $\frac{\tau}{n\sqrt{n(n+1)}}$.

To prove that $n+1$ cops suffice to catch the robber on T^n , we use change of coordinates and the argument explained above. \square

We can extend the proof to manifolds which have the Euclidean space as a covering space.

Theorem 2.24. Suppose S is an n -dimensional Euclidean manifold. Then $c(S) = 2$ and $c_0(S) = n + 1$.

Proof. The strategies are similar to those in Theorem 2.22 and Theorem 2.23, we sketch the main differences. To show that $c(S) \geq 2$, we play the game on a systole, which is a shortest non-contractible curve. Suppose the length of the systole is s , then the robber chooses agility $\tau = \frac{1}{8}s$. On the systole, one cop can not catch the robber if the agility function is $\tau = \frac{1}{8}s$, and there is a 1-Lipschitz mapping from S to the systole, which can be shown using the Gauss-Bonnet Theorem. To show that $c_0(S) \geq n + 1$, the same proof holds when the robber chooses agility $\tau = \frac{1}{8}s$. Since the $\frac{1}{8}s$ -ball around r^k can be entirely contained in the union of $\frac{1}{8}s$ -balls around c_1^k, \dots, c_n^k if and only if $r^k = c_i^k$ for some $i \in [k]$, the robber has a direction in which he can move to escape being captured in this move.

For the upper bounds, the strategies of the cops are the same, their starting position is without loss of generality the origin. We consider an appropriate copy of their starting position in the covering space, and play the game in the covering space. To show $c(S) \leq 2$ we imagine their starting positions in the covering space, so that after the first round the robber is on the line between the cops. To show $c_0(S) \leq n+1$, we imagine the cops starting positions in the covering space such that the robber is caught in a simplex. Using the same strategies as before gives the upper bound. \square

2.3.5 Hyperbolic Surfaces

In this section we turn to the Cops and Robber game on hyperbolic surfaces S . An important tool that we will be using for $c(S)$ and $c_0(S)$ is the standard fact that one cop can guard an isometric path by Lemma 2.6. We will show that if the game is played with two cops, one cop can come arbitrarily close to the robber with the help of the second cop, by playing the game in the universal covering space \mathcal{D} . In order to establish that one cop c_1 is coming closer and closer to the robber, we will need to use geometric properties of the hyperbolic plane, which we describe in the following.

First, consider Figure 2.10 and let the robber's position be X_1 and the cops position be A . The robber moves to B , while the cop moves as close to B as possible in the same time. Essentially, if their starting positions are closer together (at positions X_2 and X_3), then their end positions are closer together.

Lemma 2.25 ([W12]). Let $T(A, B, C)$ be a hyperbolic triangle with corners A, B, C , where the angle at C is a right angle. If $X_1 \in \overline{AC}$, then

$$d(A, B) - d(X_1, B) = \max_{X_2, X_3 \in \overline{AX_1}} d(X_2, B) - d(X_3, B).$$

Moreover, $d(A, B) - d(X_1, B) = d(X_2, B) - d(X_3, B)$ if and only if $X_2 = A$ and $X_3 \neq X_1$.

Proof. This is a simple application of Pythagoras' Theorem for hyperbolic triangles. Suppose $X, Y \in \overline{AC}$ with $X \in \overline{YC}$. Since \cosh is strictly increasing on the positive real axis and acosh is strictly increasing

$$\begin{aligned} d(Y, B) &= \operatorname{acosh}(\cosh(d(B, C)) \cosh(d(Y, C))) \\ &\geq \operatorname{acosh}(\cosh(d(B, C)) \cosh(d(X, C))) = d(X, B) \end{aligned}$$

with equality if and only if $X = Y$. The lemma follows by using this inequality twice,

$$d(X_2, B) - d(X_3, B) \leq d(A, B) - d(X_3, B) \leq d(A, B) - d(X_1, B).$$

Clearly, $d(X_2, B) - d(X_3, B) = d(A, B) - d(X_1, B)$ if and only if $X_2 = A$ and $X_3 = X_1$. \square

Now let the robber be at position X_3 in Figure 2.10 and the cop be at position A , the robber moves to B and the cop moves as close to B as possible in the same time. Essentially, if their starting positions are closer to C along the segment \overline{AC} while their distance is the same (their new positions are X_2 and X_1), then their end positions are closer together.

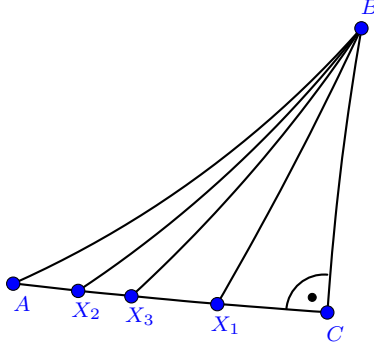


Figure 2.10: A hyperbolic right angled triangle with vertices A, B, C , the right angle is at C . The points X_1, X_2, X_3 are on the geodesic \overline{AC} .

Lemma 2.26 ([W12]). Let $T(A, B, C)$ be a hyperbolic triangle with corners A, B, C , where the angle at C is a right angle. If $X_3 \in \overline{AC}$, then

$$d(A, B) - d(X_3, B) = \max_{X_1, X_2 \in \overline{AC}, d(X_1, X_2) = d(A, X_3)} d(X_2, B) - d(X_1, B).$$

Proof. For a vertex $X \in \overline{AC}$, by Pythagoras' Theorem for hyperbolic triangles

$$d(X, B) = \operatorname{acosh}(\cosh(d(B, C)) \cosh(d(X, C))).$$

The second derivative with respect to $d(X, C)$ is

$$\frac{\partial^2 d(X, B)}{\partial d(X, C)^2} = \frac{(\cosh(d(X, C)) \cosh(d(B, C)) \sinh^2(d(B, C)))}{(-1 + \cosh^2(d(B, C)) \cosh^2(d(X, C)))^{3/2}}.$$

Therefore, $\frac{\partial^2 d(X, B)}{\partial d(X, C)^2} > 0$ for positive values of $d(B, C)$ and $d(X, C)$, hence $d(X, B)$ is convex for $d(X, C) > 0$. This means that the secant

$$\frac{d(X, B) - d(Y, B)}{d(X, C) - d(Y, C)}$$

is monotonely increasing (in both $d(X, C)$ and $d(Y, C)$). Consequently,

$$\begin{aligned} \frac{d(A, B) - d(X_1, B)}{d(A, X_1)} &= \frac{d(A, B) - d(X_1, B)}{d(A, C) - d(X_1, C)} \\ &\geq \frac{d(X_2, B) - d(X_3, B)}{d(X_2, C) - d(X_3, C)} = \frac{d(X_2, B) - d(X_3, B)}{d(X_2, X_3)}, \end{aligned}$$

and since $d(A, X_1) = d(X_2, X_3)$, this proves the lemma. \square

The next lemma helps to compare triangles where two sides have the same length.

Lemma 2.27 ([W12]). Suppose A, B, C, A', B', C' are hyperbolic triangles with $d(A, B) = d(A', B')$, $d(B, C) = d(B', C')$ and $\angle BCA > \angle B'C'A' > \frac{\pi}{2}$. Then $d(A, C) < d(A', C')$.

Proof. We will use the hyperbolic 4-parts formula

$$\cos(\angle ABC) \cosh(d(B, C)) + \sin(\angle ABC) \cos(\angle BCA) = \sinh(d(B, C)) \coth(d(A, B)),$$

which also holds by replacing A, B, C with A', B', C' . Therefore

$$\begin{aligned} & \cos(\angle ABC) \cosh(d(B, C)) + \sin(\angle ABC) \cos(\angle BCA) \\ &= \cos(\angle A'B'C') \cosh(d(B', C')) + \sin(\angle A'B'C') \cos(\angle B'C'A'). \end{aligned}$$

Since $\angle BCA > \angle B'C'A' > \pi/2$ it holds that $\angle ABC < \angle A'B'C' < \pi/2$. Now by the law of cosines

$$\cosh(d(A, C)) = \cosh(d(A, B)) \cosh(d(B, C)) - \sinh(d(A, B)) \sinh(d(B, C)) \cos(\angle ABC)$$

and also here the same formula holds by replacing A, B, C with A', B', C' , hence

$$\begin{aligned} & \cosh(d(A, C)) + \sinh(d(A, B)) \sinh(d(B, C)) \cos(\angle ABC) \\ &= \cosh(d(A', C')) + \sinh(d(A', B')) \sinh(d(B', C')) \cos(\angle A'B'C'). \end{aligned}$$

Since $\angle ABC < \angle A'B'C' < \pi/2$ and $\sinh(x)$ is positive for positive values of x , it holds that $d(A, C) < d(A', C')$, which proves the lemma. \square

Using the lemmas, we are now ready to prove our main theorem. Instead of playing the Cops and Robber game on the hyperbolic surface, we will consider the game on the universal covering space \mathcal{D} . For a player x , we will denote by x^k the player's position in \mathcal{D} after round k . We say two points A, B are on opposite sides of the geodesic h if A, B are in distinct connected components of the Poincaré disk $\mathcal{D} \setminus h$. If two points A, B are not on opposite sides, we say they are on the same side.

Theorem 2.28 ([W12]). If S is a compact hyperbolic surface, then $c(S) = 2$.

Proof. Let $s = \text{sys}(S)$ be the systolic girth of the hyperbolic surface S , which is the length of the smallest non-contractible curve.

To show that $c(S) > 1$ we play the game with one cop c and the robber r . The robber chooses the agility function $\tau \equiv \frac{s}{8}$ and initial positions such that $d(c^0, r^0) > \frac{s}{8}$. We explain the robber's strategy which he can use to stay at distance at least $\frac{\text{sys}(S)}{8} = \frac{s}{8}$ to the cop. Informally, the robber's strategy is to move in the direction opposite to the cop's position.

If $d(c^k, r^k) \geq \frac{3s}{8}$, then the robber's strategy is to stay at the same place, which means $r^{k+1} = r^k$. Then $d(c^{k+1}, r^{k+1}) \geq d(c^k, r^{k+1}) - \frac{s}{8} \geq \frac{s}{4}$. If $d(c^k, r^k) < \frac{3s}{8}$, the robber moves

in the direction opposite to the cop's position, i.e. the shortest paths from r^k to c^k and r^k to r^{k+1} meet at r^k at angle π . To argue that such a position exists with the additional assumption that $d(r^{k+1}, c^k) = d(r^k, c^k) + \frac{s}{8}$, the Gauss-Bonnet Theorem can be applied. The Gauss-Bonnet Theorem states that for a region $R \subset S$ with sectional curvature K , piecewise smooth boundary $\partial(R)$,

$$\int_R K dA + \int_{\partial(R)} k_g ds = 2\pi\chi(R),$$

where dA is the element of area of the surface, and ds is the line element along the boundary, and $\int_{\partial(R)} k_g ds$ is the sum of the corresponding integrals of the geodesic curvature k_g along the smooth portions of the boundary, plus the sum of the angles by which the smooth portions turn at the corners of the boundary. Consider the curve C which is piecewise geodesic, going from c^k to r^{k+1} along g and from r^{k+1} to c^k along an isometric path. Since the curve C has length strictly smaller than s , it has to be contractible. C bounds a region R . Since the curvature of locally isometric curves is 0, by Gauss-Bonnet

$$\int_R -1dA + \theta_1 - \pi + \theta_2 - \pi = 2\pi\chi(R),$$

where θ_1, θ_2 are the exterior angles between the locally isometric paths at r^{k+1} and c^k . Since C is contractible, the Euler characteristic of R is 1, hence $\theta_1 = \theta_2 = \pi$ and $\int_R 1dA = 0$, which means that the isometric path between c^k to r^{k+1} goes along the geodesic g , and $d(c^k, r^{k+1}) = d(c^k, r^k) + \frac{s}{8} > \frac{s}{4}$ and hence $d(c^{k+1}, r^{k+1}) > \frac{s}{8}$. In both cases the robber can stay at distance at least $\frac{s}{8}$ to the cop, which proves the lower bound.

For the upper bound, suppose we play the game with two cops c_1, c_2 and the robber r . If the robber was only escaping from cop c_1 , then by the above argument his strategy could be to stay roughly on the geodesic defined by the current positions of the robber r and cop c_1 . Since we have two cops available, we can force the robber to take a different strategy. The idea of the cops' strategy is that cop c_1 will chase the robber, while cop c_2 will force the robber to move away from the geodesic defined by r, c_1 , allowing cop c_1 to move closer to r . We will play the game on the universal covering space on the Poincaré disk \mathcal{D} . Let $D = \text{diam}(S)$.

The robber chooses an agility function τ and the starting position c_1^0, c_2^0, r^0 . Let $0 = t_0 < t_1 < t_2 < t_3 < \dots$ be a sequence of integers representing time steps such that

$$\sum_{k=t_i}^{t_{i+1}-1} \tau_k \geq 30D.$$

Our goal is to show that for every $\varepsilon > 0$ the cops c_1, c_2 have a strategy in which the cop c_1 can come ε -close to the robber r , which means the cops win the ε -approaching game. By Theorem 2.4, if the cops can win the ε -approaching game, they can win the game. We

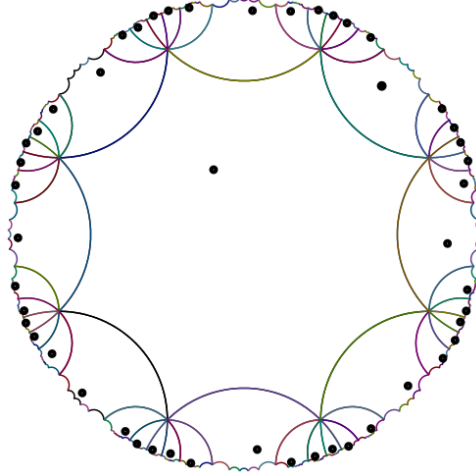


Figure 2.11: Copies of the fundamental polygon $P(4g, \frac{2\pi}{4g})$ in \mathcal{D} . Depicted is a point and one copy of this point in each of the depicted copies of the fundamental polygon.

show that if $d(c_1^{t_i}, r^{t_i}) \geq \varepsilon$ then there exists some $\delta = \delta(\varepsilon) > 0$, such that if the cops c_1, c_2 follow their strategy then either

$$d(c_1^{t_{i+1}}, r^{t_{i+1}}) \leq \varepsilon$$

or

$$d(c_1^{t_{i+1}}, r^{t_{i+1}}) \leq d(c_1^{t_i}, r^{t_i}) - \delta,$$

which means eventually the cop c_1 will be ε -close to the robber.

Let $k_0 := t_i$ for some $i > 0$. Let $r^{k_0}, c_1^{k_0}$ be a copy of the robber's and cop's position in the universal covering space \mathcal{D} , such that their distance in the universal covering space is the same as on the surface. We consider the geodesic g_0 through $r^{k_0}, c_1^{k_0}$. We explain the strategy of the cop c_2 first. Since we play the game in the covering space \mathcal{D} , we have arbitrarily many copies of the position of c_2 that we can choose from (see Figure 2.11). The starting position $c_2^{k_0}$ for cop c_2 is such that it is close to the geodesic g_0 but sufficiently far from r^{k_0} , which we make more precise in the following.

Let P be the point on g_0 at distance $10D$ to r^{k_0} that is further away from $c_1^{k_0}$. Note that there is a copy $c_2^{k_0}$ in the universal covering space which is at distance at most D from P , this will be the starting position of c_2 . We consider $h = o_{g_0}(c_2^{k_0})$, the orthogonal geodesic to g_0 through $c_2^{k_0}$. The next claim shows that the cop c_2 can reach his closest point on the geodesic g_0 in much faster time than the robber can.

Claim 2.29. $h \cap g_0$ is at distance between $9D$ and $11D$ from r^{k_0} and at distance at most D from $c_2^{k_0}$.

The closest point from $c_2^{k_0}$ to g_0 is at most the distance from $c_2^{k_0}$ to P , which is at most D . Note that the closest point from $c_2^{k_0}$ to g_0 is $h \cap g_0$ since there is a right angle between h and g_0 . The closest point from P to h is also $h \cap g_0$ since $P \in g_0$. In particular, $h \cap g_0$ is closer to P than $c_2^{k_0}$, so $d(h \cap g_0, P) \leq D$. The distance from r^{k_0} to P is $10D$, so by the triangle inequality his distance to $c_2^{k_0}$ is between $9D$ and $11D$. This proves Claim 2.29.

The strategy of c_2 is to chase the orthogonal projection of r on h . Note that by Claim 2.29 the distance from r^{k_0} to h is at least $9D$. Let B, B' be points on h at distance $8D$ from $B_0 := g_0 \cap h$. The cop c_2 can guard the path from B to B' on h , since his distance to B_0 is at most D , so his distance to B, B' is at most $9D$, which is at least the distance from r^{k_0} to B, B' . For $k \geq k_0$, let $g_k = o_h(c_1^k)$ and let $B_k = g_k \cap h$, see Figure 2.12.

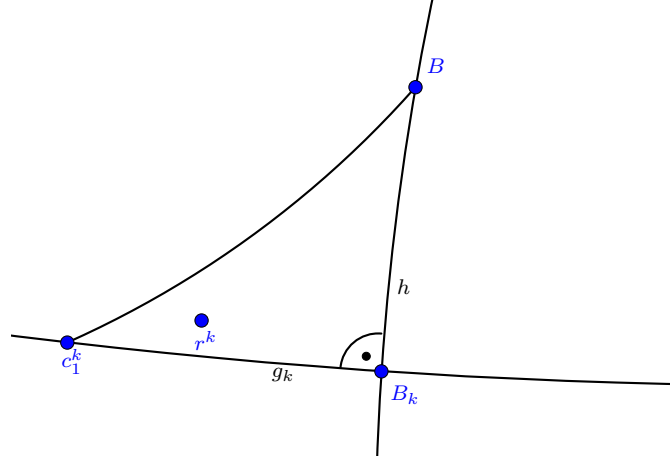


Figure 2.12: A schematic picture of cop's position c_1 and robber's position r at time step k .

Since the cop c_2 guards the path from B to B' , the robber r has to cross the geodesic segment $\overline{c_1^k B}$ (or the symmetric case $\overline{c_1^k B'}$). Since in round k the robber makes a step before the cop, the robber crosses $\overline{c_1^k B}$ in step $k + 1$.

In the following we will give a strategy of the cop c_1 , so that the best strategy for the robber r is to cross $\overline{c_1^k B}$ close to B . Suppose r^k, r^{k+1} are on the same side as B with respect to g_k . Then we move cop c_1 towards B such that:

$$\text{The robber's position } r^{k+1} \text{ and } B \text{ are on the same side of } g_{k+1}. \quad (2.3)$$

The $(k + 1)$ -st position c_1^{k+1} of cop c_1 is

- (a) the point between c_1^k and B s.t. $d(c_1^{k+1}, c_1^k) = \tau_{k+1}$ if this step does not violate (2.3),
- (b) otherwise, the closest point to r^{k+1} on the geodesic $o_h(r^{k+1})$ with $d(c_1^{k+1}, c_1^k) = \tau_{k+1}$.

The strategy is similar if the robber moves towards B' . By symmetry we can assume that the first step of the robber away from the geodesic g_0 is towards B . Now, suppose that the robber crosses g_k by going from step r^k to step r^{k+1} , see Figure 2.13. By splitting each

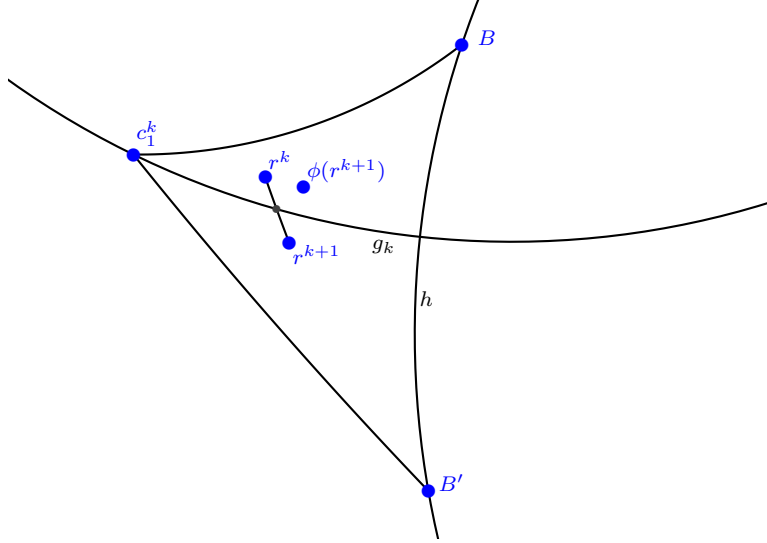


Figure 2.13: The point $\phi(r^{k+1})$ is the reflection point of r^{k+1} over g_k .

such step into two substeps we may consider the first substep as above, initial and ending position on the same side as B , and the second substep with initial and ending position on the same side as B' . In the first substep the cop c_1 moves along g_k towards the robber. In the second substep the cop imagines the robber to move to $\phi(r^{k+1})$, which is the reflection of the position r^{k+1} along g_k , and determines his position $\phi(c_1^{k+1})$ by using strategy (a) or (b). She then reflects the position $\phi(c_1^{k+1})$ along g_k to obtain c_1^{k+1} . After subdividing each of the robber's steps at most once, by symmetry we can assume the robber does not cross g_k , which means the position r^{k+1} is on the same side of the geodesic g_k as B .

Recall that in round t the robber makes a step before the cops make their step. Let t be the first round at which the robber crosses $\overline{c_1^{t-1}B}$. We can assume without loss of generality that $r^t = x \in \overline{c_1^{t-1}B}$ by subdividing the step and letting the agility at time step t be $d(x, r^{t-1})$. Let us consider the right triangle on vertices c_1^{t-1}, B_{t-1}, B , recall that $B_k = g_k \cap h$, see Figure 2.12. We define a function

$$f_t : \overline{c_1^{t-1}B} \rightarrow \mathbb{R}, \quad f_t(x) = d(c_1^{t-1}, x) - d(r^{t-1}, x).$$

The function f describes the (maximal) distance between c_1^t and $r^t = x$ given c_1^{t-1}, r^{t-1} . Note that by the triangle inequality, $f_t(x) < d(c_1^{t-1}, r^{t-1})$ unless $d(c_1^{t-1}, r^{t-1}) = 0$ since x, c_1^{t-1} and r^{t-1} are not on a common geodesic. In order to maximise his distance to cop c_1 , we show that the best choice for the robber is to move to B in his last step (we ignore that the robber would be caught by c_2).

Claim 2.30. Given fixed positions c_1^{t-1} and r^{t-1} such that r^{t-1} is in the triangle defined by c_1^{t-1}, B, B_{t-1} , it holds that

$$f_t(B) = \max_{x \in \overline{c_1^{t-1}B}} f(x)$$

Suppose $x \in \overline{c_1^{t-1}B}$ and $x \neq B$. We consider the triangle defined by x, B, r^{t-1} . Since x is on a common geodesic with c_1^{t-1} and B ,

$$f_t(B) = d(c_1^{t-1}, B) - d(r^{t-1}, B) = (d(c_1^{t-1}, x) + d(x, B)) - (d(r^{t-1}, B) - d(r^{t-1}, x)) - d(r^{t-1}, x).$$

By the triangle inequality, $d(x, B) \geq d(r^{t-1}, B) - d(r^{t-1}, x)$, hence $f_t(B)$ is at least $f_t(x) = d(c_1^{t-1}, x) - d(r^{t-1}, x)$. This proves Claim 2.30.

Let r^{k_0}, \dots, r^t be a sequence of $t - k_0$ steps such that $r^t \in \overline{c_1^{t-1}B}$ and r^k is in the interior of the triangle $c_1^{k-1}BB_k$ for $k = k_0, \dots, t - 1$ (given the prescribed strategy of cop c_1). We define

$$g(t) := \max_{r^{k_0}, \dots, r^t, \tau} d(c_1^t, r^t).$$

Note that the maximum is well-defined since S is compact and we can assume $\tau_k < D$. Hence let r^{k_0}, \dots, r^t be a sequence such that $d(c_1^t, r^t) = g(t)$. We will show that $g(t) \leq g(k_0 + 1)$ by showing that $g(t) \leq g(t - 1)$. We can assume that the last step of the cop c_1 is of type (a) (the type refers to the strategy that the cop c_1 used), otherwise the robber is caught, and $0 = g(t) \leq g(t - 1)$. We can assume $r^t = B$ by Claim 2.30. Suppose the second last step from c_1^{t-2} to c_1^{t-1} is of type (a). Then it is of advantage to the robber to move along the geodesic segment $\overline{r^{t-2}B}$ during the last two steps since

$$\begin{aligned} d(c_1^{t-2}, B) - d(r^{t-2}, B) &= d(c_1^{t-2}, c_1^{t-1}) + d(c_1^{t-1}, B) - d(r^{t-2}, B) \\ &\geq d(c_1^{t-2}, c_1^{t-1}) + d(c_1^{t-1}, B) - (d(r^{t-2}, r^{t-1}) + d(r^{t-1}, B)) \\ &\geq d(c_1^{t-1}, B) - d(r^{t-1}, B). \end{aligned}$$

Hence by maximality of r^{k_0}, \dots, r^t , we can assume $r^{t-1} \in \overline{r^{t-2}B}$. But then we can merge the last two steps $t - 2 \rightarrow t - 1$ and $t - 1 \rightarrow t$ to one step $t - 2 \rightarrow t$, since it does not change the strategy of the cop, and $g(t) \leq g(t - 1)$.

Now assume the step from c_1^{t-2} to c_1^{t-1} is of type (b). Let z_c be the intersection point of g_{t-1} and $\overline{c_1^{t-2}B}$, see Figure 2.14. By Lemma 2.25 we can assume

$$\tau_{t-1} = d(r^{t-1}, r^{t-2}),$$

otherwise decreasing τ_{t-1} (at most until $c_1^{t-1} = z_c$) is a better strategy for the robber.

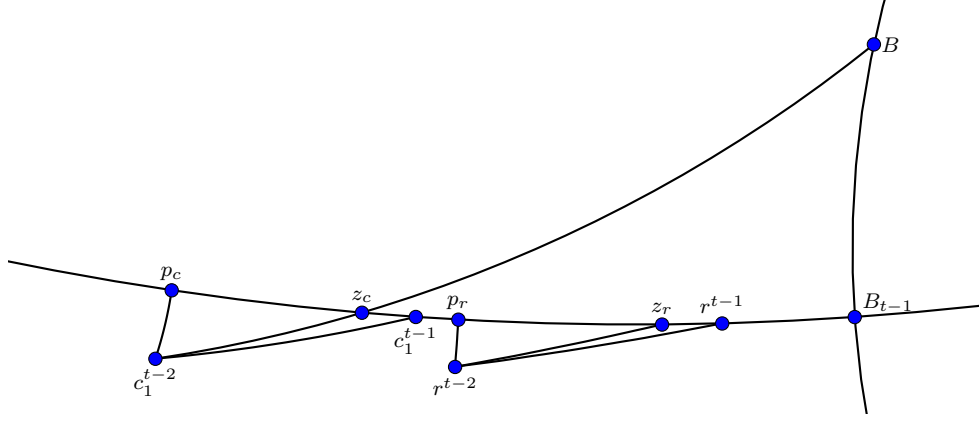


Figure 2.14: The case when the second last move of the robber is of type (b).

Let z_r^1, z_r^2 be the points on g_{t-1} such that they are at the same distance from the robber's position r^{t-2} as z_c is from the cop's position c_1^{t-2} . Let z_r^1 be closer to B_{t-1} . Note that the robber's position is either in $\overline{z_r^1 B_{t-1}}$ or in $\overline{z_r^2 z_c}$. The second case can not happen since by Lemma 2.25, $r^{t-1} = z_r$ would give $c_1^{t-1} = z_c$ and that would be a better choice for the robber, contradicting maximality of r^{k_0}, \dots, r^t . We denote $z_r = z_r^1$ and then $r^{t-1} \in \overline{z_r B_{t-1}}$, see Figure 2.14.

Claim 2.31. It is of advantage to the robber to move to z_r instead of r^{t-1} .

Let p_c, p_r be the closest points on g_{t-1} from c_1^{t-2}, r^{t-2} , respectively. This means the angles $\angle c_1^{t-2} p_c B_{t-1}, \angle r^{t-2} p_r B_{t-1}$ are right angles. There are two Lambert quadrilaterals formed by $c_1^{t-2}, p_c, B_{t-1}, B_{t-2}$ and $r^{t-2}, p_r, B_{t-1}, o_h(r^{t-2}) \cap h$, respectively. Any two sides of a Lambert quadrilateral determines the length of the other sides, see [106]. In particular, since $d(B_{t-1}, o_h(r^{t-2}) \cap h) \leq d(B_{t-1}, B_{t-2})$ and $d(p_r, B_{t-1}) < d(p_c, B_{t-1})$, it holds that

$$d(p_r, r^{t-2}) < d(p_c, c_1^{t-2}).$$

Therefore by the sine formula for hyperbolic right triangles, $\angle p_c z_c c_1^{t-2} > \angle p_r z_r r^{t-2}$ and

$$\angle c_1^{t-2} z_c c_1^{t-1} < \angle r^{t-2} z_r r^{t-1}.$$

Since $d(c_1^{t-2}, z_c) = d(r^{t-2}, z_r)$ and $d(c_1^{t-2}, c_1^{t-1}) = d(r^{t-2}, r^{t-1})$, it holds by Lemma 2.27 that $d(z_r, r^{t-1}) < d(z_c, c^{t-1})$. By Lemmas 2.26 and 2.25 we have

$$d(B, z_c) - d(B, z_r) > d(B, r^{t-1}) - d(B, c_1^{t-1}).$$

Hence it is of advantage for the robber to move to z_r instead of r^{t-1} , a contradiction to the maximality of r^{k_0}, \dots, r^t . This proves Claim 2.31, which means that the second last step of the cop is of type (a) and this means $g(t) \leq g(t-1)$.

We will establish now a positive lower bound on $d(r^{k_0}, c_1^{k_0}) - d(r^t, c_1^t)$. By Pythagoras' Theorem for hyperbolic triangles

$$\begin{aligned} d(r^t, c_1^t) &\geq \operatorname{acosh}(\cosh(d(B, B_0)) \cosh(d(c^{k_0}, B_0))) - \operatorname{acosh}(\cosh(d(B, B_0)) \cosh(d(r^{k_0}, B_0))) \\ &= \operatorname{acosh}(c_1 \cosh(d(c^{k_0}, r^{k_0}) + d(r^{k_0}, B_0))) - \operatorname{acosh}(c_1 \cosh(d(c^{k_0}, r^{k_0}) + d(r^{k_0}, B_0))), \end{aligned}$$

where $a_1 = \cosh(8D) > 1$. Note that by the mean value theorem for $x < y$

$$\operatorname{acosh}(a_1 \cosh(x)) - \operatorname{acosh}(a_1 \cosh(y)) \geq a_2(y - x)$$

where $a_2 = \min_{\xi \in [x, y]} \partial/\partial \xi(\operatorname{acosh}(a_1 \cosh(\xi)))$. Since $a_1 > 0$, the partial derivative is

$$\frac{\partial}{\partial x} \operatorname{acosh}(a_1 \cosh(x)) = \frac{a_1 \sinh(x)}{\sqrt{a_1^2 - 1 + a_1^2 \sinh^2(x)}}.$$

Taking $x = d(r^{k_0}, B_0)$ and $y = d(c_1^{k_0}, B_0)$ and since $d(c_1^{k_0}, B_0) \leq 12D$,

$$a_2 \geq \frac{a_1 \sinh(12D)}{\sqrt{a_1^2 - 1 + a_1^2 \sinh^2(12D)}} \geq 1 + \delta$$

for some $\delta > 0$. Since $y - x = d(r^{k_0}, c_1^{k_0}) \geq \varepsilon$, it follows that

$$d(r^t, c_1^t) - d(r^{k_0}, c_1^{k_0}) \geq \delta \varepsilon.$$

Recall that $k_0 = t_i$ for some i . It is left to show that $t \leq t_{i+1}$. At step k the cop c_1 is moving closer to B and h , and by the triangle inequality on the triangle c_1^{k-1}, c_1^k and $g_k \cap \overline{c_1^{k-1} B}$, she is either moving $\tau_k/2$ closer to B or $\tau_k/2$ closer to h . By the triangle inequality, $d(c_1^{k_0}, B) \leq d(c_1^{k_0}, B_0) + d(B_0, B) \leq 11D + 8D = 19D$, hence the cop either meets B or h after moving for time $30D$.

From step t_i until step t_{i+1} , the strategy of cop c_1 is to simply follow the robber, while the strategy of cop c_2 is to stay in the same position. \square

We will now turn to c_0 . We show that on a hyperbolic surface at least three cops are needed to catch the robber.

Theorem 2.32 ([W12]). If S is a hyperbolic surface, then $c_0(S) \geq 3$.

Proof. Let r^k, c_1^k, c_2^k be the robber and the cops' positions after step k . Let $s = \operatorname{sys}(S)$ be the systolic girth of the surface S . The robber chooses the following agility function $\tau \equiv \frac{s}{10}$ and starting positions r^0, c_1^0, c_2^0 where r^0 is distance more than $\frac{s}{10}$ away from c_1^0, c_2^0 . In fact, it suffices to assume that $r^0 \neq c_1^0, c_2^0$. We show that if $r^k \neq c_1^k, c_2^k$ then there exists a position r^{k+1} at distance at most $\frac{s}{10}$ from r^k with $d(r^{k+1}, c_j^k) > \frac{s}{10}$ ($j = 1, 2$), and hence the robber can escape from the cops.

Suppose $d(r^k, c_j^k) > \frac{s}{5}$. Then the robber's strategy is to stay in the same place, and $d(r^{k+1}, c_j^k) > \frac{s}{5}$. If $d(r^k, c_1^k) \leq \frac{s}{5}$ and $d(r^k, c_2^k) > \frac{s}{5}$, then the robber moves away from cop c_1 , r^{k+1} is the point at distance $\frac{s}{10}$ on the geodesic through r^k, c_1^k which is further away from c_1^k . We consider $B(r^k, \frac{s}{5})$, the disk of radius at most $\frac{s}{5}$ from r^k on S and this is isometric to a hyperbolic disk since the systolic girth on our surface S is s . In order to see that $B(r^k, \frac{s}{5})$ is isometric to a hyperbolic disk, consider $B(r^k, \frac{s}{5})$ as a disk in the universal covering space \mathcal{D} . Let $x, y \in B(r^k, \frac{s}{5})$, then the geodesic segments g between x and y in the copy of $B(r^k, \frac{s}{5})$ in the universal covering space \mathcal{D} is a locally isometric path from x to y in S . Suppose $\overline{xy} \neq g$. Then the closed path going from x to y along \overline{xy} and from y to x along g is of length less than s and consists of two paths which are locally isometric and bounds a region which is non-empty. By the same argument as in Theorem 2.28, this is not possible by the Gauss-Bonnet Theorem. It follows that $d(r^{k+1}, c_1^k) = d(r^k, c_1^k) + \frac{s}{10}$. By the triangle inequality $d(r^{k+1}, c_2^k) > \frac{s}{10}$. If $d(r^k, c_1^k) \leq \frac{s}{5}$ and $d(r^k, c_2^k) > \frac{s}{5}$ we use the same strategy by interchanging the roles of c_1, c_2 . Hence we can assume $d(r^k, c_1^k), d(r^k, c_2^k) \leq \frac{s}{5}$. Note that c_1^k, c_2^k are now in the hyperbolic disk $B(r^k, \frac{s}{5})$ of radius $\frac{s}{5}$ centred at r^k . We consider the disk $B(r^k, \frac{s}{5})$ being embedded in the Poincaré disk, and consider the geodesic h through c_1^k, c_2^k in this disk and let $o_h(r^k)$ be the orthogonal geodesic to h passing through r^k . Now let r^{k+1} be the point at distance $\frac{s}{10}$ on the geodesic $o_h(r^k)$ which is further away from g . If c_j^k is on $o_h(r^k)$ then $d(r^{k+1}, c_j^k) = d(r^k, c_j^k) + \frac{s}{10} > \frac{s}{10}$. If c_j^k is not on $o_h(r^k)$, then $\angle c_j^k, o_h(r^k) \cap h, r^{k+1}$ form a right angle and by the hyperbolic Pythagoras' theorem $d(c_j^k, r^{k+1}) > \frac{s}{10}$. \square

The following theorem shows how to capture the robber on the universal covering space \mathcal{D} , if the robber is contained in a polygon which is guarded by the cops.

Lemma 2.33 ([W12]). Suppose the robber is contained in a bounded convex polygon in the Poincaré disk \mathcal{D} where n cops guard the boundary of the polygon. Then these n cops can catch the robber.

Proof. Let the robber's position be r^0 and the cops' positions be c_1^0, \dots, c_n^0 . For all $k \geq 0$ we consider the bisectors b_j^k between the robber's position r^k and each of the cops' positions c_j^k ($j = 1, \dots, n$), and let B_j^k be the midpoint between r^k and c_j^k , see Figure 2.15. Since the k cops can contain the robber in the convex region, the bisectors b_j^0 bound a polygon P_0 containing the robber, otherwise there is a point on the boundary towards which the robber can walk and escape from the cops for infinitely long. Let $\alpha_{j,j+1}^k$ be the angle between the bisector b_j^k and b_{j+1}^k (we consider the indices modulo n) and let $P_{j,j+1}^k$ be their intersection point. The cops follow a very natural strategy, cop c_j copies the move of the robber by reflecting it along the bisector b_j and subsequently if there is any agility left she moves as close to the robber as possible. More precisely, in the k -th round the cop c_j^{k-1} will move to $o_{b_j^{k-1}}(r^k)$, as close to the robber as possible. We have to show that with this strategy the robber is eventually caught. We show our first claim.

Claim 2.34. The angles in the guarded polygon are increasing, which means

$$\alpha_{j,j+1}^k \geq \alpha_{j,j+1}^{k-1}.$$

We consider the step of the cop c_j and the cop c_{j+1} separately, imagining the cop c_j takes his turn first. Let P' be the intersection point between b_j^k, b_{j+1}^{k-1} and let α' be the angle between b_j^k, b_{j+1}^{k-1} . If $b_j^k = b_j^{k-1}$, then $\alpha' = \alpha_{j,j+1}^{k-1}$. Otherwise $b_j^k \neq b_j^{k-1}$ and note that b_j^k is orthogonal to $o_{b_j^{k-1}}(r^k)$. Since the quadrilateral $B_j^k, B_j^{k-1}, P_{j,j+1}^{k-1}, P'$ has angle sum smaller than 2π and has a right angle at B_j^{k-1} and B_j^k , it holds that the angle at P' in the quadrilateral is smaller than $\pi - \alpha_{j,j+1}^{k-1}$ but then $\alpha' > \alpha_{j,j+1}^{k-1}$. Now we consider the quadrilateral formed by $B_{j+1}^k, B_{j+1}^{k-1}, P', P_{j,j+1}^k$. By the same argument, $\alpha_{j,j+1}^k > \alpha'$. This proves Claim 2.34.

Let

$$\alpha = \min_{j \in [n]} \alpha_{j,j+1}^0$$

and

$$D = \max_{j \in [n]} d(P_{j,j+1}^0, P_{j+1,j+2}^0).$$

Claim 2.35. Let $\beta_{j,j+1}^k$ be the angle between $r^k c_j^k$ and $r^k c_{j+1}^k$. If $\alpha_{j,j+1}^k \leq (n-2)\pi/n$, then

$$\operatorname{acot}\left(\frac{\cosh(D)}{\cot((n-2)\pi/n)}\right) \leq \beta_{j,j+1}^k \leq \pi - \alpha.$$

Since $\alpha_{j,j+1}^k \leq (n-2)\pi/2$, there is a quadrilateral formed by $r^k B_j^k P_{j,j+1}^k B_{j+1}^k$ with right angles at B_j^k and B_{j+1}^k . Since a quadrilateral has angle sum at most 2π and $\alpha_{j,j+1}^k \geq \alpha$ it holds that $\beta_{j,j+1}^k \leq \pi - \alpha$. On the other hand,

$$\cot(\angle P_{j,j+1}^k r^k B_j^k) = \frac{\cosh(d(P_{j,j+1}^k, r^k))}{\cot(\angle r^k P_{j,j+1}^k B_j^k)} \leq \frac{\cosh(D)}{\cot((n-2)\pi/n)},$$

hence $\beta_{j,j+1}^k \geq \angle P_{j,j+1}^k r^k B_j^k \geq \operatorname{acot}\left(\frac{\cosh(D)}{\cot((n-2)\pi/n)}\right)$. This proves Claim 2.35.

Note that for some i and all $k \geq 0$, $\alpha_{i,i+1}^k \leq (n-2)\pi/n$ since the angle sum in a hyperbolic n -gon is upper bounded by the angle sum in an Euclidean n -gon. Without loss of generality $i = 1$. Let

$$\beta = \min\left\{\operatorname{acot}\left(\frac{\cosh(D)}{\cot((n-2)\pi/n)}\right), \alpha\right\}.$$

For $k \geq 1$ we consider the geodesic h^k through r^{k-1}, r^k . Note that h^k and $r^k c_1^k$ intersect at r^k . If the angle between h^k and $r^k c_1^k$ is in $[\pi/2 - \frac{\beta}{2}, \frac{\pi}{2})$, then the angle between h^k and $r^k c_2^k$ is at most $\pi/2 - \frac{\beta}{2}$ by Claim 2.35. Let K_i for $i = 1, 2$ be the set of rounds at which the angle

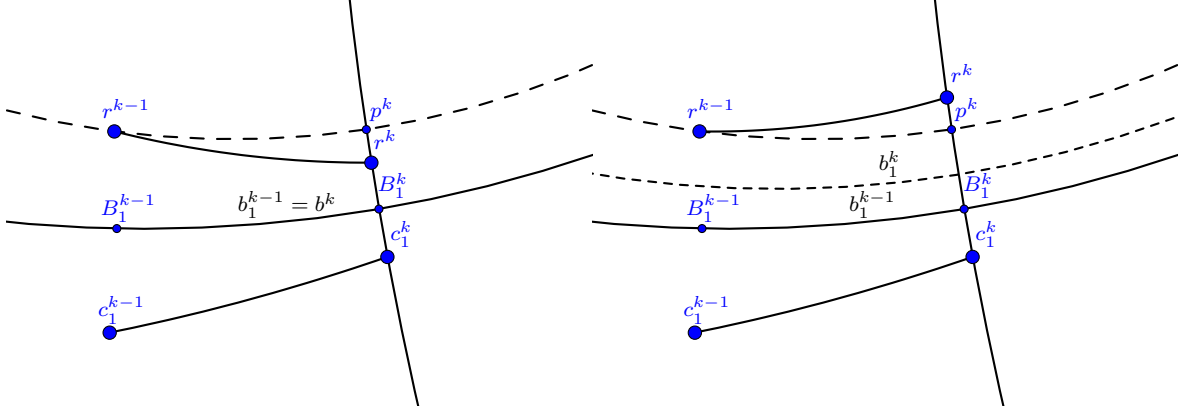


Figure 2.15: A step K_1^+ in comparison to a step K_1^- . In both cases the distance of r^k to p^k is the same and hence the move of cop c_1 is the same.

between h^k and c_j^k is at most $\pi/2 - \frac{\beta}{2}$. Without loss of generality,

$$\sum_{k \in K_1} \tau_k = \infty.$$

Suppose

$$\sum_{k \in K_1} \tau_k - d(r^k, r^{k-1}) = \infty,$$

in that case it is even easier for the cops to catch the robber. Note that while the robber is not caught, the distance between b_j^{k-1} and b_j^k is at least $\tau_k - d(r^k, r^{k-1})$. On the other side, throughout the whole game, the robber is caught in P_0 . The part of the Poincaré disk $\mathcal{D} \setminus b_j^k$ containing the cop c_j eventually surpasses P_0 , in which r^k is contained, which is a contradiction since b_j^k is a bisector.

Suppose now that

$$\sum_{k \in K_1} d(r^k, r^{k-1}) = \infty.$$

We consider the geodesic $r^k c^k$ and let p^k be the closest point to r^{k-1} on $r^k c^k$. Let K_1^+ be the time steps in K_1 in which the robber's position is closer to c_1^k than p^k and let K_1^- be the other steps, which means the robber's position c_1^k is further away from c_1^k than p^k , see Figure 2.15.

Using that $\tanh(x)$ is monotonly increasing and for small x ,

$$\tanh(x) \geq x \left(1 - \frac{x^2}{3}\right),$$

we get that

$$\sum_{k \in K_1} \tanh \left(d \left(r^k, r^{k-1} \right) \right) = \infty.$$

But then, since $\operatorname{atanh}(x) \geq x$, we also have

$$\sum_{k \in K_1} \operatorname{atanh} \left(\cos \left(\frac{\pi}{2} - \alpha \right) \right) \tanh \left(d \left(r^k, r^{k-1} \right) \right) = \infty.$$

Let us show how we can use this to end the proof. Consider the triangle $r^{k-1}p^k r^k$, with angle at most $\pi - \alpha$ at r^k . Then by Theorem 1.3,

$$d \left(r^k, p^k \right) \geq \operatorname{atanh} \left(\cos \left(\frac{\pi}{2} - \alpha \right) \right) \tanh \left(d \left(r^k, r^{k-1} \right) \right).$$

If k is a step of type K_1^- , then the distance between b_1^{k-1} and b_1^k is at least $d(r^k, p^k)$. Next, we consider the case when k is a step of type K_1^+ . Since $r^{k-1}p^k B_1^k B_1^{k-1}$ is a Lambert quadrilateral with acute angle at r^{k-1} , it holds that $d(r^{k-1}, B_1^{k-1}) \leq d(p^k, B_1^k)$. Hence $d(r^k, p^k)$ is the distance that the cop c_1 is getting closer to r in step k . But since $d(r^k, p^k) \geq \operatorname{atanh} \left(\cos \left(\frac{\pi}{2} - \alpha \right) \right) \tanh \left(d(r^k, r^{k-1}) \right)$, neither of these two can happen infinitely often, which means the robber is eventually caught. \square

We now use Lemma 2.33 to bound c_0 from above for the special surfaces $S(g)$, $S'(g)$ and $N(g)$.

Theorem 2.36 ([W12]). If $g \geq 2$, then (a) $c_0(S(g)) \leq 5$, (b) $c_0(S'(g)) \leq 6$ and (c) $c_0(N(g)) \leq 4$.

Proof. Let O be the midpoint of the fundamental polygon $P \left(4g, \frac{2\pi}{4g} \right)$. We will play the game in the universal covering space and choose the player's positions such that they are in $P \left(4g, \frac{2\pi}{4g} \right)$. We will first use the cops c_1, c_2, c_3 to guard isometric paths. We describe a strategy for c_1, c_2, c_3 that will ensure that at some time step and some $0 \leq i \leq g-1$ one cop guards the geodesic OV_{1+4i} and one cop guards the geodesic OV_{5+4i} and the robber is in one of the triangular regions $OV_{1+4i}v_{2+4i}$, $OV_{2+4i}v_{3+4i}$, $OV_{3+4i}v_{4+4i}$ or $OV_{4+4i}v_{5+4i}$. Note that as long as the cops guard OV_{1+4i} and OV_{5+4i} , the robber's moves are restricted to the specified triangles since $a_{4i+1} = a_{4i+3}^{-1}$ and $a_{4i+2} = a_{4i}^{-1}$.

We start by moving cop c_1 to the isometric path $\overline{OV_1}$, cop c_2 to the isometric path $\overline{OV_5}$ and cop c_3 to the isometric path $\overline{OV_9}$. By Lemma 2.6 we can assume that after a finite amount of time the cops guard the respective isometric paths. Now if the robber is in one of the triangles $OV_j v_{j+1}$ for some $1 \leq j \leq 8$, then we achieved our goal. Otherwise, we move cop c_2 to the isometric path $\overline{OV_{13}}$ and wait until she is guarding it. If the robber is in one of the triangles $OV_j v_{j+1}$ for $9 \leq j \leq 12$ then we are done. Otherwise we keep going in

the same way. Suppose the geodesics Ov_1, Ov_{1+4i} and Ov_{5+4i} are guarded for $i \leq g - 2$. Suppose the robber is in some triangle Ov_jv_{j+1} for $1 + 4i \leq j \leq 4g$. If $j \leq 4 + 4i$, we stop the process. Otherwise we move the cop currently guarding $\overline{Ov_{1+4i}}$ to guard $\overline{Ov_{1+4(i+2)}}$ unless $i + 2 = g$, in which case we stop the procedure. Without loss of generality cop c_1 guards Ov_1 and cop c_2 guards Ov_5 and the robber is in one of the triangles Ov_jv_{j+1} for some $1 \leq j \leq 8$. Cop c_3, c_4, c_5 will guard Ov_2, Ov_3, Ov_4 , respectively. Now the robber is captured in either $R_1 = Ov_1v_2 \cup Ov_3v_4$ or $R_2 = Ov_2v_3 \cup Ov_4v_5$. The regions R_1 and R_2 can be embedded in the universal covering space \mathcal{D} such that they form a quadrilateral which is bounded by four of the cops, respectively. By Lemma 2.33 we are done.

A similar idea can be used to show (b) and (c). For $S'(g)$, cop c_1 will stay on Ov_1 and cop c_2 will stay on Ov_{2g+1} . Cops c_3, c_4 will alternately guard the geodesic segments Ov_2, Ov_3, Ov_4, \dots and at the same time cops c_5, c_6 will alternately guard the geodesic segments $Ov_{2g+2}, Ov_{2g+3}, Ov_{2g+4}, \dots$ until the robber is caught in the region of the surface corresponding to the triangles $Ov_iv_{i+1} \cup Ov_{2g+1+i}v_{2g+2+i}$. This region is a quadrilateral in the universal covering space \mathcal{D} , and we are done by Lemma 2.33. On $N(g)$, we use three cops to capture the robber in a region $Ov_iv_{i+1} \cup Ov_{i+1}v_{i+2}$. We use two more cops to guard v_iv_{i+1} and Ov_{i+1} . Now the robber is caught in a region isomorphic to a triangle Ov_iv_{i+1} in the hyperbolic plane, and we are done by Lemma 2.33. \square

2.3.6 n-Dimensional Hyperbolic Space

The proof of Theorem 2.28 can be generalised to higher dimensional hyperbolic manifolds.

Theorem 2.37 ([W12]). If M is a compact hyperbolic manifold, then $c(M) = 2$.

Proof. Suppose the compact manifold M is \mathbb{H}^n/Γ where Γ is a torsion-free, discrete group of isometries on \mathbb{H}^n . Let D be the diameter of M . We can position the cop c_2 in the covering space such that it can guard some $n - 1$ -dimensional ball of radius $8D$ at distance between $9D$ and $11D$ from the robber's position, where the centre of the disk is on the geodesic $\overline{c_1^k r^k}$. Now at every step, we consider the positions c_1^k, r^k, r^{k+1} , they lie on a common 2-dimensional subspace of \mathcal{D}^n which is isometric to \mathcal{D}^2 and is also isometric as a subset of \mathcal{D}^n . Now the cop can use the strategies (a) and (b) outlined in Theorem 2.28 on this subspace. \square

2.3.7 Manifolds of Constant Curvature

We are ready to summarise our results about manifolds of constant curvature, such manifolds are also called *space forms*.

Theorem 2.38. Suppose M is a compact manifold of constant curvature, then $c(M) \leq 2$.

Proof. Suppose M is a real, smooth manifold, equipped with a Riemannian metric g_p . That is, M_g is a Riemannian manifold. Then if $C \neq 0$ is the curvature of M_g at each point $P \in M_g$,

equipping M with the Riemannian metric $g_p^* = |C| \cdot g_p$ gives a Riemannian manifold M_{g^*} of constant curvature 1 or -1 . Given the step function τ for M_g , we can play the game with step function $\sqrt{|C|} \cdot \tau$ on M_{g^*} instead. A step of a player from $x \in M$ to $y \in M$ of length $\tau(n)$ in M_g is a step of length $\sqrt{|C|} \cdot \tau(n)$ in M_{g^*} . Hence k cops can win the game on M_g if and only if they can win the game on M_{g^*} . By Theorem 2.18, if M_g has constant positive curvature, then the universal cover of M_{g^*} is the unit sphere by the Killing-Hopf Theorem. Similarly, the universal cover of M_g is a sphere of radius $\frac{1}{\sqrt{|C|}}$. This shows that M_g has cop number at most 2. Note that since M_g is compact there exists an $\varepsilon > 0$ such that the ε -ball around a point P in M_{g^*} is isometric to a spherical ε -ball on the sphere with radius $\frac{1}{\sqrt{|C|}}$. The robber chooses the agility function $\tau \equiv \varepsilon/4$. The $\varepsilon/4$ -ball around the robber can not be contained in the $\varepsilon/4$ -ball around the cop, so the robber has a position he can move to. Together with Theorem 2.24 and Theorem 2.37, this shows $c(M_g) = 2$ for any manifold M_g of constant curvature C . \square

Since there are graphs G with cop number at least $g^{\frac{1}{2}-o(1)}$, where g is the genus of G , and Mohar showed that for graphs of cop number at least 3 there exists a surface S of genus g with $c(S) \geq c(G)$, we can not hope that the cop number is constant in general. Mohar conjectured that the cop win number of general geodesic surfaces of genus g is close to the lower bound.

Conjecture 2.39 ([80]). Let S be a geodesic surface of genus g . Then $c(S) = O(\sqrt{g})$.

Mohar also showed that $2g + 1$ cops win the Cops and Robber game on a surface of genus $g \geq 1$ and that three cops are enough if $g = 0$. These bounds are tight for $g = 0, 1$, but for large g far from the lower bound.

Chapter 3

Random Graphs from Surfaces

A measure of quality for graph drawings is the number of edge crossings in a drawing. The *crossing number* $cr(G)$ of a graph G is the minimum number of crossings obtained by drawing G in the plane (or the sphere). One of the most fascinating unsolved problems about graph drawings is the so-called Hill's conjecture. Anthony Hill, a British artist, and Frank Harary [49] conjectured that a drawing of the complete graph on n vertices in the plane (or on the sphere) has at least $1/4 \lfloor n/2 \rfloor \lfloor (n-1)/2 \rfloor \lfloor (n-2)/2 \rfloor \lfloor (n-3)/2 \rfloor$ crossings. Hill discovered a beautiful way of drawing graphs with that many crossings, called cylindrical drawings. Many researchers have been trying to prove or disprove the conjecture over several decades or at least to find out if we can prove that the true value is close to the conjectured value for large n [85, 8]. For small values of up to 12 points the conjecture is shown to be true [46, 89]. Drawings of the complete graph K_n with crossing number $(1 + o(1)) \frac{1}{64} n^4$ can be obtained by random drawings on the sphere [83], which we will study in more depth in Section 3.3.4.

This chapter is more generally on random intersection graphs. A *(geometric) intersection graph* is the intersection graph of sets (defined by geometric objects). The vertices of the graph correspond to sets and there is an edge between two vertices in the graph if and only if their corresponding sets intersect. Before diving into the geometric results of random intersection graphs, we discuss standard random models and the celebrated recent theory of graph limits. Then, in Section 3.3 we show that the graph limit of intersection graphs of random graph drawings exists and is a graph limit of intersection graph of random geodesic segments. The results in this section appeared in [W4]. Then we study small substructures in intersection graphs of random geodesic segments, where we start with a summary of what is known for intersections of random geodesic segments in Euclidean convex sets and concentrate in particular on the square $[0, 1]^2$. We decompose a set of line segments S drawn uniformly at random from $[0, 1]^2$ into two sets, S_1, S_2 such that the number of crossings among the line segments in each set is small. This work was developed at the Crossing Number Workshop 2022 and is in preparation to be published. It is joint work with Sergio Cabello, Éva Czabarka, Ruy Fabila-Monroy, Yuga Higashikawa,

Raimund Seidel, László Székely, and Josef Tkadlec [W7]. As mentioned, we discuss random geodesic segments on the sphere and in Section 3.3.4 we give some computational results for crossing numbers of random geodesic drawings of two particular models of surfaces of higher genus.

Finally, in Section 3.4.2 we discuss intersection graphs of disks of the same radius drawn uniformly at random from $[0, 1]^2$, so called random geometric graphs. While in the first sections we study mostly small substructures in intersection graphs, in this section we study spanning substructures. This is joint work with Alberto Espuny Díaz, Lyuben Lichev and Dieter Mitsche, and is in preparation to be published [W10].

3.1 Models for Random Graphs

In the following, for $f, g : \mathbb{N} \rightarrow \mathbb{R}$ we say that $f(n) = o(g(n))$ if $\frac{f(n)}{g(n)} \rightarrow 0$ as $n \rightarrow \infty$ and that $f(n) = \omega(g(n))$ if $\frac{f(n)}{g(n)} \rightarrow \infty$ as $n \rightarrow \infty$.

3.1.1 Binomial Random Graph $G(n, p)$

The *Erdős-Rényi* graph $G(n, p)$ is the most common way of modelling a random graph on n vertices. Starting with a stable set of n vertices, each edge is included in $G(n, p)$ with probability $p \in [0, 1]$, independently from every other edge. The parameter which controls the behaviour of this random graph is $p \in [0, 1]$. Calculating the number of labelled subgraphs isomorphic to some graph H in $G(n, p)$ is straightforward. Let $\text{inj}(H, G(n, p))$ denote the number of injective graph homomorphisms from H to $G(n, p)$. Then by linearity of expectation,

$$\mathbb{E}[\text{inj}(H, G(n, p))] = p^{e(H)} n(n-1) \dots (n - v(H)),$$

and the value is in general not far from its expectation. There has been significant research in the study of large substructures in $G(n, p)$, such as spanning trees. A function $p^* = p^*(n)$ is a *threshold* for some monotone increasing property \mathcal{P} in the Erdős-Rényi graph if

$$\lim_{n \rightarrow \infty} \mathbb{P}[G(n, p) \in \mathcal{P}] = \begin{cases} 0 & \text{if } p = o(p^*), \\ 1 & \text{if } p = \omega(p^*). \end{cases}$$

Bollobás and Thomason [17] proved that every nontrivial monotone graph property has a threshold in $G(n, p)$. Thresholds have been studied for many spanning properties such as connectivity [31, 39] or Hamiltonicity [65], and further are outlined in the survey of Böttcher [20]. Montgomery [82] showed that if a tree T has bounded degree Δ then there is a constant C such that the Erdős-Rényi graph with $p = \frac{C \log n}{n}$ asymptotically almost surely (a.a.s.) contains T . Given a probability space $(\Omega, \mathcal{F}, \mathbb{P})$ and events $E_n \in \mathcal{F}$ for all $n \geq 1$,

we say that $(E_n)_{n \geq 1}$ holds *asymptotically almost surely*, if $\mathbb{P}(E_n) \rightarrow 1$ as $n \rightarrow \infty$. A related random graph model is $G(n, m)$, a graph on the vertex set $[n]$ where the set of edges is chosen uniformly at random from the m -element subsets of $\binom{[n]}{2}$.

3.1.2 Random Graphs from Graphons

The seminal work of Lovász and Szegedy [72] on graph limits introduces a very general way of generating non-balanced random graphs, so called W -random graphs. Here, W is a symmetric, measurable function $W : [0, 1] \times [0, 1] \rightarrow [0, 1]$, and such functions are called $[0, 1]$ -graphons. Graphons can be thought of as continuous adjacency matrices. The *adjacency matrix* A of a graph G on the vertex set v_1, \dots, v_n is the $n \times n$ matrix with $A_{i,j} = 1$ if $v_i \sim v_j$ and 0 otherwise. A W -random n -vertex graph $G = G(n, W)$ is a graph whose vertex set consists of n points x_1, \dots, x_n drawn uniformly at random from $[0, 1]^2$ and x_i is connected to x_j with probability $W(x_i, x_j)$. For example, if W is a $[0, 1]$ -graphon with $W \equiv p$ then $G(n, p) = G(W)$. We describe two examples of $[0, 1]$ -graphons, which arise from intersection graphs of disks and line segments, respectively. For a topological space Ω , the *Borel σ -algebra* $B(\Omega)$ is the smallest σ -algebra containing all open sets. Suppose μ is the uniform measure on the Borel σ -algebra $B([0, 1])$ of $[0, 1]$. Let x_1, x_2, \dots, x_n be a sample from the probability space $([0, 1], B([0, 1]), \mu)$ and consider the balls B_i of radius r around each point $(x_i - r, x_i + r) \cap [0, 1]$. Suppose G_n is a graph on x_1, \dots, x_n where $x_i \sim x_j$ if $B_i \cap B_j$ is non-empty. Then G_n is sampled from the graphon depicted in Figure 3.1, which is

$$W(x, y) = \begin{cases} 1 & \text{if } |x - y| < r \\ 0 & \text{otherwise.} \end{cases}$$

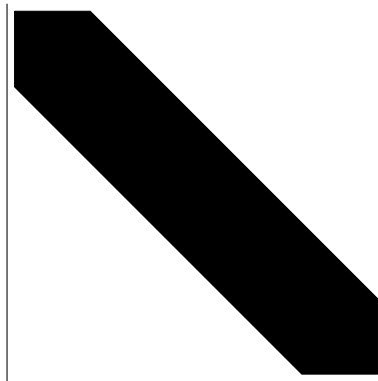


Figure 3.1: A graphon $W : [0, 1]^2 \rightarrow [0, 1]$, the values at which W is 1 are depicted in black, the value of W is 0 else. The graphon arises from the intersection graphs of random intervals of length $2r$ in $[0, 1]$ for $r = 0.2$.

Each graph G on n vertices determines a graphon $W(G)$, which can be simply obtained as follows. The graphon $W = W(G)$ has value $W(x, y) = 1$ for $x \in [\frac{i-1}{n}, \frac{i}{n}]$ and $y \in [\frac{j-1}{n}, \frac{j}{n}]$ if $i \sim j$ in G , and value $W(x, y) = 0$, otherwise. We consider a line intersection graph as an example. In Figure 3.2, we consider the intersections between green, thick line segments e_1, \dots, e_5 and blue line segments e_6, \dots, e_{10} . The adjacency matrix of this intersection graph alongside its graphon $W = W(G)$ is depicted in Figure 3.3. We can

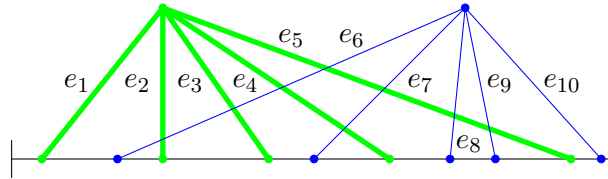


Figure 3.2: A set of edges whose intersection graph is bipartite.

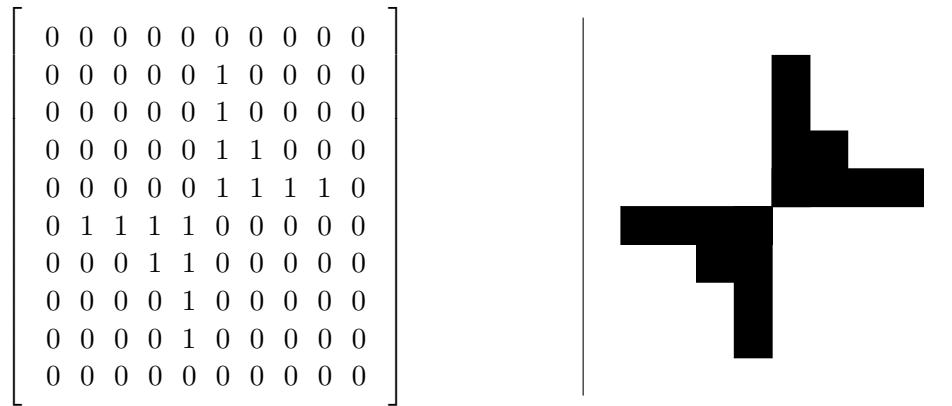


Figure 3.3: On the left the adjacency matrix of the intersection graph of the edges e_1, \dots, e_{10} . Row and column i corresponds to the edge e_i . On the right the corresponding graphon.

show that a randomly generated graph G_n from W is an intersection graph of line segments with probability 1. To see this, we replace each vertex in Figure 3.2 by a circle. We draw parallel edges to edge e_i between circles which corresponds to the number of edges of type e_i sampled. Instead of drawing multiple edges we can draw thick edges, where the thickness of the edge corresponds to the number of edges e_i sampled, or translated into a graphon W , its measure.

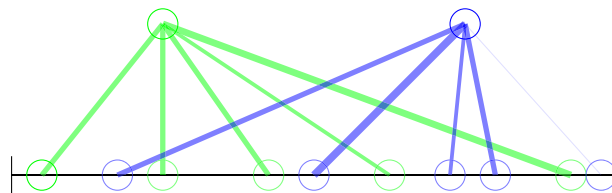


Figure 3.4: The thickness of edges determines with what density edge e_i is picked.

When taking two W -random graphs G_1, G_2 , on a large number of vertices, they look similar to each other. This similarity is usually measured in the cut-distance.

Definition. Let W, W' be graphons. The *cut distance* between W, W' is defined as

$$d_{cut}(W, W') = \inf_{\phi} \sup_{S, T \subseteq [0,1]} \left| \int_{S \times T} W(x, y) - W'(\phi(x), \phi(y)) \right|,$$

where the infimum is taken over all measure-preserving functions $\phi : [0, 1] \rightarrow [0, 1]$.

For a fixed graph H , let $k = |H|$ be its order, and let $hom(H, G)$ denote the number of graph homomorphisms $H \rightarrow G$, which is the number of maps $\phi : V(H) \rightarrow V(G)$ such that for each edge $uv \in E(H)$, $\phi(u)\phi(v) \in E(G)$. Then we define the *homomorphism density* for H as

$$t(H, G) = \frac{hom(H, G)}{|G|^k},$$

and *injective homomorphism density* by

$$t_0(H, G) = \frac{inj(H, G)}{|G|^k}.$$

Note that this is the probability that a random mapping $V(H) \rightarrow V(G)$ is a homomorphism. For a $[0,1]$ -graphon W we define

$$t(H, W) = \int_{[0,1] \times [0,1]} \prod_{ij \in E(H)} W(x_i, x_j) dx_i dx_j.$$

The definitions are compatible in the sense that for a graph G , $t_0(H, G) = t(H, W(G))$. Lovász and Szegedy [72] showed a general way of obtaining a graphon from sequences of graphs.

Theorem 3.1 ([72]). Let $(G_n)_n$ be a sequence of graphs. If the sequence $t(H, G_n)$ converges to some value $t(H)$ for every H , then there exists a limiting graphon W such that $(W(G_n))_n$ converges to W in the cut distance and $t(H, W) = t(H)$.

Therefore, when studying graph sequences, graph limit theory concentrates on small substructures in graphs of the sequence.

Small substructures of graphs are important in extremal graph theory. The theory of flag algebras by Razborov [100] has provided powerful tools for determining densities $t(H)$ for certain graph classes. One of the first results in extremal graph theory is Mantel's Theorem [74]. It says that if an n -vertex graph G has more than $\frac{n^2}{4}$ edges, then it contains a triangle. In the language of graph limits, Mantel's theorem says that if $t(K_2, G) > \frac{1}{4}$ then $t(K_3, G) > 0$. It can be further asked how small $t(K_3, G)$ can be for specific values of $t(K_2, G)$. Consider all graph G and the pairs of numbers $(t(K_2, G), t(K_3, G))$ we get a point set in the square $[0, 1]^2$. The closure of this point set in $[0, 1]^2$ gives the possible

pairs of densities $(t(K_2, W), t(K_3, W))$ for graphons W , see Figure 3.5. An upper bound for $t(K_3, W)$ in terms of $t(K_2, W)$ is given by the Kruskal-Katona Theorem [67, 61], showing that $t(K_3, W) \leq t(K_2, W)^{3/2}$. There has been a long history in proving lower bounds for $t(K_3, W)$ given $t(K_2, W) > \frac{1}{2}$. The first lower bound was given by Goodman in 1959 [43]. While Goodman's lower bound is precise if $t(K_2, W)$ is $\frac{1}{2}, \frac{2}{3}, \frac{3}{4}, \dots$ further research involved improving the lower bound in the intervals in between those points [14, 34, 71, 101], see [69]. Lovász and Simonovits [71] conjectured that the minimum number of triangles is attained by a complete k -partite graph with unequal parts. Optimising over the size of the parts leads to a cubic concave curve in each interval $[1/2, 2/3], [2/3, 3/4], [3/4, 4/5], \dots$. Razborov proved the conjecture in 2008 [101].

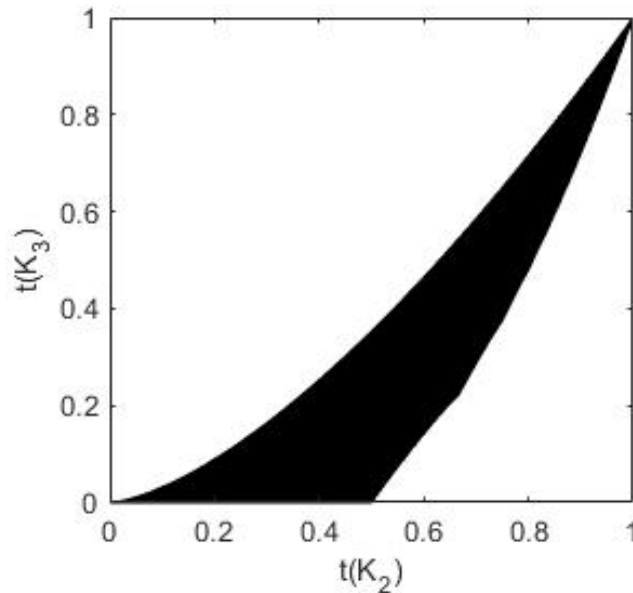


Figure 3.5: Possible values for triangle densities $t(K_3)$ given edge densities $t(K_2)$.

In the following we will be interested in $t(K_2, W)$ and $t(K_3, W)$ for graphons W which stem from random intersection graphs. First, we discuss a more general notion of graphons.

3.2 Representations of Graphons

In the previous section we considered $[0, 1]$ -graphons. Sometimes it is more natural to consider graphons as measurable symmetric functions on more general probability spaces (Ω, A, μ) , which means Ω is a set, A is a σ -algebra on Ω and μ is a probability measure. A measure μ is a *probability measure* if $\mu(\Omega) = 1$. Note that a probability measure μ can be obtained from a finite non-negative measure μ^* ($\mu^* : A \rightarrow [0, R]$ for $R > 0$), by setting $\mu = \frac{1}{\mu^*(\Omega)}\mu^*$. A graphon on (Ω, A, μ) is a symmetric measurable function $W : \Omega \times \Omega \rightarrow [0, 1]$.

Densities of such a graphon W are accordingly defined as

$$t(H, W) = \int_{[0,1] \times [0,1]} W(x, y) d\mu(x) d\mu(y).$$

We give an example of Diaconis, Holmes and Janson [25] on intersection graphs of intervals in $[0, 1]$ (see also [69]). Let $J = \{(x, y) \in [0, 1] : x \leq y\}$, and define

$$W((x_1, y_1), (x_2, y_2)) = \begin{cases} 1 & \text{if } [x_1, y_1] \cap [x_2, y_2] \neq \emptyset, \\ 0 & \text{otherwise.} \end{cases}$$

Every probability measure μ on the Borel sets in J gives rise to a graphon W on $(J, B(J), \mu)$ and more surprisingly, all interval graph limits arise this way. Whereas the graphon W has a nice representation on $[0, 1]^4$, finding a representation on $[0, 1]^2$ seems difficult

Suppose W_i is a graphon on a probability space (Ω_i, A_i, μ_i) for $i = 1, 2$. The general cut distance is defined as

$$\delta_{\square}(W_1, W_2) = \inf_{J, \phi_1, \phi_2} \sup_{S, T \in A} \left| \int_S \int_T W_1(\phi_1(x), \phi_1(y)) - W_2(\phi_2(x), \phi_2(y)) d\mu(x) d\mu(y) \right|,$$

where the infimum is taken over all probability spaces $J = (\Omega, A, \mu)$ and measure-preserving functions $\phi_i : \Omega \rightarrow \Omega_i$. Borgs, Chayes and Lovász [18] proved that the representation of a graphon does not matter up to what is called a weak isomorphism.

Theorem 3.2 ([18]). Suppose W_i is a graphon on a probability space (Ω_i, A_i, μ_i) for $i = 1, 2$. If $t(H, W_1) = t(H, W_2)$ for every simple graph H , then $\delta_{\square}(W_1, W_2) = 0$. Further, there exists a probability space (Ω, A, σ) and measure-preserving maps $\phi_i : \Omega \rightarrow \Omega_i$ for $i = 1, 2$ such that $W_1 \circ \phi_1 = W_2 \circ \phi_2$ almost everywhere.

We showcase the independence of the representation by considering the cut distance. It is a straightforward corollary of Theorem 3.2 that δ_{\square} satisfies the triangle inequality.

Corollary 3.3. Let W_i be a graphon on a probability space (Ω_i, A_i, μ_i) for $i = 1, 2, 3$, then

$$\delta_{\square}(W_1, W_3) \leq \delta_{\square}(W_1, W_2) + \delta_{\square}(W_2, W_3).$$

Proof. Suppose ϕ_i is a measure-preserving map from the probability space (Ω, A, μ) to (Ω_i, A_i, μ_i) for $i = 1, 2$ and σ_j a measure-preserving map from the probability space (Ω', A', μ') to (Ω_j, A_j, μ_j) for $j = 2, 3$. Let $\varepsilon > 0$ and ϕ_i be such that

$$\sup_{S, T \in A} \left| \int_S \int_T W_1(\phi_1(x), \phi_1(y)) - W_2(\phi_2(x), \phi_2(y)) d\mu(x) d\mu(y) \right| \leq \delta_{\square}(W_1, W_2) + \varepsilon.$$

Let σ_j be such that

$$\sup_{S,T \in A'} \left| \int_S \int_T W_2(\sigma_2(x), \sigma_2(y)) - W_3(\sigma_3(x), \sigma_3(y)) d\mu'(x) d\mu'(y) \right| \leq d_{\square}(W_2, W_3) + \varepsilon.$$

There exists a probability space (Σ, B, π) and a measure-preserving map ρ such that $W_2 \circ \phi_2 \circ \rho = W_2 \circ \sigma_2 \circ \rho$ almost everywhere. But then

$$\begin{aligned} d_{\square}(W_1, W_3) &\sup_{S,T \in B} \leq \left| \int_S \int_T W_1(\phi_1(\rho(x)), \phi_1(\rho(y))) - W_3(\sigma_3(\rho(x)), \sigma_3(\rho(y))) d\pi(x) d\pi(y) \right| \\ &\leq \sup_{S,T \in B} \left| \int_S \int_T W_1(\phi_1(\rho(x)), \phi_1(\rho(y))) - W_2(\phi_2(\rho(x)), \phi_2(\rho(y))) d\pi(x) d\pi(y) \right| \\ &\quad + \sup_{S,T \in B} \left| \int_S \int_T W_2(\phi_2(\rho(x)), \phi_2(\rho(y))) - W_3(\sigma_3(\rho(x)), \sigma_3(\rho(y))) d\pi(x) d\pi(y) \right| \\ &\leq d_{\square}(W_1, W_2) + d_{\square}(W_2, W_3) + 2\varepsilon. \end{aligned}$$

Since this is true for all $\varepsilon > 0$, the triangle inequality follows. \square

From the triangle inequality it follows naturally that the cut distance does not depend on the representation of a graphon.

Corollary 3.4. For graphons F_1, F_2, F_3 such that for all graphs H it holds that $t(H, F_1) = t(H, F_2)$, then

$$d_{\square}(F_1, F_3) = d_{\square}(F_2, F_3).$$

Proof. This follows from applying the triangle inequality,

$$d_{\square}(F_1, F_3) \leq d_{\square}(F_1, F_2) + d_{\square}(F_2, F_3) = d_{\square}(F_2, F_3),$$

and by symmetry, the corollary follows. \square

In the following we will be interested in probability spaces $J_S = (S, B(S), \mu)$ where S is an Euclidean, spherical or hyperbolic compact surface, $B(S)$ is the Borel σ -algebra on S and μ is their respective normalised area (or volume) measure. For intersection graphs of geodesic segments we will consider products of these spaces $J_S \times J_S$.

3.3 Random Intersection Graphs of Geodesic Segments

Generating random geodesic segments is a generalisation of throwing Buffon Needles (see, e.g. [56] or [112]), where we allow the needles to have different lengths. Let $J = (S, B, \mu)$ be a probability space. Random geodesic segments L_1, \dots, L_n can be modelled

by taking the product measure space $J \times J$ and sample n tuples (x, y) with $x, y \in S$. To obtain random geodesic segments we follow these two steps:

- Sample a set of X pairs of points from $S \times S$ with respect to $\mu \times \mu$.
- For a tuple of points (x_i, y_i) , let L_i be a geodesic segment between x_i and y_i .

Let $X_n(S, \mu)$ be the intersection graph of L_1, \dots, L_n . The expected number of edges in the intersection graph $X_n(S, \mu)$ is a well studied parameter when μ is a uniform distribution on convex sets in the Euclidean plane (see [96]), on the sphere [83] (and [W4]) and on the torus [47]. The intersection graph can be modelled by the following graphon,

$$W_{S, \mu}((x_1, y_1)(x_2, y_2)) = \begin{cases} 1 & \text{if } L_1 \text{ and } L_2 \text{ intersect,} \\ 0 & \text{else.} \end{cases}$$

The limiting edge density in $X_n(S, \mu)$ is then $t(K_2, W_{S, \mu})$.

In the following we want to draw a comparison between intersection graphs of line segments and intersection graphs of graph embeddings. A *geodesic drawing* of a graph G is a drawing of G in a geodesic space, such that each edge is a geodesic segment. A μ -*random drawing* of a graph G is a geodesic drawing obtained from a μ -random set of points representing the vertices $V(G)$. For an example of a μ -random drawing on the sphere see Figure 3.6. In a non-degenerate graph drawing no two vertices are mapped to the same

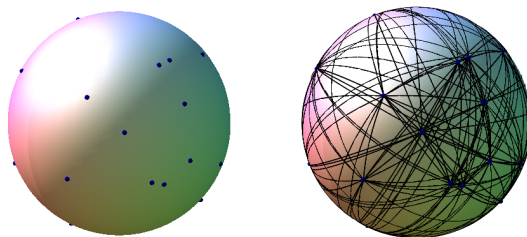


Figure 3.6: A uniformly random drawing of a complete graph on the sphere.

point and a vertex is not mapped to the interior of a simple curve that defines an edge. We say a probability measure μ is non-degenerate, if a μ -random drawing of a complete graph K_n is non-degenerate with probability one. If D_n is a drawing of an n -vertex graph G_n , then we associate the *crossing graph* X_n to D_n , whose vertices are the edges of D_n , and two of them are adjacent in X_n if they cross in D_n . This means the crossing graph X_n is a subgraph of the intersection graph of the edges in the drawing D_n , it is the intersection graph of the set of edges when we delete the endpoints from each drawn edge. We show that the sequence of drawings converges.

Theorem 3.5 (See [W4]). Let $(G_n)_n$ be a sequence of n -vertex graphs on $\Omega(n^2)$ edges. Let μ be a non-degenerate probability measure on a surface S . Let D_n be a μ -random

drawing, and let X_n be its crossing graph. The sequence of graphs $(X_n)_n$ is convergent with probability 1 to $W_{S,\mu}$.

The idea of the proof of Theorem 3.5 is that k edges from $(G_n)_n$ are with a.a.s. independent, therefore they are a random sample from $J_S \times J_S$ where $J_S = (S, B(S), \mu)$. We will make this idea formal.

Definition. For given X_n , let $\phi : V(H) \rightarrow V(X_n)$ and we define the random variable $y_{H,\phi}$ on X_n to be

$$y_{H,\phi}(X_n) = \begin{cases} 1 & \text{if } \phi \text{ is a graph homomorphism } H \rightarrow X_n \\ 0 & \text{otherwise} \end{cases}$$

and denote its expectation by

$$E_\phi := \mathbb{E}[y_{H,\phi}].$$

Note that E_ϕ is not the same for every ϕ . For example, if H is a complete graph, then $E_\phi = 0$ whenever $im(\phi)$ contains edges that share a vertex, as those edges never cross and hence are not adjacent in the crossing graph.

Lemma 3.6 ([W4]). Let $(X_n)_n$ be a sequence of the crossing graphs of μ -random geodesic drawings D_n of G_n for $n = 1, 2, \dots$, and let H be a fixed graph of order k . Then

$$\lim_{n \rightarrow \infty} \frac{1}{|X_n|^k} \sum_{\phi: V(H) \rightarrow V(X_n)} E_\phi = t(H, W_{S,\mu}).$$

Proof. Let $im(\phi) = \{v_1 w_1, \dots, v_k w_k\}$. Then if $|\{v_1, \dots, v_k, w_1, \dots, w_k\}| = 2n$, the line segments are independent and

$$\mathbb{E}[y_{H,\phi}] = t(H, W_{S,\mu}).$$

Moreover, there are $O(n^{2k-1})$ choices for ϕ for which $|\{v_1, \dots, v_k, w_1, \dots, w_k\}| < 2n$ and the result follows. \square

Let us now consider the sum of the above defined random variables

$$Y_H := \sum_{\phi: V(H) \rightarrow V(X_n)} y_{H,\phi}, \tag{3.1}$$

and note that $Y_H(X_n) = hom(H, X_n)$ and $\mathbb{E}[Y_H] = \sum_{\phi: V(H) \rightarrow V(X_n)} E_\phi$. The aim is to show that Y_H is in general not far from its expectation. This then gives us the tool to show the existence of $\lim_{n \rightarrow \infty} \frac{|Y_H|}{|X_n|^k} = t(H)$ with probability 1.

Proposition 3.7 ([W4]). Let Y_H be defined as in (3.1). Then we have

$$\text{var}(Y_H) = O(n^{4k-2}).$$

Proof of Proposition 3.7. By definition,

$$\begin{aligned} \text{var}(Y_H) &= \mathbb{E}[(Y_H - \mathbb{E}[Y_H])^2] \\ &= E \left[\left(\sum_{\phi: V(H) \rightarrow V(X_n)} y_{H,\phi} - E_\phi \right)^2 \right] \\ &= \sum_{\phi: V(H) \rightarrow V(X_n)} \sum_{\phi': V(H) \rightarrow V(X_n)} \mathbb{E}[(y_{H,\phi} - E_\phi)(y_{H,\phi'} - E_{\phi'})]. \end{aligned} \quad (3.2)$$

For independent variables $y_{H,\phi}$ and $y_{H,\phi'}$ the expectation $\mathbb{E}[(y_{H,\phi} - E_\phi)(y_{H,\phi'} - E_{\phi'})]$ equals zero so we only need to consider those pairs ϕ and ϕ' for which $y_{H,\phi}$ and $y_{H,\phi'}$ are dependent.

The events “ ϕ is a graph homomorphism $H \rightarrow X_n$ ” and “ ϕ' is a graph homomorphism $H \rightarrow X_n$ ” are independent if $\text{im}(\phi) = \{e_1, \dots, e_k\} = \{v_1 w_1, \dots, v_k w_k\}$ and $\text{im}(\phi') = \{e'_1, \dots, e'_k\} = \{v'_1 w'_1, \dots, v'_k w'_k\}$ satisfy

$$|\{v_1, \dots, v_k, w_1, \dots, w_k\} \cap \{v'_1, \dots, v'_k, w'_1, \dots, w'_k\}| \leq 1.$$

But note that for these sets to share at least two points we have $\binom{n}{2}$ choices for those two special points and at most $(n^{2k-2})^2$ for the remaining ones. The number of edges (e_1, \dots, e_k) that can be formed by a set of vertices in $X_n \{v_1, \dots, v_k, w_1, \dots, w_k\}$ does not depend on n , so we have at most $O(n^{4k-2})$ pairs $y_{H,\phi}$ and $y_{H,\phi'}$ that are dependent as ϕ and ϕ' are defined by (e_1, \dots, e_k) and (e'_1, \dots, e'_k) only. Note that for each pair

$$|\mathbb{E}[(y_{H,\phi} - \mu_\phi)(y_{H,\phi'} - \mu_{\phi'})]| \leq 1$$

since $|y_{H,\phi}(X_n) - \mu_\phi| \leq 1$ for every X_n . Summing up those expectations over the dependent variables, (3.2) gives $\text{var}(Y_H) = O(n^{4k-2})$. \square

Proof of Theorem 3.5. By Proposition 3.7 and Chebyshev's inequality there exists a constant C such that

$$\text{Pr} \left[|Y_H - \mathbb{E}[Y_H]| \geq kCn^{2k-1} \right] \leq \frac{1}{k^2}.$$

Now if we choose $k = k(n)$ appropriately such that $k(n)n^{-1}$ converges to zero and the sum $\sum_{n=1}^{\infty} \frac{1}{k(n)^2}$ is finite we can use the Borel-Cantelli Lemma. For example, we can choose

$k = n^{3/4}$ and using Lemma 3.6 we get

$$\begin{aligned} Pr \left[\left| \frac{|Y_H|}{|X_n|^k} - t(H, W_{S,\mu}) \right| - \left| t(H, W_{S,\mu}) - \frac{\mathbb{E}[Y_H]}{|X_n|^k} \right| \geq \frac{Cn^{2k-1/4}}{|X_n|^k} \right] &\leq \frac{1}{n^{3/2}} \\ \implies Pr \left[\left| \frac{|Y_H|}{|X_n|^k} - t(H, W_{S,\mu}) \right| \geq \frac{C'}{n^{1/4}} \right] &\leq \frac{1}{n^{3/2}}, \end{aligned}$$

for some constant C' . Then the Borel-Cantelli Lemma implies the following.

Claim 3.8. For each fixed H , $\frac{|Y_H|}{|X_n|^k} \rightarrow t(H, W_{S,\mu})$ with probability 1.

Given that for each H , $t(H, X_n) \rightarrow t(H, W_{S,\mu})$ with probability 1, and since the probabilities are countably additive, it follows with probability 1 that $t(H, X_n) \rightarrow t(H, W_{S,\mu})$ for every H . Consequently, the sequence of random crossing graphs $(X_n)_n$ is convergent with probability 1. This proves Claim 3.8 and hence Theorem 3.5. \square

Let G_n be an n -vertex graph where the vertex set is partitioned into sets $V_{n,1}, \dots, V_{n,k}$. Let $e_d : [k]^2 \rightarrow [0, 1]$, we will call e_d an *edge density function* if it is symmetric and for its image it holds that

$$\sum_i e_d(i, i) + \frac{1}{2} \sum_{i \neq j} e_d(i, j) = 1.$$

We say $(V_{n,1}, \dots, V_{n,k})_n$ is an e_d -proportional vertex partition of $(V(G_n))_n$ if

$$e_d(i, j) = \lim_{n \rightarrow \infty} \frac{e(V_{n,i}, V_{n,j})}{e(G_n)},$$

for every $1 \leq i \leq j \leq k$, where $e(V_{n,i}, V_{n,j})$ is the number of edges with one endpoint in $V_{n,i}$ and one endpoint in $V_{n,j}$. A $\mu = (\mu_1, \mu_2, \dots, \mu_k)$ -*random drawing* of a partitioned graph G_n with partition $(V_{n,1}, \dots, V_{n,k})$ is a geodesic drawing of G_n where $V_{n,i}$ is a μ_i -random set of points and edges are geodesic segments.

Theorem 3.9 ([W4]). Let $(G_n)_n$ be a sequence of n -vertex graphs on $\Omega(n^2)$ edges and let e_d be an edge density function. Let the sequence of partitions $(V_{n,1}, \dots, V_{n,k})_n$ be an e_d -proportional vertex partition of $(V(G_n))_n$. Let μ_i be a non-degenerate probability measure on a surface S , $i = 1, \dots, k$. Let D_n be a $\mu = (\mu_1, \mu_2, \dots, \mu_k)$ random drawing of G_n , and let X_n be its crossing graph. The sequence of graphs $(X_n)_n$ is convergent with probability 1 and there is a graphon $W = W_{S,\mu,e_d}$ for $\mu = (\mu_1, \mu_2, \dots, \mu_k)$ that is the limit of this convergent sequence.

We will omit the proof as it is very similar to the proof of Theorem 3.5. A special case of this theorem was proven in [W4].

3.3.1 The Euclidean Square $[0, 1]^2$ and Sylvester's Four Point Problem

Random geodesic drawings are often studied due to their close connection to graph drawings. For μ -random drawings D_n of the complete graph K_n on a surface S , where μ is non-degenerate, the crossing number is in expectation

$$\mathbb{E}(\text{cr}(D_n)) = \frac{t(K_2, W_{S,\mu}) n(n-1)(n-2)(n-3)}{8}.$$

In the following we will be interested in studying the densities $t(H, W_{S,\mu})$, with a particular focus on $H = K_2$ which relates to crossing numbers. We will first consider subsets of the Euclidean plane, then the torus as an Euclidean surface and finally spherical and hyperbolic surfaces. A *geometric drawing* of a graph is a geodesic drawing in the Euclidean plane which means edges are drawn as straight line segments

Given a convex, finite set D in the Euclidean plane, what is the probability $q(D)$ that four points taken uniformly at random form a convex four-gon? We will call $q(D)$ the *four point probability* of D . Sylvester originally asked about the four point probability of four points chosen at random from the Euclidean plane [107], but this question is not well-defined, which is why we restrict to finite sets D [96, 108]. The four point probability is related to crossings of random straight line segments. Four points are in convex position in the Euclidean plane if and only if the geometric drawing of K_4 whose vertices are mapped to the four points has one crossing. Since four points define three pairs of non-adjacent segments,

$$q(D) = 3t(K_2, W_{D,\mu}),$$

where μ is the uniform distribution on D . It was shown that

$$\frac{2}{3} \leq q(D) \leq 1 - \frac{35}{12\pi^2}.$$

The lower bound is attained when D is a triangle, the upper bound is attained when D is an ellipse, which was shown by Blaschke (see [95]). Table 3.1 contains the four point probabilities for other convex sets D [62, 113, 115]. We will focus in this section on the unit square $S = [0, 1]^2$. A clever technique to work with point sets in the unit square was developed by Valtr [111], and he used it to prove the following theorem.

Theorem 3.10 ([111]). If μ is a uniform distribution on $[0, 1]^2$, then a μ -random set of k points is in convex position with probability

$$\left(\frac{\binom{2k-2}{k-1}}{k!} \right)^2.$$

D	$q(D)$	approx
triangle	$\frac{2}{3}$	0.66667
square	$\frac{25}{36}$	0.69444
pentagon	$\frac{2}{45}(18 - \sqrt{5})$	0.70062
hexagon	$\frac{683}{972}$	0.70267
ellipse	$1 - \frac{35}{12\pi^2}$	0.70448

Table 3.1: Sylvester four point probabilities.

Considering a set of points p_1, \dots, p_k drawn uniformly at random from $S = [0, 1]^2$, Valtr considers the *bounding box* of the k points which is the smallest axis-parallel rectangle R that contains p_1, \dots, p_k . He computes the probability that the bounding box has width close to w and height close to h . Then he computes the probability that the point set p_1, \dots, p_k satisfies the property of interest (in his case, convexity) conditioned on the bounding box of p_1, \dots, p_k having dimensions roughly $w \times h$. We will explain the technique more precisely. The first step consists of a discretisation of the point set. Let $Q_{w,h} = [w] \times [h]$ be the points of an integer grid. Valtr compares two events,

A : k independently uniformly selected points in $[0, 1]^2$ satisfy property X

and

A_m : k independently uniformly selected points in $Q_{m,m}$ satisfy property X ,

where X is a property that is invariant under scaling and translation. We consider the following function $f : ([0, 1]^2)^k \rightarrow \{0, 1\}$,

$$f(p_1, \dots, p_k) = \begin{cases} 1 & \text{if } p_1, \dots, p_k \text{ satisfy property } X, \\ 0 & \text{otherwise.} \end{cases}$$

If f is Riemann-integrable, and property X is invariant under homothety, then

$$\lim_{m \rightarrow \infty} A_m = A.$$

In order to approximate A_m , Valtr's strategy considers the bounding box $R = R(p_1, \dots, p_k)$ of a point set p_1, \dots, p_k . We denote by $d(R)$ the dimensions of the rectangle, i.e. $d(R) = w \times h$ for some positive integers w, h . He then followed that

$$\mathbb{P}(A_m) = \sum_{w=1}^m \sum_{h=1}^m \mathbb{P}(A_m \mid d(R(P_1, \dots, P_m)) = w \times h) (m+1-w)(m+1-h), \quad (3.3)$$

where $(m+1-w)(m+1-h)$ is the number of bounding boxes of size $w \times h$ in $Q_{m,m}$. To calculate $\mathbb{P}(A_m)$, it is hence enough to calculate $\mathbb{P}(A_m \mid d(R))$.

Sometimes it is easier to consider point sets in $Q_{m,m}$, such that their bounding box contains at most one point on each of its bounding sides. We say that $p_1, \dots, p_k \in Q_{m,m}$ is a point set in *axis-general position* if no two points among p_1, \dots, p_k have the same x or the same y -coordinate. Suppose k is fixed and $m \rightarrow \infty$. Then

$$\lim_{m \rightarrow \infty} \mathbb{P}(p_1, \dots, p_k \in Q_{m,m} \text{ are in axis-general position}) = 1,$$

hence we can assume that the points are in axis-general position.

3.3.2 Coloured Crossing Number in $[0, 1]^2$

We will consider a coloured version of Sylvester's four point problem on the unit square to which we will apply Valtr's bounding box strategy. Let χ be a colouring of a set of line segments L into two colours, red and blue. Let $\text{cr}(L, \chi)$ be the number of monochromatic crossings of L , that is, of edges of the same colour that cross. A *geometric graph* is a geometric drawing of a graph. If H is a geometric graph, then $\text{cr}(H, \chi) = \text{cr}(L, \chi)$ where L is the set of line segments defined by the edges of H . If χ is a random edge colouring of L , in which every edge is assigned one of two colours with probability $\frac{1}{2}$, then linearity of expectation implies that

$$E[\text{cr}(L, \chi)] = \frac{1}{2} \text{cr}(L).$$

Recently, Aichholzer et al. showed that there exists a constant $c > 0$, such that if H is a complete geometric graph, then there exists a 2-colouring of the edges, χ , of H such that

$$\text{cr}(H, \chi) \leq \left(\frac{1}{2} - c\right) \text{cr}(H).$$

In the following we consider the case when two line segments are chosen uniformly at random from the unit square $[0, 1]^2$. We show the following theorem.

Theorem 3.11 ([W7]). Let S be a set of four points chosen independently and uniformly at random from a square. Join every pair of points of S with a straight line segment. colour each such edge red if it has positive slope and blue otherwise. Then the probability that S defines a pair of crossing edges of the same colour is equal to $\frac{1}{4}$.

Let χ_{slope} be the edge colouring of H in which an edge is coloured red if it has positive slope and blue otherwise. Theorem 3.11 implies that if the vertices of H are chosen

uniformly at random from a square then

$$E[\text{cr}(H, \chi_{\text{slope}})] = \frac{1}{4} \binom{n}{4} = \left(\frac{1}{2} - \frac{7}{50}\right) \frac{25}{36} \binom{n}{4} = \left(\frac{1}{2} - \frac{7}{50}\right) E[\text{cr}(H)],$$

where the second inequality follows from Sylvester's four point probability on the square, see Table 3.1. The constant $7/50$ is significantly larger than the constant c of Aichholzer et al. for the generic case. Incidentally, this idea of assigning different colours to edges depending on the slope was used by Blažek and Koman [12], to obtain a (conjectured) crossing optimal drawing of the complete graph K_n as follows. Place n points in a regular polygon; for every pair of vertices u and v , if the line segment uv has positive slope then draw this edge as diagonal of the polygon, otherwise draw this edge as a chord on the outside of the polygon.

In order to prove Theorem 3.11, we will use Valtr's bounding box strategy to determine:

A_m : A uniformly random set of 4 points from $Q_{m,m}$ in axis-general position defines a monochromatic crossing

We decompose the relevant sets depending on the number of points placed at the corners of the bounding box, which we will denote by $Q_{w,h}$. The four corners of $Q_{w,h}$ are the points that lie on two sides simultaneously: $\{0, w\} \times \{0, h\}$. The four sides of $Q_{w,h}$ are the subsets $\{0\} \times [h]$ (left side), $\{w\} \times [h]$ (right side), $[w] \times \{0\}$ (bottom side), and $[w] \times \{h\}$ (top side).

Definition. For each $i = 0, \dots, 4$, let $A_{w,h}^{(i)}$ be the number of sets $S \in \binom{Q_{w,h}}{4}$ satisfying the following:

- the bounding box of S is precisely $Q_{w,h}$;
- S is in axis-general convex position;
- the diagonals of the convex quadrilateral defined by S are of the same colour; and
- exactly i of the points of S are corners of $Q_{w,h}$.

If at least three corners of a bounding box are occupied, then the point set is not in axis-general position, therefore

$$A_{w,h}^{(4)} = A_{w,h}^{(3)} = 0.$$

We denote

$$A_{w,h} := \sum_{i=0}^2 A_{w,h}^{(i)}.$$

and we use p_1, \dots, p_4 to denote the points in the sets $S \in \binom{Q_{w,h}}{4}$ we consider. For each point $p_i \in S$, we use (x_i, y_i) for its coordinates.

Claim 3.12.

$$A_{w,h}^{(0)} = \frac{w^2 h^2}{2} + O(w^2 h + w h^2).$$

Proof. In this case, the four points of S are on the sides of $Q_{w,h}$ and none of them lie in a corner. Without loss of generality, we assume that p_1, p_2, p_3, p_4 lie on the top, bottom, left and right sides of $Q_{w,h}$, respectively. Thus, the diagonals that cross are $\overline{p_1 p_2}$ and $\overline{p_3 p_4}$. There are $(w-1)(w-2)$ choices for $\overline{p_1 p_2}$ and $(h-1)(h-2)$ choices for $\overline{p_3 p_4}$, as none of the points can be a corner and the segments can not be horizontal or vertical since they are in axis-general position. Exactly half of the choices for $\overline{p_1 p_2}$ are red since there are no vertical edge segments, and exactly half of the choices of $\overline{p_3 p_4}$ are red since there are no horizontal edge segments, and those choices are independent. Thus,

$$A_{w,h}^{(0)} = \frac{(w-1)(w-2)(h-1)(h-2)}{2} = \frac{w^2 h^2}{2} + O(w^2 h + w h^2).$$

□

To estimate the number of integer points inside a convex region of the plane, there is a tight, classical bound given by Nosarzewska [86], which we simplify to the following rough statement:

Theorem 3.13 ([86]). Let K be a convex and compact set in the plane with area A and perimeter L . Then

$$|\mathbb{Z}^2 \cap K| = A + O(1 + L).$$

We will use this theorem to calculate $A_{w,h}^{(1)}$.

Claim 3.14.

$$A_{w,h}^{(1)} = \frac{2}{3} w^2 h^2 + O(w^2 h + w h^2).$$

Proof. Without loss of generality assume that p_1 is the point in a corner of $Q_{w,h}$. Suppose that p_1 is in the bottom-left corner. The other three cases are analogous. To have bounding box $Q_{w,h}$, one point of S , say p_2 , is on the right side of $Q_{w,h}$, and another point of S , say p_3 , is in the top side of $Q_{w,h}$. Note that $\overline{p_1 p_2}, \overline{p_1 p_3}$ are red, while $\overline{p_2 p_3}$ is blue, see Figure 3.7. For S to define a pair of crossing edges of the same colour, the remaining point of S , p_4 , must lie in K or K' , where:

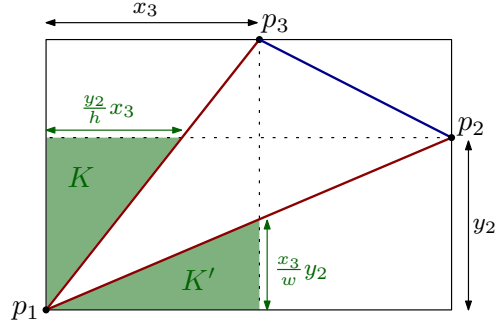


Figure 3.7: The case $A_{w,h}^{(1)}$ with a point at the bottom-left corner.

- $K = K(p_2, p_3)$ is the region above the line supporting $\overline{p_1 p_3}$, below the horizontal line through p_2 , and to the right of the vertical line through p_1 ;
- $K' = K'(p_2, p_3)$ is the region below the line supporting $\overline{p_1 p_2}$, to the left of the vertical line through p_3 , and above the horizontal line through p_1 .

Note that K and K' are interior disjoint triangles. By considering the four possible corners for the point p_1 and the possible locations of p_2 and p_3 , we have

$$A_{w,h}^{(1)} = 4 \sum_{y_2=1}^{h-1} \sum_{x_3=1}^{w-1} (|Q_{w,h} \cap K| + |Q_{w,h} \cap K'| + O(w+h)).$$

Since the regions K and K' are convex and have perimeter $O(w+h)$, we can use Theorem 3.13, hence

$$A_{w,h}^{(1)} = 4 \sum_{y_2=1}^{h-1} \sum_{x_3=1}^{w-1} (\text{area}(K) + \text{area}(K') + O(w+h)).$$

Recall that $p_i = (x_i, y_i)$ are the coordinates of point p_i ($i = 1, \dots, 4$). Then

$$\begin{aligned} \text{area}(K) &= \frac{1}{2} \cdot y_2 \cdot \frac{y_2}{h} x_3, \\ \text{area}(K') &= \frac{1}{2} \cdot x_3 \cdot \frac{x_3}{w} y_2. \end{aligned}$$

Therefore,

$$\begin{aligned}
A_{w,h}^{(1)} &= 4 \sum_{y_2=1}^{h-1} \sum_{x_3=1}^{w-1} \left(\frac{1}{2h} y_2^2 x_3 + \frac{1}{2w} x_3^2 y_2 + O(w+h) \right) \\
&= \left(\frac{2}{h} \sum_{y_2=1}^{h-1} y_2^2 \sum_{x_3=1}^{w-1} x_3 \right) + \left(\frac{2}{w} \sum_{x_3=1}^{w-1} x_3^2 \sum_{y_2=1}^{h-1} y_2 \right) + O(w^2 h + h^2 w) \\
&= \frac{2 \cdot h^3 \cdot w^2}{h \cdot 3 \cdot 2} + \frac{2 \cdot w^3 \cdot h^2}{w \cdot 3 \cdot 2} + O(w^2 h + h^2 w) = \frac{2}{3} w^2 h^2 + O(w^2 h + h^2 w).
\end{aligned}$$

□

Claim 3.15.

$$A_{w,h}^{(2)} = \frac{1}{3} w^2 h^2 + O(w^2 h + w h^2).$$

Proof. Since there are no points on a common horizontal or vertical line, we only count the number of sets S with two points on opposite corners of $Q_{w,h}$. Suppose that one point of S , say p_1 , is in the bottom-left corner and another point, say p_2 , is in the top-right corner. The case when the points are in the other pair of opposing corners is analogous. Note that the segment $\overline{p_1 p_2}$ is red. See Figure 3.8.

Let p_3 and p_4 be the remaining points of S . We say a point is above $\overline{p_1 p_2}$ if it is above the line supporting $\overline{p_1 p_2}$, and otherwise we say it is below. We count separately the sets S with p_3 and p_4 on the same side of $\overline{p_1 p_2}$ and with p_3 and p_4 on opposite sides of $\overline{p_1 p_2}$. More precisely, we define:

- Let $C_{w,h}^{(2)}$ be the number of sets $\{p_1, p_2, p_3, p_4\} \in \binom{Q_{w,h}}{4}$ contributing to $A_{w,h}^{(2)}$ such that p_1 is the bottom-left corner, p_2 is the top-right corner, and p_3, p_4 are on opposite sides of $\overline{p_1 p_2}$.
- Let $D_{w,h}^{(2)}$ be the number of sets $\{p_1, p_2, p_3, p_4\} \in \binom{Q_{w,h}}{4}$ contributing to $A_{w,h}^{(2)}$ such that p_1 is the bottom-left corner, p_2 is the top-right corner, and p_3, p_4 are on the same side of $\overline{p_1 p_2}$.

We then have

$$A_{w,h}^{(2)} = 2 \cdot (C_{w,h}^{(2)} + D_{w,h}^{(2)}),$$

where the factor 2 comes from choosing p_1, p_2 as the endpoints of the other diagonal.

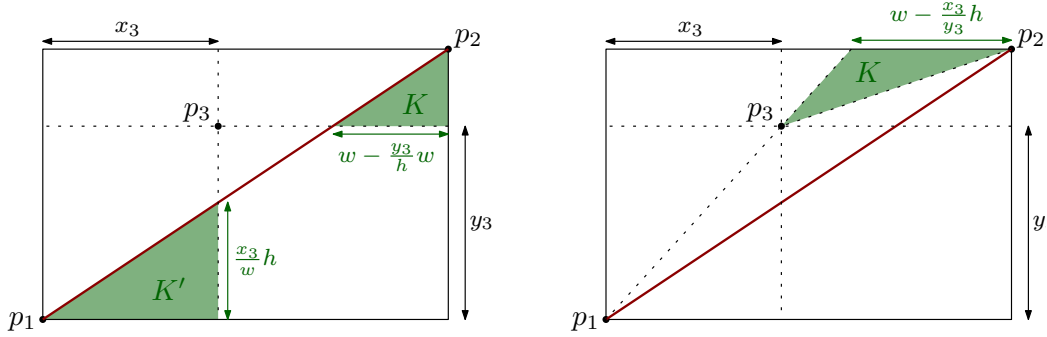


Figure 3.8: The case $A_{w,h}^{(2)}$ with points at the bottom-left and top-right corner. The left depicts the case $C_{w,h}^{(2)}$ and the right figure the case $D_{w,h}^{(2)}$.

Let us estimate $C_{w,h}^{(2)}$. Without loss of generality, let us denote by p_3 the point above $\overline{p_1p_2}$, and thus p_4 is below $\overline{p_1p_2}$, see Figure 3.8. For each choice of p_3 , if the segment $\overline{p_3p_4}$ is to be red, the point p_4 must lie in K or K' , where:

- $K = K(p_3)$ is the region below $\overline{p_1p_2}$, above the horizontal line through p_3 , and to the left of the vertical line through p_2 ;
- $K' = K'(p_3)$ is the region below $\overline{p_1p_2}$, to the left of the vertical line through p_3 , and above the horizontal line through p_1 .

Note that K and K' are interior disjoint triangles. Thus,

$$C_{w,h}^{(2)} = \sum_{p_3 \text{ above } \overline{p_1p_2}} (|Q_{w,h} \cap K| + |Q_{w,h} \cap K'| + O(w+h)).$$

The areas of the regions K, K' are

$$\begin{aligned} \text{area}(K) &= \frac{1}{2} \cdot w \left(1 - \frac{y_3}{h}\right) \cdot (h - y_3), \\ \text{area}(K') &= \frac{1}{2} \cdot x_3 \cdot \frac{x_3}{w} h. \end{aligned}$$

Therefore by Theorem 3.13,

$$\begin{aligned}
C_{w,h}^{(2)} &= \sum_{y_3=1}^h \sum_{x_3=1}^{\lfloor y_3 w/h \rfloor} \left(\frac{w}{2h} \cdot (h - y_3)^2 + \frac{h}{2w} \cdot x_3^2 + O(w + h) \right) \\
&= \sum_{y_3=1}^h \frac{w}{2h} \cdot \frac{y_3 w}{h} \cdot (h - y_3)^2 + \sum_{y_3=1}^h \frac{h}{6w} \cdot \left(\frac{y_3 w}{h} \right)^3 + O(w^2 h + h^2 w) \\
&= \frac{w^2}{2h^2} \cdot \frac{h^4}{12} + \frac{w^2}{6h^2} \cdot \frac{h^4}{4} + O(w^2 h + w h^2) \\
&= \frac{1}{12} w^2 h^2 + O(w^2 h + w h^2).
\end{aligned}$$

We continue now estimating $D_{w,h}^{(2)}$. Let us consider the case when both points p_3 and p_4 are above $\overline{p_1 p_2}$; the other case is analogous. Because of symmetry, we can denote by p_3 the point with smallest x coordinate, see Figure 3.8. In this case, for each choice of p_3 , the point p_4 must lie in $K = K(p_3)$: the region below the line supporting $\overline{p_1 p_3}$, above the line supporting $\overline{p_2 p_3}$, and below the horizontal line through p_2 . Hence,

$$D_{w,h}^{(2)} = 2 \sum_{p_3 \text{ above } \overline{p_1 p_2}} (|Q_{w,h} \cap K| + O(w + h))$$

The region K is a triangle and, using that the slope of $\overline{p_1 p_3}$ is $\frac{y_3}{x_3}$, we obtain that K has base (on $y = h$) equal to $w - \frac{x_3}{y_3} h$ and height equal to $h - y_3$, see Figure 3.8. Therefore,

$$\text{area}(K(p_3)) = \frac{1}{2} \cdot \left(w - \frac{x_3}{y_3} h \right) (h - y_3) = \frac{1}{2} \left(w(h - y_3) - x_3 \left(\frac{h^2}{y_3} - h \right) \right).$$

By Theorem 3.13,

$$\begin{aligned}
D_{w,h}^{(2)} &= 2 \sum_{y_3=1}^h \sum_{x_3=0}^{\lfloor y_3 w/h \rfloor} \frac{1}{2} \left(w(h - y_3) - x_3 \left(\frac{h^2}{y_3} - h \right) + O(w + h) \right) \\
&= \sum_{y_3=1}^h \left(w(h - y_3) \left(\frac{y_3 w}{h} \right) - \frac{1}{2} \cdot \left(\frac{y_3 w}{h} \right)^2 \left(\frac{h^2}{y_3} - h \right) \right) + O(w^2 h + h^2 w) \\
&= \sum_{y_3=1}^h \left(\left(\frac{w^2}{h} (h - y_3) y_3 \right) - \left(\frac{w^2}{2} y_3 \right) + \left(\frac{w^2}{2h} y_3^2 \right) \right) + O(w^2 h + h^2 w) \\
&= \left(\frac{w^2}{h} \left(\frac{h^3}{6} \right) \right) - \left(\frac{w^2}{2} \left(\frac{h^2}{2} \right) \right) + \left(\frac{w^2}{2h} \left(\frac{h^3}{3} + O(h^2) \right) \right) + O(w^2 h + w h^2) \\
&= \frac{1}{12} w^2 h^2 + O(w^2 h + w h^2).
\end{aligned}$$

Using the computed values we conclude that

$$\begin{aligned}
A_{w,h}^{(2)} &= 2 \cdot \left(\frac{1}{12}w^2h^2 + O(w^2h + wh^2) + \frac{1}{12}w^2h^2 + O(w^2h + wh^2) \right) \\
&= \frac{1}{3}w^2h^2 + O(w^2h + wh^2).
\end{aligned}$$

□

This finishes the estimates of each single value $A_{w,h}^{(i)}$. Adding them we have that

$$A_{w,h} = w^2h^2 \left(\frac{1}{2} + \frac{2}{3} + \frac{1}{3} \right) + O(w^2h + wh^2) = \frac{3}{2}w^2h^2 + O(w^2h + wh^2).$$

We summarise our findings.

Lemma 3.16 ([W7]). There are $\frac{3}{2}w^2h^2 + O(w^2h + wh^2)$ sets $S \in \binom{Q_{w,h}}{4}$ such that: the points of S are in convex and axis-general position, the bounding box of S is $Q_{w,h}$, and both diagonals of the convex quadrilateral defined by S have positive slope or both diagonals have negative slope.

Proof of Theorem 3.11. By Equation 3.3 the number of quadrilaterals that define a monochromatic crossing is

$$\begin{aligned}
&\sum_{w=1}^m \sum_{h=1}^m \left(\frac{3}{2}w^2h^2 + O(w^2h + wh^2) \right) (m^2 - (w+h)m + wh + O(m)) \\
&= \left(\sum_{w=1}^m \frac{1}{2}w^2m^5 - \frac{1}{2}w^3m^4 + \frac{3}{8}w^2m^5 + \frac{3}{8}w^3m^4 \right) + O(m^7) \\
&= \frac{1}{6}m^8 - \frac{1}{8}m^8 - \frac{1}{8}m^8 + \frac{3}{32}m^8 + O(m^7) \\
&= \frac{1}{96}m^8 + O(m^7).
\end{aligned}$$

Dividing by $\binom{m^2}{4} \cdot \frac{m^8}{24}$ gives the probability $\frac{1}{4}$ for a monochromatic quadrilateral. □

We believe that colouring by positive and negative slope is the best that can be done for using a two range colouring. A *two range colouring* is given by angles $\alpha, \beta \in [0, 360]$ with $\alpha < \beta$, line segments are blue if they can be obtained from a segment on the x -axis by translation and rotation by some angle $\gamma \in [\alpha, \beta]$ in counter-clockwise direction and red otherwise. It would be nice to find a proof that colouring by positive and negative slope is in fact the best that can be done for these types of colouring.

3.3.3 Torus with Euclidean Metric

We will turn our attention back to μ -random drawings and the parameter $t(K_2, W_{S,\mu})$. If S is a torus with an Euclidean metric, a random drawing on the torus depends on the choice

of metric. Recall the fundamental polygon of a torus which stems from a Voronoi cell of a lattice in the Euclidean plane where a parallelogram defined by the lattice is spanned by two vectors t_1, t_2 where we can assume $t_1 = (1, 0)$. Taking the most natural lattice, $t_1 = (1, 0)$, $t_2 = (0, 1)$, turns out to be the worst model for random drawings if we want to minimise crossings. Guy, Jenkyns and Schaar [47] showed that a random drawing of K_n on the torus with rectangular fundamental polygon (Figure 1.4 (a)) has $\approx \frac{5}{432}n^4 = 0.01157..n^4$ crossings. Elkies [29] recently showed that the metric which minimises the crossing number stems from a plane tiling with the parallelogram spanned by the vectors $(0, 1)$ and $(1/2, \sqrt{3}/2)$ (Figure 1.4 (b)). A uniformly random geodesic drawing of K_n has $\approx \frac{11}{972}n^4 = 0.01131..n^4$ crossings. This is the best upper bound for toroidal drawings of the complete graph so far.

3.3.4 Sphere

Moon [83] showed that picking n points uniformly at random from the sphere and connecting them by shortest paths gives a drawing of K_n with expected number of crossings $\frac{1}{64}n(n-1)(n-2)(n-3)$, which is the same multiplicative constant as in Hill's conjecture. We extended Moon's result to the case where the points are picked with respect to a more general probability distribution. The distribution only needs to be *non-degenerate*, which means the probability that three points lie on a common great circle is zero, and *antipodally-symmetric* which means for every measurable set $A \subseteq \mathbb{S}^2$ the measure of its antipodal set \bar{A} is the same, $\mu(A) = \mu(\bar{A})$.

Theorem 3.17 (See [W4] for a different proof.). Let μ be a non-degenerate antipodally symmetric probability distribution on the unit sphere \mathbb{S}^2 . Then $t(W_{\mathbb{S}^2, \mu}, K_2) = \frac{1}{8}$.

Proof. Let ϕ_1 be the identity map on \mathbb{S}^2 and ϕ_2 be the map that sends a point to its antipodal point. Since μ is antipodal, ϕ_1, ϕ_2 are measure-preserving automorphisms on $(\mathbb{S}^2, B(\mathbb{S}^2), \mu)$. Note that for $i_1, i_2, j_1, j_2 \in \{1, 2\}$

$$t(W_{\mathbb{S}^2, \mu}, K_2) = \int_{(\mathbb{S}^2)^4} W_{\mathbb{S}^2, \mu}((\phi_{i_1}(x_1), \phi_{j_1}(y_1)), (\phi_{i_2}(x_2), \phi_{j_2}(y_2))) dx_1 dy_1 dx_2 dy_2, \quad (3.4)$$

since ϕ_1, ϕ_2 are measure-preserving. We denote by \bar{x} the antipodal point of x . We consider the great circle C_1 that contains $x_1, y_1, \bar{x}_1, \bar{y}_1$ and the great circle C_2 that contains the points $x_2, y_2, \bar{x}_2, \bar{y}_2$. As already observed by Elkies and Mohar [29, 78], C_1, C_2 cross exactly twice. Therefore,

$$2 = \int \sum_{i_1, i_2, j_1, j_2 \in \{0, 1\}} W_{S, \mu}((\phi_{i_1}(x_1), \phi_{j_1}(y_1)), (\phi_{i_2}(x_2), \phi_{j_2}(y_2))) dx_1 dy_1 dx_2 dy_2. \quad (3.5)$$

From equation 3.4 and 3.5 it follows that

$$t(W_{\mathbb{S}^2, \mu}, K_2) = \frac{2}{24} = \frac{1}{8}.$$

□

From this we can easily deduce the crossing probability of a μ -random drawing of the complete graph.

Corollary 3.18 (See [W4]). Let μ be a non-degenerate antipodally symmetric probability distribution on the unit sphere \mathbb{S}^2 . Let D_n be a μ -random drawing of K_n . Then $\mathbb{E}(\text{cr}(K_n)) = \frac{1}{64}(n-4)(n-3)(n-2)(n-1)$.

Proof. If two pairs of edges share a common vertex, then they do not cross. There are

$$\frac{1}{8}n(n-1)(n-2)(n-3)$$

pairs of edges that do not share a common vertex, and the result follows by linearity of expectation. □

In the following we will consider drawings of the complete bipartite graph $K_{N,N}$, where vertices in one part are drawn at random from the sphere with respect to some probability measure μ_1 and vertices in the other part are drawn at random from the sphere with respect to some probability measure μ_2 . Let $V_{N,1}$ and $V_{N,2}$ denote the parts of the bipartition of $K_{N,N}$. Recall the definition of e_d -proportional from Section 3.3. The vertex partition $(V_{N,1}, V_{N,2})_N$ is an e_d -proportional vertex partition of $K_{N,N}$ for $e_d : \{1, 2\}^2 \rightarrow \{0, 1\}$ with $e(1, 1) = e(2, 2) = 0$ and $e(1, 2) = e(2, 1) = 1$, and we call this particular e_d the *edge density function of $K_{N,N}$* . Hence Theorem 3.9 applies. In the following we say shortly a (μ_1, μ_2) -random drawing of $K_{N,N}$ for a (μ_1, μ_2) -random drawing of $K_{N,N}$ partitioned into its parts $V_{N,1}, V_{N,2}$.

Corollary 3.19 (See [W4]). Let D_N be a (μ_1, μ_2) -random drawing of $K_{N,N}$. Then the expected number of crossings is $E(\text{cr}(K_{N,N})) = \frac{1}{16}N^2(N-1)^2$.

Proof. If two pairs of edges share a common vertex, then they do not cross. There are

$$2 \binom{N}{2} \binom{N}{2}$$

pairs of edges that do not share a common vertex. Each such pair crosses with probability $\frac{1}{8}$ by a generalisation of Theorem 3.17. □

We turn our attention to triangle densities.

Question 3.20. Let e_d be the edge density function of $K_{N,N}$. Given $\mu = (\mu_1, \mu_2)$ such that $t(K_2, W_{\mathbb{S}^2, \mu, e_d}) = \frac{1}{8}$, what are possible values for $t(K_3, W_{\mathbb{S}^2, \mu, e_d})$?

For brevity we will call $W(\mu_1, \mu_2) = W_{\mathbb{S}^2, \mu, e_d}$ for $\mu = (\mu_1, \mu_2)$, where e_d is the edge density function of $K_{N,N}$. The rest of this section is concerned with computing possible values for the triangle density $t(K_3, W(\mu_1, \mu_2))$ and proving the following theorem.

Theorem 3.21 ([W4]). For fixed $r > 0$ let μ_1 and μ_2 be uniform distributions over two pairs of antipodal circles on \mathbb{S}^2 of radius r each and let $W(\mu_1, \mu_2)$ be the crossing graph limit of the corresponding drawings. Then

$$\frac{83}{3 \cdot 2^{12}} + O(r) \leq t(K_3, W(\mu_1, \mu_2)) \leq \frac{1}{3 \cdot 2^5} + O(r),$$

and these bounds are best possible. Further, every value in the interval $(\frac{83}{12288}, \frac{128}{12288})$ is possible for the triangle density $t(K_3)$.

We will prove this theorem by turning to the discrete setting. We fix a drawing D_4 of the complete bipartite graph $K_{4,4}$ where each part consists of two antipodal pairs of vertices on \mathbb{S}^2 as in Figure 3.9.

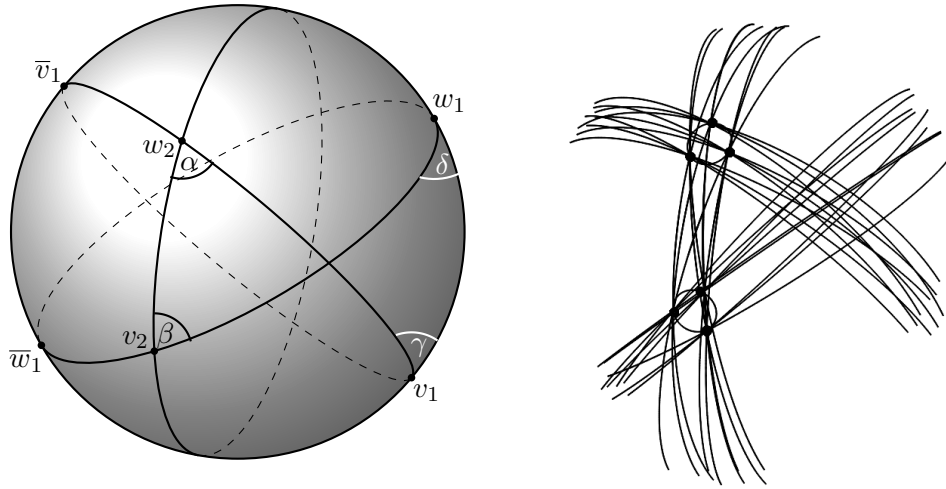


Figure 3.9: The left part shows a drawing D_4 of a $K_{4,4}$ on parts $\{v_1, \bar{v}_1, v_2, \bar{v}_2\}$ and $\{w_1, \bar{w}_1, w_2, \bar{w}_2\}$. The angles α and β are in the triangle formed by w_2 , v_2 and a crossing, whereas γ and δ are in a triangle formed by v_1 , w_1 and the same crossing. The right-hand side shows part of a $D_4^{(3)}$ drawing with the circles of w_2 and v_2 each containing 3 vertices and with nine edges for each incident bundle emanating from these two nodes.

We will be considering a *blowup drawing* $D_4^{(n)}$ of D_4 for which we replace each vertex from D_4 with a circle of some small radius $r = r(n)$ that is centred at that vertex, and position n evenly spaced vertices on that circle. These n vertices will be referred to as the *node* of the corresponding vertex of $K_{4,4}$. We also assume that all $8n$ vertices obtained in this way are in general position. In that way, each edge of $K_{4,4}$ is replaced by a complete bipartite graph between the corresponding nodes which we call the *edge bundle*. This means for $N = 4n$ that $D_4^{(n)}$ is a drawing of $K_{N,N}$. In what follows, we discuss the number of triangles in the intersection graph (of edges in $D_4^{(n)}$) when n grows large. To simplify our discussion about triangles, we first classify the crossings in $D_4^{(n)}$.

In the blowup drawing $D_4^{(n)}$, we distinguish three types of crossings, depending on what they stem from, as depicted in Figure 3.10.

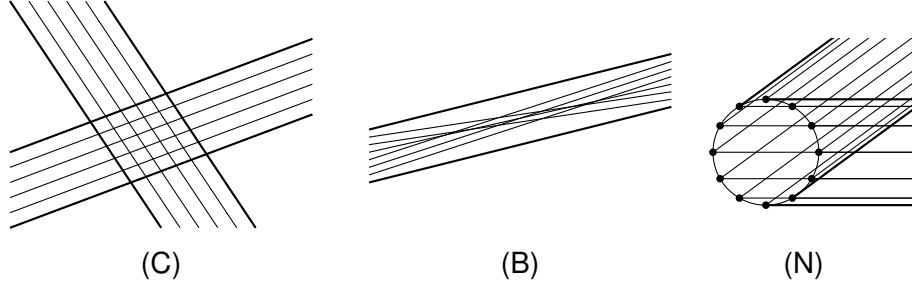


Figure 3.10: Possible crossings in the blow up: Bundle-bundle crossings (C), bundle crossings (B) and node crossings (N).

Let us define these types (B), (C), and (N) more precisely and state their count.

- (C) Two edge-bundles cross in a small neighbourhood of a previous crossing in D_4 . We call these *bundle-bundle crossings* (C). Since each edge-bundle consists of n^2 edges, this gives n^4 bundle-bundle crossings for each crossing in D_4 .
- (B) Two edges cross within a bundle. We call these *bundle crossings* (B). Here we have $\binom{n}{2}^2$ crossings per bundle assuming $r(n) \ll n^{-1}$ and a suitable rotation of the circles.
- (N) Two edge-bundles cross at a node. We call these *node crossings* (N). Let $\alpha \in (0, \pi)$ be the angle between two incident edges e, f in D_4 which were blown up to the edge-bundles, and let cr_α be the resulting number of node crossings between the edges in the corresponding edge-bundles. Then we have: $\text{cr}_\alpha + \text{cr}_{\pi-\alpha} = \frac{n^3(n-1)}{2}$.

To help us with counting crossings of type (N) below, we first prove the following Lemma.

Lemma 3.22 ([W4]). Let A and B be two nodes corresponding to adjacent vertices in D_4 and let $x \in A$. If the geodesics from x to B intersect the circle C_A corresponding to A , we denote by L_x the set of vertices in A that are on the smallest circular arc that contains those intersections. Then $|L_x| = O(rn)$. Moreover, if $W_y = \{x \in A \mid y \in L_x\}$, then $|W_y| = O(rn)$.

Proof. Note that the length of L_x is $O(r^2/d)$, where d is the distance from A to B (see Figure 3.11). As we consider the distance d to be constant, the number of vertices y such that $y \in L_x$ is $O(r^2n/(2\pi r)) = O(rn)$. Moreover, since the angles at y and x , as shown in Figure 3.11, are almost the same as d is large compared to r , we also have $|W_y| = O(rn)$. \square

In the following we discuss and count the crossings of each type.

- (C) Two edge-bundles cross in a small neighbourhood of a previous crossing in D_4 . (We assume that $r(n)$ is small.) We call these *bundle-bundle crossings* (C). Since each edge-bundle consists of n^2 edges, this gives n^4 bundle-bundle crossings for each crossing in D_4 .

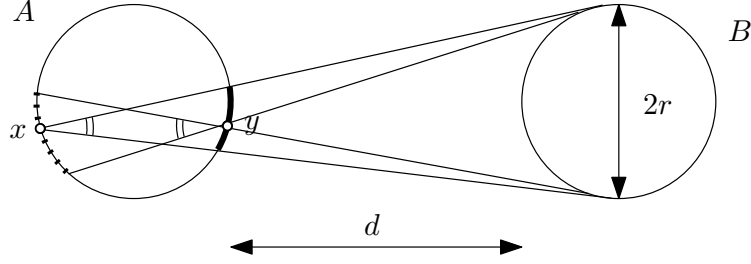


Figure 3.11: L_x are the vertices on the arc between the extremal two edges leading from x to B . The dashed arc in this figure contains vertices in W_y .

- (B) Two edges cross within a bundle. We call these *bundle crossings* (B). Here we have $\binom{n}{2}^2$ crossings per bundle if $r(n) \ll n^{-1}$ and suitably rotated circles considering the following elementary argument:

Claim 3.23. Let $D_{A,B}$ be the subdrawing of $D_4^{(n)}$ consisting of all edges between two nodes A, B corresponding to two adjacent vertices of D_4 . If $r(n) \ll n^{-1}$ and the cycles are suitably rotated, then $\text{cr}(D) = \binom{n}{2}^2$.

Proof. Any 4-tuple of two vertices from A and two vertices from B determines precisely one crossing, and each crossing corresponds to precisely one such 4-tuple of vertices. \square

If we drop the restriction $r(n) \ll n^{-1}$ and consider general r the picture looks slightly different. Referring to Figure 3.11 we can see that if $y \in L_x$ then the pair x, y does not contribute (B) crossings with any pair of vertices in B . For another pair of vertices w, z in B we can see that the edges from x to w, z and from y to the antipodals \bar{w}, \bar{z} contribute two crossings. Hence generally we have $\binom{n}{2}^2 + O(rn^4)$ bundle crossings and $O(rn^4)$ additional node crossings.

- (N) Two edge-bundles cross at a node. We call these *node crossings* (N). Let $\alpha \in (0, \pi)$ be the angle between two incident edges e, f in D_4 which were blown up to the edge-bundles, and let cr_α be the resulting number of node crossings between the edges in the corresponding edge-bundles. We consider one bundle to be horizontal whereas the other bundle is counterclockwise at angle α . We partition the edges from the bundle at angle α into four sets depending on which vertex in the node they are adjacent to. Starting at the top vertex, we enumerate the vertices clockwise along the cycle. The first $\frac{\pi-\alpha}{2\pi}n$ vertices¹ belong to part (A), the next $\frac{\alpha}{2\pi}n$ vertices belong to part (B), then we have $\frac{\pi-\alpha}{2\pi}n$ vertices belonging to part (C) and the last $\frac{\alpha}{2\pi}n$ vertices

¹The numbers of nodes in each part are rounded up or down, but these changes will make our counts of crossings deviate only in a lower order term and can thus be neglected.

belong to part (D) as in Figure 3.12. Assuming the circle radius r is small enough, all edges in one bundle are almost parallel to each other up to an error term that depends on r . For each vertex x we introduce two sets of vertices, S_x and W_x . Let $y \in S_x$ if all horizontal edges incident with y cross all edges at angle α that are incident with x , and let $W_x = \{y \in A \mid x \in L_y\}$ where L_y is defined as in Lemma 3.25 with respect to the horizontal edges. If x is the i -th vertex in (A) then $|S_x| = 2i + O(rn)$ and $|W_x| = O(rn)$. If x is in (B) then $|S_x| = \frac{\pi - \alpha}{\pi}n + O(rn)$ and $|W_x| = O(rn)$. If x is in (C) then a similar count as in (A) applies if we enumerate those vertices starting at the last vertex in (C). If $x \in (D)$ then S_x is empty and $|W_x| = O(rn)$. Note that each pair x, y such that $y \in S_x$ contributes n^2 crossing and if $y \in W_x$ then the contribution is $O(n^2)$ crossing. Finally the number of crossings is

$$\begin{aligned} \text{cr}_\alpha(r) &= 2 \left(\sum_{i=1}^{(\pi - \alpha)n/2\pi} (2i + O(rn)) \cdot n^2 \right) + \left(\frac{\alpha}{2\pi} n^2 \right) \left(\frac{\pi - \alpha}{\pi} + O(rn) \right) n^2 \\ &= \frac{\pi - \alpha}{2\pi} \cdot n^4 + O(rn^4 + n^3). \end{aligned}$$

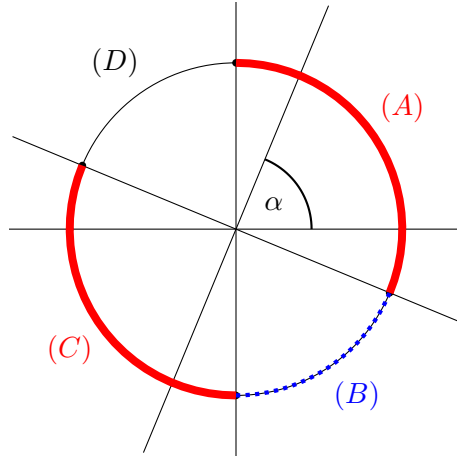


Figure 3.12: (A), (B), (C) and (D) are special areas of vertices of a node. An illustration where $0 < \alpha \leq \frac{\pi}{2}$.

Let us observe that $\text{cr}_\alpha + \text{cr}_{\pi - \alpha} = \frac{n^3(n-1)}{2}$. This formula, which is exact, can be obtained directly by considering all four bundles arriving to a node as shown in Figure 3.13. It is apparent from the figure that the total number of crossings, which is equal to $2 \text{cr}_\alpha + 2 \text{cr}_{\pi - \alpha}$, can be counted by considering every ordered pair (x, y) of distinct vertices in the node and observing that the horizontal edges incident with x and the angle α edges incident with y leaving in both directions from each vertex yield n^2 crossings.

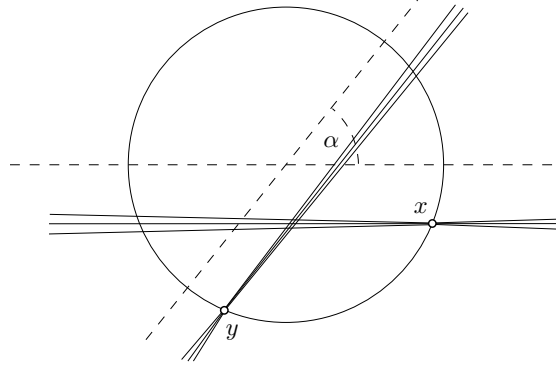


Figure 3.13: An illustration of the antipodal argument for the total number of node crossings at one of the nodes. The edges incident with any x and y ($x \neq y$) yield precisely n^2 node crossings.

The crossings in a triangle need to stem from bundle-bundle crossings (C), bundle crossings (B) or node crossings (N) as specified above. We first prove the following lemma.

Lemma 3.24 ([W4]). Let D_4 be a spherical drawing of a $K_{4,4}$ where each part consists of two pairs of antipodal vertices. Then no edge in D_4 is crossed twice.

Proof. Let the parts of the $K_{4,4}$ be $A = \{v_1, \bar{v}_1, v_2, \bar{v}_2\}$ and $B = \{w_1, \bar{w}_1, w_2, \bar{w}_2\}$. Note that the edge v_1w_1 can only be crossed by an edge between the other antipodal pairs, i.e. $v_2w_2, v_2\bar{w}_2, \bar{v}_2w_2, \bar{v}_2\bar{w}_2$. All of them lie on the great circle defined by v_2w_2 so in fact only one of these edges can cross v_1w_1 . By symmetry the same holds for the other edges. \square

We classify the triangles in the intersection graph of the blowup drawing $D_4^{(n)}$ as follows. We assign each crossing (which is an edge in the intersection graph) a *type* (C), (B), or (N) depending on whether it is a bundle-bundle, within bundle or a node crossing. We say a triangle $c_1c_2c_3$ is of *type* $(l(c_1)l(c_2)l(c_3))$ where $l(c_i)$ is the type of crossing c_i .

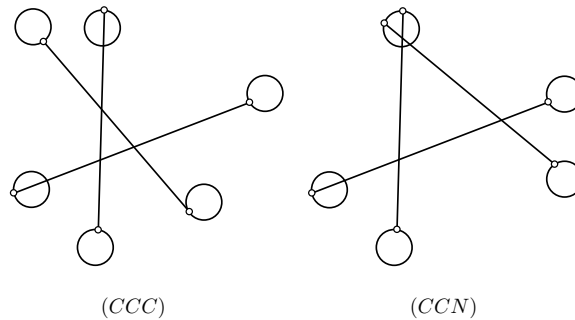


Figure 3.14: Triangles of type (CCC) and (CCN).

The above lemma shows that there are no (CCC) or (CCN) triangles in $D_4^{(n)}$. Also note that (CBB), (BBN) and (CBN) are not possible in general since BB suggests that all edges are from the same bundle and the bundled edges in (CBN) cross the third edge either at a

node or at a bundle-bundle crossing but not at both. Triangles of type (NNN) either appear at three different nodes or at one node. However, we can not have (NNN) triangles at three different nodes since $K_{4,4}$ is bipartite and hence triangle-free. By the following lemma, the number of (NNN) triangles with all three crossings at one node is only of order rn^6 and can therefore be neglected.

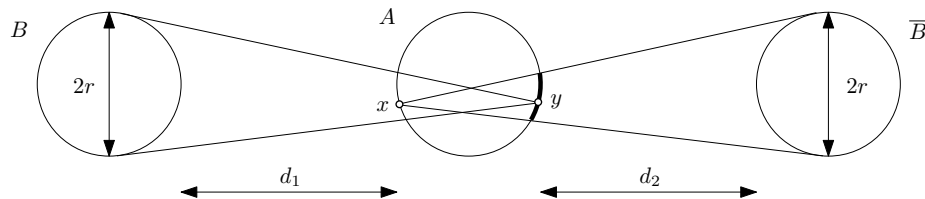


Figure 3.15: Two edges from node A leading to antipodal nodes B and \bar{B} can cross. If $d = \min\{d_1, d_2\}$ and $r \leq d$, then $|L_x| = O(rn)$.

Lemma 3.25 ([W4]). The number of (NNN) triangles in $D_4^{(n)}$ that correspond to three edges at the same node is $O(rn^6)$. Moreover, if $r(n) \ll n^{-1}$, there are no such triangles.

Proof. Let us refer to Figure 3.15 and consider the possibility that an edge incident with a vertex y and leading to a node B crosses an edge incident with a vertex x that leads to the antipodal node \bar{B} . If the geodesics from x to \bar{B} intersect the circle C_A corresponding to A , we denote by L_x the set of vertices in A that are on the smallest circular arc that contains those intersections.

Then it is easy to see that either $x \in L_y$ or $y \in L_x$ (or both as shown in the figure). It can be shown (details can be found in the full paper) that the number of cases where $y \in L_x$ or $x \in L_y$ is $O(rn)$. In particular, if $r \ll n^{-1}$ then L_x is empty. For each such pair x, y , the number of vertices z whose incident edges leading to a node different from B and \bar{B} make an (NNN) crossing triangle with two edges incident with x and y , respectively, is $O((t+r)n)$, where t is the number of vertices on the arc between x and y . We define the parameter l which is the number of vertices in the node A between x and the lowest point on the circle of A (assuming that x is in the lower half of the circle and on the left side). Then $t \in [2l - \Theta(rn), 2l + \Theta(rn)]$. This gives the following upper bound for the number of such triples (x, y, z) :

$$4 \sum_{l=1}^{n/4} O(rn)O(2l + rn) = O(rn^3).$$

Finally, since each such triple involves $O(n^3)$ triples of mutually crossing edges incident with x, y, z , we confirm that the number of considered (NNN) triangles is $O(rn^6)$. \square

We are left with the following four cases.

(CNN) We consider pairwise crossings of three edges such that two cross at a bundle-bundle crossing and the third edge crosses one edge each at one node each. These

crossings depend on the angles $\alpha, \beta, \gamma, \delta$ as depicted in Figure 3.9. By Section (N) the number of pairs of vertices x, y such that all edges at angle α incident to x cross all horizontal edges incident to y is $\frac{\pi-\alpha}{2\pi}n^2 + O(rn^2 + n)$. It is easy to see that the number of crossings we get in the triangle including α and β is $(\frac{\pi-\alpha}{2\pi})(\frac{\pi-\beta}{2\pi})n^6 + O(rn^6 + n^5)$. We have a similar count for the angles γ and δ . Then we have to add three other contributions corresponding to other crossings in D_4 . The antipodal crossing involves a triangles with α, β and γ, δ , whereas the other two crossings involve triangles with α, γ and β, δ . Overall, this gives $\frac{2}{n^2}(\text{cr}_\alpha + \text{cr}_\delta)(\text{cr}_\gamma + \text{cr}_\beta) + O(rn^6 + n^5)$ triangles of this kind.

(BBB) We consider pairwise crossings of three edges such that all edges are from one bundle. For each bundle we get $\binom{n}{3}^2 + O(rn^6)$ such triangles by Section (B). There are 16 bundles so in total we have $\sim \frac{4}{9}n^6 + O(rn^6)$ triangles of the type (BBB).

(CCB) We consider pairwise crossings of three edges such that two edges are in one bundle and cross the third edge at a bundle-bundle crossing. There are $2\binom{n}{2}^2n^2 + O(rn^6)$ triangles per each crossing in D_4 . We have 4 crossings so in total $\sim 2n^6 + O(rn^6)$ triangles of this kind.

(BNN) We consider pairwise crossings of three edges such that two are in the same bundle and cross the third edge at a node. The argument is analogous to the one for crossings of type (N). Starting at the top vertex, we enumerate the vertices clockwise along the cycle as in Figure 3.12. We consider an edge at angle α which ends in the i -th vertex in part (A) and its crossings to horizontal edges. From Section (N), we know that $|S_i| = 2i + O(rn)$, where S_i is as defined there. We can choose from $\binom{2i+O(rn)}{2}$ pairs of left endpoints and $\binom{n}{2}$ pairs of right endpoints for a triangle. The number of triangles with an edge ending in i and another edge ending in a vertex in $W_x = \{y \in A \mid x \in L_y\}$ is of order $O(rn^4)$, where L_y is defined as in the proof of Lemma 3.25. We consider now edges at angle α ending in a vertex x in (B). Note that $|S_x| = \frac{\pi-\alpha}{\pi}n + O(rn)$. We can choose for any one of $\binom{\frac{\pi-\alpha}{\pi}n+O(rn)}{2}$ pairs of left endpoints $\binom{n}{2}$ pairs of right endpoints for a triangle. The number of triangles with another edge ending in a vertex in W_x is of order $O(rn^4)$. The contribution of triangles from edges in (C) is the same as for edges in (A). Hence the number of triangles of type (BNN) is

$$2 \left(n \sum_{i=1}^{(\pi-\alpha)n/2\pi} \binom{2i}{2} \cdot \binom{n}{2} \right) + \left(\frac{\alpha}{2\pi}n^2 \right) \cdot \left(\frac{\pi-\alpha}{\pi}n \right) \binom{n}{2} + O(rn^6 + n^5).$$

For α and $\pi - \alpha$ added together, this gives

$$\frac{1}{12}n^6 - \frac{\alpha(\pi-\alpha)}{8\pi^2}n^6 + O(rn^6 + n^5).$$

Now note that for two bundles at angle α we can choose one of the bundles to contain the bundled edges. This gives two options. At each node we have two pairs of bundles meeting at angle α and two pairs of bundles meeting at angle $\pi - \alpha$. (In addition to these

possibilities we get further (BNN) triangles from two bundles at the same node that lead to antipodal nodes and correspond to the value of $\alpha = \pi$. They give only $O(rn^6 + n^5)$ triangles.) If $\alpha, \beta, \gamma, \delta$ are the angles as in Figure 3.9, the overall number of (BNN) triangles is

$$\frac{\alpha(\alpha - \pi) + \beta(\beta - \pi) + \gamma(\gamma - \pi) + \delta(\delta - \pi)}{\pi^2} n^6 + \frac{8}{3} n^6 + O(rn^6 + n^5).$$

If we leave out smaller order terms, the total number of triangles in the intersection graph by summing up the number of (CNN), (BBB), (CCB) and (BNN) triangles is

$$\frac{\alpha^2 + \beta^2 + \gamma^2 + \delta^2 - \pi(\alpha + \beta + \gamma + \delta)}{\pi^2} n^6 + \frac{(2\pi - \alpha - \delta)(2\pi - \gamma - \beta)}{2\pi^2} n^6 + \frac{46}{9} n^6.$$

Theorem 3.26 ([W4]). Given a drawing D_4 of a $K_{4,4}$ where each part has two antipodal pairs, let $D_4^{(n)}$ be the blowup drawing, and let $\alpha, \beta, \gamma, \delta$ be the angles defined above. Then the limiting triangle density $t(K_3)$ of the sequence $D_4^{(1)}, D_4^{(2)}, \dots$ is equal to

$$\frac{3}{2^{12}\pi^2} \left((2\pi - \alpha - \delta)(2\pi - \gamma - \beta) + 2(\alpha^2 + \beta^2 + \gamma^2 + \delta^2) - 2\pi(\alpha + \beta + \gamma + \delta) \right) + \frac{23}{3 \cdot 2^{10}} + O(r).$$

Proof. We have determined the number of triangles in the intersection graphs. Dividing by the number of possible triangles in the intersection graph, $\binom{16n^2}{3} = \frac{16^3}{6} n^6 + O(n^5)$, gives the triangle density. \square

Finally, let us show that the crossing graphs of drawings $D_4^{(n)}$ can be interpreted as certain graphons.

Theorem 3.27 ([W4]). For fixed $r > 0$ let μ_1 and μ_2 be uniform distributions over two pairs of antipodal circles on \mathbb{S}^2 of radius r each and let $W(\mu_1, \mu_2)$ be the crossing graph limit of corresponding drawings. If we consider blow-up drawings $D_4^{(n)}$ w.r.t. the centres of the circles of radius r , then the crossing graphs of $D_4^{(n)}$ converge and their limit is the graphon $W(\mu_1, \mu_2)$.

Proof. All we need to show is that the density $t_1(H)$ in the random case limit and the density $t_2(H)$ of the blow-up drawing limit are the same for each graph H . Let $k = |H|$ be the number of vertices of H and let $\phi : V(H) \rightarrow [k]$ be a bijection. For distinct points $x_1, \dots, x_k, y_1, \dots, y_k$ in \mathbb{S}^2 , let $X(x_1, \dots, x_k, y_1, \dots, y_k)$ be the intersection graph of the geodesic segments x_1y_1, \dots, x_ky_k . Consider the following function

$$f(x_1, \dots, x_k, y_1, \dots, y_k) = \begin{cases} 1, & \text{if } v \mapsto x_{\phi(v)}y_{\phi(v)} \text{ is a hom. } H \rightarrow X(x_1, \dots, y_k), \\ 0, & \text{otherwise.} \end{cases}$$

Let S_1 and S_2 be the two circles on which μ_1 and μ_2 are defined, respectively. Since f as defined above is measurable because $f^{-1}(1)$ is open, we can represent $t_1(H)$ as

$$t_1(H) = \frac{1}{(8\pi r)^k} \int_{x \in S_1^n \times S_2^n} f(x) dx.$$

In order to approximate $t_1(H)$ consider a set C_n which consists of n equidistant points on each of the cycles from S_1, S_2 . Let $\pi_n : S_1 \cup S_2 \rightarrow C_n$ be the function that maps a points from $S_1 \cup S_2$ to its closest point in X . Let g_n be a function $g_n : (S_1 \cup S_2)^{2n} \rightarrow (C_n)^{2n}$ that applies π_n componentwise. Then $f_n = f \circ g_n$ converges pointwise to f on $S_1^n \times S_2^n$. By the bounded convergence theorem

$$t_1(H) = \frac{1}{(8\pi r)^k} \int_{x \in S_1^n \times S_2^n} f(x) dx = \frac{1}{(8\pi r)^k} \lim_{n \rightarrow \infty} \int_{x \in S_1^n \times S_2^n} f_n(x) dx = t_2(H).$$

□

The theorem shows that the same values for triangle densities in the (μ_1, μ_2) -random setting hold as for the blow-up limit in Theorem 3.26.

Proof of Theorem 3.21. By Theorem 3.27 we can refer to Theorem 3.26 to find the extremal bounds. We give a proof for the upper bound first, which is attained if all angles are close to zero as in Figure 3.16. This is optimal since rewriting the equation from Theorem 3.26 gives

$$\begin{aligned} & \frac{3}{2^{12}\pi^2} (4\pi^2 - 4\pi(\alpha + \beta + \gamma + \delta) + (\alpha + \delta)(\gamma + \beta) + 2\alpha^2 + 2\beta^2 + 2\gamma^2 + 2\delta^2) \\ & \quad + \frac{23}{3 \cdot 2^{10}} + O(r) \\ & \leq \frac{3}{2^{12}\pi^2} (-4\pi(\alpha + \beta + \gamma + \delta) + (2\pi)(\gamma + \beta) + 2\pi\alpha + 2\pi\beta + 2\pi\gamma + 2\pi\delta) \\ & \quad + \frac{1}{3 \cdot 2^5} + O(r) \\ & \leq \frac{1}{3 \cdot 2^5} + O(r). \end{aligned}$$

The claimed value in the lower bound in Theorem 3.26 is attained for $\alpha = \beta = \gamma = \delta = \frac{\pi}{2}$. To construct an example where all values are close to $\frac{\pi}{2}$, we exchange v_1 and \bar{v}_1 with w_1 and \bar{w}_1 in Figure 3.16, respectively. To show that we can not do better we first prove the following claim.

Claim 3.28. Let $\alpha, \beta, \gamma, \delta$ be as in Figure 3.9. Then $\alpha + \beta + \gamma + \delta < 2\pi$.

We refer to Figure 3.9. Let T be the triangle formed by w_2, v_2 and the crossing c of the segments w_2v_1 and v_2w_1 . Let T' be the triangle formed by \bar{v}_1, \bar{w}_1 and the crossing c and note that T' contains T . Note that the angle a at \bar{v}_1 and the angle b at \bar{w}_1 in T' are $a = \pi - \gamma$

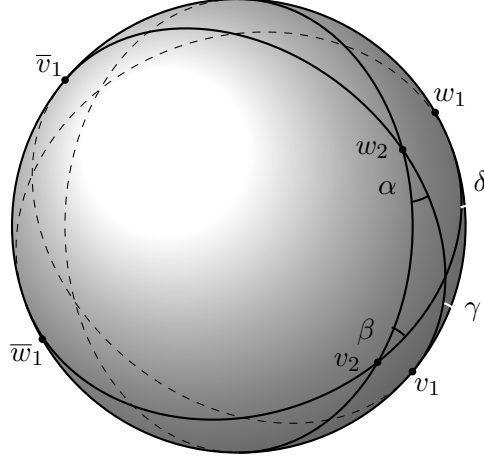


Figure 3.16: If w_2, v_2 approach w_1, v_1 , respectively, then all angles $\alpha, \beta, \gamma, \delta$ converge to zero.

and $b = \pi - \beta$. As T is within T' its area is smaller and hence its angular defect is smaller which is proportional to the angle sum. This tells us that $\alpha + \beta < a + b = 2\pi - \gamma - \delta$ which proves the claim.

Let $\alpha = \frac{\pi}{2} + a$, $\beta = \frac{\pi}{2} + b$, $\gamma = \frac{\pi}{2} + c$ and $\delta = \frac{\pi}{2} + d$. Omitting $O(r)$ terms, the associated triangle density is

$$\begin{aligned} & \frac{3}{2^{12}\pi^2} \left((\pi - a - d)(\pi - c - b) + 2a^2 + 2b^2 + 2c^2 + 2d^2 - 2\pi^2 \right) + \frac{23}{3 \cdot 2^{10}} \\ &= \frac{83}{3 \cdot 2^{12}} + \pi(-a - b - c - d) \\ & \quad + \frac{1}{2}(a + b + c + d)^2 + \frac{1}{2}(a - d)^2 + \frac{1}{2}(b - c)^2 + a^2 + b^2 + c^2 + d^2 \end{aligned}$$

and it attains its global minimum at $a = b = c = d = 0$ as $-a - b - c - d \geq 0$ by Claim 3.28.

As we can come from every arrangement of four antipodal pairs of points to every other arrangement by continuously changing the points, and since r can be arbitrary small, every triangular density in the interval $(\frac{83}{12288}, \frac{128}{12288})$ can be attained with one of these graphons. \square

3.3.5 Hyperbolic Surfaces

On hyperbolic surfaces, the geometry is more complex, and so far we can only show numerical results for the number of crossings in random geodesic drawings where segments are chosen with respect to the uniform distribution. We start by considering random geodesic segments on the hyperbolic disk D_R of radius R . For a point chosen uniformly at random from D_R , the angle θ with respect to the centre of the disk is picked uniformly from

the interval $[0, 2\pi]$. The distance r from the centre is distributed as

$$dr = \frac{\sinh(r)}{\cosh(R) - 1}.$$

This means that for a large radius R the points are likely to be close to the boundary of the disk. Four points on the boundary of a disk form a quadrilateral, so intuitively, the larger R , the higher the crossing probability. Formally one can prove this by considering the expected area $E(\text{Area}(T))$ of a triangle T formed by three points chosen uniformly at random from D_R . If a fourth point is within this triangle, then the four points do not form a convex quadrilateral. On the other hand, if we do not have a convex quadrilateral, then one of the four points is in the convex hull formed by the other three points. We have four choices for the point that is not on the boundary of the convex hull, hence if $\text{Area}(D_R)$ is the area of D_R then

$$q(D_R) = \frac{\text{Area}(D_R) - 4 \cdot E(\text{Area}(T))}{\text{Area}(D_R)} = \frac{\cosh(R) - 1 - \frac{2}{\pi} \cdot E(\text{Area}(T))}{\cosh(R) - 1}.$$

In a hyperbolic plane, $\text{Area}(T) \leq \pi$ and hence $q(D_R) \rightarrow 1$ for $R \rightarrow \infty$. Computationally, determining how $\text{Area}(T)$ behaves with respect to the radius of the disk R can be done by solving the following integral

$$\mathbb{E}(\text{Area}(T)) = \frac{1}{\text{Area}(D_R)^3} \int_{A \in D_R} \int_{B \in D_R} \int_{C \in D_R} \text{Area}(T_{A,B,C}) \, dA \, dB \, dC. \quad (3.6)$$

where $T_{A,B,C}$ is the triangle on points A, B, C . There are two strategies to solve this integral. We can use a direct formula for the area [54] or use that in the hyperbolic plane $\text{Area}(T_{A,B,C}) = \pi - \angle ABC - \angle CAB - \angle BCA$, and hence $\mathbb{E}(\text{Area}(T)) = \pi - 3 \cdot \mathbb{E}(\angle ABC)$.

We have seen that for Euclidean convex sets D , Sylvester's four point probability is minimised when the convex set D is a triangle. Now suppose Δ_R is an equilateral triangle in the hyperbolic plane with vertices at distance R from the circumcentre. The probability that four random points chosen from Δ_R form a convex quadrilateral is for very small R close to the value for an Euclidean triangle, $2/3$. Computationally, for increasing R , the probability for a convex quadrilateral decreases, which is exactly the opposite behaviour as for the disk, see Figure 3.17.

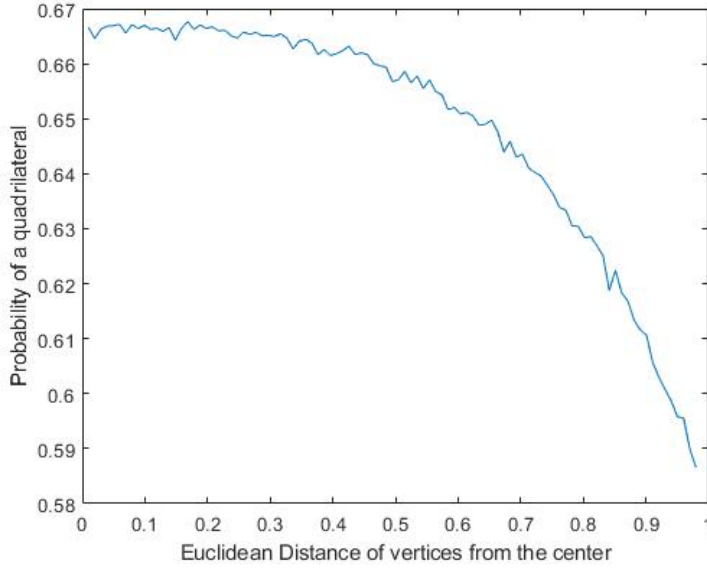


Figure 3.17: Sylvester’s four point probability for an equilateral triangle with growing hyperbolic radius r_H , which was translated into Euclidean radius $r_E = \tanh(\frac{r_H}{2})$.

We turn now to computing crossing probabilities on a standard model of the double torus. Computationally, the probability for a crossing in the double torus $S(2)$ is approximately 0.0886. A random such drawing of K_n would then approximately have $0.0886 \cdot 3 \cdot \binom{n}{4} \approx 0.011075n^4$ crossings since there are $3 \cdot \binom{n}{4}$ pairs of segments which do not share a common vertex. The algorithm used to compute these crossing probabilities for $S(2)$ can be found in Appendix A. In the following we describe the algorithm. In order to pick random points on $S(2)$, we consider $P(8, \frac{\pi}{4})$ embedded centrally in the Poincaré disk and pick random points from $P(8, \frac{\pi}{4})$. In order to do this, we note that $P(8, \frac{\pi}{4})$ is the Voronoi cell of the centre when considering the Voronoi diagram on all copies of the centre in the covering space. We pick a point randomly from the disk with the same radius as $P(8, \frac{\pi}{4})$, that is with hyperbolic radius $R = \text{acosh}\left(\cot\left(\frac{\pi}{4g}\right)^2\right)$. Recall that the radius of a point is then distributed with density

$$dr = \frac{\sinh(r)}{\cosh(R) - 1} = \frac{\sinh(r)}{\cosh\left(\text{acosh}\left(\cot\left(\frac{\pi}{4g}\right)^2\right)\right) - 1},$$

whereas the angle is distributed uniformly over 2π . Then, we check if the point is closer to the midpoint of $P(8, \frac{\pi}{4})$ or the midpoint of one of its adjacent copies (which means copies that share an edge with the central fundamental polygon). Figure 3.18 shows a random sample of such points.

For $n = 10000$ times we sample four points w_1, w_2, w_3, w_4 (in the implementation w_i is denoted as $wtuples[i]$) and find the geodesics between w_1, w_2 (and w_3, w_4). In order to do

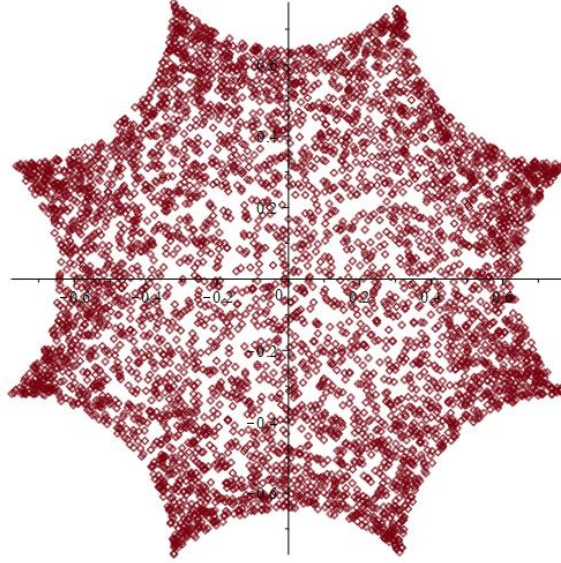


Figure 3.18: A random point set in $S(2)$.

so we let w_1 be represented by its copy in $P(8, \frac{\pi}{4})$, while w_2 ranges over all copies of nearby fundamental polygons, which is, fundamental polygons which share a vertex with the central polygon. It is possible to show that this is sufficient, by showing that if a representation of a geodesic segment in $S(2)$ represented in the Poincaré disk crosses two boundary edges of fundamental polygons, then those edges have to share a common vertex (in the Poincaré disk). Figure 3.19 depicts the copies of one such point. After finding geodesics between w_1, w_2 and w_3, w_4 represented in the Poincaré disk such that $w_1, w_3 \in P(8, \frac{\pi}{4})$, we fix the geodesic segment $w_1 w_2$ but go over all nearby representations of the geodesic segment $w_3 w_4$. If one of those representations of $w_3 w_4$ crosses the fixed representation of $w_1 w_2$, then the segments cross, otherwise they do not cross.

3.4 Random Intersection Graphs of Disks

This section considers random intersection graphs of disks of the same radius $\frac{r}{2}$. Intersection graphs of disks are easier to describe than intersection graphs of line segments since they are defined by one point on a surface S , their centre, and line segments are defined by two points on a surface, their endpoints. We will not only consider the dense case (the radius r is constant) but also consider r converging to 0 for the number of disks going to infinity.

3.4.1 Random Geometric Graph $G^d(n, r)$

The model for random disks on a surface is the random geometric graph (RGG) model. RGGs on the Euclidean plane are commonly either studied via a Poisson process (Gilbert

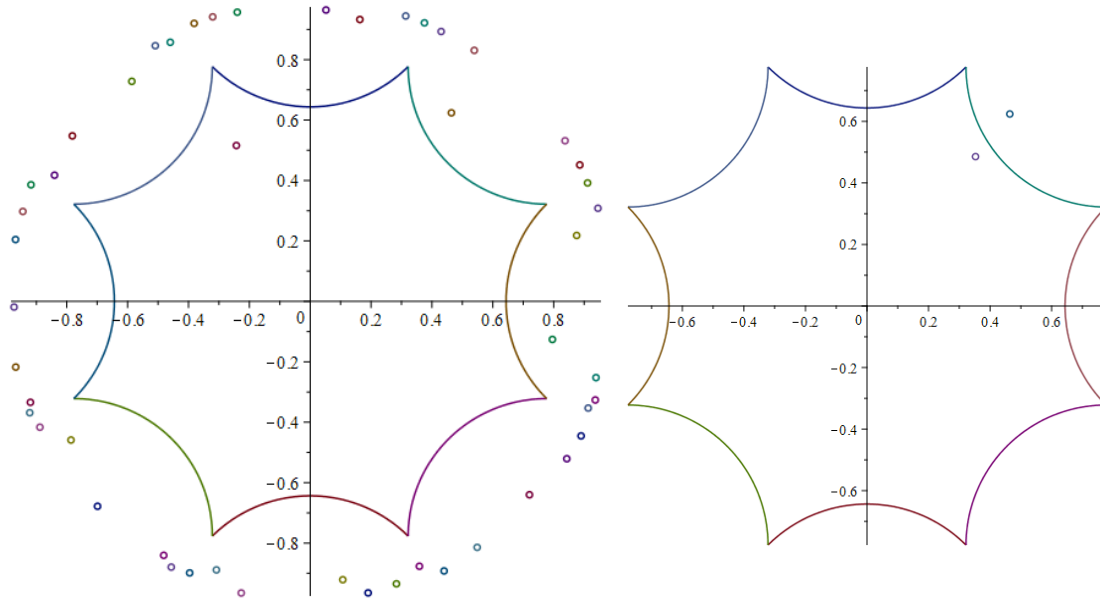


Figure 3.19: On the left, copies of a point w_2 . On the right, a polygon which contains a point w_1 and the closest copy of w_2 to w_1 . The geodesic segment between them on the Poincaré disk is as long as their distance on the surface.

Model [40]), or by choosing n points uniformly at random from $[0, 1]^2$ (see e.g. the monograph by Penrose [92]). Both models are intimately related such as $G(n, p)$ is related to $G(n, m)$. In the following we will concentrate on the second model. Suppose S is a set of finite measure with metric d , then we define the graph $G_S(n, r)$:

- $V(G_S(n, r)) = X$ is a set of points picked at random with respect to the uniform distribution on S .
- $V(G_S(n, r)) = X$ and $\{x, y\} \in E(G_S(n, r))$ if and only if $d(x, y) < r$.

We will mostly concentrate on $G_q^d(n, r)$, a random geometric graph on $S = [0, 1]^d$ equipped with the ℓ^q -metric. We will drop the parameter q if there is no specific norm we refer to and write $G^d(n, r) = G_q^d(n, r)$. Thresholds in RGGs can be analogously defined to those in the Erdős-Rényi graph: a function $r^* = r^*(n)$ is a threshold for some monotone increasing property \mathcal{P} in the random geometric graph $G_p^d(n, r)$ if

$$\lim_{n \rightarrow \infty} \mathbb{P}[G^d(n, r) \in \mathcal{P}] = \begin{cases} 0 & \text{if } r = o(r^*), \\ 1 & \text{if } r = \omega(r^*). \end{cases}$$

Thresholds for connectivity [7, 94], Hamiltonicity [26], treewidth and treedepth [75] have been studied for RGGs. A real-world application of RGGs are for example wireless networks or statistical classifications of individuals based on numerical measurements of d attributes for each individual (see [92]). Sometimes random geometric graphs $G_S(n, r)$ are

considered on more complex metric spaces S . Hyperbolic geometric graphs use the hyperbolic plane as a model to depict popularity versus similarity problems [90].

3.4.2 Thresholds for Spanning Substructures

In this section we show that the intersection graph $G_1^d(n, r)$ basically behaves like a power of a grid. For constant r we used this implicitly when considering Sylvester's four point probabilities, since we assumed that a random point sets from a square can be approximated by an integer lattice. Here we consider $r \rightarrow 0$. When dealing with independent random variables, we will use the following Chernoff bound (see, e.g., the book of Janson, Łuczak and Ruciński [57, Corollary 2.3]).

Lemma 3.29 (See [57]). Let X be the sum of n mutually independent Bernoulli random variables and let $\mu := \mathbb{E}[X]$. Then, for all $0 < \delta < 1$ we have that

$$\mathbb{P}[X \geq (1 + \delta)\mu] \leq e^{-\delta^2\mu/3}$$

and

$$\mathbb{P}[X \leq (1 - \delta)\mu] \leq e^{-\delta^2\mu/2}.$$

Given some positive integer k , we denote by G^k the k -th power of G , which is the graph defined by setting $V(G^k) := V(G)$ and $E(G^k) := \{\{u, v\} \subseteq V(G) : u \neq v, \text{dist}_G(u, v) \leq k\}$. Given two positive integers m and d , we will write $L_{m;d}$ to denote the graph with vertex set $[m]^d$ where two vertices are joined by an edge if their coordinates are equal in all but one dimension, where they differ by exactly one unit. We denote by $\lceil \cdot \rceil : \mathbb{R} \rightarrow \mathbb{Z}$ the rounding up function.

Lemma 3.30 ([W10]). Suppose $X = \{x_1, \dots, x_n\}$ are n points chosen uniformly at random from $I = [0, 1]$ and suppose the point set is labelled such that $x_1 \leq x_2 \leq \dots \leq x_n$. Fix positive integers $\ell \in [n]$ and $s \leq \frac{n}{9 \log \ell}$, and define $n_i = \lceil \frac{in}{\ell} \rceil$ for all $i \in [\ell - 1]$. Then,

$$x_{n_i} \in \left[\left(\frac{i}{\ell} - \sqrt{\frac{s \log \ell}{n}} \right), \left(\frac{i}{\ell} + \sqrt{\frac{s \log \ell}{n}} \right) \right] \text{ for all } i \in [\ell - 1]$$

with probability at least

$$1 - 2(\ell - 1)e^{-\frac{1}{7}s \log \ell}.$$

Proof. We write $\delta := \sqrt{\frac{s \log \ell}{n}}$. Then, if $\frac{i}{\ell} \geq \delta$,

$$\begin{aligned}
\mathbb{P}\left(\left|x_{n_i} - \frac{i}{\ell}\right| \geq \delta\right) &= \mathbb{P}\left(x_{n_i} \leq \frac{i}{\ell} - \delta\right) + \mathbb{P}\left(x_{n_i} \geq \frac{i}{\ell} + \delta\right) \\
&\geq \mathbb{P}\left(\left|[0, \frac{i}{\ell} - \delta] \cap X\right| \geq \frac{in}{\ell}\right) + \mathbb{P}\left(\left|[0, \frac{i}{\ell} + \delta] \cap X\right| \leq \frac{in}{\ell} + 1\right) \\
&= \mathbb{P}\left(\left|[0, \frac{i}{\ell} - \delta] \cap X\right| \geq \left(1 + \delta \left(\frac{i}{\ell} - \delta\right)^{-1}\right) \left(\frac{i}{\ell} - \delta\right) n\right) \\
&\quad + \mathbb{P}\left(\left|[0, \frac{i}{\ell} + \delta] \cap X\right| \leq \left(1 + \delta \left(\frac{i}{\ell} + \delta + \frac{1}{n}\right)^{-1}\right) \left(\frac{i}{\ell} + \delta + \frac{1}{n}\right) n\right) \\
&\leq e^{-\delta^2(i/\ell - \delta)^{-1}n/3} + e^{-\delta^2(i/\ell + \delta + 1/n)^{-1}n/3} \\
&\leq 2e^{-\delta^2(i/\ell + \delta + 1/n)^{-1}n/3},
\end{aligned} \tag{3.7}$$

where we use the Chernoff bound in Lemma 3.29. If $\frac{i}{\ell} < \delta$, then the interval $[0, \frac{i}{\ell} - \delta]$ is empty, so the same result holds by considering only the case $x_{n_i} \geq \frac{i}{\ell} + \delta$. By (3.7) for $\delta = \sqrt{\frac{s \log \ell}{n}} \leq \frac{1}{3}$, we have

$$\mathbb{P}\left(\left|x_{n_i} - \frac{i}{\ell}\right| \geq \sqrt{\frac{s \log \ell}{n}}\right) \leq 2e^{-\frac{1}{7}s \log \ell},$$

where we used that $\frac{1}{3}(\frac{i}{\ell} + \delta + \frac{1}{n})^{-1} \geq \frac{1}{7}$ for all $i \in [\ell - 1]$. A union bound over all $i \in [\ell - 1]$ gives

$$\mathbb{P}\left(\forall i : \left|x_{n_i} - \frac{i}{\ell}\right| \geq \sqrt{\frac{s \log \ell}{n}}\right) \leq 2(\ell - 1)e^{-\frac{1}{7}s \log \ell},$$

as desired. \square

We denote by $G_1^d(n, r)$ the random geometric graphs where distances are in ℓ^1 -metric, which means two vertices are connected if their ℓ^1 -distance is at most r . In the following theorem, we ignore integer parts when these do not influence the argument; in particular, by $L_{m;d}^c$ we mean $L_{m;d}^{\lfloor \cdot \rfloor}$ where $\lfloor \cdot \rfloor : \mathbb{R} \rightarrow \mathbb{Z}$ is the rounding down function.

Theorem 3.31 ([W10]). Let $d \geq 1$ be a fixed integer and $n = m^d$ for some integer $m \geq 1$. Suppose that $r = \omega\left(\sqrt{\frac{\log n}{n}}\right)$. Then, for every $\varepsilon > 0$, a.a.s. $L_{m;d}^{(1-\varepsilon)rm} \subset G_1^d(n, r) \subset L_{m;d}^{(1+\varepsilon)rm}$.

Proof. Fix $\varepsilon > 0$ and let X_1, \dots, X_n be the random variables which generate the vertex set of $G_1^d(n, r)$ in $[0, 1]^d$. Fix $r' := \frac{r}{6dC}$ for some integer C such that $\frac{1}{C} \leq \varepsilon$. We map

$$y(w) = \left(\frac{w_1 - 1}{m}, \dots, \frac{w_d - 1}{m}\right),$$

and we write $B_z = \{y(w) : w \in W_z\}$.

Note that two vertices are joined by an edge (in $L_{m;d}$) if and only if the ℓ^1 -distance of their images in the above embedding equals $\frac{1}{m}$. We will map each vertex w in $L_{m;d}$ to a point $x(w) \in X_1, \dots, X_n$ such that for all w , it holds a.a.s. that

$$\|y(w) - x(w)\|_1 \leq d\|y(w) - x(w)\|_\infty = \frac{r}{2C}. \quad (3.8)$$

We will first argue how to prove the theorem using (3.8). Fix two vertices v, w in $L_{m;d}$ and suppose that $vw \in E(L_{m;d}^{(1-1/C)rm})$, or equivalently that $\|y(v) - y(w)\|_1 \leq (1 - \frac{1}{C})r$. Then, combining (3.8) and the triangle inequality shows that $\|x(v) - x(w)\|_1 \leq r$, so $x(v) \sim x(w)$. This shows $L_{m;d}^{(1-1/C)rm} \subset G_1^d(n, r)$. Conversely, if $x(v) \sim x(w)$ is an edge in $G_1^d(n, r)$, then $\|x(v) - x(w)\|_1 \leq r$. Again, by (3.8) and the triangle inequality we obtain that $\|y(v) - y(w)\|_1 \leq (1 + \frac{1}{C})r$, which shows that $G_1^d(n, r) \subset L_{m;d}^{(1+1/C)rm}$. Since C was chosen such that $\frac{1}{C} \leq \varepsilon$, this proves Theorem 3.31.

The rest of the proof is concerned with establishing a mapping from the vertices of the grid $V(L_{m;d})$ to the vertices of the random geometric graph $V(G_1^d(n, r))$ which a.a.s. satisfies (3.8). We define the projection onto the j -th coordinate by $\sigma_j : \mathbb{R}^d \rightarrow \mathbb{R}$. Assume without loss of generality that $\sigma_1(X_1) \leq \sigma_1(X_2) \leq \dots \leq \sigma_1(X_n)$. We partition the point set X_1, \dots, X_n into ℓ parts A_1, \dots, A_ℓ where $\ell := \lceil \frac{1}{r'} \rceil \leq \frac{6dC}{r} + 1 \leq \frac{6dC+1}{r}$. Define $k_0 = 0$, and for $i \in [\ell]$, let $k_i = \frac{in}{\ell}$. In a similar way, we label the vertices v_1, \dots, v_n of $L_{m;d}$ so that $\sigma_1(v_1) \leq \sigma_1(v_2) \leq \dots \leq \sigma_1(v_n)$ (breaking ties arbitrarily). We define $W_i = \{v_{k_{i-1}+1}, \dots, v_{k_i}\}$. By analogy, we partition the point sets $(A_i)_{i=1}^\ell$ and the vertex sets $(W_i)_{i=1}^\ell$ according to their second coordinate into ℓ parts. Then, we partition the resulting sets according to the third coordinate, and so on. For two sets A, A' , we write $\sigma_i(A) \leq \sigma_i(A')$ if $\sigma_i(a) \leq \sigma_i(a')$ for all $a \in A, a' \in A'$. Thus, for all $k \in [d-1]$ and $z \in [\ell]^k$, we define recursively $A_{z_1}, \dots, A_{z_\ell} \subset A_z$ and $W_{z_1}, \dots, W_{z_\ell} \subset W_z$ where A_{z_j} and W_{z_j} contain $\frac{|A_z|}{\ell} = \frac{|W_z|}{\ell}$ points, and for all $i < j \leq \ell$,

$$\sigma_{k+1}(A_{zi}) \leq \sigma_{k+1}(A_{zj}) \text{ and } \sigma_{k+1}(W_{zi}) \leq \sigma_{k+1}(W_{zj}).$$

We define the function x so that for all $z \in \mathbb{R}^d$, x maps bijectively the vertices in W_z to the points in A_z . This is possible since the sets have the same number of vertices. It remains to show that this mapping satisfies (3.8) a.a.s. We will show that a.a.s. for every $z = (z_1, \dots, z_d)$,

$$A_z, B_z \subset \prod_{i=1}^d \left[\frac{z_i - 1}{\ell} - r', \frac{z_i}{\ell} + r' \right]. \quad (3.9)$$

Then, for every pair of points $a \in A_z, b \in B_z$, a and b are at ℓ^∞ -distance at most $\frac{1}{\ell} + 2r' \leq 3r' = \frac{r}{2dC}$, which proves that (3.8) is satisfied.

To begin with, fix $k \in [d-1]$ and $z = (z_1, \dots, z_k)$. By construction A_z contains $\frac{n}{\ell^k}$ vertices. Hence, by Lemma 3.30 with $s = 14d$, for all $i \in [\ell-1]$,

$$A_{z_1 z_2 \dots z_k i} \in [0, 1]^k \times \left[\frac{i-1}{\ell} - \sqrt{\frac{14d \log \ell}{n\ell^{-d+1}}}, \frac{i}{\ell} + \sqrt{\frac{14d \log \ell}{n\ell^{-d+1}}} \right] \times [0, 1]^{d-k-1} \quad (3.10)$$

with probability at least

$$1 - 2(\ell-1)e^{-2d \log \ell} = 1 - \frac{2(\ell-1)}{\ell^{2d}}.$$

By the union bound on the complementary events for all $z \in \bigcup_{k=0}^{d-1} [\ell]^k$, Property (3.10) holds with probability at least

$$1 - 2 \sum_{i=0}^{d-1} \ell^i (\ell-1) e^{-2d \log \ell} \geq 1 - 2\ell^{-d} = 1 - o(1).$$

It remains to show that for all sufficiently large n ,

$$\sqrt{\frac{14d \log \ell}{n\ell^{-d+1}}} \leq r'.$$

Using that $\ell \leq \frac{6dC+1}{r} \leq (6dC+1)^{d+1} \sqrt{\frac{n}{\log(n)}}$ (so in particular $n\ell^{1-d} \gg \omega(1)$) and that $\sqrt{\frac{14d \log \ell}{n\ell^{-d+1}}}$ is an increasing function of ℓ , we obtain that

$$\sqrt{\frac{14d \log \ell}{n\ell^{1-d}}} \leq \sqrt{\frac{28d \log \left(\sqrt[d+1]{\frac{n}{\log n}} \right)}{n \left(\sqrt[d+1]{\frac{n}{\log n}} \right)^{1-d}}} = O \left(\sqrt[d+1]{\frac{\log(n)}{n}} \right) = o(r').$$

This proves (3.9) for A_z .

We turn our attention to W_z . First, consider W_1, \dots, W_ℓ . It holds that

$$\left[\frac{m(i-1)}{\ell} + 2, \frac{mi}{\ell} - 1 \right] \times [m]^{d-1} \subset W_i \subset \left[\frac{m(i-1)}{\ell}, \frac{mi}{\ell} + 1 \right] \times [m]^{d-1}. \quad (3.11)$$

Consider now W_z for $z \in [m]^k$ recursively for $k = 2, \dots, d$. We let R_z be the *bounding box* of W_z , which is the smallest axis-parallel rectangle that contains W_z . Suppose the bounding box R_z of W_z satisfies

$$R_z = \left(\prod_{j=1}^k \left[\frac{(z_j-1)m}{\ell} + C_{z_j}, \frac{z_j m}{\ell} + D_{z_j} \right] \right) \times [m]^{d-k},$$

where $|C_{z_j}|, |D_{z_j}| \leq C_k, D_k$ for some positive integers C_k, D_k . We consider $W_{z_1}, \dots, W_{z_\ell}$. Note that for $j \in [m]$ the size of the points in W_z with $k+1$ st coordinate j is $|W_z \cap \sigma_{k+1}^{-1}(j)| = \theta\left(\frac{n}{\ell^{k+1}}\right)$. Note that the sets $|W_z \cap \sigma_{k+1}^{-1}(j)|$ and $|W_z \cap \sigma_{k+1}^{-1}(i)|$ differ by at most the number of points on the boundary of

$$\left(\prod_{j=1}^k \left[\frac{(z_j - 1)m}{\ell} + C_{z_j}, \frac{z_j m}{\ell} + D_{z_j} \right] \right),$$

which is of order $O\left(\frac{m^k}{\ell^k}\right)$, see Figure 3.20.

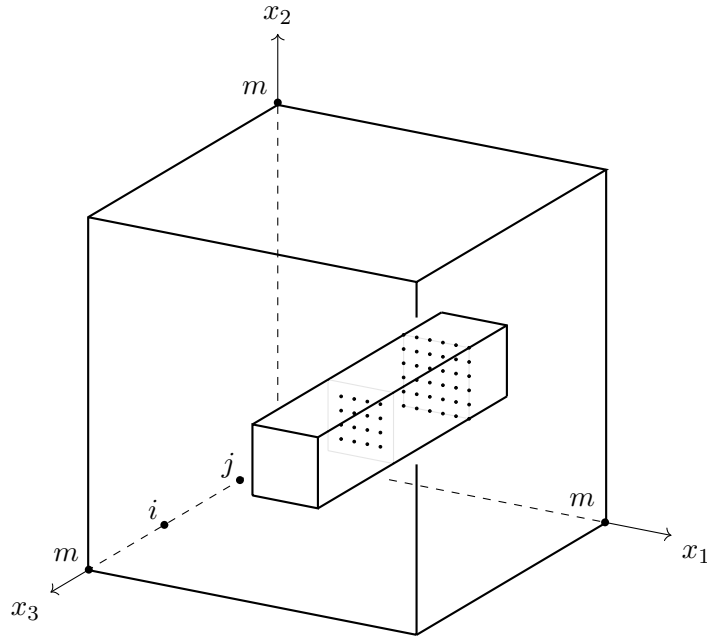


Figure 3.20: A picture of a bounding box $R_{z_1 z_2}$ of a point set $W_{z_1 z_2}$. The number of points in $W_{z_1 z_2} \cap \sigma_3(i)$ and $W_{z_1 z_2} \cap \sigma_3(j)$ differs by the number of points in $\sigma_3(i)$ which are on the boundary of R_{z_1, z_2} .

Since $\frac{m^{k+1}}{\ell^k} = O\left(\frac{n}{\ell^{k+1}}\right)$, the bounding box R_{z_i} of W_{z_i} satisfies

$$R_{z_i} = \left(\prod_{i=1}^k \left[\frac{(z_j - 1)m}{\ell} + O(1), \frac{z_j m}{\ell} + O(1) \right] \right) \times \left[\frac{(i-1)m}{\ell} + O(1), \frac{im}{\ell} + O(1) \right] \times [m]^{d-k-1}.$$

But this means that for $z \in [m]^d$ the set B_z is contained in

$$\prod_{i=1}^d \left[\frac{(z_j - 1)}{\ell} - O\left(\frac{1}{m}\right), \frac{z_j}{\ell} + O\left(\frac{1}{m}\right) \right]$$

Since $\frac{1}{m} = o(r')$, this shows (3.9) for B_z . □

Scientists in parallel computing are interested in embedding different types of graphs into powers of grids and hypercubes, since they are used in several large-scale parallel computers [81]. The smallest power of a square grid in which binary trees of the same size can be embedded was determined up to a small error [50]. Hence we get a natural corollary.

Corollary 3.32. Suppose $n = 2^k + 1$ and $k \rightarrow \infty$. If $r \geq (1 + \varepsilon) \frac{\sqrt{2}}{\log(n)}$ then a.a.s. there is an embedding of the spanning binary tree in $G_1^2(n, r)$.

Question 3.33 (Espuny Díaz). What parameters of a sequence of spanning trees $(T_n)_n$ determine its threshold in $G^d(n, r)$, (i.e. the threshold that ensures that T_n can be embedded a.a.s.)?

A natural lower bound comes from the fact that T_n is spanning, hence $G^2(n, r)$ has to be connected. The threshold of connectivity for $G_2^2(n, r)$ is $\sqrt{\log n / (\pi n)}$ [93]. Another lower bound comes from the diameter of the tree. For large n , a uniformly random set of n points in $[0, 1]^2$ contains a point x_i and a point x_j close to opposite corners of $[0, 1]^2$, hence their ℓ^2 -distance is $d(x_i, x_j) \geq (1 - o(1))\sqrt{2}$. The shortest path between x_i and x_j in $G_2^2(n, r)$ is at least of length $(1 - o(1))\sqrt{2}/r$. Hence if a tree T_n can be embedded in $G_2^2(n, r)$ then $r \geq (1 - o(1))\sqrt{2} / \text{diam}(T_n)$. Similarly, note that the maximum degree of a vertex in $G_2^2(n, r)$ is $(1 + o(1))\pi r^2 n$. So $\Delta(T_n) \leq (1 + o(1))\pi r^2 n$ where $\Delta(T_n)$ is the maximum degree of a vertex in T_n , hence $r \geq \sqrt{\Delta(T_n) / (\pi n)}$. Imagine connecting two stars of size k with a path of length ℓ . Then if both k and ℓ are linear then the degree of the centre of the stars is the limiting property (with $r = \omega(1)$) and not the diameter. The minimum degree bound is generalisable to the sum of degrees of vertices that are close to each other. Recall the result of Montgomery [82] that there is a constant C such that the Erdős-Rényi graph with $p = C \log n / n$ contains a.a.s. every tree T with maximum degree Δ . Motivated by Corollary 3.32, it would be nice to show a similar result for random geometric graphs.

Question 3.34. For every $\Delta > 0$, is there a constant $C = C(\Delta)$ such that the random geometric graph $G_q^2(n, \frac{C}{\log(n)})$ a.a.s. contains a copy of every tree with n vertices and maximum degree at most Δ ?

Chapter 4

Decomposing Drawings into Plane Subdrawings

In Section 3.3.2 we studied decompositions of geometric drawings into two subdrawings, such that the number of crossings in each of the subdrawings is small. In this chapter we are interested in decompositions of drawings into a large collection of subdrawings such that each subdrawing is plane. An easy decomposition can be achieved by taking stars around every vertex, since the corresponding edges do not cross. In this chapter we consider similar decompositions, we fix a certain geometric graph G (for example a star graph) and ask how well we can decompose a geometric drawing into (plane) subdrawings of G . This chapter is joint work with Daniel W. Cranston, Jiayi Nie and Jacques Verstraëte [W8] and was partly developed at the 2021 Graduate Research Workshop in Combinatorics.

4.1 Large Substructures

A *packing* of a graph H is a collection of edge-disjoint subgraphs of H . If the packing covers all edges of H , we call it a *decomposition* or *partition*, see Figure 4.1. If H is a

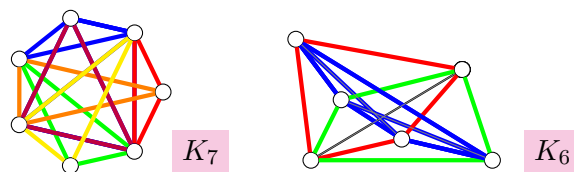


Figure 4.1: A partition of K_7 into plane C_3 's and a K_6 with a C_4 packing. The grey edges are edges which are not covered by a C_4 .

geometric graph, a *subgraph* of H is a geometric graph G which can be embedded in the drawing of H . G is *plane* if none of the edges of G cross (in the embedding of G in H).

We will be mostly concerned with packings and partitions of complete geometric graphs into small plane subgraphs. A fundamental open question in the area of packing plane subgraphs into geometric graphs is the following.

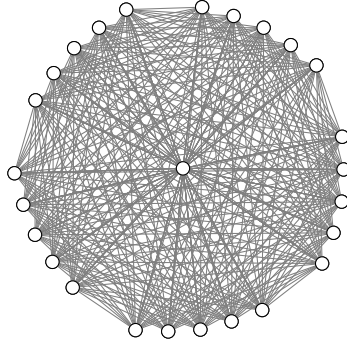


Figure 4.2: A drawing of the complete graph K_{26} which can not be decomposed into $\lfloor \frac{26}{2} \rfloor$ spanning trees. The vertices are in general position and all vertices except the central vertex are on the convex hull.

Question 4.1. Is there a constant $c < 1$ such that every complete geometric graph can be partitioned into at most cn plane subgraphs?

The case $c = 1$ is easy, because a partition into stars centred at every vertex gives n plane subgraphs. Bose, Hurtado, Rivera-Campo and Wood [19] showed that each geometric drawing of the complete graph can be partitioned into $n - \sqrt{\frac{n}{12}}$ plane subgraphs which is the current best result. If the point set of the geometric graph is convex, it was shown that the graph can be partitioned into $\lfloor \frac{n}{2} \rfloor$ plane subgraphs [10] and less is not possible since there are $\lfloor \frac{n}{2} \rfloor$ edges which pairwise cross. This shows that c from Question 4.1 is at least $\frac{1}{2}$. The subgraphs in such an optimal packing of a complete convex geometric graph can be taken as spanning trees, even spanning paths. It is natural to ask whether it is possible to pack $\lfloor \frac{n}{2} \rfloor$ plane spanning trees into every geometric complete graph, which is a strong version of Question 4.1. Obenaus and Orthaber showed that this is not possible in general [88], and they also showed that there is a complete geometric graph that can not be partitioned into $\lfloor \frac{n}{2} \rfloor$ plane subgraphs. An example of a complete geometric graph that can not be partitioned into $\lfloor \frac{n}{2} \rfloor$ plane subgraphs (in particular, plane spanning trees) is the graph in Figure 4.2. The current best construction shows that it is possible to pack $\lfloor \frac{n}{3} \rfloor$ plane spanning trees into every geometric drawing of the complete graph [11]. There is significant further research [2, 10, 11, 19, 88, 110] about packing large plane trees into geometric graphs.

It is interesting to note that edge colourings of planar graphs H are a special case of partitioning general graphs (not necessarily complete graphs) into few plane subgraphs [3]. From a straight-line drawing of H , slightly extend all line segments, so that they cross at the vertices of H , and nowhere else. A partition of the resulting graph into plane subgraphs gives an edge colouring of H and vice versa. For the class of planar graphs with maximum degree $\Delta = 3$ it was shown that it is NP-complete [51] to decide whether a planar graph is Δ or $\Delta + 1$ -edge colourable, while for $\Delta = 4$ or $\Delta = 5$ it is conjectured to be NP-hard

to make this decision. Planar graphs with $\Delta \geq 7$ are Δ -edge colourable [102] and it was conjectured that graphs with $\Delta = 6$ are Δ -edge colourable.

4.2 Small Substructures

Whereas previous research was concentrated on packing large plane structures into geometric graphs, in this work we commence the research of packing small plane graphs into geometric graphs. This is related to Wilson's theorem on graph packing [114], which originates from design theory.

Theorem 4.2 (Wilson, 1976). For every graph G and n large enough, K_n has a partition into copies of G if and only if

- $e(G)$ divides $\binom{n}{2}$,
- the greatest common divisor of the vertex degrees in G divides $n - 1$.

We will consider the same problem as Wilson, with the extra assumption that the complete graph is a geometric graph and the partition is into plane copies of G . We denote by $\mathcal{P}(G)$ the set of all plane geometric drawings of G and H_n is a complete geometric graph on n vertices. The sequence $\{H_n\}_{n \geq 1}$ can be *asymptotically packed by* $\mathcal{P}(G)$ if there is a $\mathcal{P}(G)$ -packing of H_n that covers all but $o(n^2)$ edges of H_n . In other words, if $p(H, \mathcal{P}(G))$ is the maximum size of a $\mathcal{P}(G)$ -packing in H , then $\{H_n\}_{n \geq 1}$ can be asymptotically packed by $\mathcal{P}(G)$ if

$$\lim_{n \rightarrow \infty} \frac{p(H_n, \mathcal{P}(G))e(\mathcal{P}(G))}{e(H_n)} = 1.$$

G is *geometric-packable* if every sequence $\{H_n\}_{n \geq 1}$ can be asymptotically packed by $\mathcal{P}(G)$.

$\mathcal{P}(C_3)$ is geometric-packable due to the existence of Steiner Triple Systems. To generalize this result, we consider plane geometric packing problems for planar *Hamiltonian graphs*, that is, planar graphs that contain a Hamiltonian cycle. We prove the following result.

Theorem 4.3 ([W8]). If G is a planar Hamiltonian graph, then $\mathcal{P}(G)$ is not geometric-packable unless G is the 3-cycle C_3 , the 4-cycle C_4 , or one of the four graphs $\Theta_1, \Theta_2, \Theta_3, \Theta_4$ shown in Figure 4.3. Further, $\mathcal{P}(G)$ is geometric-packable if G is one of C_3, C_4 , and Θ_1 .

The result is proven in two parts. First we show packability of C_3, C_4 and θ_1 (Proposition [W8]) and then the non-packability results in Proposition [W8].

4.2.1 Packability

In this section we consider geometric-packability of C_3, C_4 and Θ_1 (see Figure 4.3). We show later that almost all other graphs are not geometric-packable, except for possibly

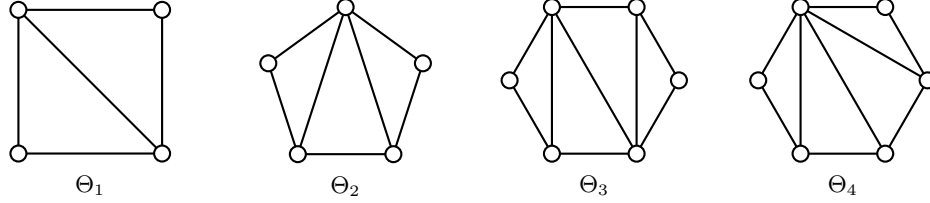


Figure 4.3: Four plane triangulated cycles. The first, Θ_1 , is geometric-packable. For each of the remaining three, the question of geometric-packability remains open.

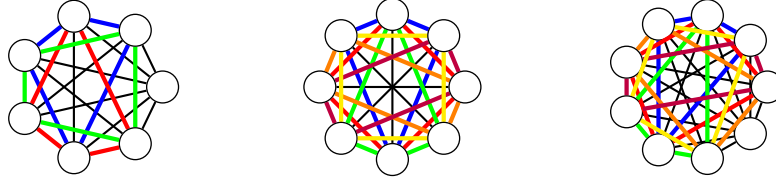


Figure 4.4: Packing C_4 's into a sequence of convex drawings.

Θ_2 , Θ_3 , and Θ_4 as depicted in Figure 4.3. Figure 4.4 shows packings of C_4 's into convex geometric graphs.

Proposition 4.4 ([W8]). $\mathcal{P}(G)$ is geometric-packable if G is C_3 , C_4 , or Θ_1 .

Proof. $\mathcal{P}(C_3)$ is geometric-packable due to the existence of Steiner Triple System. We consider the set of plane 4-cycles, $\mathcal{P}(C_4)$. Let D_n be a geometric drawing in the plane of the complete graph K_n . By symmetry, assume that v_1 is on the convex hull of the vertices v_1, \dots, v_n . Assume further that v_2, \dots, v_n appear in clockwise order around v_1 , with edges v_1v_2 and v_1v_n on the convex hull. The cycles $v_1, v_i, v_{\lceil n/2 \rceil}, v_{\lceil n/2 \rceil + i}$, for each $i \in \{2, \dots, \lceil n/2 \rceil - 1\}$, are plane and disjoint; so we add them all to our $\mathcal{P}(C_4)$ -packing. Further, these cycles cover all but 3 edges incident to v_1 or $v_{\lceil n/2 \rceil}$. Now we delete v_1 and $v_{\lceil n/2 \rceil}$ from the drawing D_n to get a drawing D_{n-2} of K_{n-2} . We continue recursively, ending when the drawing has at most 3 vertices. Each time we delete vertices, we discard $O(1)$ uncovered incident edges. Thus, the resulting packing covers all but $O(n)$ edges of D_n .

Now we consider the set of plane 4-cycles with a chord, $\mathcal{P}(\Theta_1)$. Let D_n be an arbitrary geometric drawing in the plane of K_n . Let $f(n) = 2n \log_2 n$. We prove by induction on n that there exists a Θ_1 -packing of D_n that covers all but at most $f(n)$ edges.

Let $m = \lfloor n/4 \rfloor$. By the Ham Sandwich Theorem, there exist two straight lines partitioning the plane into 4 parts P_1, P_2, P_3, P_4 , in clockwise order, where each part contains at least m vertices, see Figure 4.5.

Ignoring up to 3 vertices, we pick m vertices in each part. We denote these vertices by $v_{i,j}$, where $i \in \{1, \dots, 4\}$ and $j \in \{1, \dots, m\}$.

Let D'_n be the spanning subgraph of D_n whose edge set consists of all edges with endpoints in distinct parts, except for those with one endpoint in each of P_2 and P_4 . Let \mathcal{F}_n be a collection of copies of plane Θ_1 whose vertex set is $\{v_{1,j}, v_{2,k}, v_{3,j+k}, v_{4,k}\}$ and whose

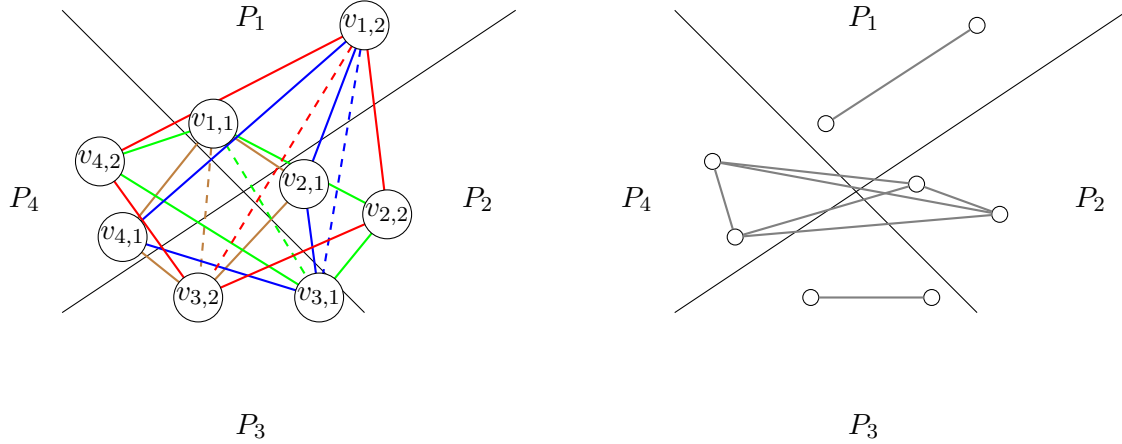


Figure 4.5: The inductive step in packing Θ_1 .

chord is $\{v_{1,j}, v_{3,j+k}\}$, with $j, k \in \{1, \dots, m\}$; here each second index is modulo m . It is easy to check that this is a Θ_1 -packing of D'_n that covers all but at most $3n$ edges.

Note that $D_n \setminus D'_n$ consists of three complete components, one induced by $P_2 \cup P_4$, and the others induced by P_1 and P_3 . Thus, by induction, there exists a Θ_1 -packing of D_n such that the number of uncovered edges is at most $f(n/2) + 2f(n/4) + 3n \leq f(n)$, as desired. \square

While we will show that most graphs are not geometric-packable, the plane geometric packing problem is still open for 3 planar Hamiltonian graphs: Θ_2 , Θ_3 , and Θ_4 , see Figure 4.3. In Theorem 4.12 we show that, in fact, each can be packed when the vertices of the complete geometric graphs are in strictly convex position. We conjecture the following.

Conjecture 4.5 ([W8]). $\mathcal{P}(G)$ is geometric-packable when G is one of Θ_2 , Θ_3 , and Θ_4 .

4.2.2 Convex-Nonpackable CGGs

In this section we show that almost all graphs are not geometric-packable. To show this, we show that they can not be packed into a sequence of convex complete graphs.

A *convex geometric graph* (CGG for short) G is a geometric graph whose vertices are in strictly convex position; Figure 4.3 shows four examples. We denote the vertices of G by v_0, v_1, \dots, v_{n-1} and assume these vertices appear in clockwise (cyclic) order on the boundary of their convex hull (indexing is modulo n). Every subset of $V(G)$ that is contiguous with respect to its cyclic order is an *interval*. A pair $\{v_i, v_{i+1}\}$ of $V(G)$ is an *extremal pair*. For every pair $\{x, y\}$ in a CGG, the *length* of $\{x, y\}$, denoted by $\ell(x, y)$, is the minimum length of a path from x to y using only extremal pairs. For example, in Figure 4.6, $\ell(x, y) = \ell(y, x) = 2$.

Informally, two CGGs are convex-isomorphic if some graph isomorphism between them preserves the cyclic order of all vertices. Formally, CGGs G_1 and G_2 are *convex-isomorphic*

if there is a bijective function $f : V(G_1) \rightarrow V(G_2)$ such that for every pair of vertices $x, y \in V(G_1)$: (i) $\ell(x, y) = \ell(f(x), f(y))$; (ii) $\{x, y\} \in E(G_1)$ if and only if $\{f(x), f(y)\} \in E(G_2)$. A CGG H contains a CGG G if some subgraph of H is convex-isomorphic to G . Given CGGs G and H , a G -packing of H is a collection of edge-disjoint subgraphs of H that are convex-isomorphic to G . Let $p(H, G)$ be the maximum size of a G -packing in H . Let \mathcal{K}_n be the complete CGG on n vertices. In particular, let $p(n, G) = p(\mathcal{K}_n, G)$. For example, if G is a 4-cycle with a crossing, then $p(6, G) = 3$. Figure 4.6 shows a construction proving the lower bound. (The upper bound holds since $\lfloor \binom{6}{2}/4 \rfloor = 3$.)

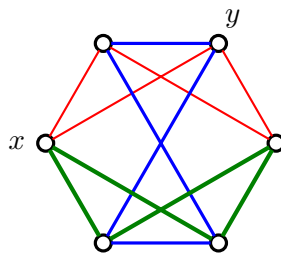


Figure 4.6: When G is a 4-cycle with a crossing, $p(6, G) = 3$.

Recall the definition of asymptotically packed. Further, G is *convex-packable* if G asymptotically packs into \mathcal{K}_n . That is, G is convex-packable if there exist G -packings of \mathcal{K}_n that cover all but $o(n^2)$ edges. Finally, a CGG is *plane* if no two of its edges cross.

Clearly, for a graph G , if $\mathcal{P}(G)$ is geometric-packable and there is only one way to draw G as a plane CGG, then G , as a plane CGG, is convex-packable. Let \mathcal{C}_k denote the convex plane k -cycle. Note that \mathcal{C}_3 and \mathcal{C}_4 are convex-packable by Proposition 4.4; so we naturally ask: Is \mathcal{C}_5 convex-packable? The answer is No. In fact, for all $k \geq 5$, the average length of the edges in a copy of \mathcal{C}_k in \mathcal{K}_n is at most n/k ; hence the average length of all edges covered by a \mathcal{C}_k -packing of \mathcal{K}_n is also at most n/k . In contrast, the average length of all edges in \mathcal{K}_n is $(1 + o(1))n/4$. So when $k \geq 5$, no \mathcal{C}_k -packing can cover all but $o(n^2)$ edges of \mathcal{K}_n .

By extending this average length argument, we find a necessary condition (Lemma 4.6) for a CGG to be convex-packable. Currently, this is our only tool to prove that a CGG is not convex-packable. But for many CGGs, it is enough. We use this argument to prove the convex-nonpackability of most plane Hamiltonian CGGs. A set of edges $\{e_1, e_2, \dots, e_k\}$ of a convex geometric graphs G is *convex* if for each edge e_i , all other edges e_j lie on the same side of the line determined by e_i . For example, in Figure 4.7, the set of blue edges is convex while the set of red edges is not.

The following lemma is our key tool for proving convex-nonpackability.

Lemma 4.6 ([W8]). Let G be a CGG. If G is convex-packable, then there exists $f : E(G) \rightarrow \mathbb{R}^+$ that satisfies the following two conditions: (i) Every set of edges S satisfies $\sum_{e \in S} f(e) \geq |S|^2/(4e(G))$ and (ii) every convex set of edges A satisfies $\sum_{e \in A} f(e) \leq 1$.

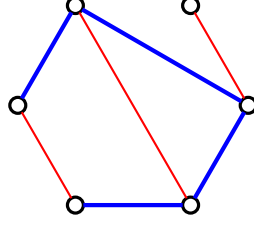


Figure 4.7: The set of thick blue edges is convex, but the set of thin red edges is not.

Proof. For each positive integer n , let \mathcal{F}_n be a G -packing of \mathcal{K}_n that covers all but $o(n^2)$ edges. This means that $|\mathcal{F}_n| = (1 - o(1))\binom{n}{2}/e(G)$. For every $e \in G$ and every copy G' of G in \mathcal{K}_n , let $l_{G'}(e)$ denote the length in \mathcal{K}_n of the edge $F_{G,G'}(e)$. For every edge $e \in G$, let $f_n(e)$ be the average length of the edges in \mathcal{F}_n corresponding to edge e , divided by n ; that is,

$$f_n(e) := \frac{\sum_{G' \in \mathcal{F}_n} l_{G'}(e)}{n|\mathcal{F}_n|}.$$

Let S be a set of edges of G , and denote by $\mathcal{F}_n(S)$ the set of edges in \mathcal{K}_n that are covered in \mathcal{F}_n by edges of S . Note that $|\mathcal{F}_n(S)| = |S||\mathcal{F}_n| = (1 - o(1))\frac{|S|}{e(G)}\binom{n}{2}$. Further, the average length of edges in $\mathcal{F}_n(S)$ is at least

$$(1 - o(1))\frac{|S|}{4e(G)}n,$$

since that is precisely the average when $\mathcal{F}_n(S)$ consists of the $|\mathcal{F}_n(S)|$ shortest edges in \mathcal{K}_n , those with length at most $(1 - o(1))\frac{|S|}{e(G)}\frac{n}{2}$. Thus, we have

$$\frac{\sum_{e \in S} f_n(e)}{|S|} \geq (1 - o(1))\frac{|S|}{4e(G)},$$

which we rewrite as

$$\sum_{e \in S} f_n(e) \geq (1 - o(1))\frac{|S|^2}{4e(G)}.$$

Let A be a convex set of edges of G . For each $G' \in \mathcal{F}_n$, by definition $\sum_{e \in A} l_{G'}(e) \leq n$. Now summing over all $G' \in \mathcal{F}_n$ (by the definition of $f_n(e)$ above) gives

$$\sum_{e \in A} f_n(e) = \frac{\sum_{G' \in \mathcal{F}_n} \sum_{e \in A} l_{G'}(e)}{n|\mathcal{F}_n|} \leq 1.$$

Since $\{f_n\}_{n \geq 1}$ is a sequence of bounded functions with finite domain, there exists a subsequence $\{f_{n_i}\}_{i \geq 1}$ such that $f_{n_i}(e)$ converge for all $e \in G$. Let f be the function on $E(G)$ such that $f(e) = \lim_{i \rightarrow \infty} f_{n_i}(e)$. Now f satisfies (i) and (ii) from the statement of the theorem. \square

We can argue that a CGG G is not convex-packable by showing that the function f that would be guaranteed by Lemma 4.6 cannot exist. Using an edge length argument similar

to the proof of condition (ii), we can further show that a CGG G has no perfect convex-packing¹, i.e. $p(n, G) < e(K_n)/e(G)$. Suppose G is the plane C_4 . The average edge length in every \mathcal{K}_n is strictly greater than $n/4$, but the average edge length in every C_4 -packing is at most $n/4$. Therefore, no plane C_4 -packing covers all edges of \mathcal{K}_n .

Proposition 4.7 ([W8]). Let G be a CGG and let k be the maximum size of a convex set of edges of G . If $e(G) < k^2/4$, then G is not convex-packable.

Proof. We prove the contrapositive. Assume that G is convex-packable and let f be the function guaranteed by Lemma 4.6. Let A be a convex set of edges of size k . Combining the two conditions in Lemma 4.6 gives

$$1 \geq \sum_{e \in A} f(e) \geq \frac{k^2}{4e(G)}.$$

Simplifying gives $e(G) \geq k^2/4$, as desired. □

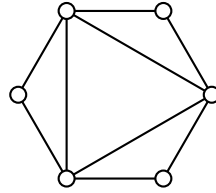


Figure 4.8: Θ_5 is not convex-packable.

Proposition 4.8 ([W8]). If G is a plane Hamiltonian CGG, then G is not convex-packable unless G is one of $C_3, C_4, \Theta_1, \Theta_2, \Theta_3$, or Θ_4 (the latter four of these are shown in Figure 4.3). In particular, Θ_5 is not convex-packable.

Proof. Let G be a plane CGG formed by adding t chords to C_k . We suppose that G is convex-packable, and apply Proposition 4.7. When $k = 5$, we have $e(G) \geq \lceil 25/4 \rceil = 7$; when $k = 6$, we have $e(G) \geq 9$; and when $k \geq 7$, we have $e(G) \geq k^2/4 > 2k - 3$, which contradicts the planarity of G . So the only remaining candidates for a plane convex-packable Hamiltonian CGG are the plane cycles C_3, C_4 , the four CGGs in Figure 4.3 and the CGG Θ_5 in Figure 4.8.

Suppose, for contradiction, that Θ_5 is convex-packable and let f be the function guaranteed by Lemma 4.6. Let A_1 be the convex set consisting of the 6 edges on the outer 6-cycle and let A_2 be the convex set consisting of the 3 chords. The two conditions in Lemma 4.6 give

$$2 \geq \sum_{e \in A_1} f(e) + \sum_{e \in A_2} f(e) = \sum_{e \in A_1 \cup A_2} f(e) \geq \frac{9^2}{4 \cdot 9} = 9/4,$$

¹By Rödl Nibble, if a graph has a perfect convex packing into some \mathcal{K}_n , then it is convex-packable.

which is a contradiction. □

If we restrict the geometric graphs that we pack to be both plane and also convex, then every planar Hamiltonian graph, other than the triangle, is not geometric-packable. Let $\mathcal{P}^*(G)$ be the set of all plane geometric drawings of G whose vertices are in strictly convex position; note that $\mathcal{P}^*(G) \subset \mathcal{P}(G)$. For example, if C_4 is the 4-cycle and G_1, G_2, G_3 are the geometric graphs in Figure 4.9, then $G_1 \notin \mathcal{P}(C_4)$ and $G_2 \in \mathcal{P}^*(C_4)$ and $G_3 \in \mathcal{P}(C_4) \setminus \mathcal{P}^*(C_4)$.

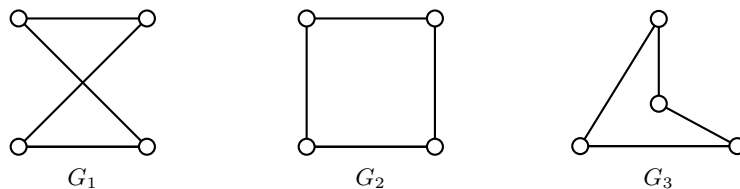


Figure 4.9: $G_1 \notin \mathcal{P}(C_4)$ and $G_2 \in \mathcal{P}^*(C_4)$ and $G_3 \in \mathcal{P}(C_4) \setminus \mathcal{P}^*(C_4)$.

Theorem 4.9 ([W8]). If G is a Hamiltonian graph, then $\mathcal{P}^*(G)$ is not geometric-packable unless G is C_3 . Further, $\mathcal{P}^*(C_3)$ is geometric-packable.

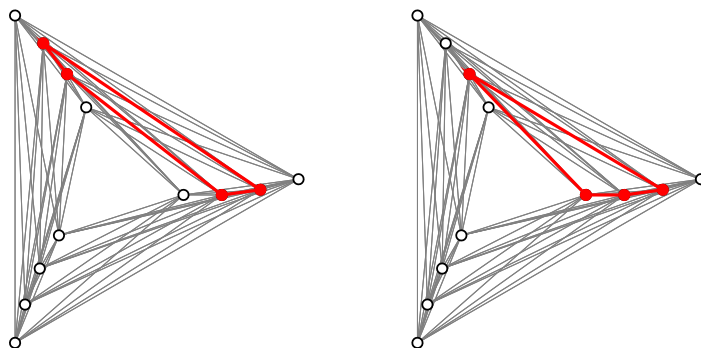


Figure 4.10: Two convex C_4 's in D_{12} .

Proof. $\mathcal{P}^*(C_3)$ is geometric-packable due to the existence of Steiner Triple Systems. Propositions 4.7 and 4.8 imply the geometric-nonpackability of $\mathcal{P}^*(G)$ for all Hamiltonian graph G unless G is one of $C_3, C_4, \Theta_1, \Theta_2, \Theta_3$ and Θ_4 . What remains to be done is to construct D_1, D_2, \dots , a sequence of drawings of the complete graph, such that it cannot be packed by $\mathcal{P}^*(G)$ when G is one of $C_4, \Theta_1, \Theta_2, \Theta_3$ and Θ_4 .

We show that the generalisation of the graph in Figure 4.10, which we define below, is not $\mathcal{P}^*(C_4)$ -packable. We only consider drawings D_n when $n \equiv 0 \pmod 3$, since we can get D_{n-1} and D_{n-2} by deleting one or two vertices from D_n .

For each $i \in \{1, \dots, \frac{n}{3}\}$, we let $v_i := (i, i^2/(2n^2))$. The importance of the second coordinate is simply to keep the points $v_1, \dots, v_{n/3}$ in general convex position. We form $v_{i+\frac{n}{3}}$ and $v_{i+\frac{2n}{3}}$ from v_i by rotating (around $(0,0)$) 120 and 240 degrees counterclockwise. Let

$A := \{v_1, \dots, v_{\frac{n}{3}}\}$, $B := \{v_{\frac{n}{3}+1}, \dots, v_{\frac{2n}{3}}\}$, and $C := \{v_{\frac{2n}{3}+1}, \dots, v_n\}$. We claim that we cannot pack many convex C_4 's into the drawing on v_1, \dots, v_n . The reason is that each convex C_4 has at least two edges within the sets A, B, C . To see this, consider a set S with two points from A , one point from B , and one point from C . The key observation is that the more inner point from A is not on the convex hull of S . (This can be verified by finding the line determined by the two points in A and showing that it intersects the interior of the line segment determined by the points in B and C . But we omit these routine calculations.) Hence, in every convex C_4 , all four points must come from at most two of A, B , and C . It is easy to check that the only types of convex C_4 's are the two highlighted in Figure 4.10. But at most $3\left(\frac{n}{3}\right)$ edges go between different sets from A, B, C . Hence, each packing of convex C_4 's has at most $\frac{n^2}{3.4}(1 + o(1))$ copies of C_4 ; so it covers at most $\frac{2}{3}(1 + o(1))$ of all edges.

By similar arguments, $\{D_n\}_{n \geq 1}$ cannot be asymptotically packed by $P^*(G)$ when G is one of $\Theta_1, \Theta_2, \Theta_3$ and Θ_4 . \square

4.2.3 Strong Packability

We have shown that most Hamiltonian graphs are not convex-packable, except for the plane cycles C_3 and C_4 and the four CGGs $\Theta_1, \Theta_2, \Theta_3$ and Θ_4 . In this section we show that Θ_2, Θ_3 and Θ_4 are convex-packable. For each even integer n , and all integers ℓ such that $1 \leq \ell < n/8$, we take all copies of C_4 with edges of lengths $2\ell, n/2 - 2\ell, 2\ell - 1, n/2 - 2\ell + 1$, in clockwise order; see Figure 4.11. Clearly these copies of C_4 form a C_4 -packing of \mathcal{K}_n and the number of edges uncovered is $O(n)$; thus the packing is almost perfect.

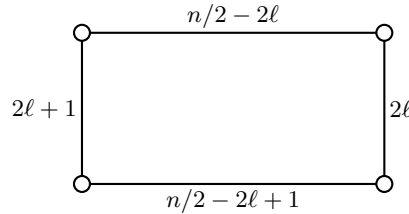


Figure 4.11: A typical C_4 in an asymptotic C_4 -packing of the convex complete graphs.

To generalise the example above, that C_4 is convex-packable, we need the following definitions. Let G be a subgraph of \mathcal{K}_n . The *length set* of G , denoted L_G , is a subset of $\{1, 2, \dots, \lfloor n/2 \rfloor\}$ such that $i \in L_G$ if and only if some edge $e \in G$ has length in \mathcal{K}_n equal to i .

Definition. A CGG G is *strongly packable* if for each $n \geq 1$ there exists S_n , a set of subsets of $\{1, 2, \dots, \lfloor n/2 \rfloor\}$, with the following three properties:

1. All sets in S_n are pairwise disjoint and have size $e(G)$; and
2. For all $A \in S_n$, there exists a subgraph G_A of \mathcal{K}_n that is convex-isomorphic to G such that $L_{G_A} = A$; and

$$3. \sum_{A \in S_n} |A| = |S_n|e(G) = (1 - o(1))n/2.$$

Further, we say $\{S_n\}_{n \geq 1}$ is a sequence of *packable length-set collections* of G .

Lemma 4.10 ([W8]). Let G be a CGG. If G is strongly packable, then G is also convex-packable.

Proof. Let $\{S_n\}_{n \geq 1}$ be a sequence of collections of sets that satisfy all three properties in Definition 4.2.3, i.e., a sequence of packable length-set collections of G . We construct a sequence of G -packings $\{\mathcal{F}_n\}_{n \geq 1}$ that covers all but $o(n^2)$ edges of $\{\mathcal{K}_n\}_{n \geq 1}$. Fix an arbitrary positive integer n' . For each $A \in S_{n'}$, we add to $\mathcal{F}_{n'}$ the subgraph G_A convex-isomorphic to G in $\mathcal{K}_{n'}$ with lengths in A , as well as the $n - 1$ copies of G formed from G_A by rotations.

Each edge e in $\mathcal{K}_{n'}$ of some length l , where $l \in \{1, \dots, \lfloor n'/2 \rfloor\}$, is covered by $\mathcal{F}_{n'}$ if and only if $l \in \bigcup_{A \in S_{n'}} A$. Since $\{S_n\}_{n \geq 1}$ is a sequence of packable length-set collections of G , Property 3 of Definition 4.2.3 implies that the number of lengths not covered by $\bigcup_{A \in S_n} A$ is $o(n)$. Thus, the number of edges not covered by $\{\mathcal{F}_n\}_{n \geq 1}$ is $o(n^2)$, as desired. \square

Consider a CGG G with vertex set $\{v_0, \dots, v_{m-1}\}$. A CGG \tilde{G} is a *reflection* of G along an edge $\{v_0, v_t\}$ if \tilde{G} has the same vertex set as G and a pair of vertices $\{v_i, v_j\}$ form an edge of \tilde{G} if and only if either (a) $\{i, j\} \in \{0, \dots, t\}$ and $\{v_{t-i}, v_{t-j}\} \in E(G)$ or (b) $\{i, j\} \in \{0, \dots, m-1\} \setminus \{1, \dots, t-1\}$ and $\{v_i, v_j\} \in E(G)$. Reflections are illustrated in Figure 4.14 (in Section 4.2.4).

Lemma 4.11 ([W8]). If a CGG G is strongly packable, then so is each of its reflections.

Proof. Let \tilde{G} be a reflection of G and let $\{S_n\}_{n \geq 1}$ be a sequence of collections of packable length-sets of G . Fix an arbitrary positive integer n' . For each $A \in S_{n'}$, let H be a copy of G in $\mathcal{K}_{n'}$ such that $L_H = A$. Clearly $\mathcal{K}_{n'}$ also contains a copy \tilde{H} of \tilde{G} such that $L_{\tilde{H}} = L_H = A$ (which is the reflection of H along the image of the edge of the reflection from G to \tilde{G}). Therefore, $\{S_n\}_{n \geq 1}$ is also a sequence of collections of packable length-sets of \tilde{G} . Hence \tilde{G} is also strongly packable. \square

Theorem 4.12 ([W8]). All plane Hamiltonian CGGs are not convex-packable, except for the two plane cycles \mathcal{C}_3 and \mathcal{C}_4 and the four CGGs $\Theta_1, \Theta_2, \Theta_3$ and Θ_4 shown in Figure 4.3, which are all convex-packable.

Proof. Propositions 4.7 and 4.8 imply the non-packability of all plane Hamiltonian CGGs, except for $\mathcal{C}_3, \mathcal{C}_4, \Theta_1, \Theta_2, \Theta_3$ and Θ_4 . Recall that \mathcal{C}_3 is convex-packable due to the existence of Steiner Triple Systems, and they are also strongly packable by a result of Rose Pelsesohn [91]. \mathcal{C}_4 and Θ_1 are convex-packable by Proposition 4.4.

We now consider Θ_2, Θ_3 , and Θ_4 . We will show that they are all (strongly) packable. To show that a CGG is strongly packable, it suffices to give a sequence of packable length-set collections. We label the edges of Θ_2 as in Figure 4.12.

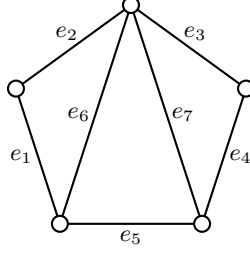


Figure 4.12: An edge labelling of Θ_2 used to show it is strongly packable.

Let $n = 28x$, for some positive integer x . We construct a collection of length-sets for Θ_2 in \mathcal{K}_n . If $28 \nmid n$, then we simply ignore the edges incident to at most 27 vertices in \mathcal{K}_n . Since the number of ignored edges is $O(n)$, they do not affect whether or not our packing covers $(1 - o(1))\binom{n}{2}$ edges. Thus, we assume $n = 28x$ without loss of generality.

We extend the idea of a length-set to a *length-vector*. Each length-vector for Θ_2 is an ordered 7-tuple of positive integers that form a length-set. Here the j th entry of a length-vector is the length in some copy of Θ_2 of the image of edge e_j , as labeled in Figure 4.12. We use the following $2x - 3$ length-vectors:

$$(7x + 1 - 7i, 2 + 14i, 5 + 14i, 7x + 6 - 7i, 14x - 14i - 14, \\ 7x + 3 + 7i, 7x + 11 + 7i), \quad 0 \leq i \leq x - 2$$

and

$$(-4 + 7i, 14x + 12 - 14i, 14x + 9 - 14i, 4 + 7i, 14i - 21, \\ 14x + 8 - 7i, 14x + 13 - 7i), \quad 2 \leq i \leq x - 1.$$

As in the proof of Lemma 4.10, for each length-vector above, we add to \mathcal{F}_n some copy of G with edges lengths given by that length-vector, as well as the $n - 1$ non-trivial rotations of that copy of G . Note that the 7 coordinates of each length-vector lie in distinct residue classes modulo 7. This observation makes it easy to check that the length-sets of these $2x - 3$ length-vectors are pairwise disjoint. Thus the number of edge lengths in these length-vectors is $7(2x - 3) = (1 - o(1))n/2$, and the number of edges covered by this Θ_2 -packing is $(1 - o(1))\binom{n}{2}$. So Θ_2 is strongly packable.

The proofs that Θ_3 and Θ_4 are strongly packable mirror that above for Θ_2 . So we just give the length-vectors (which are identical for Θ_3 and Θ_4) and the edge labellings in Figure 4.13.

$$(2x - 2i, 5x + i, 7x - i, 2x + 2i, 9x - i, 2x - 1 - 2i, \\ 7x + i + 1, 2x + 1 + 2i, 5x - i), \quad 1 \leq i \leq x - 1.$$

□

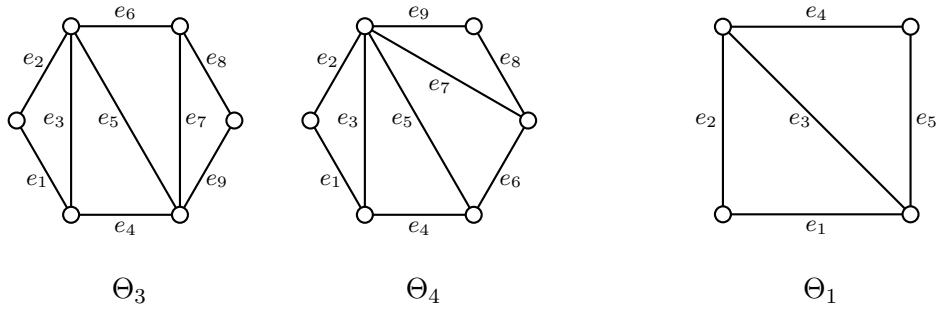


Figure 4.13: Edge labellings showing that Θ_3 , Θ_4 , and Θ_1 are all strongly packable.

In fact, we can also show that Θ_1 is strongly packable using the edge labelling in Figure 4.13 and the following collections of vectors (we assume, without loss of generality, that $n = 20x$):

$$(5i + 2, 5i + 3, 10i + 5, 10x - 5i - 1, 10x - 5i - 4), \quad 0 \leq i < x - 1,$$

$$(5i + 2, 5i - 2, 20x - 10i, 10x - 5i - 1, 10x - 5i + 1), \quad x < i < 2x - 1.$$

4.2.4 Paths and Caterpillars

So far, we only considered Hamiltonian plane graphs. This last section is on packing a (small) tree into convex drawings of the complete graph.

Note that every plane path can be uniquely transformed into a convex plane caterpillar by reflections. (See Figure 4.14, where in each step we reflect with respect to the bold red edge). Thus, by Lemma 4.11, a plane path is strongly packable if and only if its corresponding convex plane caterpillar is strongly packable.

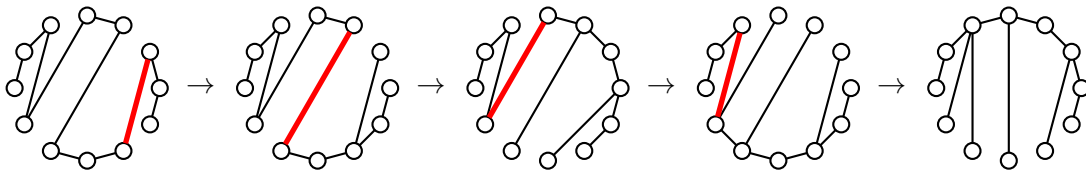


Figure 4.14: A plane path is transformed into a convex plane caterpillar.

By Proposition 4.7, we know that a plane path with k edges is not convex-packable if it has more than $2\sqrt{k}$ extremal edges. Equivalently, a plane convex caterpillar is not convex-packable if it has more than $2\sqrt{k} - 2$ edges in the spine. Let $f(k)$ be the maximum number of extremal edges of a convex-packable plane path with k edges. So we have $f(k) \leq 2\sqrt{k}$ for all positive integers k . We conjecture that this is sharp.

Conjecture 4.13 ([W8]). $f(k) = (2 - o(1))\sqrt{k}$ as $k \rightarrow \infty$.

In the rest of this section, we construct two types of strongly packable convex plane caterpillars, both show $f(k) \geq (1 + o(1))\sqrt{2k}$ as $k \rightarrow \infty$.

Theorem 4.14 ([W8]). Let s be a positive integer. Let G be a plane convex caterpillar with vertices v_1, \dots, v_s, v_{s+1} in clockwise order on the spine such that each of v_2, \dots, v_s has no adjacent leaf. If $s(s+3) \leq 2e(G)$, then G is strongly packable.

If we let $s(s+3) = 2e(G)$, then we have a plane convex caterpillar with $s(s+3)/2$ edges among which $s+2$ edges are extremal. This implies that $f(k) \geq (1 + o(1))\sqrt{2k}$.

Proof. Let $k := e(G)$. Without loss of generality, assume n is a multiple of $2k$ and let $x := n/(2k)$. We construct copies G_m of G in \mathcal{K}_n for each $m \in \{1, \dots, x-1\}$ such that $\{L_{G_m}\}$ is a packable length-set collection of G . Let t_1 and t_2 denote the numbers of leaves adjacent to v_1 and v_{s+1} ; by symmetry, we assume $t_2 \geq t_1$. Denote the leaf edges incident to v_1 (resp. to v_{s+1}) by $e_{s+1}, e_{s+2}, \dots, e_{s+t_1}$ (resp. $e_{s+t_1+1}, e_{s+t_1+2}, \dots, e_{s+t_1+t_2}$).

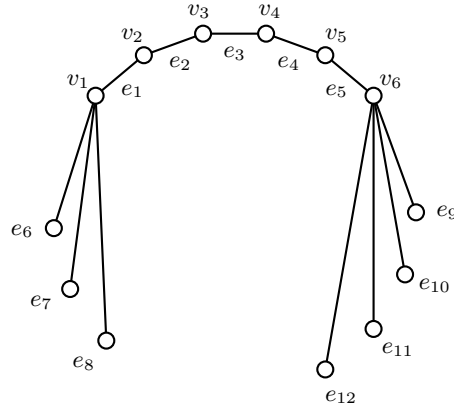


Figure 4.15: An edge-labelling of a caterpillar where all leaves are adjacent to either v_1 or v_{s+1} .

Let G_m be a copy of G in \mathcal{K}_n , and let $\ell_m(e) := \ell(F_{G,G_m}(e))$, i.e., $\ell_m(e)$ is the length in \mathcal{K}_n of the edge of G_m corresponding to the edge e of G . We will show, for each $m \in \{1, \dots, x-1\}$, that there exists G_m with

$$\ell_m(e_i) = \begin{cases} (i-1)x + m & i \in \{1, \dots, s\} \\ sx + (m-1)t_1 + (i-s) & i \in \{s+1, \dots, s+t_1\} \\ n/2 - (m+1)t_2 + (i-s-t_1) & i \in \{s+t_1+1, \dots, s+t_1+t_2\}. \end{cases}$$

Let S_n be the collection of sets L_{G_m} for all $m \in \{1, \dots, x\}$. It is straightforward to check that these sets are pairwise disjoint, and thus that S_n is a packable length-set collection. In particular, spine edges all have lengths in $\{1, \dots, sx\}$; leaf edges incident to v_1 have lengths in $\{sx+1, \dots, sx+t_1x\}$, and leaf edges incident to v_{s+1} have lengths in $\{sx+t_1x +$

$1, \dots, n/2\}$. Since $\sum_{m=1}^{x-1} |L_{G_m}| = (1 - o(1))n/2$, we only need to check that G contains the desired copies G_m , with no edges crossing. It suffices to verify that the edges e_{s+t_1} and $e_{s+t_1+t_2}$ in each copy do not cross. Recall that $t_2 \geq t_1$. Thus, for each $m \in \{1, \dots, x-1\}$, because

$$\begin{aligned} & \sum_{i=1}^s \ell_m(e_i) + \ell_m(e_{s+t_1}) + \ell_m(e_{s+t_1+t_2}) \\ &= \sum_{i=1}^s ((i-1)x + m) + sx + mt_1 + n/2 - (m+1)t_2 + t_2 \\ &= \frac{s(s-1)x}{2} + sm + sx + mt_1 + n/2 - mt_2 \\ &< \frac{s(s+3)x}{2} + n/2 \leq k(n/2k) + n/2 = n. \end{aligned}$$

□

Theorem 4.15 ([W8]). Let l , and a_1, \dots, a_{s+1} be positive integers. Let G be a plane convex caterpillar with vertices v_1, \dots, v_s, v_{s+1} in clockwise order on the spine such that each v_i is adjacent to a_i leaves. If there exists a permutation $\sigma_1, \dots, \sigma_{s-1}, \sigma_s$ of the set $1, \dots, s$ such that $\sigma_i \leq \min\{a_i, a_{i+1}\}$ for all $i \in \{1, \dots, s\}$, then G is strongly packable.

If we let $a_i = i$ and $\sigma_i = i$, then we have a packable plane convex caterpillar with $(s^2 + 5s + 3)/2$ edges among which $s+2$ are extremal. This implies, again, $f(k) \geq (1 + o(1))\sqrt{2k}$.

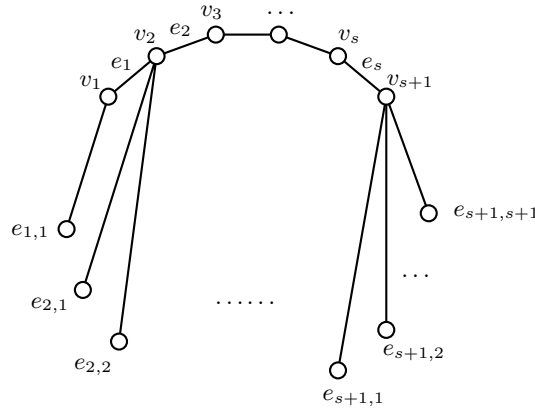


Figure 4.16: An edge-labelling of a caterpillar where v_i is adjacent to i leaves for all $1 \leq i \leq s+1$.

The proof of Theorem 4.15 is similar to that of Theorem 4.14. The main difference is that now we must ensure that the final leaf edge incident with v_i does not cross with the first leaf edge incident with v_{i+1} , for each $i \in \{1, \dots, s+1\}$. That is the role of the permutation σ , which controls the length of each edge on the spine. More precisely, letting $x := n/(2k)$, in each copy of G the edge e_i has length between $(\sigma_i - 1)x$ and $\sigma_i x - 1$.

Proof. Let $k := e(G)$. Without loss of generality, assume n is a multiple of $2k$ and let $x := n/(2k)$. For each $m \in \{1, \dots, x - k^2\}$, we will construct a copy G_m of G in \mathcal{K}_n such that $\{L_{G_m}\}$ is a packable length-set collection of G . Let e_1, \dots, e_s be the edges on the spine, where $e_i = \{v_i, v_{i+1}\}$, and let $e_{i,1}, \dots, e_{i,a_i}$ be the edges connecting v_i to its a_i leaves in counterclockwise order. Let G_m be a copy of G in \mathcal{K}_n , and let $\ell_m(e) := \ell(F_{G,G_m}(e))$; that is, $\ell_m(e)$ is the length of the edge of G_m corresponding to the edge e of G . We will show, for all $m \in \{1, \dots, x - k^2 - 2\}$, that there exists G_m with

$$\begin{aligned} \ell_m(e_i) &= (\sigma_i - 1)x + m, & i \in \{1, \dots, s\} \\ \ell_m(e_{i,t}) &= (s + \sum_{j=1}^{i-1} a_j)x + i \cdot k + m \cdot a_i + t, & i \in \{1, \dots, s+1\} \text{ and } t \in \{1, \dots, a_i\}. \end{aligned}$$

First, we verify that each edge length ℓ_m is less than $n/2$. Since $\sigma_i \leq s$ and $m < x$, we have $\ell_m(e_i) < \sigma_i x \leq sx \leq k(n/(2k)) = n/2$; and for all $a_i \neq 0$ we have

$$\ell_m(e_{i,t}) \leq (s + \sum_{j=1}^{i-1} a_j)x + k^2 + (x - k^2 - 1)a_i \leq e(G)x - 1 < \frac{n}{2}.$$

We need to check that edges e_{i,a_i} and $e_{i+1,1}$ do not cross, for all $i \in \{1, \dots, s\}$ in each copy of G . It suffices to check that $\ell_m(e_{i,a_i}) + \ell_m(e_i) \leq \ell_m(e_{i+1,1})$ for all $i \in \{1, \dots, s\}$ and all $m \in \{1, \dots, x - k^2 - 2\}$. Note that

$$\begin{aligned} \ell_m(e_{i+1,1}) - \ell_m(e_{i,a_i}) - \ell_m(e_i) &= (s + \sum_{j=1}^i a_j)x + (i+1)k + ma_{i+1} + 1 \\ &\quad - (s + \sum_{j=1}^{i-1} a_j)x - ik - (m+1)a_i - (\sigma_i - 1)x - m \\ &= (a_i - \sigma_i + 1)x + (a_{i+1} - a_i - 1)m + k - a_i + 1 \end{aligned}$$

If $a_{i+1} \geq a_i$, then (since $a_i \geq \sigma_i$, by assumption) we have

$$\ell_m(e_{i+1,1}) - \ell_m(e_{i,a_i}) - \ell_m(e_i) \geq x - m + k - a_i + 1 \geq k - a_i + 1 > 0.$$

On the other hand, if $a_{i+1} < a_i$, then (since $m \leq x$) we have

$$\ell_m(e_{i+1,1}) - \ell_m(e_{i,a_i}) - \ell_m(e_i) \geq (a_i - a_{i+1} + 1)(x - m) + k - a_i + 1 \geq k - a_i + 1 > 0.$$

Hence such G_m exist for all $m \in \{1 \dots x - k^2\}$. Let S_n be the collection of sets consisting of L_{G_m} for all $m \in \{1, \dots, x - k^2 - 2\}$. It is easy to check that sets in S_n are pairwise disjoint and $\sum_{m=1}^x |L_{G_m}| = (1 - o(1))n/2$. Therefore, G is strongly packable. \square

Chapter 5

Spectral Graph Theory for Graph Drawings

This chapter presents a new graph drawing algorithm using semidefinite programming. We start with two classical, related graph drawing methods, Tutte's spring embeddings and spectral embeddings. This chapter is joint work with Matthew DeVos and Danielle Rogers. It is currently in preparation for publication [W9].

5.1 Tutte's Spring Embedding

The classical theorem of Fáry [32] states that every planar graph admits a geometric drawing in the plane without edge crossings. The proof is by induction and it can be shown using Euler's Formula and the Art Gallery Theorem. The proof can not be generalised for graphs that are embeddable in general surfaces. In fact, Hubbard et al. [55] show that for large g there exists a graph G of genus g , such that a.a.s. for $g \rightarrow \infty$ a random hyperbolic metric on a surface of genus g does not admit a shortest path embedding of G , where the probability measure is proportional to the Weil-Petersson volume on moduli space.

In Tutte's famous paper "How to draw a graph" he shows a different way of obtaining Fáry's result. The proof idea can be described by an experiment:

The vertices of a graph G are represented by steel rings and edges are represented by springs (of natural length zero). Take a (not necessarily geometric) embedding of a planar, 3-connected graph G and a facial cycle C . Place the steel rings of the vertices of the cycle in convex position. Now let the other vertices move freely. The vertices move into an equilibrium position in which the springs are still. The final position of the vertices induces a geometric plane drawing of G , for an example see Figure 5.1.

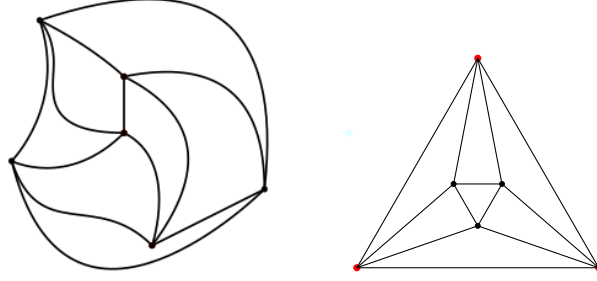


Figure 5.1: An example of Tutte's spring embedding on the right. The vertices of the outer face of the general drawing (left) are mapped to vertices of a triangle (right), which are on the outer face of the spring embedding.

In the equilibrium position, each vertex is the barycentre of its adjacent neighbours. The geometric drawing has an additional nice property, each face is a convex polygon. Let u_i be the position vector of vertex v_i . Then the barycentre condition yields

$$u_i = \frac{1}{\deg(v)} \sum_{v_j v_i \in E(G)} u_j.$$

Let the energy of a representation $U = [u_1, \dots, u_n]$ of a graph G be defined as

$$\text{energy}(U, G) = \sum_{v_i v_j \in E(G)} \|u_i - u_j\|^2. \quad (5.1)$$

It turns out that the energy of a geometric drawing of G with a fixed outer cycle C is minimised when all vertices $V(G) \setminus V(C)$ satisfy the barycentre condition, hence the representation is a spring embedding. To see this, we can write $u_i = [u_{1,i}, u_{2,i}]^T$ and

$$\text{energy}(U, G) = \sum_{v_i v_j \in E(G)} (u_{1,i} - u_{1,j})^2 + (u_{2,i} - u_{2,j})^2. \quad (5.2)$$

The energy of a representation U is minimised when for each $v_i \in V(G) \setminus C$

$$\frac{\partial(\text{energy}(U, G))}{\partial u_{1,i}} = \frac{\partial(\text{energy}(U, G))}{\partial u_{2,i}} = 0,$$

and hence

$$\sum_{v_j: v_i v_j \in E(G)} 2(u_{1,i} - u_{1,j}) = \sum_{v_j: v_i v_j \in E(G)} 2(u_{2,i} - u_{2,j}) = 0.$$

Rewriting the second equation gives the barycentre condition.

5.2 Eigenvector Embeddings of Graphs

Already in 1970 Hall [48] observed that the minimisation problem of Equation 5.1 together with additional constraints is related to low eigenvalues of the Laplacian of a graph. The *Laplacian* $L = L(G)$ of a graph G with vertex set v_1, \dots, v_n is the $n \times n$ matrix with $L_{i,i} = \deg(v_i)$, $L_{i,j} = -1$ if $v_i \sim v_j$ and $L_{i,j} = 0$ else. A direct calculation shows that for the Laplacian $L = L(G)$ and every vector x of length n it holds that

$$x^T Lx = \sum_{v_i v_j \in E(G)} (x_i - x_j)^2 = \text{energy}(x^T, G).$$

In the following we will denote by w_1, \dots, w_k the row vectors of U . By a generalisation of Equation 5.2,

$$\text{energy}(U, G) = \sum_{i=1}^k w_i^T L w_i.$$

When minimising the energy of a graph representation, additional constraints are needed since otherwise the energy of a graph is minimised by representing each vertex by the same vector, for example the all zeroes vector. The classical constraint added is

$$w_i \cdot w_j = \delta_{ij}. \tag{5.3}$$

Since $\|w_i\| = 1$, the solution $w_i = 0$ is not valid and since w_i is orthogonal to w_j for $i \neq j$ the solution $w_i = \frac{1}{\sqrt{n}}(1, \dots, 1)$ for $1 \leq i \leq k$ is not valid (if $k \geq 2$). Hence both constraints $w_i \cdot w_i = 1$ and $w_i \cdot w_j = 0$ for $i \neq j$ are necessary to ensure that the vertices are not mapped to the same point. These constraints are met by an orthogonal basis of eigenvectors w_1, \dots, w_k associated with the k smallest eigenvalues $\lambda_1^L \leq \dots \leq \lambda_k^L$ of the Laplacian L of G , and this choice minimises the energy among all choices satisfying constraint 5.3. This led to the study of eigenvector drawings [33, 48, 66, 70, 97]. We present the spectral graph drawing algorithm in Algorithm 1. Usually the first eigenvector is omitted for regular graphs, since adding or deleting it does not change the drawing (it is simply lifted, since the first eigenvector is the all ones vector $\mathbf{1}$).

Algorithm 1: Spectral Graph Drawing Algorithm.

Input: A Laplacian A of a graph G on the vertex set v_1, \dots, v_n

Result: A geometric drawing of G in \mathbb{R}^k

1. Compute the eigenvectors w_2, \dots, w_k to the eigenvalues $\lambda_2^L, \dots, \lambda_{k+1}^L$.
2. Let U be the representation matrix formed by the rows w_2, \dots, w_k .
3. Let the column u_i be the representation of vertex v_i .

Eigenvector drawings are nice since they are computable in polynomial time. Eigenvectors of the Laplacian and generalised Laplacians can be used in applications for graph drawings [45, 66]. However, spectral methods have their limitations. For example, spectral drawings of planar graphs in the plane can have crossings if the graph is not regular and the first two eigenvectors are considered [44]. But graph representations are not only used to visualise a graph but also for example for partitioning, clustering, ranking or finding of large components (see [13]). Further, in applications of graph drawings other energy-based algorithms are considered [4, 53].

In the following we will be interested in minimising the energy of a graph representation using a different set of constraints. We want to minimise the energy of a graph representation U with respect to

$$\|\mathbf{u}_i\| = 1 \text{ for each } 1 \leq i \leq n. \quad (5.4)$$

$$\text{The origin is the barycentre of } \mathbf{u}_1, \dots, \mathbf{u}_n. \quad (5.5)$$

The first constraint ensures that the representations $\mathbf{u}_1, \dots, \mathbf{u}_n$ of the vertices $\mathbf{v}_1, \dots, \mathbf{v}_n$ all have the same length and in particular no vertex is mapped to the origin. The second constraint ensures that the vertices are not mapped to a single point. The constraints give the graph representation a geometric flavour, the vertices are drawn on an a sphere. If U satisfies the constraints 5.4 and 5.5, we say U is a *unit barycentre 0 representation* of G .

5.3 Drawings of Distance Regular Graphs

Classic spectral drawings are those of (2-skeletons of) Platonic solids, see Figure 5.2.



Figure 5.2: Platonic solids.

Optimal spectral drawings in three dimensional space of the graphs of Platonic solids are up to rotation unique since the eigenspace of the second smallest eigenvector of the Laplacian is 3-dimensional. Platonic solids are distance regular graphs. *Distance regular graphs* are graphs such that the number of vertices which are simultaneously at distance j from a vertex v and at distance k from a vertex w depends only on j , k , and the distance between v and w . For distance regular graphs, optimising the energy of a representation with respect to the constraint 5.3 or with respect to the constraints 5.4 and 5.5 yields a common solution. By omitting the $\mathbf{1}$ vector as an eigenvector for constraint 5.3, w_1, \dots, w_k can be taken as vectors from the second smallest eigenspace of $L = L(G)$. By a result of Godsil [41, Lemma 1.2, Corollary 6.2] there exists an orthonormal basis for the eigenspace of the second smallest eigenvalue of the Laplacian $Eig(\lambda_2^L)$ in a distance regular graph such that the representation formed by rows of basis vectors is a unit barycentre $\mathbf{0}$ representation. The following observation shows that this is optimal.

Observation 5.1. If U is a unit barycentre $\mathbf{0}$ representation of a connected regular graph G , then

$$\text{energy}(U, G) = \sum_{i=1}^k w_i^T L w_i \geq \lambda_2^L \sum_{i=1}^k w_i^T w_i = \lambda_2^L \sum_{i=1}^k \sum_{i=1}^n U_{i,i} \stackrel{5.4}{=} \lambda_2^L v(G),$$

and equality holds if and only if for all i the row vector w_i is an eigenvector associated with λ_2^L .

The inequality in the observation follows from basic Linear Algebra of the Rayley quotient since each row vector \mathbf{w}_i is orthogonal to the all ones vector $\mathbf{1}$, which is the eigenvector to the smallest eigenvalue λ_1^L .

To showcase that our set of chosen constraints is natural, we consider vertex-transitive graphs. *Vertex-transitive* graphs are graphs whose automorphism group $Aut(G)$ is transitive. An *automorphism* of a graph G is a permutation σ of $V(G)$, such that (u, v) is an edge if and only if $(\sigma(u), \sigma(v))$ is an edge.

Observation 5.2. For each connected vertex-transitive graph G there exists a unit barycentre $\mathbf{0}$ representation U of a connected vertex-transitive graph G such

- every two edges that are in a common orbit of the automorphism group have the same length
- the energy of the representation is $\lambda_2^L \cdot v(G)$.

Proof. Let \mathbf{w} be a row vector that is a λ_2^L eigenvector, hence it is orthogonal to $\mathbf{1}$. Let $Aut(G) = \{\sigma_1, \dots, \sigma_t\}$ and for $i = 1, \dots, t$ let w_i be the vector obtained from \mathbf{w} by applying the permutation σ_i to the indices. It follows from vertex transitivity that the matrix with rows w_1, \dots, w_t has all columns of the same norm. So an appropriate scaling of the matrix with columns $\mathbf{r}_1, \dots, \mathbf{r}_t$ is a unit barycentre $\mathbf{0}$ representation of G and Proposition 5.3 shows that it is optimal. Further, taking an edge (i, j) and letting $(\mathbf{w})_i, (\mathbf{w})_j$ be the value of \mathbf{w} in position i, j , respectively. It follows that for every $\sigma \in Aut(G)$

$$\|\mathbf{u}_i - \mathbf{u}_j\|^2 = \sum_{k=1}^t ((w)_{\sigma_k(i)} - (w)_{\sigma_k(j)})^2 = \sum_{k=1}^t ((w)_{\sigma_k(\sigma(i))} - (w)_{\sigma_k(\sigma(j))})^2 = \|\mathbf{u}_{\sigma(i)} - \mathbf{u}_{\sigma(j)}\|^2,$$

which show that edges in the same orbit of the automorphism group have the same length. \square

The nice property here is that edges from the same orbit have the same length. Although the automorphism group can be very large, the representation U has rank at most n , which means we can reduce to the case with only n row vectors by an orthogonal transformation.

5.4 Semidefinite Graph Drawing Algorithm

In the following we define a semidefinite program from which we can obtain a polynomial time approximation algorithm to a unit barycentre $\mathbf{0}$ representation of G . Goemans and Williamsons approximation algorithm for MAXIMUM CUT [42] inspire our study of representations using semidefinite programming. A *maximum cut* is an edge-cut in G which maximizes the number of edges in the cut. MAXIMUM CUT is one of the first problems that was shown to be NP-complete. Goemans and Williamson introduce a semidefinite programming relaxation of MAXIMUM CUT. This (polynomially-solvable) relaxation is that of finding a spherical graph representation of an n -vertex graph G in \mathbb{R}^n which maximizes the energy. Remarkably, Goeman's and Williamson show that choosing a random hyperplane through the origin of the sphere then gives an edge-cut with expected size of approximately .868 times the size of the true maximum cut.

If $U = [\mathbf{u}_1, \dots, \mathbf{u}_n]$ is a unit barycentre $\mathbf{0}$ representation of G , we define

$$\rho(G, U) = \sum_{ij \in E(G)} \langle \mathbf{u}_i, \mathbf{u}_j \rangle.$$

We define $\rho(G)$ to be the maximum of $\rho(G, U)$ over all unit barycentre $\mathbf{0}$ representations U of G (which must exist by compactness). Under the constraints 5.3 and 5.5 minimising $\text{energy}(U, G)$ is equivalent to maximising $\rho(U, G)$, since

$$\begin{aligned} \|\mathbf{u}_i - \mathbf{u}_j\|^2 &= \langle \mathbf{u}_i - \mathbf{u}_j, \mathbf{u}_i - \mathbf{u}_j \rangle \\ &= \|\mathbf{u}_i\|^2 + \|\mathbf{u}_j\|^2 - 2\langle \mathbf{u}_i, \mathbf{u}_j \rangle \\ &= 2 - 2\langle \mathbf{u}_i, \mathbf{u}_j \rangle. \end{aligned}$$

In the following we will consider the adjacency matrix $A(G)$ and the parameter $\rho(G)$ instead of the Laplacian $L(G)$ and $\text{energy}(G)$. Let the eigenvalues of the adjacency matrix $A = A(G)$ be $\lambda_1 \geq \lambda_2 \geq \dots \geq \lambda_n$.

Corollary 5.3 ([W9]). If G is a regular graph, then $\rho(G) \leq \frac{\lambda_2}{2}v(G)$. Furthermore $\rho(G, R) = \frac{\lambda_2}{2}v(G)$ if and only if every row of R is a λ_2 -eigenvector of the adjacency matrix of G .

For every $1 \leq i \leq n$ the matrix C_i is an $n \times n$ matrix with a 1 in position i, i and 0 everywhere else. We use J to denote an $n \times n$ matrix with all entries 1. We will call upon standard properties of positive semidefinite matrices and semidefinite programming. In particular we define the *dot product* of two $n \times n$ matrices A and B to be $A \bullet B = \text{trace}(A^\top B)$.

<p><i>Primal Program (Primal):</i></p> <p>Maximise: $\frac{1}{2}A \bullet X$ Subject To: $C_i \bullet X = 1$ for $i = 1, \dots, n$ $J \bullet X = 0$ $X \succeq 0$</p>	<p><i>Dual Program (Dual):</i></p> <p>Minimise $\sum_{i=1}^n y_i$ Subject To: $-\sum_{i=1}^n y_i \cdot C_i - y_{n+1} \cdot J \preceq -\frac{1}{2}A$</p>
---	---

Theorem 5.4 ([W9]). The optimum value of the above primal program is $\rho(G)$. Moreover, if $X = R^\top R$ is a feasible matrix optimising this program, then R is a unit barycentre $\mathbf{0}$ representation of G maximising ρ (and thus minimising energy).

Proof. Let $R = [\mathbf{u}_1, \dots, \mathbf{u}_n]$ be an $m \times n$ matrix representing the graph G and let $X = R^\top R$. The i, i coordinate of X is $\langle \mathbf{u}_i, \mathbf{u}_i \rangle$ so the first condition in the Primal Program is equivalent to R being a unit representation. The second condition in this program is equivalent to R having barycentre $\mathbf{0}$ as shown by the following calculation:

$$J \bullet X = \text{Trace}(J^\top X) = \sum_{i=1}^n \sum_{j=1}^n X_{ij} = \sum_{i=1}^n \sum_{j=1}^n \langle \mathbf{u}_i, \mathbf{u}_j \rangle = \left\langle \sum_{i=1}^n \mathbf{u}_i, \sum_{j=1}^n \mathbf{u}_j \right\rangle.$$

It follows that X is a feasible matrix for the program if and only if R is a unit barycentre $\mathbf{0}$ representation of G . Now we have

$$\frac{1}{2}A \bullet X = \sum_{ij \in E(G)} \langle \mathbf{u}_i, \mathbf{u}_j \rangle = \rho(G, R)$$

so the value of this program on a feasible matrix $X = R^\top R$ is precisely $\rho(G, R)$. Our result now follows from the Cholesky decomposition theorem. \square

From this we can set up an alternative graph drawing algorithm.

Algorithm 2: Semidefinite Graph Drawing Algorithm

Input: Adjacency matrix A of an n -vertex graph G

Result: A geometric representation of G in one of $\mathbb{R}^1, \dots, \mathbb{R}^n$

1. For a graph G , solve *Primal* to obtain an optimal matrix X_G .
 2. Use the Cholesky decomposition to obtain a representation matrix R_G with $X_G = R_G^\top R_G$.
-

If we want to get a representation in a particular dimension, for example in dimension $k = 2$, we can perform the following additional steps.

3. If $\text{rank}(R_G) \leq k$ then let R'_G be an orthogonal transformation of R_G where all but the first k rows are zero rows. Take for the representations u_1, \dots, u_n the column vector of R'_G .
4. If $\text{rank}(R_G) > k$ then take a random orthogonal transformation of R_G to obtain R'_G . Take for the representations u_1, \dots, u_n the first k entries of the column vectors of R'_G .
5. If vertices i and j are adjacent in G then draw a straight line between their placements.

An approximate solution to the given semidefinite program can be computed in polynomial time since the Frobenius norm of the solution space is polynomially bounded in n [38]. Standard algorithms for the Cholesky decomposition run in $O(n^3)$ time [38]. Therefore, the above gives us a way to approximately compute $\rho(G)$ and to construct a minimum energy unit barycentre $\mathbf{0}$ representation of a graph in polynomial time. Figure 5.3 shows drawings of Platonic solids drawn by our semidefinite program which Danielle Rogers implemented in SageMath.

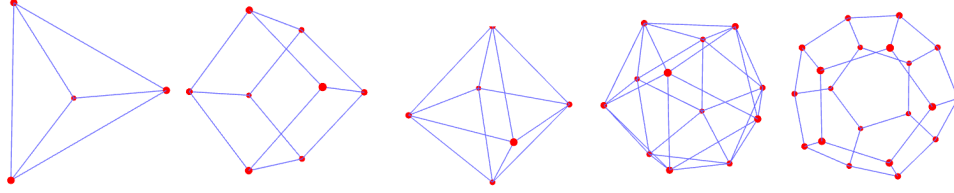


Figure 5.3: Semidefinite drawings of Platonic solids.

Next we will show that for the graphs of interest to us the primal and dual are well behaved.

5.4.1 Strong Duality

A semidefinite program is *strongly dual* if both the Primal and Dual programs achieve the same optimum.

Theorem 5.5 ([W9]). If G is regular then Primal and Dual are strongly dual.

Proof of Theorem 5.5. Suppose G is a regular graph on n vertices. We show strong duality by showing that there exists a feasible point $\mathbf{y} = (y_1, y_2, \dots, y_{n+1})$ for *Dual* such that

$$M = -\frac{1}{2}C + \sum_{i=1}^n y_i A_i + y_{n+1} J \succ 0,$$

which is enough by [38, Theorem 4.1.1]. Set $y_i = \frac{\lambda_2}{2} + 1$ for $i = 1, \dots, n$ and $y_{n+1} = \frac{\lambda_1 - \lambda_2}{2n}$, then

$$M = -\frac{1}{2}C + \left(\frac{\lambda_2}{2} + 1\right)I + \frac{\lambda_1 - \lambda_2}{2n}J.$$

All that is left to show is that M is positive definite. The eigenvalues of $-\frac{1}{2}C + (\frac{\lambda_2}{2} + 1)I$ are

$$\left\{ \frac{-\lambda_1 + \lambda_2}{2} + 1, 1, \dots, \frac{-\lambda_n + \lambda_2}{2} + 1 \right\}$$

and all eigenvalues are positive except for $\frac{-\lambda_1 + \lambda_2}{2} + 1$ which has eigenvector $\mathbf{1}$. The negative eigenvalue gets lifted up by adding $\frac{\lambda_1 - \lambda_2}{2n}J$, as $\mathbf{1}$ is an eigenvector of $\frac{\lambda_1 - \lambda_2}{2n}J$ with eigenvalue $\frac{\lambda_1 - \lambda_2}{2n}$ and noting that the other eigenvalues of $\frac{\lambda_1 - \lambda_2}{2n}J$ are 0, so each eigenvector of $-\frac{1}{2}C + (\frac{\lambda_2}{2} + 1)I$ is an eigenvector of M . \square

5.5 The Energy of Regular Graphs

In the following we show that almost all regular graphs have ρ asymptotically close to the upper bound. We start by considering regular graphs with large girth and show that such graphs have ρ asymptotically close to the upper bound. Our argument is based on a lovely

theorem of Nilli [84] who showed how to construct vectors orthogonal to $\mathbf{1}$ that are close to λ_2 eigenvectors (in the sense of Rayleigh quotient). In particular, the multiplicative factor that appears in our theorem is the same as that from the paper of Nilli.

Next we introduce the vectors that will be used here and in the forthcoming subsection on random regular graphs. We define the *distance* between an edge e and a vertex v (edge e') to be the minimum distance between an end of e and v (an end of e'). For every edge e and non-negative integer s we define $V_s(e)$ to be the set of vertices at distance s to e . Now let e, \bar{e} be edges at distance at least $2k + 2$ in a d -regular graph G and construct the row vector $\mathbf{w}_{e, \bar{e}}$ (indexed by $V(G)$) as follows:

$$(\mathbf{w}_{e, \bar{e}})_j = \begin{cases} (d-1)^{\frac{-s}{2}}, & \text{if } j \in V_s(e) \text{ for some } s \leq k \\ -(d-1)^{\frac{-s}{2}}, & \text{if } j \in V_s(\bar{e}) \text{ for some } s \leq k \\ 0, & \text{else} \end{cases} \quad (5.6)$$

The key feature of the vector $\mathbf{w}_{e, \bar{e}}$ is the following bound.

Lemma 5.6 ([W9]). Let G be a d -regular graph, let e, \bar{e} be edges with distance greater than $2k + 2$ and assume that the subgraph induced by all vertices at distance at most k to e (\bar{e}) has no cycle. Then using A for the adjacency matrix of G we have

$$\|\mathbf{w}_{e, \bar{e}}\|^2 = 4(k+1) \quad \text{and} \quad \mathbf{w}_{e, \bar{e}} A \mathbf{w}_{e, \bar{e}}^\top = 4 + 8k\sqrt{d-1}.$$

Proof. It follows from our assumption on induced subgraphs that $|V_s(e)| = 2(d-1)^s = |V_s(\bar{e})|$ holds for all $0 \leq s \leq k$. Therefore $\|\mathbf{w}_{e, \bar{e}}\|^2 = 2 \sum_{s=0}^k |V_s(e)| (d-1)^{-s} = 4(k+1)$ as claimed. For two disjoint subsets, say U, W of $V(G)$ we let $e(U, W)$ denote the number of edges with one end in U and the other in W . A similar argument to that for vertices then shows that $e(V_s(e), V_{s+1}(e)) = 2(d-1)^{s+1} = e(V_s(\bar{e}), V_{s+1}(\bar{e}))$ holds for all $0 \leq s \leq k-1$.

The only edges $uv \in E(G)$ for which $\mathbf{w}_{e, \bar{e}}$ assigns both u and v nonzero weight are as follows: e, \bar{e} , and those edges with one end in $V_s(e)$ ($V_s(\bar{e})$) and the other in $V_{s+1}(e)$ ($V_{s+1}(\bar{e})$) for some $0 \leq s \leq k-1$. Our result now follows from the calculation below.

$$\begin{aligned} \mathbf{w}_{e, \bar{e}} A \mathbf{w}_{e, \bar{e}}^\top &= 2 \sum_{ij \in E(G)} (\mathbf{w}_{e, \bar{e}})_i (\mathbf{w}_{e, \bar{e}})_j \\ &= 2 \left(2 + 2 \sum_{s=0}^{k-1} (d-1)^{-s-\frac{1}{2}} e(V_s(e), V_{s+1}(e)) \right) \\ &= 4 + 8k\sqrt{d-1} \quad \square \end{aligned}$$

Next we use these vectors to find good representations for regular graphs of high girth.

Theorem 5.7 ([W9]). Let G be d -regular with girth $g > 2k + 1$, then

$$\left(2\sqrt{d-1} - \frac{2\sqrt{d-1}-1}{k+1}\right) \frac{v(G)}{2} \leq \rho(G).$$

Proof. We will use the preceding lemma to construct a family of row vectors for a representation matrix that implies the desired bound. We claim that we may choose two enumerations of the edges of our graph $e_1, \dots, e_{e(G)}$ and $\bar{e}_1, \dots, \bar{e}_{e(G)}$ with the property that e_i and \bar{e}_i have distance at least $2k + 2$ for $1 \leq i \leq e(G)$. To prove the claim, construct a bipartite graph H where each side of the bipartition corresponds to $E(G)$ and an edge is present in H if the corresponding edges of G have distance at least $2k + 2$ (in G). It now follows from the girth assumption that H is regular and the desired enumerations are implied by the presence of a perfect matching in H .

Now define W be the matrix with rows $\mathbf{w}_1, \dots, \mathbf{w}_{e(G)}$ where $\mathbf{w}_i = \mathbf{w}_{e_i, \bar{e}_i}$. It follows from our girth assumption that any column of W can be transformed into any other column of W by permuting entries and changing signs. So, in particular any two columns of W have the same norm. Lemma 5.6 implies that the sum of the squares of the norms of the rows of W is $e(G)4(k+1) = \frac{d}{2}v(G)4(k+1)$ so defining $t = \sqrt{\frac{1}{2}d \cdot 4(k+1)}$ the matrix $W' = \frac{1}{t}$ is a unit barycentre $\mathbf{0}$ representation of G . The result is then given by the following calculation:

$$\begin{aligned} \rho(G) &\geq \rho(G, W') \\ &= \frac{1}{2} \sum_{k=1}^{e(G)} \frac{1}{t^2} \mathbf{w}_i A \mathbf{w}_i^\top \\ &= \frac{e(G)}{2t^2} (4 + 8k\sqrt{d-1}) \\ &= \frac{v(G)}{2} \left(2\sqrt{d-1} - \frac{2\sqrt{d-1}-1}{k+1}\right). \quad \square \end{aligned}$$

Before proving our final result on the behaviour of ρ for random regular graphs we require one straightforward result. Here we let $\mathbb{R}^+ = \{x \in \mathbb{R} \mid x \geq 0\}$ and for a function $f : S \rightarrow \mathbb{R}^+$ and a subset $A \subseteq S$ we let $f(A) = \sum_{x \in A} f(x)$.

Lemma 5.8 ([W9]). Let $G = (V, E)$ be a complete graph and let $f : V \rightarrow \mathbb{R}^+$. If

$$(\star) \quad f(v) \leq \frac{1}{2}f(V) \text{ for every } v \in V,$$

then there exists $g : E \rightarrow \mathbb{R}^+$ satisfying $\sum_{e \sim v} (g(e))^2 = f(v)$ for every $v \in V$.

Proof. We proceed by induction on $|V|$. As a base case, when $|V| = 1$ condition (\star) implies that $f = 0$ so the result holds by taking $g = 0$. More generally, observe that whenever (\star) is tight, i.e. there exists $v \in V$ with $f(v) = \frac{1}{2}f(V)$, then we have a solution given by

setting $g(uv) = \sqrt{f(u)}$ for every $u \in V \setminus \{v\}$ and setting $g(e) = 0$ for edges e not incident with v . Now we suppose there is no such vertex and choose distinct vertices $x, y \in V$ with $0 < f(x) \leq f(y)$. Consider the complete graph $G' = G - x$ with weight function $f' : V(G') \rightarrow \mathbb{R}^+$ given by $f'(y) = f(y) - f(x)$ and $f'(z) = f(z)$ for all $z \in V \setminus \{x, y\}$. If G' (and f') satisfy (\star) then the result follows by applying induction and then modifying this solution by giving the edge xy the value $\sqrt{f(x)}$. Otherwise there exists $v \in V \setminus \{x, y\}$ violating (\star) (in the graph G'), hence $f(v) > \frac{f(y)-f(x)}{2} + \frac{1}{2} \sum_{z \in V \setminus \{x, y\}} f(z)$. In this case we let $f'' : V \rightarrow \mathbb{R}^+$ be given by $f''(z) = f(z) - \frac{1}{2}f(V) + f(v)$ for $z = x, y$ and $f''(z) = f(z)$ for every $z \in V \setminus \{x, y\}$. Now the graph G and the weight function f'' satisfy (\star) . However, v is tight so the result holds for G and f'' (as shown above). Modifying this solution to change the value on the edge xy from 0 to $\sqrt{\frac{1}{2}f(V) - f(v)}$ gives a solution in the original graph. \square

Theorem 5.9 ([W9]). Let G be a random regular graph with degree d . For every $\varepsilon > 0$ the inequality

$$\left(2\sqrt{d-1} - \varepsilon\right) \frac{v(G)}{2} \leq \rho(G) \leq \left(2\sqrt{d-1} + \varepsilon\right) \frac{v(G)}{2}$$

holds asymptotically almost surely.

Proof. The upper bound follows from Proposition 5.3 and a remarkable result by J. Friedmann [36] showing that the second largest eigenvalue of a d -regular graph is asymptotically almost surely smaller than $2\sqrt{d-1} + \varepsilon$. Hence we only have to show the lower bound. We will denote $n := v(G)$. Our proof uses that the expected number of cycles of length at most $2k+1$ in a random d -regular graph is asymptotically smaller than some constant $C_{d,k}$ [116]. Since the number of cycles of length at most $2k+1$ is a non-negative random variable, by Markov's inequality, with probability at least $1 - C_{d,k} \cdot (\log n)^{-1}$ there are no more than $\log(n)$ cycles of length at most $2k+1$. Therefore, we may suppose that G is a random d -regular graph for which there are no more than $\log(n)$ cycles of length at most $2k+1$.

As in the previous theorem we claim that we may enumerate the edges e_1, \dots, e_m and $\bar{e}_1, \dots, \bar{e}_m$ so that e_i and \bar{e}_i have distance at least $2k+2$. As before, to prove the claim, we construct a bipartite graph H where each side of the bipartition corresponds to $E(G)$ and an edge is present in H if the corresponding edges of G have distance at least $2k+2$ (in G). Since the number of edges at distance less than $2k+2$ is bounded above by a function of d and k , for G suitably large the graph H will have m vertices on each side of the bipartition and minimum degree greater than $\frac{m}{2}$, thus implying the existence of a perfect matching.

Fix two vertices $x, y \in V(G)$. Now define I to be the set of all $1 \leq i \leq m$ for which the graph induced by all vertices at distance at most k from e_i and all vertices at distance at most k from \bar{e}_i does not contain a cycle and does not contain either x or y . Note that by our assumptions we have $|I| \geq m - Cd^k \log(n)$ for some constant C . Now define a matrix W (starting from the empty matrix) by adding the row vector $\mathbf{w}_i = \mathbf{w}_{e_i, \bar{e}_i}$ for every $i \in I$.

As we did in the previous subsection, we set $t = \sqrt{\frac{1}{2}d(4k+1)}$ and define $W' = \frac{1}{t}W$. For every vertex v let \mathbf{u}_v be the column of W' associated with v and observe that $\|\mathbf{u}_v\|^2 \leq 1$. For every vertex v define $f(v) = 1 - \|\mathbf{u}_v\|^2$ and note that $f(x) = f(y) = 1$ and $f(v) \leq 1$ for every vertex. Therefore, by the previous lemma we may choose for every pair of distinct vertices, u, v a weight w_{uv} so that $f(v) = \sum_{u \in V(G) \setminus \{v\}} w_{uv}^2$. Now for every $w_{uv} > 0$ add a row vector to W' with a w_{uv} at vertex u a $-w_{uv}$ at vertex v , and all other entries 0. The matrix W'' obtained at the end of this process has all columns of norm 1 and all rows summing to zero so W'' is a suitable representation of G and

$$\begin{aligned} \rho(G) &\geq \rho(G, W'') \\ &\geq \frac{1}{2} \sum_{i \in I} \frac{1}{t^2} \mathbf{w}_i A \mathbf{w}_i^\top \\ &= \frac{|I|}{2t^2} (4 + 8k\sqrt{d-1}) \\ &= \frac{|I|}{d} \left(2\sqrt{d-1} - \frac{2\sqrt{d-1}-1}{k+1} \right). \end{aligned}$$

Recall that $|I| \geq m - 2(2k+2)(d^{k+1}) \log(n)$. We have

$$\begin{aligned} &\frac{1}{d}|I| \left(2\sqrt{d-1} - \frac{2\sqrt{d-1}-1}{k+1} \right) \\ &\geq \frac{1}{d} \left(m - 2(2k+2)(d^{k+1}) \log(n) \right) \left(2\sqrt{d-1} - \frac{2\sqrt{d-1}-1}{k+1} \right) \\ &\geq \frac{v(G)}{2} 2\sqrt{d-1} - \frac{v(G)}{2} \left(\frac{2\sqrt{d-1}-1}{k+1} \right) \\ &\quad - 4(2k+2)d^k \sqrt{d-1} \log(n). \end{aligned}$$

Recall that we have chosen k sufficiently large such that $\frac{2\sqrt{d-1}-1}{k+1} \leq \frac{\epsilon}{2}$. As well because k is fixed, $4(2k+2)d^k \sqrt{d-1} \log(n)$ is $\leq n \cdot (\frac{\epsilon}{2})$ for sufficiently large n . Hence we have

$$\rho(G) \geq \frac{v(G)}{2} (2\sqrt{d-1} - \epsilon).$$

This completes the proof. □

5.6 Spectral Graph Drawings for Graphs of Higher Genus

Recently, new methods have been developed to draw toroidal graphs, which are graphs of genus 1. One such example is the Petersen graph. It is edge transitive, but a random projection of its unit barycentre 0 representation to two dimensional space does not preserve the property that every edge has the same length, see Figure 5.4. There exists an embed-

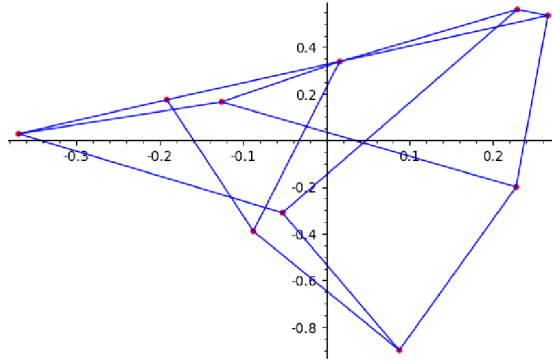


Figure 5.4: A semidefinite drawing of the Petersen graph.

ding of the Petersen graph on the flat torus where every edge has the same length. It can be obtained by placing an appropriately spaced grid on the covering space, the Euclidean plane, and rotating the grid appropriately. Kang and Wu [60] showed how to obtain it with spectral methods. They also provided toroidal spectral drawings of other vertex-transitive graphs such as K_5 , K_6 , K_7 , $K_{3,3}$, the Heawood graph, the Möbius-Kantor graph $G(8, 3)$, the Nauru graph $G(12, 5)$ and grids. They asked if there are methods of drawing vertex-transitive graphs of higher genus g on a surface of genus g , starting with $g = 2$. A first question would be which surface to choose for the embedding.

Chapter 6

Conclusion

In this thesis, we studied surfaces and graphs embedded on them. In Chapter 2 we showed that two cops can win the Cops and Robber game on surfaces of constant curvature. This is in strong contrast to general surfaces, since surfaces of genus g exists where $g^{\frac{1}{2}-\varepsilon}$ cops can not win the Cops and Robber game. In Chapter 3 and Chapter 4 we considered graph drawings or decompositions of graph drawings with few number of crossings, whereas in Chapter 5 we minimised the energy of graph representations. One result to highlight is that we determined that most graphs are not geometric packable, which is in contrast to Wilson's theorem which states that every graph G is packable, which means there is a packing of G in K_n that covers all but $o(n^2)$ edges.

6.1 Open Questions

Recall that Mohar [80] showed that $2g + 1$ cops are enough to win the Cops and Robber game on a surface of genus g . The lower bound from the Cops and Robber game on graphs gives a lower bound of $g^{\frac{1}{2}-o(1)}$ for surfaces of genus g . A natural direction of work would be to improve the gap. While strategies from the Cops and Robber game on graphs ([21, 30, 104]) could lead to an improvement of the linear factor, it would be fundamental to show whether $o(g)$ cops are enough to win the Cops and Robber game on a surface of genus g . Similarly, upper bounds on catching the robber would be interesting, although they are more difficult to obtain. We showed that the number of cops needed to catch the robber on the special surface $S(g)$ is between 3 and 5. If the lower bound is not tight, it is not clear to us how to improve it. Hence a tight bound on the number of cops needed to win the Cops and Robber game on $S(g)$ would be interesting. A further question is, if a surface has high cop number, does there exists a graph with high cop number that is embeddable in the surface such that edges are geodesic segments?

In Chapter 3 we studied random graph models through intersection graphs of geometric objects. Given random line segments drawn uniformly at random from $[0, 1]^2$ and a partition of the segments into two parts, is there a better strategy to partition them than by positive

and negative slope? We believe that it is the best way to partition the edges when the strategy is to assign one range of angles for each colour class but do not have a formal proof yet. How about partitioning line segments drawn uniformly at random from other convex sets in the plane? Or how about the sphere or the torus? These are questions that would be interesting to investigate further. In Section 3.3.4 we considered triangle densities of geodesic segment intersection graphs drawn where geodesic segments are drawn at random with respect to a special probability measure μ on the sphere. However, we have not determined the triangle density when μ is the uniform distribution on the sphere, which is a natural question to ask. For triangle densities it seems more difficult to simplify the problem using symmetries such as we did for edge densities. It could be simpler to determine subgraph densities, such a triangle densities, of the intersection graph of n line segments drawn uniformly at random from $[0, 1]^2$. For line segments in $[0, 1]^2$ methods like Valtr's bounding box strategy could be used.

In Section 3.4 we showed that if $r = \omega\left(\sqrt[d+1]{\frac{\log n}{n}}\right)$ then a.a.s. the random geometric graph $G_1^d(n, r)$ behaves like a power of the grid. Is it possible to improve the bound to $r = \omega\left(\sqrt[d]{\frac{\log n}{n}}\right)$? If $r = o\left(\sqrt[d]{\frac{\log n}{n}}\right)$, then $G_1^d(n, r)$ is a.a.s. disconnected, hence does not contain any spanning structure. Further, we asked in Section 3.4 if for every $\Delta > 0$, there exists a constant C such that the random geometric graph $G^d(n, \frac{C}{\log(n)})$ a.a.s. contains every tree with maximum degree at most Δ ? We could show that more general graphs than s -ary trees can be embedded in $G^d(n, \frac{C}{\log(n)})$ for large enough C , but are far from the full result. A start would be to consider $\Delta = 3$. Lastly, what can be said about spanning substructures of intersection graphs of disks of radius r drawn uniformly at random from a hyperbolic square?

In Section 5 we proposed a semidefinite program which computes a representation of regular graphs G with small energy. Recall the question of Kang and Wu about natural embeddings of vertex-transitive graphs of genus $g \geq 2$. For hyperbolic surfaces of genus $g \geq 2$, surfaces of the same genus g can exhibit different geometries. Which surfaces are most natural for embeddings of vertex-transitive graphs?

6.2 Work not in this Thesis

There are several works that are not mentioned in this thesis that we worked on during the preparation of this thesis. We shortly present the papers that are available online at this moment.

We studied the MINIMUM DOMINATING SET (MDS) problem on planar graphs. Planar graphs are well studied due to their topological applications. With Marthe Bonamy, Linda Cook and Carla Groenland we considered MDS on outerplanar graphs [W2], which are graphs that can be embedded in the plane such that all vertices share a face (usually, the

outer face). We showed that in the LOCAL model, there exists a 5-approximation algorithm for MDS, which is tight. A lower bound for approximating MDS on planar graphs is 7. The tools we developed for outerplanar graphs can be used to give an approximation algorithm on planar graphs that gives a similar bound to the current best upper bound, which gives an $(11 + \varepsilon)$ -approximation for MDS on planar graphs.

Planar graphs motivate the study of structural graph theory, they are K_5 and $K_{3,3}$ -minor free. During the Graph Theory Workshop held at Bellairs Research Institute in March 2022 we studied graphs that have no k disjoint triangles as induced minors and showed that they have logarithmic treewidth [W1]. As a consequence, many NP-hard problems such as MINIMUM DOMINATING SET, MINIMUM VERTEX COVER, MINIMUM COLORING and MAXIMUM INDEPENDENT SET are polynomial time solvable in this graph class. We also study MAXIMUM INDEPENDENT SET on graphs excluding a friendship graph as an induced minor as well as graphs excluding a disjoint union of triangles and one four-cycle [W5]. With Nicolas Bousquet and Théo Pierron [W6] we studied the structure of $K_{2,\ell}$ -minor free graphs. We give a simple proof that 3-connected $K_{2,\ell}$ -minor free graphs with minimum degree at least 5 and no twins of degree 5 have bounded size. This work generalises an unpublished result by Ding [28] and simplifies the proof.

As mentioned in the introduction, one of the first problems studied on planar graphs is vertex colouring. Edge colouring a graph G is tightly related to vertex colouring by considering the line graph of G . We studied connected greedy edge colouring [W3], where the vertices are ordered in a connected fashion and coloured greedily with respect to this order. We showed that the minimum number of colours needed for connected greedy colouring in a subcubic graph is at most 4, and for a bipartite graph it is the same number of colours as for classical edge colouring.

With Natasha Morrison, JD Nir, Sergey Norin and Paweł Rzażewski we worked on a Turán-type problem [W14] during the Cross-Community Collaborations in Combinatorics Workshop (22w5107) at the Banff International Research Station. Turán's theorem says that the r -partite Turán graph maximises the number of edges among all graphs which do not contain K_{r+1} as a subgraphs, which means it maximised the density. We show that for every graph H , if r is large enough as a function of H , the r -partite Turán graph maximises the number of copies of H among all K_{r+1} -free graphs on a given number of vertices.

With Alberto Espuny Díaz, Lyuben Lichev and Dieter Mitsche [W11] we studied thresholds for the appearance of certain spanning trees in the random geometric graph, motivated by Question 3.33.

Lastly, I would like to mention that with Matt DeVos and Danielle Rogers we worked on two more problems in spectral graph theory. We studied the Network Laplacian of a graph, and we showed a novel proof of correctness of the Gomory-Hu tree theorem. The results have not been published yet, but the research has been an integral part of my PhD experience. They appeared in the master thesis of Danielle Rogers.

Author's Publications

- [W1] Marthe Bonamy, Édouard Bonnet, Hugues Déprés, Louis Esperet, Colin Geniet, Claire Hilaire, Stéphan Thomassé, and Alexandra Wesolek. Sparse graphs with bounded induced cycle packing number have logarithmic treewidth. In *Proceedings of the 2023 Annual ACM-SIAM Symposium on Discrete Algorithms (SODA)*, pages 3006–3028. SIAM, Philadelphia, PA, 2023.
- [W2] Marthe Bonamy, Linda Cook, Carla Groenland, and Alexandra Wesolek. A tight local algorithm for the minimum dominating set problem in outerplanar graphs. In *35th International Symposium on Distributed Computing*, volume 209 of *LIPICs. Leibniz Int. Proc. Inform.*, pages 13– 18. Schloss Dagstuhl. Leibniz-Zent. Inform., Wadern, 2021.
- [W3] Marthe Bonamy, Carla Groenland, Carole Muller, Jonathan Narboni, Jakub Pekárek, and Alexandra Wesolek. A note on connected greedy edge colouring. *Discrete Appl. Math.*, 304:129–136, 2021.
- [W4] Marthe Bonamy, Bojan Mohar, and Alexandra Wesolek. Limiting crossing numbers for geodesic drawings on the sphere. In *International Symposium on Graph Drawing and Network Visualization*, pages 341–355. Springer, 2020.
- [W5] Édouard Bonnet, Julien Duron, Colin Geniet, Stéphan Thomassé, and Alexandra Wesolek. Maximum independent set when excluding an induced minor: $K_1 + tK_2$ and $tC_3 \uplus C_4$. *arXiv preprint arXiv:2302.08182*, 2023.
- [W6] Nicolas Bousquet, Théo Pierron, and Alexandra Wesolek. A note on highly connected $K_{2,\ell}$ -minor free graphs. *arXiv preprint arXiv:2301.02133*, 2023.
- [W7] Sergio Cabello, Éva Czabarka, Ruy Fabila-Monroy, Yuga Higashikawa, Raimund Seidel, László Székely, Josef Tkadlec, and Alexandra Wesolek. A note on the 2-colored rectilinear crossing number of random point sets in the unit square. *In preparation*.
- [W8] Daniel W. Cranston, Jiayi Nie, Jacques Verstraëte, and Alexandra Wesolek. On asymptotic packing of geometric graphs. *Discrete Appl. Math.*, 322:142–152, 2022.

- [W9] Matt DeVos, Danielle Rogers, and Alexandra Wesolek. On minimizing the energy of a spherical graph representation. *In preparation*.
- [W10] Alberto Espuny Díaz, Lyuben Lichev, Dieter Mitsche, and Alexandra Wesolek. High powers of grids in random geometric graphs. *In preparation*.
- [W11] Alberto Espuny Díaz, Lyuben Lichev, Dieter Mitsche, and Alexandra Wesolek. Sharp threshold for embedding balanced spanning trees in random geometric graphs. *arXiv preprint arXiv:2303.14229*, 2023.
- [W12] Vesna Iršič, Bojan Mohar, and Alexandra Wesolek. Cops and robber on hyperbolic manifolds. *In preparation*.
- [W13] Vesna Iršič, Bojan Mohar, and Alexandra Wesolek. Cops and robber game in higher-dimensional manifolds with spherical and Euclidean metric. *C. R. Math. Acad. Sci. Soc. R. Can.*, 44(3):50–68, 2022.
- [W14] Natasha Morrison, JD Nir, Sergey Norin, Paweł Rzażewski, and Alexandra Wesolek. Every graph is eventually Turán-good. *Journal of Combinatorial Theory, Series B*, 162:231–243, 2023.

Bibliography

- [1] Marco Abate and Francesca Tovena. *Curves and surfaces*, volume 55 of *Unitext*. Springer, Milan, 2012.
- [2] Oswin Aichholzer, Thomas Hackl, Matias Korman, Marc Van Kreveld, Maarten Löffler, Alexander Pilz, Bettina Speckmann, and Emo Welzl. Packing plane spanning trees and paths in complete geometric graphs. *Information Processing Letters*, 124:35–41, 2017.
- [3] Oswin Aichholzer, Johannes Obenaus, Joachim Orthaber, Rosna Paul, Patrick Schnider, Raphael Steiner, Tim Taubner, and Birgit Vogtenhuber. Edge partitions of complete geometric graphs (part 2). *arXiv preprint arXiv:2112.08456*, 2021.
- [4] Noam Aigerman and Yaron Lipman. Orbifold Tutte embeddings. *ACM Transactions on Graphics*, 34(6):190–1, 2015.
- [5] Martin Aigner and M. Fromme. A game of cops and robbers. *Discrete Appl. Math*, 8:1–12, 1984.
- [6] James W. Anderson. Convexity, area, and trigonometry. In *Hyperbolic Geometry*, pages 111–151. Springer, 1999.
- [7] Martin JB Appel and Ralph P. Russo. The connectivity of a graph on uniform points on $[0, 1]^d$. *Statistics & Probability Letters*, 60(4):351–357, 2002.
- [8] József Balogh, Bernard Lidický, and Gelasio Salazar. Closing in on Hill’s conjecture. *arXiv preprint arXiv:1711.08958*, 2017.
- [9] Riccardo Benedetti and Carlo Petronio. *Lectures on hyperbolic geometry*. Springer Science & Business Media, 1992.
- [10] Frank Bernhart and Paul C. Kainen. The book thickness of a graph. *Journal of Combinatorial Theory, Series B*, 27(3):320–331, 1979.
- [11] Ahmad Biniiaz and Alfredo García. Packing plane spanning trees into a point set. *Computational Geometry*, 90:101653, 2020.

- [12] Jaroslav Blažek and Milan Koman. A minimal problem concerning complete plane graphs. *Theory of graphs and its applications, Czech. Acad. of Sci*, pages 113–117, 1964.
- [13] Drago Bokal, Martin Juvan, and Bojan Mohar. A spectral approach to graphical representation of data. *Informatica (Slovenia)*, 28(3):233–238, 2004.
- [14] Béla Bollobás. Relations between sets of complete subgraphs. In *Proceedings of the Fifth British Combinatorial Conference (Univ. Aberdeen, Aberdeen, 1975)*, Congressus Numerantium, No. XV, pages 79–84. Utilitas Math., Winnipeg, Man., 1976.
- [15] Béla Bollobás, Gábor Kun, and Imre Leader. Cops and robbers in a random graph. *Journal of Combinatorial Theory, Series B*, 103(2):226–236, 2013.
- [16] Béla Bollobás, Imre Leader, and Mark Walters. Lion and man—can both win? *Israel J. Math.*, 189:267–286, 2012.
- [17] Béla Bollobás and Andrew Thomason. Threshold functions. *Combinatorica*, 7(1):35–38, 1987.
- [18] Christian Borgs, Jennifer Chayes, and László Lovász. Moments of two-variable functions and the uniqueness of graph limits. *Geom. Funct. Anal.*, 19(6):1597–1619, 2010.
- [19] Prosenjit Bose, Ferran Hurtado, Eduardo Rivera-Campo, and David R. Wood. Partitions of complete geometric graphs into plane trees. *Computational Geometry*, 34(2):116–125, 2006.
- [20] Julia Böttcher. Large-scale structures in random graphs. In *BCC*, pages 87–140, 2017.
- [21] Nathan Bowler, Joshua Erde, Florian Lehner, and Max Pitz. Bounding the cop number of a graph by its genus. *arXiv preprint arXiv:1911.01758*, 2019.
- [22] Peter Bradshaw. A proof of the Meyniel conjecture for abelian cayley graphs. *Discrete Mathematics*, 343(1):111546, 2020.
- [23] Henry R. Brahana. Systems of circuits on two-dimensional manifolds. *Annals of Mathematics*, pages 144–168, 1921.
- [24] Hallard T. Croft. 'Lion and man': A postscript. *J. Lond. Math. Soc.*, 39:385–390, 1964.
- [25] Persi Diaconis, Susan Holmes, and Svante Janson. Interval graph limits. *Ann. Comb.*, 17(1):27–52, 2013.
- [26] Josep Díaz, Dieter Mitsche, and Xavier Pérez. Sharp threshold for hamiltonicity of random geometric graphs. *SIAM Journal on Discrete Mathematics*, 21(1):57–65, 2007.

- [27] Reinhard Diestel. *Graph theory*, volume 173 of *Graduate Texts in Mathematics*. Springer, Berlin, fifth edition, 2018.
- [28] Guoli Ding. Graphs without large $K_{2,n}$ -minors. *arXiv preprint arXiv:1702.01355*, 2017.
- [29] Noam D. Elkies. Crossing numbers of complete graphs. In *The mathematics of various entertaining subjects. Vol. 2*, pages 218–249. Princeton Univ. Press, Princeton, NJ, 2017.
- [30] Joshua Erde and Florian Lehner. Improved bounds on the cop number of a graph drawn on a surface. In *Extended Abstracts EuroComb 2021*, pages 111–116. Springer, 2021.
- [31] Paul Erdős and Alfréd Rényi. On random graphs I. *Publicationes Mathematicae*, 6(1):290–297, 1959.
- [32] István Fáry. On straight-line representation of planar graphs. *Acta Sci. Math.*, 11:229–233, 1948.
- [33] Miroslav Fiedler. A property of eigenvectors of nonnegative symmetric matrices and its application to graph theory. *Czechoslovak Math. J.*, 25(100)(4):619–633, 1975.
- [34] David C. Fisher. Lower bounds on the number of triangles in a graph. *J. Graph Theory*, 13(4):505–512, 1989.
- [35] Peter Frankl. Cops and robbers in graphs with large girth and Cayley graphs. *Discrete Appl. Math.*, 17(3):301–305, 1987.
- [36] Joel Friedman. *A proof of Alon’s second eigenvalue conjecture and related problems*. American Mathematical Soc., 2008.
- [37] Jean Gallier and Dianna Xu. *A guide to the classification theorem for compact surfaces*, volume 9 of *Geometry and Computing*. Springer, Heidelberg, 2013.
- [38] Bernd Gärtner and Jiri Matousek. *Approximation Algorithms and Semidefinite Programming*. Springer Science & Business Media, 2012.
- [39] Edgar N. Gilbert. Random graphs. *The Annals of Mathematical Statistics*, 30(4):1141–1144, 1959.
- [40] Edgar N. Gilbert. Random plane networks. *Journal of the Society for Industrial and Applied Mathematics*, 9(4):533–543, 1961.
- [41] Chris D. Godsil. *Algebraic Combinatorics*. Chapman and Hall Mathematics Series. Chapman & Hall, New York, 1993.

- [42] Michel X. Goemans and David P. Williamson. Improved approximation algorithms for maximum cut and satisfiability problems using semidefinite programming. *J. Assoc. Comput. Mach.*, 42(6):1115–1145, 1995.
- [43] Adolph W. Goodman. On sets of acquaintances and strangers at any party. *Amer. Math. Monthly*, 66:778–783, 1959.
- [44] Craig Gotsman. On graph partitioning, spectral analysis, and digital mesh processing. In *2003 Shape Modeling International.*, pages 165–171. IEEE, 2003.
- [45] Craig Gotsman, Xianfeng Gu, and Alla Sheffer. Fundamentals of spherical parameterization for 3d meshes. *ACM Trans. Graph.*, 22(3):358363, jul 2003.
- [46] Richard K. Guy. Crossing numbers of graphs. In *Graph theory and applications (Proc. Conf., Western Michigan Univ., Kalamazoo, Mich., 1972; dedicated to the memory of J. W. T. Youngs)*, Lecture Notes in Math., Vol. 303, pages 111–124. Springer, Berlin, 1972.
- [47] Richard K Guy, Tom Jenkyns, and Jonathan Schaer. The toroidal crossing number of the complete graph. *Journal of Combinatorial Theory*, 4(4):376–390, 1968.
- [48] Kenneth M. Hall. An r -dimensional quadratic placement algorithm. *Management science*, 17(3):219–229, 1970.
- [49] Frank Harary and Anthony Hill. On the number of crossings in a complete graph. *Proc. Edinburgh Math. Soc. (2)*, 13:333–338, 1962/63.
- [50] Ralf Heckmann, Ralf Klasing, Burkhard Monien, and Walter Unger. Optimal embedding of complete binary trees into lines and grid. *Journal of Parallel and Distributed Computing*, 49(1):40–56, 1998.
- [51] Ian Holyer. The NP-completeness of edge-coloring. *SIAM J. Comput.*, 10(4):718–720, 1981.
- [52] Heinz Hopf. Zum Clifford-Kleinschen Raumproblem. *Math. Ann.*, 95(1):313–339, 1926.
- [53] Kai Hormann, Konrad Polthier, and Alia Sheffer. Mesh parameterization: theory and practice. In *ACM SIGGRAPH ASIA 2008 courses*, pages 1–87. 2008.
- [54] Blue (<https://math.stackexchange.com/users/409/blue>). Area of a right angled hyperbolic triangle as function of side lengths. Mathematics Stack Exchange. URL:<https://math.stackexchange.com/q/1469983> (version: 2015-10-10).

- [55] Alfredo Hubard, Vojtěch Kaluža, Arnaud De Mesmay, and Martin Tancer. Shortest path embeddings of graphs on surfaces. *Discrete & Computational Geometry*, 58(4):921–945, 2017.
- [56] Yukinao Isokawa. Buffon’s short needle on the sphere. *Bull. Fac. Ed. Kagoshima Univ. Natur. Sci.*, 51:17–36, 2000.
- [57] Svante Janson, Tomasz Łuczak, and Andrzej Ruciński. *Random graphs*. Wiley-Interscience Series in Discrete Mathematics and Optimization. Wiley-Interscience, New York, 2000.
- [58] Camille Jordan. Sur la déformation des surfaces. *Journal de mathématiques pures et appliquées*, pages 105–109, 1866.
- [59] Gwenaël Joret, Marcin Kamiński, and Dirk O. Theis. The cops and robber game on graphs with forbidden (induced) subgraphs. *Contrib. Discrete Math.*, 5(2):40–51, 2010.
- [60] Ming-Hsuan Kang and Jing-Wen Gu. Toroidal spectral drawing. *Axioms*, 11(3):137, 2022.
- [61] Gyula Katona. A theorem of finite sets. In *Theory of Graphs (Proc. Colloq., Tihany, 1966)*, pages 187–207. Academic Press, New York, 1968.
- [62] Maurice G. Kendall and Patrick A. P. Moran. *Geometrical probability*. Griffin’s Statistical Monographs & Courses, No. 10. Hafner Publishing Co., New York, 1963.
- [63] Wilhelm Killing. Ueber die Clifford-Klein’schen Raumformen. *Math. Ann.*, 39(2):257–278, 1891.
- [64] Kyle Klein and Subhash Suri. Pursuit evasion on polyhedral surfaces. In *International Symposium on Algorithms and Computation*, pages 284–294. Springer, 2013.
- [65] János Komlós and Endre Szemerédi. Limit distribution for the existence of hamiltonian cycles in a random graph. *Discrete mathematics*, 43(1):55–63, 1983.
- [66] Yehuda Koren. Drawing graphs by eigenvectors: theory and practice. *Computers & Mathematics with Applications*, 49(11-12):1867–1888, 2005.
- [67] Joseph B. Kruskal. The number of simplices in a complex. In *Mathematical optimization techniques*, pages 251–278. Univ. California Press, Berkeley, Calif., 1963.
- [68] John E. Littlewood. *Littlewood’s miscellany*. Cambridge University Press, Cambridge, 1986. Edited and with a foreword by Béla Bollobás.

- [69] László Lovász. *Large networks and graph limits*, volume 60 of *American Mathematical Society Colloquium Publications*. American Mathematical Society, Providence, RI, 2012.
- [70] László Lovász and Alexander Schrijver. On the null space of a Colin de Verdière matrix. volume 49, pages 1017–1026. 1999.
- [71] László Lovász and Miklós Simonovits. On the number of complete subgraphs of a graph. II. In *Studies in pure mathematics*, pages 459–495. Birkhäuser, Basel, 1983.
- [72] László Lovász and Balázs Szegedy. Limits of dense graph sequences. *J. Combin. Theory Ser. B*, 96(6):933–957, 2006.
- [73] Tomasz Łuczak and Paweł Prałat. Chasing robbers on random graphs: zigzag theorem. *Random Structures & Algorithms*, 37(4):516–524, 2010.
- [74] Willem Mantel. Problem 28. *Wiskundige Opgaven*, 10:60–61, 1907.
- [75] Dieter Mitsche and Guillem Perarnau. On treewidth and related parameters of random geometric graphs. *SIAM Journal on Discrete Mathematics*, 31(2):1328–1354, 2017.
- [76] August F. Möbius. Zur Theorie der Polyëder und der Elementarverwandtschaft. *Gesammelte werke*, 2:519–559, 1886.
- [77] Bojan Mohar. Notes on cops and robber game on graphs. *arXiv preprint arXiv:1710.11281*, 2017.
- [78] Bojan Mohar. On a conjecture by anthony hill. *arXiv preprint arXiv:2009.03418*, 2020.
- [79] Bojan Mohar. Min-max theorem for the game of cops and robber on geodesic spaces. *ArXiv e-prints*, December 2021.
- [80] Bojan Mohar. The game of cops and robber on geodesic spaces. *ArXiv e-prints*, May 2022.
- [81] Burkhard Monien, Ralf Diekmann, Rainer Feldmann, Ralf Klasing, Reinhard Lüling, Knut Menzel, Thomas Römke, and Ulf-Peter Schroeder. Efficient use of parallel & distributed systems: From theory to practice. *Computer Science Today*, pages 62–77, 1995.
- [82] Richard Montgomery. Spanning trees in random graphs. *Advances in Mathematics*, 356:106793, 2019.
- [83] John W. Moon. On the distribution of crossings in random complete graphs. *J. Soc. Indust. Appl. Math.*, 13:506–510, 1965.

- [84] Alon Nilli. On the second eigenvalue of a graph. *Discrete Mathematics*, 91(2):207–210, 1991.
- [85] Sergey Norin. Presentation at the BIRS Workshop on geometric and topological graph theory. <https://www.birs.ca/events/2013/5-day-workshops/13w5091/videos/watch/201310011538-Norin.html>. Accessed: 05-February-2023.
- [86] Maria Nosarzewska. Évaluation de la différence entre l'aire d'une région plane convexe et le nombre des points aux coordonnées entières couverts par elle. *Colloq. Math.*, 1:305–311, 1948.
- [87] Richard Nowakowski and Peter Winkler. Vertex-to-vertex pursuit in a graph. *Discrete Mathematics*, 43(2-3):235–239, 1983.
- [88] Johannes Obenaus and Joachim Orthaber. Edge partitions of complete geometric graphs (part 1). *arXiv preprint arXiv:2108.05159*, 2021.
- [89] Shengjun Pan and R. Bruce Richter. The crossing number of K_{11} is 100. *J. Graph Theory*, 56(2):128–134, 2007.
- [90] Fragkiskos Papadopoulos, Maksim Kitsak, M Ángeles Serrano, Marián Boguná, and Dmitri Krioukov. Popularity versus similarity in growing networks. *Nature*, 489(7417):537–540, 2012.
- [91] Rose Peltesohn. Eine Lösung der beiden Heffterschen Differenzenprobleme. *Compositio Math.*, 6:251–257, 1939.
- [92] Mathew Penrose et al. *Random Geometric Graphs*, volume 5. Oxford University Press, 2003.
- [93] Mathew D. Penrose. The longest edge of the random minimal spanning tree. *The Annals of Applied Probability*, 7(2):340–361, 1997.
- [94] Mathew D. Penrose. On k -connectivity for a geometric random graph. *Random Structures & Algorithms*, 15(2):145–164, 1999.
- [95] Norbert Peyerimhoff. Areas and intersections in convex domains. *Amer. Math. Monthly*, 104(8):697–704, 1997.
- [96] Richard E Pfeifer. The historical development of JJ Sylvester's four point problem. *Mathematics Magazine*, 62(5):309–317, 1989.
- [97] Tomaž Pisanski and John Shawe-Taylor. Characterizing graph drawing with eigenvectors. *Journal of Chemical Information and Computer Sciences*, 40(3):567–571, 2000.

- [98] Photchchara Pisantechakool and Xuehou Tan. On the conjecture of the smallest 3-cop-win planar graph. In *International Conference on Theory and Applications of Models of Computation*, pages 499–514. Springer, 2017.
- [99] Alain Quilliot. *Jeux et pointes fixes sur les graphes*. PhD thesis, Ph. D. Dissertation, Université de Paris VI, 1978.
- [100] Alexander A. Razborov. Flag algebras. *J. Symbolic Logic*, 72(4):1239–1282, 2007.
- [101] Alexander A. Razborov. On the minimal density of triangles in graphs. *Combin. Probab. Comput.*, 17(4):603–618, 2008.
- [102] Daniel P. Sanders and Yue Zhao. Planar graphs of maximum degree seven are class I. *J. Combin. Theory Ser. B*, 83(2):201–212, 2001.
- [103] Numan Satimov and Atamurat Kuchkarov. On the solution of a model differential pursuit-evasion game on a sphere. *Uzbek. Mat. Zh*, 1:45–50, 2000.
- [104] Bernd SW Schröder. The copnumber of a graph is bounded by $\lceil 3/2 \text{ genus}(g) \rceil + 3$. In *Categorical perspectives*, pages 243–263. Springer, 2001.
- [105] John Stillwell. *Geometry of surfaces*. Universitext. Springer-Verlag, New York, 1992.
- [106] Wilson Stothers. Hyperbolic geometry. <http://www.maths.gla.ac.uk/wws/cabripages/hyperbolic/hyperbolic0.html>. Accessed: 16-January-2023.
- [107] James J. Sylvester. Mathematical question 1491. *Educ. Times J. Coll. Precept*, 17:20, 1864.
- [108] James J. Sylvester. On a special class of questions on the theory of probabilities. *Birmingham British Association Report*, 35:8–9, 1865.
- [109] Carsten Thomassen. The Jordan-Schönflies theorem and the classification of surfaces. *The American Mathematical Monthly*, 99(2):116–130, 1992.
- [110] Hazim M. Trao, Gek L. Chia, Niran A. Ali, and Adem Kilicman. On edge-partitioning of complete geometric graphs into plane trees. *arXiv preprint arXiv:1906.05598*, 2019.
- [111] Pavel Valtr. Probability that n random points are in convex position. *Discrete & Computational Geometry*, 13(3-4):637–643, 1995.
- [112] Elias Wegert and Lloyd N. Trefethen. From the Buffon needle problem to the Kreiss matrix theorem. *Amer. Math. Monthly*, 101(2):132–139, 1994.
- [113] Eric W. Weisstein. Sylvester’s four-point problem. <https://mathworld.wolfram.com/SylvestersFour-PointProblem.html>, 2004. Accessed: 05-February-2023.

- [114] Richard M. Wilson. Decompositions of complete graphs into subgraphs isomorphic to a given graph. In *Proceedings of the Fifth British Combinatorial Conference (Univ. Aberdeen, Aberdeen, 1975)*, Congressus Numerantium, No. XV, pages 647–659. Utilitas Math., Winnipeg, Man., 1976.
- [115] WSB Woolhouse. Some additional observations on the four-point problem. *Mathematical Questions and their Solutions from the Educational Times*, 7:81, 1867.
- [116] Nicholas C. Wormald. The asymptotic distribution of short cycles in random regular graphs. *Journal of Combinatorial Theory, Series B*, 31(2):168–182, 1981.

Appendix A

Code for finding crossing probability of $S(2)$

The Maple code can be downloaded at:

<https://github.com/alexweso/hyperbolic-surface-maple.git>.

[> *unassign~(⟨anames(user)⟩)* :

Introduction

We will computationally approximate the probability that two random segments on the double torus $S(2)$ cross. The number of pairs of random segments we check is *ntuples* and crossing will be the number of times a pair of segments crosses.

```
[> ntuples := 10000 ;
      crossing := 0 ;
      ntuples := 10000
      (1.1)
```

The following procedure determines if given four points *point1*, *point2*, *point3* and *point4* in the Poincaré disk, the two geodesic segments *point1point2* and *point3point4* cross (*ans*=1) or if they do not cross (*ans*=0). None of the geodesics can go through the origin, which happens with probability 0 for random segments (computationally, with very small probability).

```
[> with(Student[Statistics]) :
      with(LinearAlgebra) :
      UseHardwareFloats := false :
      with(geometry) :
      cross := proc(point1, point2, point3, point4)
      local ans, point1inverse, point3inverse, xcoord, x2coord, x, x2, c1, c2;
      ans := 0;
      point1inverse :=  $\frac{1}{\text{evalf}(\text{abs}(\text{point1}))^2} \cdot \text{point1}$ ;
      circle(c1, [point(A, Re(point1), Im(point1)), point(B, Re(point2), Im(point2)), point(C,
      Re(point1inverse), Im(point1inverse))] ) :
      xcoord := coordinates(center(c1));
      x := xcoord[1] + I·xcoord[2];
      point3inverse :=  $\frac{1}{\text{evalf}(\text{abs}(\text{point3}))^2} \cdot \text{point3}$ ;
      circle(c2, [point(A2, Re(point3), Im(point3)), point(B2, Re(point4), Im(point4)),
      point(C2, Re(point3inverse), Im(point3inverse))] ) :
      x2coord := coordinates(center(c2));
      x2 := x2coord[1] + I·x2coord[2];
      if evalf(abs(x - point3)) < evalf(abs(x - point1)) < evalf(abs(x - point4))
      or evalf(abs(x - point4)) < evalf(abs(x - point1)) < evalf(abs(x - point3)) then
      if evalf(abs(x2 - point1)) < evalf(abs(x2 - point3)) < evalf(abs(x2 - point2))
      or evalf(abs(x2 - point2)) < evalf(abs(x2 - point3)) < evalf(abs(x2 - point1)) then
      ans := 1;
      end if;
      end if;
      return ans;
      end proc;
```

We create the Euclidean coordinates of the vertices of the fundamental polygon of $S(2)$ where $v[i]$ for $i = 1, \dots, 8$ are vertices of the 8-gon in clockwise order. $r1$ is the Euclidean distance of the points from the origin.

```

> with(ArrayTools) :
> v := [seq(0, i=1..8)]:
> r1 := evalf(sqrt(2*(sqrt(2)-1))) :
> for i from 1 to 8 do
v[i] := evalf(r1*exp(I*Pi*(i-1)/4));
end do:

```

In order to find the geodesic on the covering space between two points on a surface, we will fix a copy of one point x and consider the copies of point y on copies of the fundamental polygon which are close. In order to find its copies, we initialize two functions.

```

> vert := 1/sqrt(sqrt(2)) * exp(I*Pi/8) :
> midpt := 1/2 * sqrt(2*(1+sqrt(2))) :
> ffinal := (k, z) -> exp(-k*Pi/4 * I) * (-exp(-I*Pi/2)
. ( (exp(k*Pi/4 * I) * z) - v[4] )
conjugate(-v[4]) * (exp(k*Pi/4 * I) * z) + 1 ) :
ffinal2 := (k, z) -> exp(-k*Pi/4 * I) * (-exp(I*Pi/2)
. ( (exp(k*Pi/4 * I) * z) - v[2] )
conjugate(-v[2]) * (exp(k*Pi/4 * I) * z) + 1 ) :
> copies := proc(point)
local S;
S := [evalf(point),
seq(evalf(ffinal(k, point)), k in [0, 1, 4, 5]),
seq(evalf(ffinal2(k, point)), k in [0, 1, 4, 5]),
seq(evalf(ffinal(k, ffinal2(k+1, point))), k in [0, 4]),
seq(evalf(ffinal(k, ffinal(k-1, point))), k in [1, 5]),
seq(evalf(ffinal(k, ffinal2(k-1, point))), k in [1, 5]),
seq(evalf(ffinal(k, ffinal(k-3, point))), k in [0, 4]),
seq(evalf(ffinal2(k, ffinal(k-1, point))), k in [1, 5]),
seq(evalf(ffinal2(k, ffinal2(k+3, point))), k in [1, 5]),
seq(evalf(ffinal2(k, ffinal(k+1, point))), k in [0, 4]),
seq(evalf(ffinal2(k, ffinal2(k+1, point))), k in [0, 4]),
seq(evalf(ffinal(k, ffinal(k-1, ffinal2(k, point)))), k in [1, 5]),
seq(evalf(ffinal(k, ffinal2(k-1, ffinal2(k, point)))), k in [1, 5]),
seq(evalf(ffinal(k, ffinal2(k+1, ffinal2(k+4, point))))), k in [0, 4]],

```

```

seq(evalf(ffinal2(5 - k, ffinal2(k, ffinal(k + 1, point)))), k in [0, 4]),
seq(evalf(ffinal2(k + 1, ffinal(k, ffinal(k - 3, point)))), k in [0, 4]),
seq(evalf(ffinal(5 - k, ffinal(k, ffinal2(k - 1, point)))), k in [1, 5]),
seq(evalf(ffinal2(k - 1, ffinal(k, ffinal(k - 1, point)))), k in [1, 5]),
seq(evalf(ffinal2(k - 1, ffinal2(k, ffinal(k - 1, point)))), k in [1, 5]),
seq(evalf(ffinal2(k - 4, ffinal(5 - k, ffinal(k, ffinal2(k - 1, point))))), k in [1, 5]),
seq(evalf(ffinal2(k - 4, ffinal2(k - 1, ffinal(k, ffinal(k - 1, point))))), k in [1, 5]),
seq(evalf(ffinal(k, ffinal2(k - 1, ffinal2(k, ffinal(k - 1, point))))), k in [1, 5]),
seq(evalf(ffinal(k - 5, ffinal(k, ffinal2(k - 1, ffinal2(k, point))))), k in [1, 5])
];
return S;
end proc:

```

Given point1 in the fundamental polygon, we find the closest copy of point2 in the covering space.

```

> closest := proc(point1, point2)
local S, s, dist1, dist, y2;
y2 := point2;
S := copies(point2);

dist1 := evalf( arccosh( 1 +  $\frac{2 \cdot \text{abs}(point1 - point2)^2}{(1 - \text{abs}(point1)^2) \cdot (1 - \text{abs}(point2)^2)}$  ) );

for s from 2 to nops(S) do
dist := evalf( arccosh( 1 +  $\frac{2 \cdot \text{abs}(point1 - S[s])^2}{(1 - \text{abs}(point1)^2) \cdot (1 - \text{abs}(S[s])^2)}$  ) );
if dist < dist1 then
dist1 := dist;
y2 := evalf(S[s]);
end if;
end do;
return y2;
end proc:

```

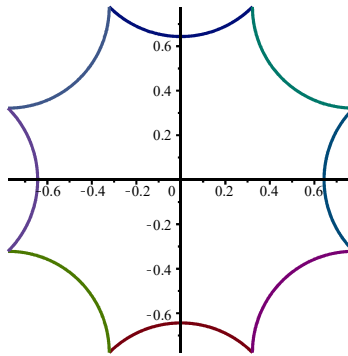
We show how the previously defined functions work by an example.

```

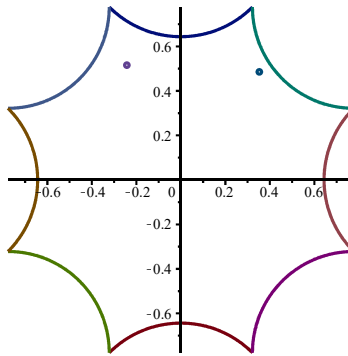
[> g := Im(vert) :
[> h := abs(midpt - vert) :
[> ang := evalf( 2 * arcsin(  $\frac{g}{h}$  ) ) :
[> npoints := 100 :
[> points4plot := [seq(0, i = 1 .. npoints) ] :
[> for i from 1 to npoints do
points4plot[i] := evalf( midpt + ( exp(  $\frac{ang \cdot i}{npoints} I$  ) * (vert - midpt) ) ) :
end do:
[> pointsarray := Array(points4plot) :
[> Extend( pointsarray, evalf( exp(  $\frac{\text{Pi}}{4} I$  ) * pointsarray ) ) :
[> with(plots) :

```

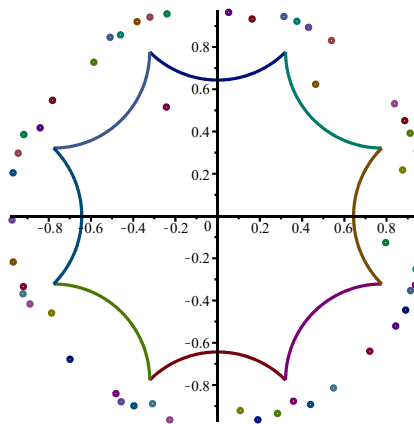
```
> complexplot( { seq( exp( (2*j)*Pi/I ) * (midpt + (exp( ang*t*I ) * (vert - midpt))), j=1
..8 ) }, t=0..1 );
```



```
> examplepoint1 := evalf(0.60*exp(2*Pi*I*0.15)) :
> examplepoint2 := evalf(0.57*exp(2*Pi*I*0.32)) :
> complexplot( { examplepoint1 + 0.01*exp(2*Pi*t*I), examplepoint2 + 0.01*exp(2*Pi*t*I),
seq( exp( (2*j)*Pi/I ) * (midpt + (exp( ang*t*I ) * (vert - midpt))), j=1..8 ) }, t=0..1 )
;
```



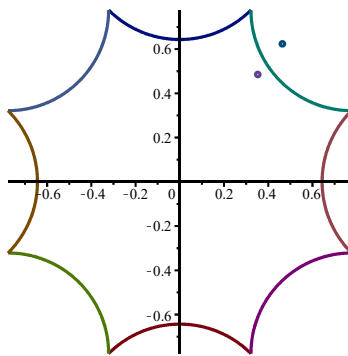
```
> S := copies(examplepoint2) :
> complexplot( { seq(S[j] + 0.01*exp(2*Pi*t*I), j=1..nops(S)), seq( exp( (2*j)*Pi/I )
*(midpt + (exp( ang*t*I ) * (vert - midpt))), j=1..8 ) }, t=0..1 );
```



```

> examplepoint2close := closest(examplepoint1, examplepoint2) :
> complexplot( { examplepoint1 + 0.01 · exp(2 · Pi · t · I), examplepoint2close + 0.01 · exp(2 · Pi · t
· I), seq( exp( (2 · j) · Pi / 8 · I) · (midpt + (exp(ang · t · I) · (vert - midpt))), j = 1 .. 8) }, t = 0
.. 1);

```



```

> x := cross( examplepoint2close, examplepoint1, vert · exp( Pi / 4 · I), vert );
x := 1
(6.1)

```

We sample the segments and determine whether they cross. The pairs of points are saved in the Array wtuples. In the first while loop, we sample points uniformly at random from the disk that contains the fundamental polygon. If the fundamental polygon contains the point, then we keep it, otherwise we discard it. In that way we generate uniformly random points on the fundamental polygon.
 In order to determine the segments and the crossings, the first point firstp of the first segment will be the first random point. The second point secondp will be the closest copy of the second

random point in the covering space. Hence the geodesic between firstp and secondp in the covering space is the shortest path between firstp and secondp on the surface. To determine if there is a crossing with the second segment, the third point thirdp and fourth point fourthp will range over copies of the third and fourth random point.

```

[> distH := [seq(0, i = 1 ..8) ] :
[> with(Statistics) :
[> with(RandomTools) :
> for tuples from 1 to ntuples do
x := 1 :
wtuples := Array([ ]) :
while x < 5 do
y := 0;
samp := Sample(UniformRandomVariable(0, 1), 2) :
#Sample two points uniformly at random between 0 and 1
r := tanh( arccosh(1 + (2 + 2·sqrt(2))·samp[1]) / 2 );
#r is a radius chosen uniformly w.r.t a hyperbolic disk
z := evalf(r·exp(2·Pi·I·samp[2])) :
#2 Pi samp[2] is a random angle, here z is in polar coordinates
distH0 := evalf(arccosh(1 + (2 + 2·sqrt(2))·samp[1]));
for i from 1 to 8 do
distH[i] := evalf( arccosh( evalf( 1 + ( 2·abs(v[i] - z)2 / ((1 - abs(z)2)·(1 - r2) ) ) ) ) );
if distH0 > distH[i] then
y := 1;
end if;
end do;
if y=0 then
Append(wtuples, z) :
++x;
end if;
end do;
firstp := evalf(wtuples[1]);
secondp := closest(firstp, wtuples[2]);
p4 := closest(wtuples[3], wtuples[4]);
p3 := closest(wtuples[4], wtuples[3]);
SetsForSegments3 := copies(wtuples[3]);
SetsForSegments4 := copies(p4);
segmentcross := 0;
for l from 1 to nops(SetsForSegments3) do
thirdp := evalf(SetsForSegments3[l]);
forthp := evalf(SetsForSegments4[l]);
if cross(firstp, secondp, thirdp, forthp) = 1 then
segmentcross := 1;
end if;
end do;
SetsForSegments3b := copies(p3);
SetsForSegments4b := copies(wtuples[4]);
for l from 1 to nops(SetsForSegments3b) do

```



```

thirdp := evalf(SetsForSegments3b[l]);
forthp := evalf(SetsForSegments4b[l]);
if cross(firstp, secondp, thirdp, forthp) = 1 then
  segmentscross := 1;
end if;
end do;
if segmentscross = 1 then
  crossing := ++ crossing ;
end if;
end do;

```

▼ **The fraction of pairs of segments that cross compared to all pairs of segments.**

```

> ability :=  $\frac{\text{crossing}}{\text{ntuples}}$ ;

```

$$\text{ability} := \frac{887}{10000}$$

(8.1)